

A Reproduced Copy
OF

N86-13357

LIBRARY COPY

5 1986

LANGLEY RESEARCH CENTER
LIBRARY, NASA
LANGLEY STATION
HAMPTON, VIRGINIA

Reproduced for NASA

by the

NASA Scientific and Technical Information Facility

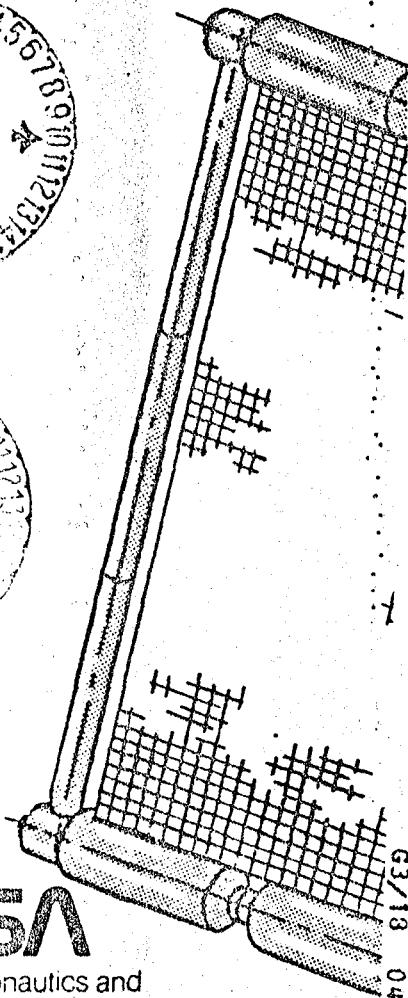
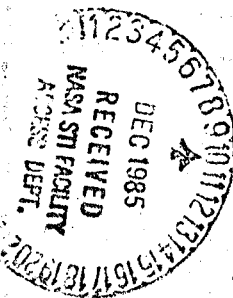
3 1176 01306 5389

100

JSC-18555

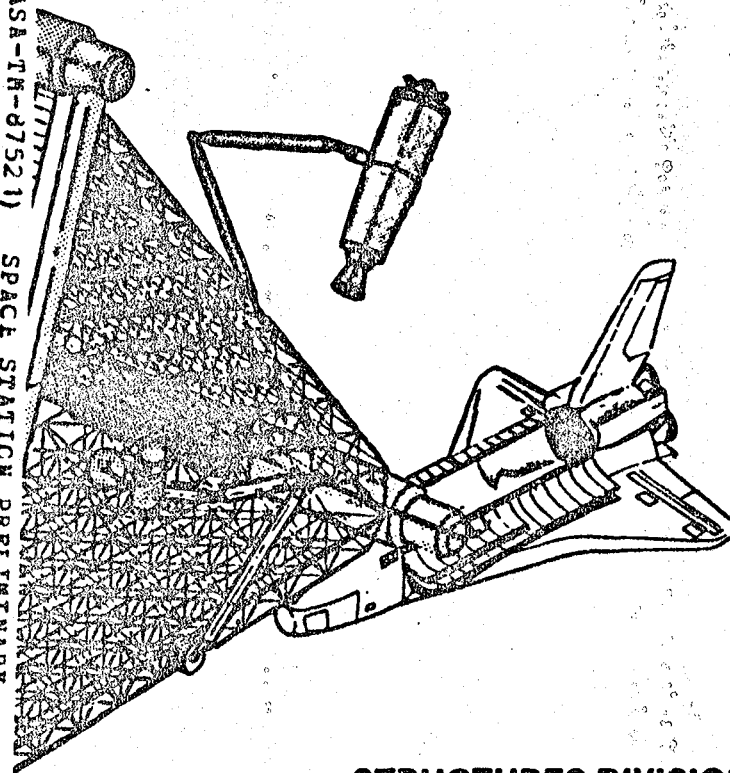
SPACE STATION

PRELIMINARY DESIGN REPORT



(NASA-TM-87521) SPACE STATION PRELIMINARY
DESIGN REPORT (NASA) 252 P HC A12/HF A01

CSC1 22B



G3/18 UNCLAS
04915

N86-13357

STRUCTURES DIVISION
ENGINEERING AND DEVELOPMENT
DIRECTORATE

SEPTEMBER 1982



National Aeronautics and
Space Administration

Lyndon B. Johnson Space Center
Houston, Texas

N86-13357#

FORWARD

This report contains the results of the preliminary design and analysis that was performed by the Structures Division's Preliminary Space Station Design Team, during the 3-month period between June 14 and September 15, 1982. This team was organized in the following way

Team Director:	Dr. William C. Schnieider
Thermal Analysis:	Richard Parish Robert Vogt
On-orbit Dynamics Analysis:	John Schliesing Reg Berka Barbara Hernandez Ron Maynard
Structural Design and Analysis Deployable Truss:	Herbert Kavanaugh Dr. Frederick Stebbins
Handling Equipment:	Clarence Wesselski
Holddown Attachments:	Dr. Kornel Nagy
Module Design:	Herbert Kavanaugh Jim McMahon Peter Taylor
Buildup Sequence:	P. Donald Smith Clarence Wesselski
Materials:	Sam Glorioso
Report Preparation:	Patricia Longacre
Special Editor:	Orvis Pigg
Outside Space Station Consultants:	Robert Ried Robert Wren

TABLE OF CONTENTS

Section	Page
<u>Summary</u>	1
0 <u>Introduction</u>	3.1
0.1 Background.....	3.1
0.2 General Plan.....	4
0.3 Evolution to the Final Configuration.....	6
0.4 Description of Triangular Space Station Configuration....	11
0.5 Configuration.....	13
1.0 <u>Space Station Thermal Analysis</u>	16
1.1 Thermal Design Objectives.....	16
1.2 Thermal Analysis.....	17
1.2.1 Thermal Radiation Geometric Math Model.....	17
1.2.2 Thermal Conduction Math Model.....	19
1.2.3 Analytical Results.....	24
1.2.4 Conclusions.....	35
1.3 Radiator Concepts.....	40
1.4 Possible Design Refinements.....	40
1.4.1 Structurally Enclosed Modules.....	40
1.4.2 Thermal Comparison with Baseline.....	41
2.0 <u>Space Station On-orbit Dynamic Analysis</u>	48
2.1 Objectives.....	48
2.2 Introduction.....	48

TABLE OF CONTENTS (CONT'D)

Section	Page
2.3 Orbital Altitude Analysis.....	50
2.3.1 Atmosphere Model.....	51
2.3.2 STS Payload Performance.....	51
2.3.3 Orbit Decay Time.....	52
2.3.4 Orbit Maintenance Methodology.....	54
2.4 Attitude Control Analysis.....	56
2.4.1 Disturbance Torques.....	57
2.4.1.1 Aerodynamic Torque.....	58
2.4.1.2 Gravity Gradient Torque.....	61
2.4.2 Attitude Control Assessment.....	62
2.5 Conclusions.....	75
3.0 <u>Structural Design and Analysis</u>	
3.1 Deployable Truss.....	79
3.1.1 Introduction.....	79
3.1.2 Truss Requirements.....	79
3.1.3 Truss Concept Study.....	80
3.1.4 Truss Loading.....	85
3.1.5 Truss Materials Study.....	90
3.1.6 Space Station Frame Geometry.....	94
3.1.7 Truss Member Sizing and Weight Analysis.....	95
3.1.8 Payload Packaging Analysis.....	102
3.1.9 Deployable Joint and Fitting Study.....	109
3.1.10 Space Deployment Concept.....	115
3.1.11 Conclusions and Recommendations.....	120
3.1.12 References.....	124

TABLE OF CONTENTS (CONT'D)

Section	Page
3.2 <u>Handling Equipment</u>	125
3.2.1 Requirements.....	126
3.2.2 The Manipulator Concept.....	127
3.2.3 Loads and Stresses.....	132
3.2.3.1 Operational Stresses.....	135
3.2.3.1.1 Stiffnesses.....	141
3.2.3.1.2 Maximum Velocities.....	153
3.2.3.1.3 Tetratruss Member Loads and Stresses.....	154
3.2.4 Manipulator Operations.....	158
3.2.4.1 OTV Handling.....	158
3.2.4.2 Moving Base of Manned Manipulators.....	158
3.2.4.3 Inside and Outside Conversion.....	160
3.2.4.4 Shuttle Docking.....	160
3.2.5 Stowage of the Manipulators.....	166
3.2.6 Conclusions.....	168
3.3 <u>Holddown Attachments</u>	170
3.3.1 Introduction.....	170
3.3.2 Attachment Interfaces.....	172
3.3.2.1 Attachment at Truss Nodal Points.....	172
3.3.2.2 Attachment at Truss Diagonals.....	172
3.3.3 Orbiter Transfer Vehicle (OTV) Holddown Attachments.....	174
3.3.3.1 OTV Trunnion Attach with Tripod.....	176
3.3.3.2 Handling Fixture Attach.....	179
3.3.3.3 OTV Berthing Fixture Attach.....	182

TABLE OF CONTENT (CONT'D)

Section	Page
3.3.4 Orbiter Berthing to Station.....	183
3.3.4.1 Orbiter Berthing with Baseline Docking Tunnel.....	184
3.3.4.2 Alternate Orbiter Berthing Concepts.....	187
3.3.5 Attachment of Auxilliary Equipment to Station.....	189
3.3.5.1 Storage Tank Attachment.....	189
3.3.5.2 Tubing and Cable Tray Attachment.....	192
3.3.6 Attachment of Satellites to Station.....	193
3.4 <u>Module Design</u>	195
3.4.1 Introduction.....	195
3.4.2 Module Design Requirements.....	195
3.4.3 Module Configuration.....	202
3.4.3.1 Module Skin Thickness.....	202
3.4.3.2 End Closure Design.....	206
3.4.3.3 Weld Joint Design.....	209
3.4.3.4 Supporting Analysis.....	210
3.4.4 Meteoroid Protection.....	214
3.4.5 Module Weight.....	215
3.4.6 Manufacturing Summary.....	218
3.4.6.1 Materials Selection.....	218
3.4.6.2 Fabrication Considerations.....	219
3.4.6.3 Cassinian, Elliptic, and Spherical Dome Fabrication.....	220
3.4.6.4 Conic and Flat Bulkhead Dome Fabrication.....	222
3.4.6.5 Fabrication Cost Comparison.....	222
3.4.6.6 Fabrication Summary and Recommendations.....	224

TABLE OF CONTENTS (CONT'D)

Section	Page
3.4.7 Tunnels.....	225
3.4.8 Conclusions and Recommendations.....	229
3.4.9 References.....	231
4.0 <u>Buildup Sequence</u>	232
Delivery Flight Number 1.....	232
Delivery Flight Number 2.....	233
Delivery Flight Number 3.....	236
Delivery Flight Number 4.....	236
Delivery Flight Numbers 5, 6, 7, and 8.....	240
5.0 Concluding Remarks.....	244

SUMMARY

This report summarizes a 3-month engineering effort by Structures Division personnel to define a structurally efficient and stable Shuttle launched Space Station. Potential uses for the Space Station were established to be

- a) Servicing and construction of orbital transfer vehicles (OTV) for launch to geosynchronous orbit
- b) Satellite servicing and repair
- c) Laboratory industrial manufacturing and experiments
- d) Large antenna technology (buildup and servicing)
- e) Earth observation
- f) Communications
- g) Space observation

Based on a detailed study of these potential uses, efficient and maximum operation dictates that the Space Station, regardless of configuration, must have a large, flat, stiff structure to serve as a work base to which the OTV, satellites, etc. are attached during their construction and/or servicing. Furthermore, this platform to be lightweight, should be a trussed structural element, and to minimize Extravehicular Activity (EVA), should also be deployable. Thus, it was concluded that one critical element of any Space Station should be a planar truss that can be constructed on the ground, packaged for transportation in the Shuttle, and deployed in space.

Another element that is considered critical to a functional and cost effective Space Station, is the Universal Module. Universal Modules are structural shells with the same design and construction regardless of their function (habitat, lab, etc). These modules can be used for various purposes by tailoring the internal arrangement (equipment, partitions, etc) to meet the specific function.

To minimize the changes in gravity gradient torques and the overall dynamic characteristics that can occur when the large masses (associated with OTV, satellites etc) are attached, removed, and moved around on the Space Station, transient masses should be placed as near the Space Station center of mass as possible.

The demands of antennas and solar cells for accurate positioning and the requirements of adequate stiffness to avoid undesirable structural distortions are considered serious and thereby will dictate the design. Therefore, one further characteristic essential to the primary structure is a high rigidity of the assembled components when they form the full operational Space Station.

The Space Station configuration that has these essential features consists of three large erectable trusses, six modules, and three tunnel systems (see figure O.V). In two Shuttle flights a habitable but limited operational station can be delivered to orbit. For a fully operational Space Station eight flights are required.

Sufficient engineering was performed to demonstrate the feasibility of this Space Station configuration, and insure that no major design problems would exist. The configuration presented in this study is such that it can be further expanded (as desired) to a much larger Space Station (see figure O.VI) by adding more trusses and modules, and the resulting configuration would possess the same general characteristics as the original.

0 INTRODUCTION

0.1 Background

With the present reality of an operational Space Shuttle, the energy of the aerospace community can now be focused on the establishment of a permanent Space Station. During the past 20 years numerous studies have been performed that resulted in various space laboratories, bases, and stations utilizing different launch vehicles. Recently, preliminary studies (e.g., Rockwell and Boeing) have been completed using the space shuttle. These studies (and the resulting configurations), while of great value, leave much to be desired relative to structural design and providing inherent capabilities to meet long term Space Station needs such as space basing an OTV, satellite servicing and space construction.

To arrive at a Space Station design that provided the needed capabilities and which was strongly influenced by structural and thermal considerations and to more deeply involve key personnel in the Space Station design effort (previously occupied with Shuttle design certification and analysis) a Preliminary Space Station Design Team was formed. This team is composed of eight full-time and six part-time engineers with expertise in the areas of preliminary structural design, rigid body dynamics and control, thermal analysis, and materials. The time allocated to this initial design effort was the 3-month period between June 14 through September 15, 1982.

0.2 General Plan

The general design and analysis plan followed by the team is shown in figure 0.I.

GENERAL PLAN
SPACE STATION
PRELIMINARY DESIGN TEAM

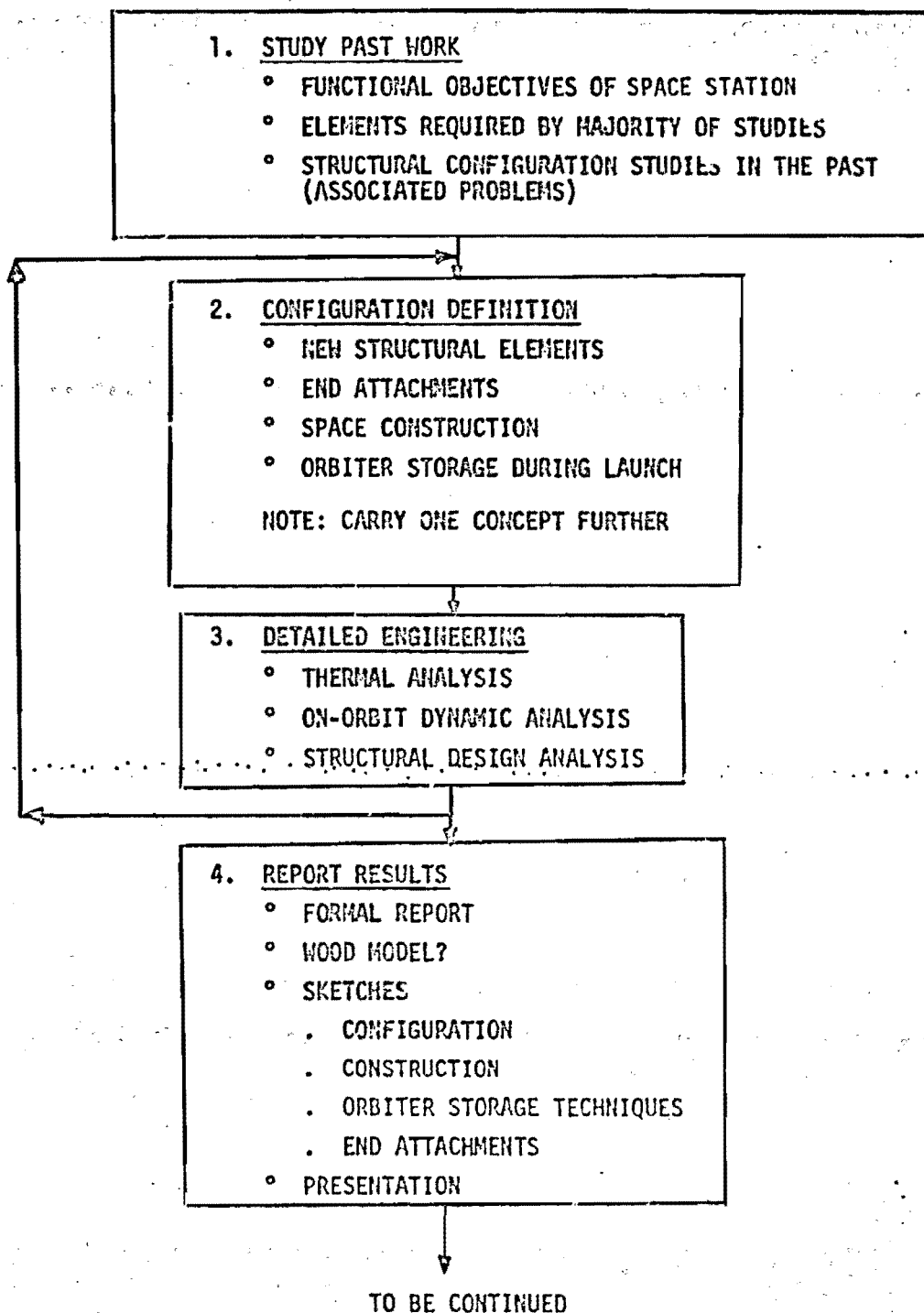


FIGURE 0.1

0.3 Evolution to the Final Configuration

After completing the first block of the general plan (past work studied) various concepts were proposed by the team. Three of the initial configurations entertained were

1. The Erectable Rigid Spheres
2. The Building Block
3. The Erectable Hexagonal Hanger

A sketch of each is shown in figures 0.II, 0.III, 0.IV.

Each configuration had a number of advantageous features. For example, the Erectable Rigid Spheres configuration eliminated the need for solar cell orientation, utilized gravity gradient stabilization and was composed essentially of erectable structure. The Building Block offered a very compact side by side module configuration which minimized the cable and tubing lengths, utilized minimum length solar arrays (i.e., no flexible beams) and provided for shirtsleeve servicing of the solar array drives. The Erectable Hexagonal Hanger configuration utilized solar cells rigidly attached to the trusses and provided for internal center of gravity location which contributes to greater overall control and good center of gravity management.

The Erectable Hexagonal Hanger seemed to have the best potential for meeting the general Space Station objectives. The six sided structure, as initially envisioned, would have a tendency to distort cross-sectionally unless the corners were made extremely stiff and consequently heavy. To minimize this tendency, the

TWO RIGID SPHERES

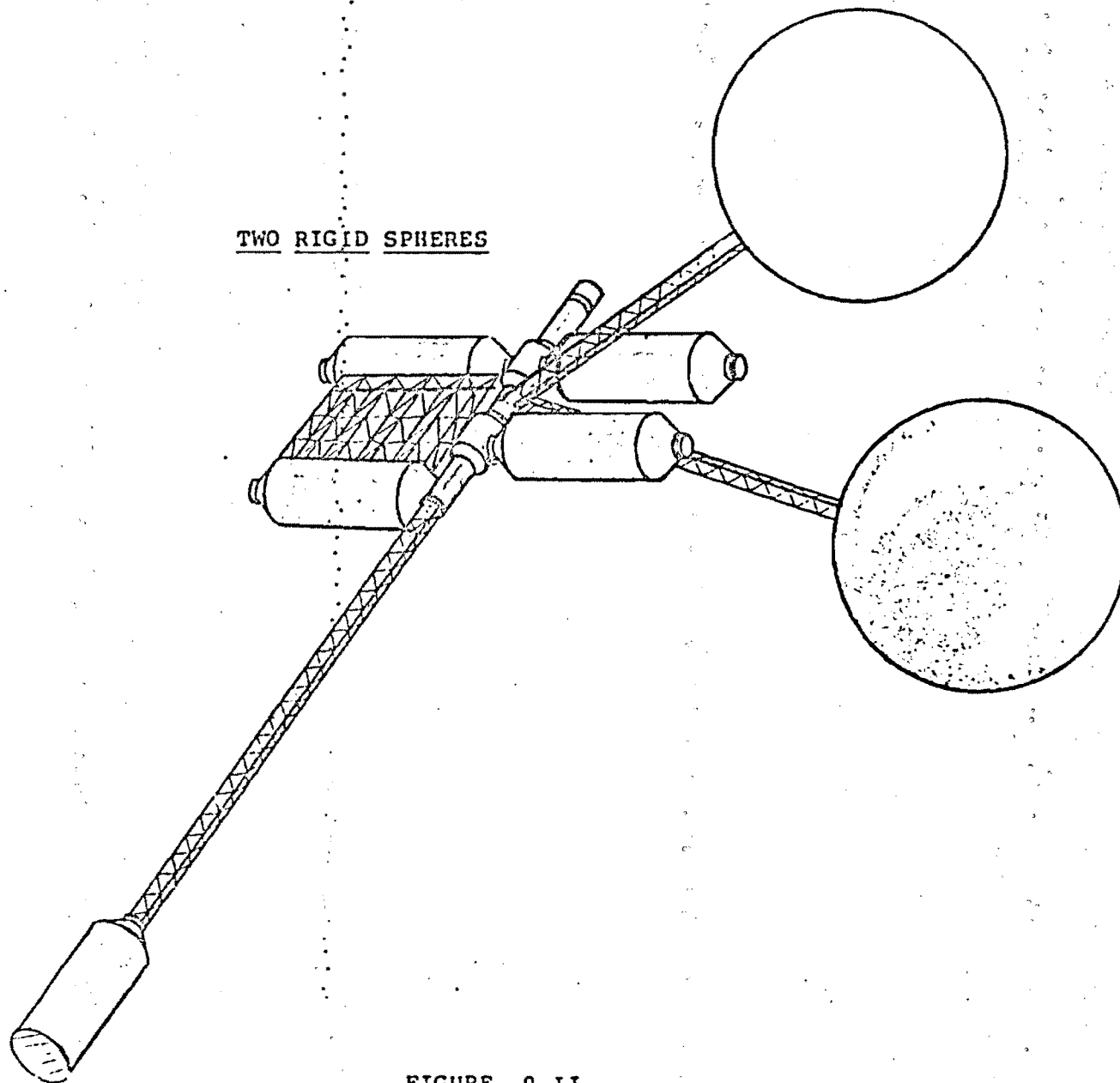


FIGURE 0.11

BUILDING BLOCK

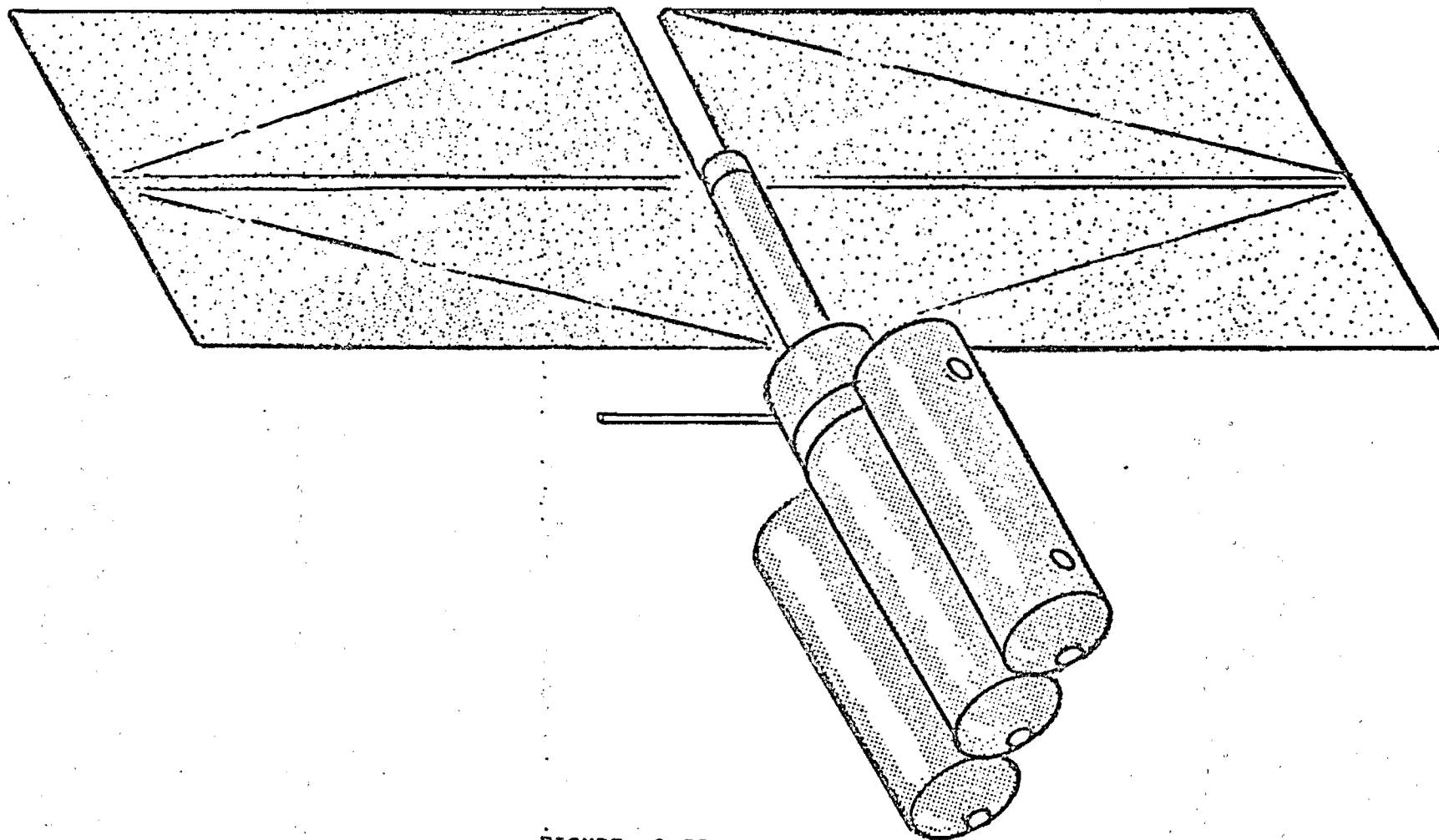


FIGURE 0.III

ERECTABLE HEXAGONAL HANGER

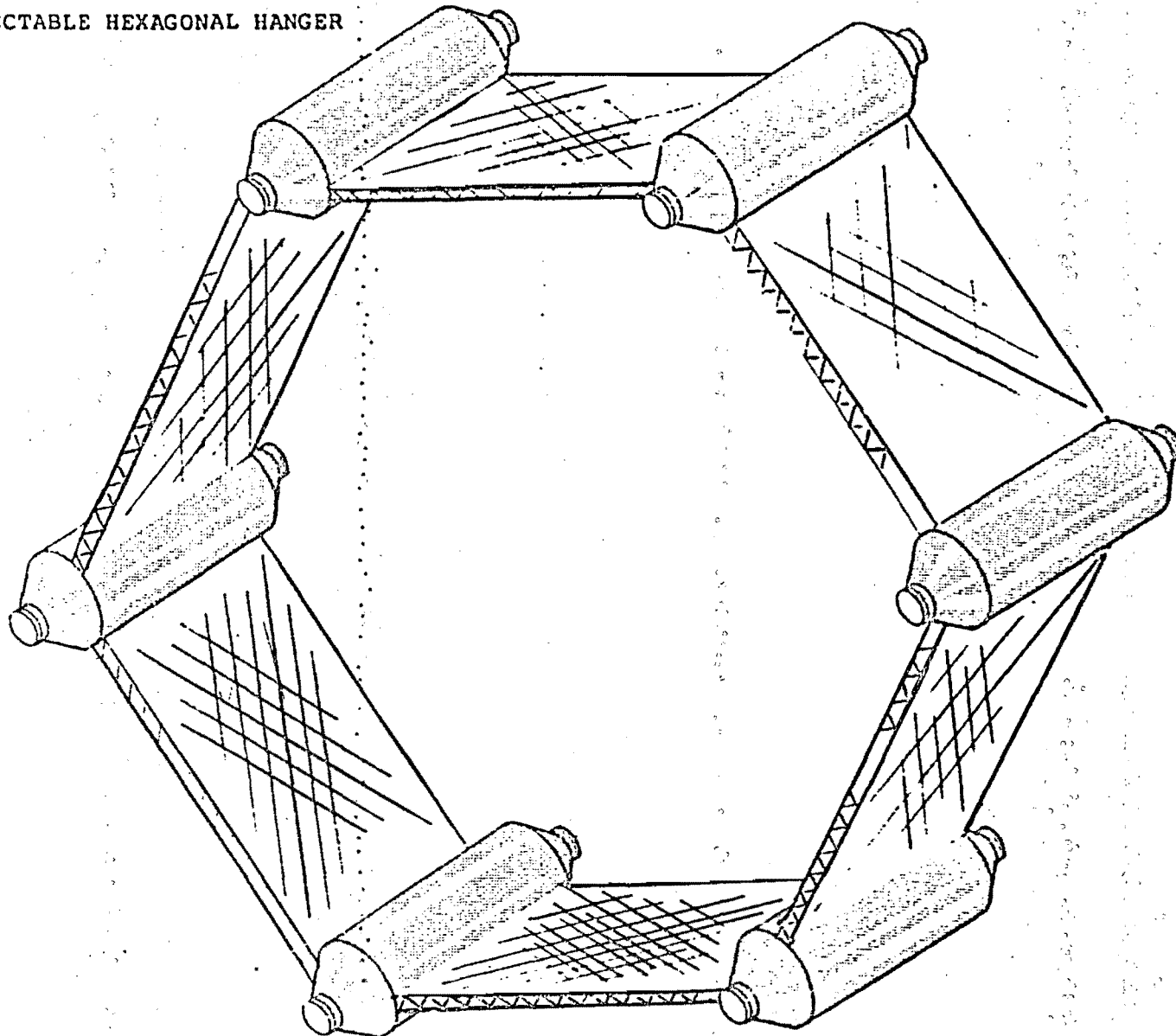


FIGURE 0.IV

decision was made to use a 3-sided, inherently stable, cross section for the configuration. This triangular configuration, after some slight modifications, was chosen for the detailed engineering analysis (square 3 of general plan).

0.4 Description of Triangular Space Station Configuration

The baseline configuration for the design analysis is comprised of six modules and three deployable tetratruss flat platforms assembled in such a way that an open triangular shaped structure (see figure 0.V) is formed. Each of the three apexes has two modules (figure 0.V, item 1) and each of the three flat sides are the tetratruss platforms. Tentatively there are two habitat modules, two service modules, a logistic module and a lab module. Each module is approximately 14 feet diameter and 46 feet long. Each platform is approximately 125 feet long, 70 feet wide, and 8.4 feet thick. Three connecting tunnels (figure 0.V, item 3) run between apexes and join the modules so that all modules are accessible to one another. These tunnels are pressurized, and about 6 feet in diameter, and have a telescoping feature that permits them to be stowed in the midfuselage bay. Item 4 of figure 0.V is the solar panel that is fastened to the outside of one of the tetratruss platforms, sized to supply 50 kw of electrical power... Item 5 of figure 0.V is one of the two radiator panels (mounted to the outside surface of the remaining two platforms) that radiates excess heat to space. Item 6 of figure 0.V is a manipulator system to move and work with payloads such as, OTV's, satellites, tanks, etc. The entire assembly is about 90 feet long and the distance between apexes is 138 feet.

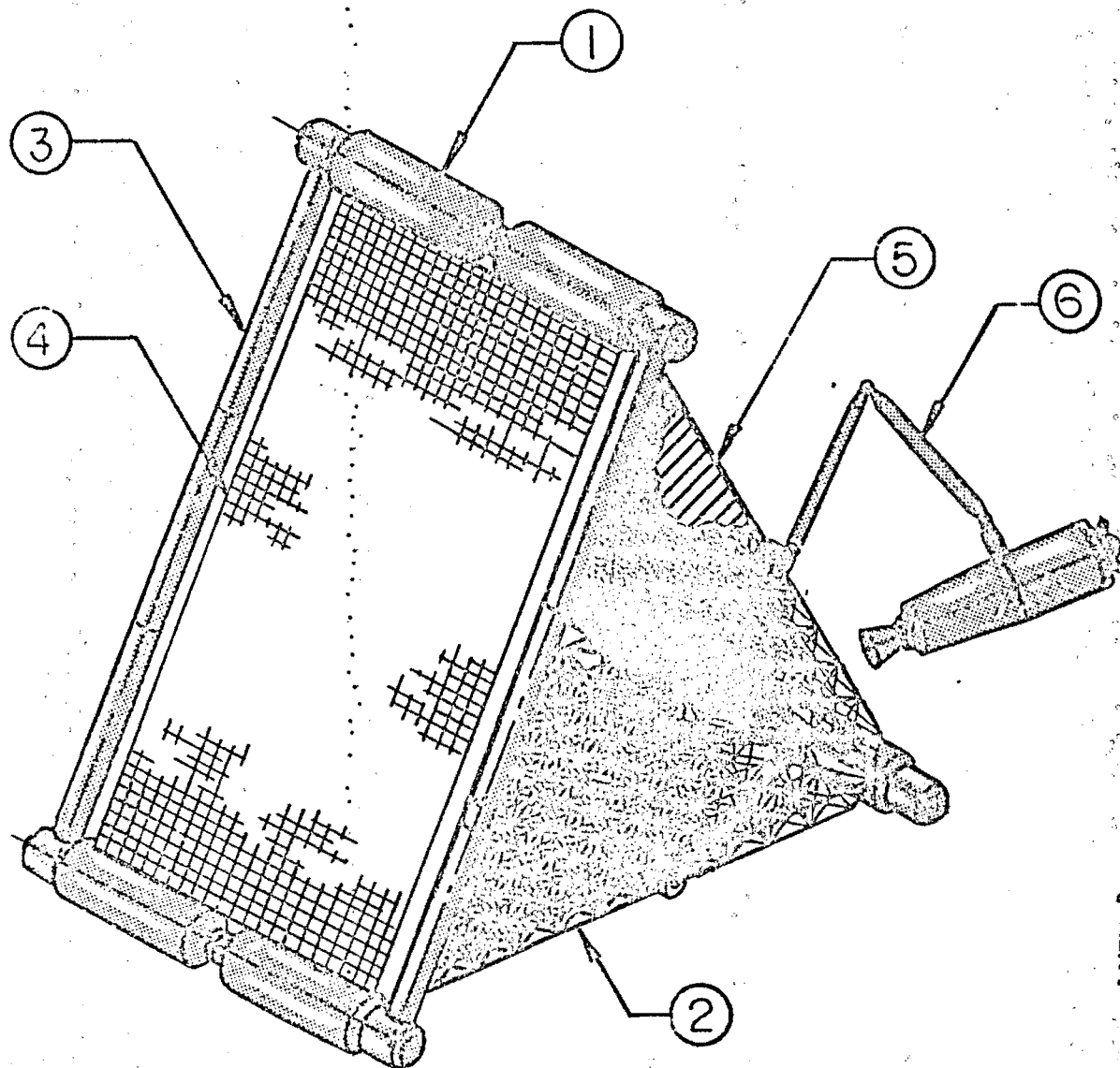


FIGURE 0.V

ORIGINAL PAGE IS
OF POOR QUALITY

0.5 Configuration

This configuration affords the following advantages

The three structural trusses (forming the largest Space Station component) are fabricated on the ground, collapsed, launched in the Shuttle, and erected in space. The structural trusses are designed to require minimum EVA during construction.

The configuration buildup sequence can be tailored to the Space Station funding schedule. The first three flights comprise a Space Station (trusses, habitat module, and a service module). Additional modules and handling equipment will be brought up on later flights as funding becomes available.

The solar cells, used for electricity generation, are attached to one of the stiff truss sides and therefore eliminates the problems associated with very flexible solar panels.

The center of mass of the basic Station is located internal to the structure which allows for ease of control and center of gravity management during OTV and satellite servicing.

The open truss construction of the sides offer excellent work areas for OTV and satellite servicing as well as large antenna construction.

The modules are cylindrical units that fit nicely into the Orbiter payload bay for delivery, and are designed such that the

structure is used to accommodate the launch loads as well as the loads induced through the trusses by daily operations. The configuration, while baselined as inertially oriented, can be easily oriented to earth since very low gravity gradient torques are experienced.

The thruster units for Space Station orientation are three in number and are located at the very stiff and strong corners of the truss triangles. This eliminates the need for additional weight required by thrust loads.

The basic Triangular Station configuration can easily be expanded by the addition of trusses and modules. This configuration, when expanded, resembles a honeycomb (figure O.VI).

ORIGINAL PAGE IS
OF POOR QUALITY

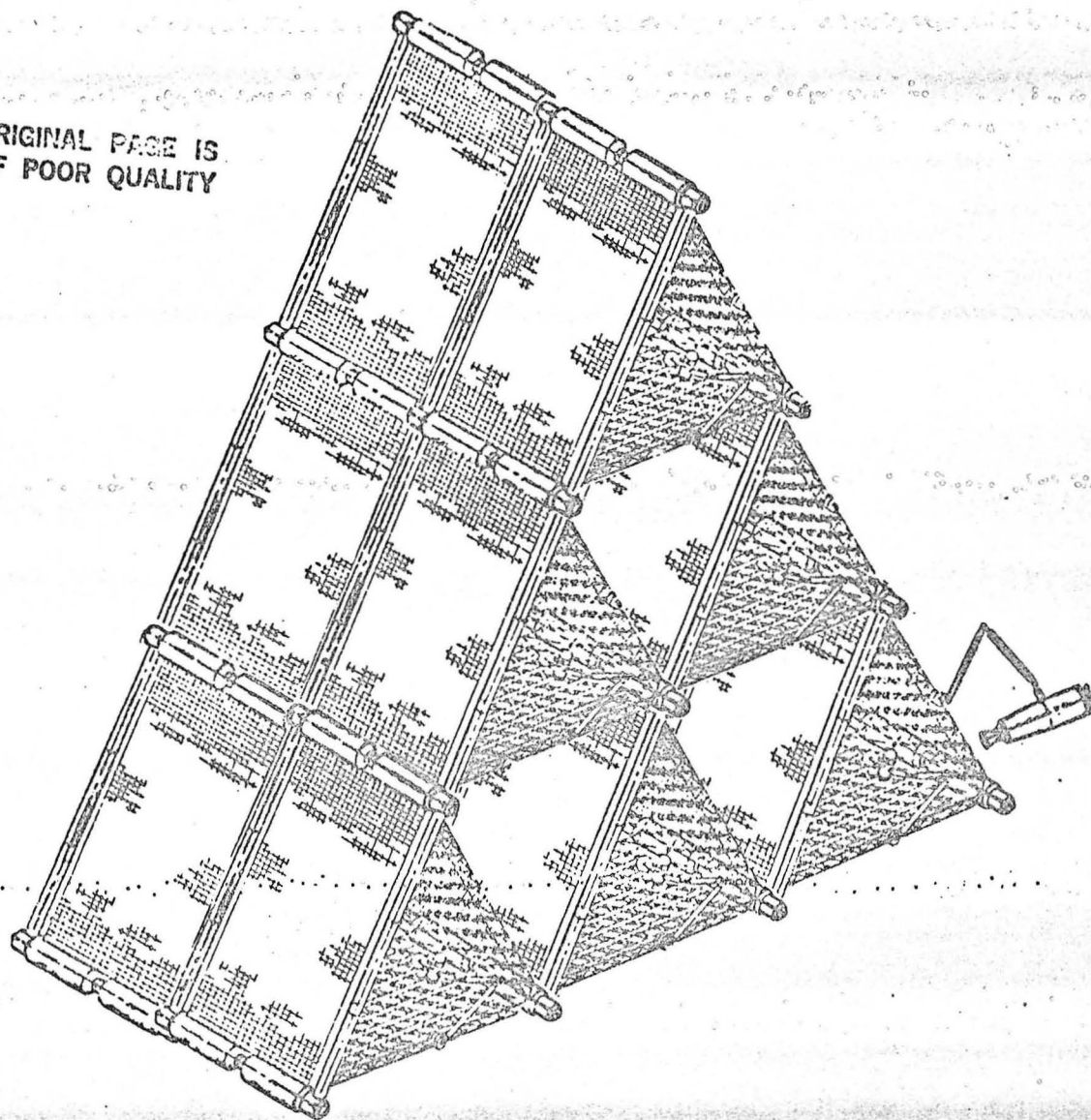


FIGURE O.VI

1.0 Space Station Thermal Analysis

1.1 Thermal Design Objectives

The primary thermal design objectives addressed in this study are:

- (1) Efficient space station thermal energy management.
- (2) Verification of acceptable temperature levels of structural components.
- (3) Maintenance of habitat module wall temperature levels above the condensation point.
- (4) Assessment of configuration sensitivity to thermal coatings and insulations.

Efficient thermal energy management in a space station concept should begin with a structure that maximizes passive thermal control. This is accomplished by selection of appropriate coatings and insulations with properties tailored for long duration attitudes in Earth's orbit.

A preliminary thermal analysis was performed on the triangular configuration in order to assure a thermally efficient design. This involved a rough sizing of insulations and specification of coating characteristics. It was also necessary to confirm that the solar arrays would have adequate back-side radiation capability to operate at as low a temperature as possible, enhancing power generation efficiency. Truss structure temperature levels and possible gradient ranges were to be established to justify radiator placement and to predict thermal stresses in the structure.

One of the primary goals of the thermal design is to maintain the habitable module inner pressure vessel wall at a temperature higher than the internal dewpoint

temperature (i.e., greater than approximately 50°F) to prevent condensation on the module walls. This would be accomplished by reducing strong circumferential gradients in the wall. These gradients are controlled by balancing the influence of the external environment against the internal heat load. Designing for a controlled heat rejection capability through the walls of the modules enables wall surface temperatures to be maintained at desired levels while reducing the internal load imposed on an active thermal control system.

Another objective of the thermal design involved assessing the sensitivity of the configuration to thermal coatings, assuming various insulation effectivities. The thermal coatings determine the amount of heat flux that is absorbed and rejected on the surface of the structure while the insulation modulates this flux into and out of the internal compartments. The sensitivity would preferably be low due to degradation that will occur to the coatings. Additionally, an insensitive configuration would imply that less exotic coatings could initially be utilized, reducing build-up and refurbishment costs.

1.2 Thermal Analysis

Thermal math models were constructed to assist in the analysis of the proposed configuration and to enable assessment of thermal control materials. The thermal radiation analysis system (TRASYS) was used to determine heat loads to the external surfaces of the vehicle and the systems improved numerical differencing analyzer (SINDA) enabled temperatures to be computed from these flux levels.

1.2.1 Thermal Radiation Geometric Math Model

To accurately assess the influence of the external thermal environment on the proposed configurations, a TRASYS geometric math model was developed. As shown in figure 1.1, modules and tunnels are represented by closed cylindrical shapes while the

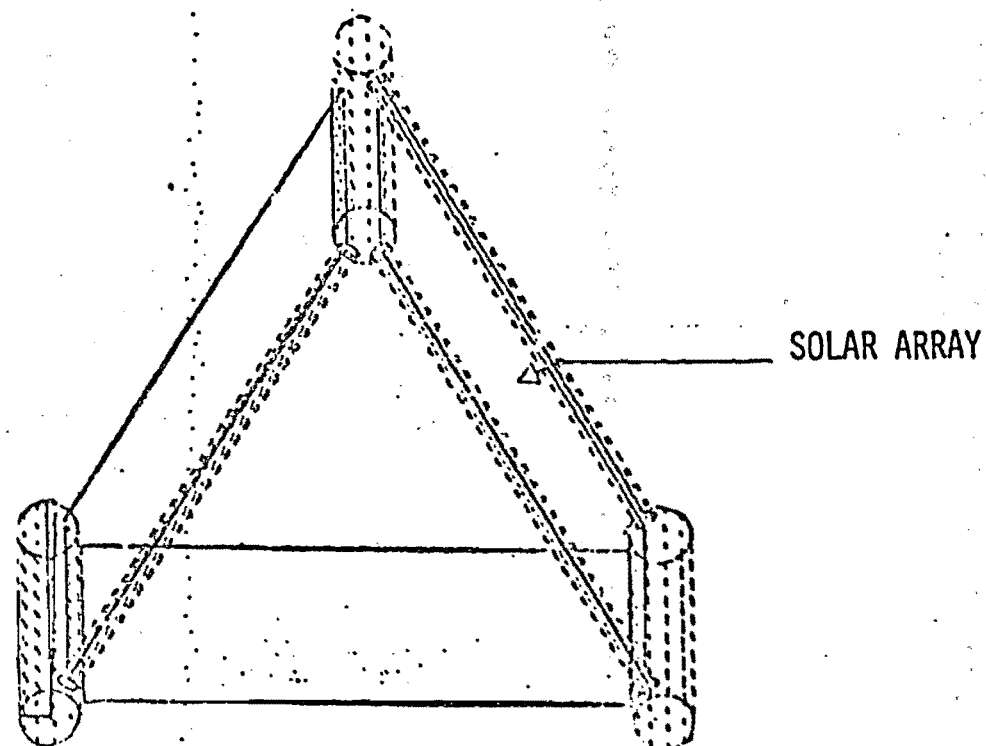


FIGURE 1.1 TRASYS CONFIGURATION

solar arrays and trusswork are represented by planar surfaces. Initial TRASYS analysis resulted in the calculation of form factors between surfaces, taking into account multiple inter-reflections between the surfaces, and between the surfaces and space.

Using these form factors, several cases were run assuming various solar wavelength absorptivities of surface coatings ($\alpha_s = 0.2, 0.3$ and 0.5). These absorptivities are to represent preferred, as well as degraded, coating properties. The infrared emissivity was assumed to remain constant at a value of 0.9 . Solar array absorptivity and emissivity were set at 0.7 and 0.9 , respectively. The result of this analysis was a set of radiation conductors which are utilized in the SINDA thermal network.

An additional output of the TRASYS analysis is the incident and absorbed heat flux on surface nodes. These are computed by inputting orbital altitude, inclination and vehicle orientation with respect to the earth and sun. The heat rates are the sum of albedo, planetary, and direct solar influences during the designated orbit.

Absorbed heat fluxes at a number of points throughout the orbit can be input into the SINDA analysis for a transient analysis or an average absorbed flux can be input for a steady-state analysis. To represent this configuration study, the orbital altitude was taken to be 250 statute miles at an inclination of 28.5° . The vehicle attitude was with the solar array surface oriented towards the sun during the orbit (i.e., solar inertial).

1.2.2 Thermal Conduction Math Model

While the TRASYS math model depicts the effect of the external environment on the surface of the vehicle, the SINDA math model utilizes these influences to predict temperatures at the surfaces and throughout the structure. An example of a

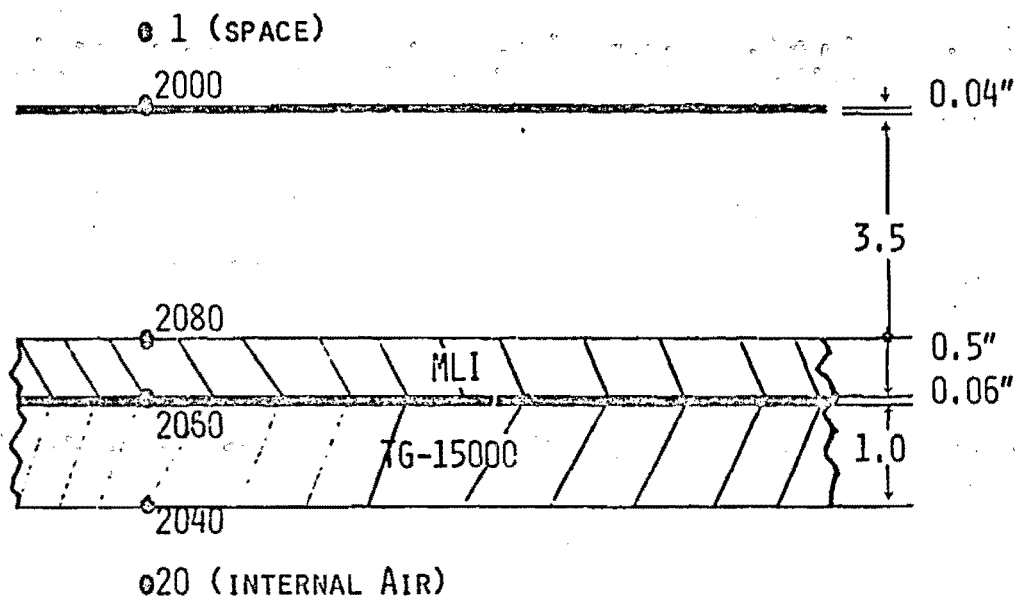
module and tunnel representation and nodalization is given in figure 1.2.

The module structure is assumed to be an aluminum pressure vessel 0.06-in. thick. The walls of the pressure vessel are covered with an internal fibrous batt-type insulation and an external multiple-layer insulation (MLI). The internal insulation assumes TG-15000 type properties, given in reference 1, although that particular material may not be suitable for habitable areas without some form of coating. The nominal thickness of the internal insulation is 1 inch. Multiple layer insulation was chosen for the external surface of the module because of its extremely low conductivity in a low pressure environment. The nominal MLI was comprised of 81 layers of embossed single-aluminized mylar with an uncompressed thickness of approximately 0.5 in. Properties of this insulation are given in reference 2. Standing off from the module pressure vessel wall at approximately 4 inches is an aluminum micro-meteoroid shield of 0.04 inch thickness.

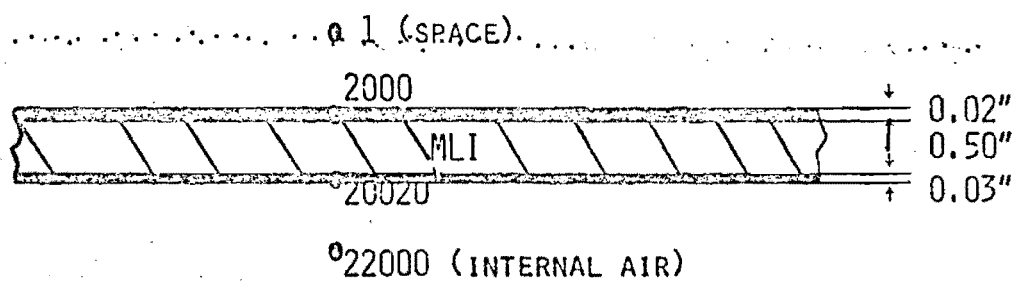
The tunnels are modeled with an inner wall thickness of 0.03 inch and an outer shield thickness of 0.02 inch, both of which are aluminum separated by 0.5 inch of MLI of the type previously mentioned. The internal air convection coefficient for both the tunnels and modules was computed to be approximately 0.15 Btu/hr ft²°F. The module air temperature is held at 70°F, while the tunnel air temperature is allowed to float. This allows a calculation of the minimum required internal heat load to maintain a module at shirt sleeve conditions. The surplus heat load would be rejected through the radiator loop. Tunnel air temperatures are assumed to float to assess the impact of non-continuous environmental control in those volumes.

Properties for the trusses were assumed to be similar to those of aluminum, so are modeled as being of equivalent conductance of a sheet 0.0045 inch thick. This

MATH MODEL NODALIZATION



HABITAT/SERVICE/LAB MODULE WALL
CROSS - SECTION



TUNNEL WALL CROSS-SECTION

FIGURE 1.2 SINDA THERMAL

is definitely an area where greater modeling accuracy is required, but is beyond the scope of the present study. Truss attachments to the modules are adiabatic because of the proposed small area of attachment, so have only a radiative influence upon the modules and tunnels.

The solar cells will be cooled by their backside radiation ability, so the backside emissivity is assumed to be 0.9 with the front side solar absorptivity of 0.7. Thermal conductivity and capacitance is modeled as being an aluminum sheet of 0.1 inch thickness. This is also an area that requires more detailed modeling to accurately depict the array and structure components.

Internal heat load in the modules, generated by electronics, power conditioning equipment, and environmental control hardware will be rejected to space via heat pipe radiators. Single-sided radiators which radiate from only one side rather than two, are capable of rejecting roughly 31 watts/ft² while operating at approximately 60°F with a 13 watt/ft² environmental heat load. This would imply that for a module heat load of approximately 50 kw., as computed in reference 3, a radiative surface of approximately 2800 ft² would be required. To model the affects of this heat load on the configuration, certain truss nodes, shown in figure 1.3, are held at 60°F. The nodes comprise a total of 10,800 ft² of radiator area for the six modules. This area would have the capability of rejecting approximately 180 kw of thermal energy. The purpose of oversizing the required radiator area is to assess what the effects of radiative blockage to space and additional heat load would be on the solar array.

Using the above mentioned mathematical modeling parameters, a steady-state analysis was run to determine long duration temperature levels. Insulation effective-

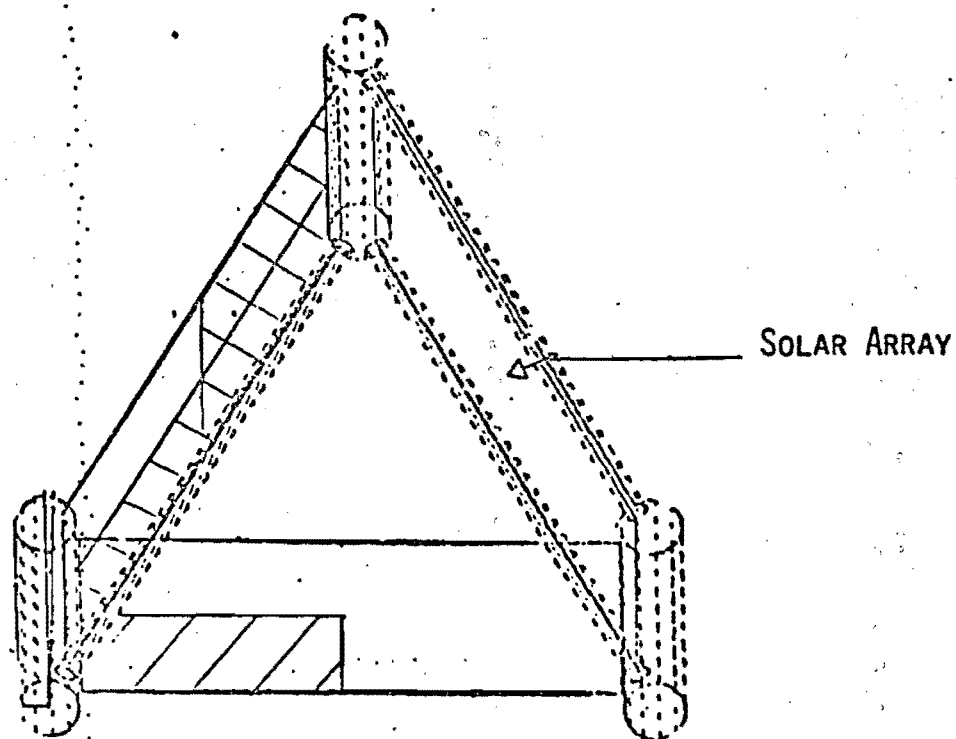


FIGURE 1.3 HEAT PIPE RADIATOR PLACEMENT

ness and coating characteristics were then varied parametrically to ascertain the configuration sensitivity to degraded properties.

1.2.3 Analytical Results

Tables 1.1 through 1.3 reiterate the assumptions made for the baseline triangular configuration. A steady-state thermal analysis, using these parameters with a surface solar absorptivity of 0.2 and an average orbital external heating rate, was carried out to establish a temperature distribution in the structure. Figure 1.4 shows a nodal breakdown of the configuration with surface temperatures indicated in the appropriate areas. As shown in the figure, the largest thermal gradient (of approximately 101°F) appears on a sunlit module micrometeoroid bumper shield. However, the shadowed module surface also experiences a gradient due to the warming effects of the radiators and radiated heat from the solar array on the front of the module versus the large view to space on the backside. Gradients within the truss structure are relatively small (100°), with side to side gradients being somewhat larger (approximately 150°). Tunnel air temperature varies from -9°F on a sunlit side to -38°F on the shadowed side.

The solar array temperature, as with the other temperatures in the steady-state analysis, indicates the orbital average temperature. Silicon solar cells at the indicated temperatures of approximately 100°F (38°C) should operate at an efficiency of roughly 85% of their sunlight conversion efficiency according to figure 1.5 from reference 4. However, due to the orbital variation of impressed heating rates, array temperatures would vary widely. To assess what these variations would be, a transient analysis was carried out. Figure 1.6 illustrates the predicted temperature range of the solar cells. This indicates that peak temperatures would be approximately 150°F. At these high temperatures, conversion efficiency would be reduced by 27%. When compared to a configuration which does not include the heat rejection capabilities of

TABLE 1.1 ANALYTICAL ASSUMPTIONS

STRUCTURE	SURFACE PROPERTIES	EXTERNAL SKIN	INTERNAL SKIN	EXTERNAL INSULATION	INTERNAL INSULATION	CONSTANT TEMP
MODULE	$s = 0.2$ $= 0.9$	0.04 INCH 2219 Al 4 INCHES OFF INTERNAL SKIN	0.05 INCH 2219 Al	MLI - 81 LAYERS EMBOSSED SINGLE- ALUMINIZED MYLAR 0.5 INCH	TG-15000 1 INCH	INTERNAL
TUNNEL	$s = 0.2$ $= 0.9$	0.02 INCH 2219 Al 0.5 INCH OFF INTERNAL SKIN	0.03 INCH 2219 Al	SAME AS ABOVE	NONE	No
TRUSS	$s = 0.2$ $= 0.8$	0.0045 INCH 2219 Al	-	-	-	No
SOLAR ARRAY	$s = 0.7$ $= 0.9$	0.1 INCH 2219 Al	-	-	-	No
RADIATORS	$s = 0.2$ $= 0.9$	0.1 INCH 2219 Al	-	-	-	60°F

TABLE 1.2 MULTIPLE LAYER INSULATION
CONDUCTIVITY

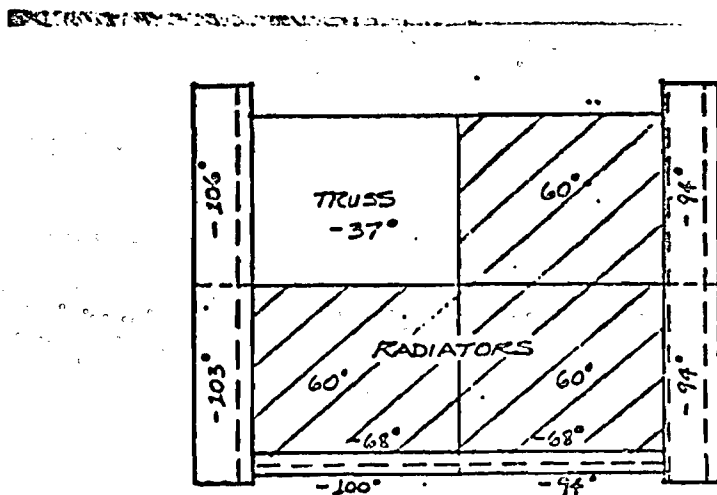
(AT $< 1 \times 10^{-6}$ PSI)

TEMPERATURE °F	BTU/HR FT ² °F
-400	0.000076
- 10	0.000076
35	0.000086
80	0.000105
125	0.000180
170	0.00031
215	0.00076

TABLE 1.3 TG-15000 CONDUCTIVITY

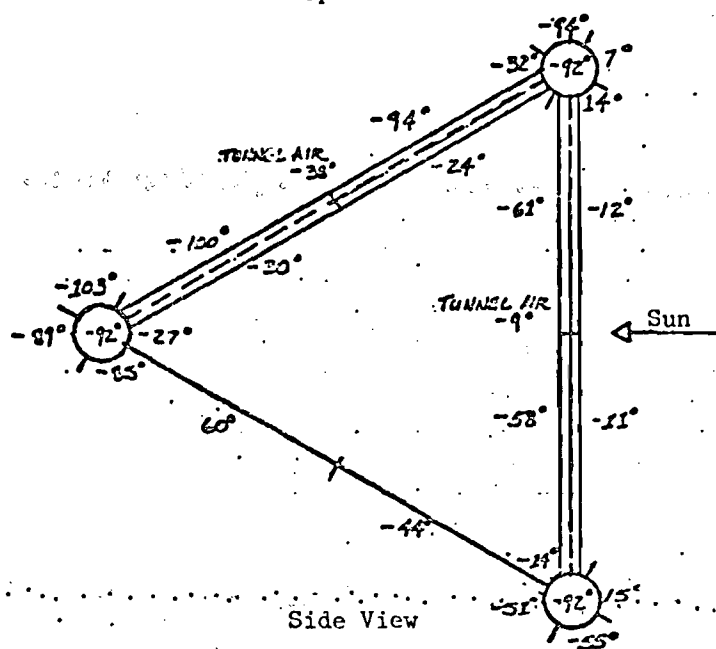
(AT 1 ATMOSPHERE)

TEMPERATURE °F	BTU/HR FT ² °F
-200	0.0093
- 50	0.0146
100	0.0195
250	0.0255
400	0.0320

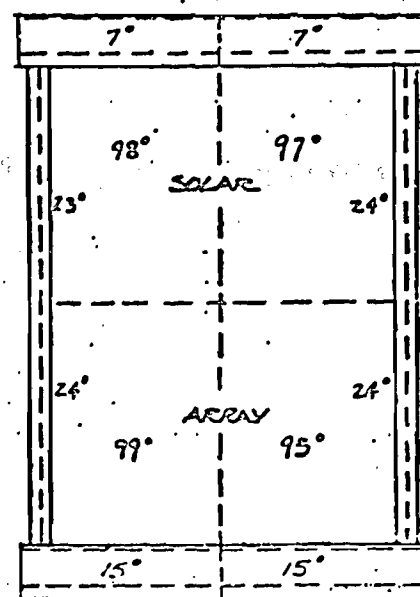


ORIGINAL PAGE IS
OF POOR QUALITY

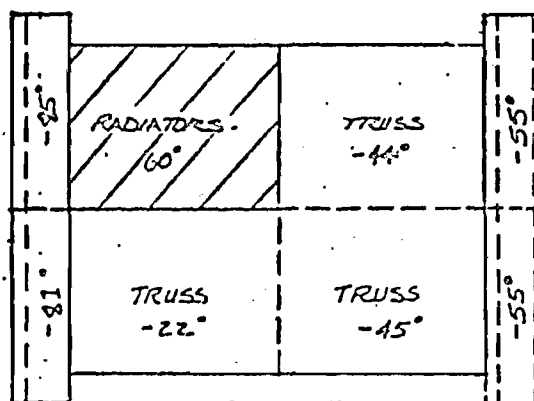
Top View



Side View



Front View



Bottom View

FIGURE 1.4 Surface Temperatures ($^\circ\text{F}$); $\alpha_s = 0.2$

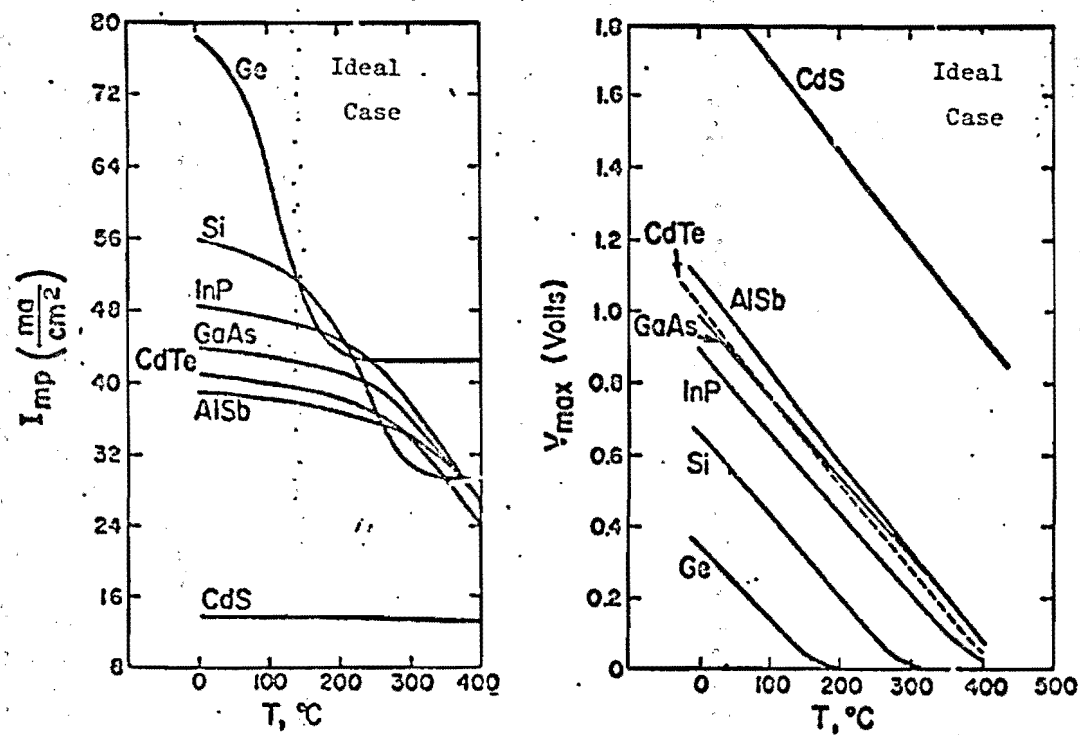


Figure 1.5 Variation of Voltage and Current Outputs from Selected Photovoltaic Materials as a Function of Temperature.

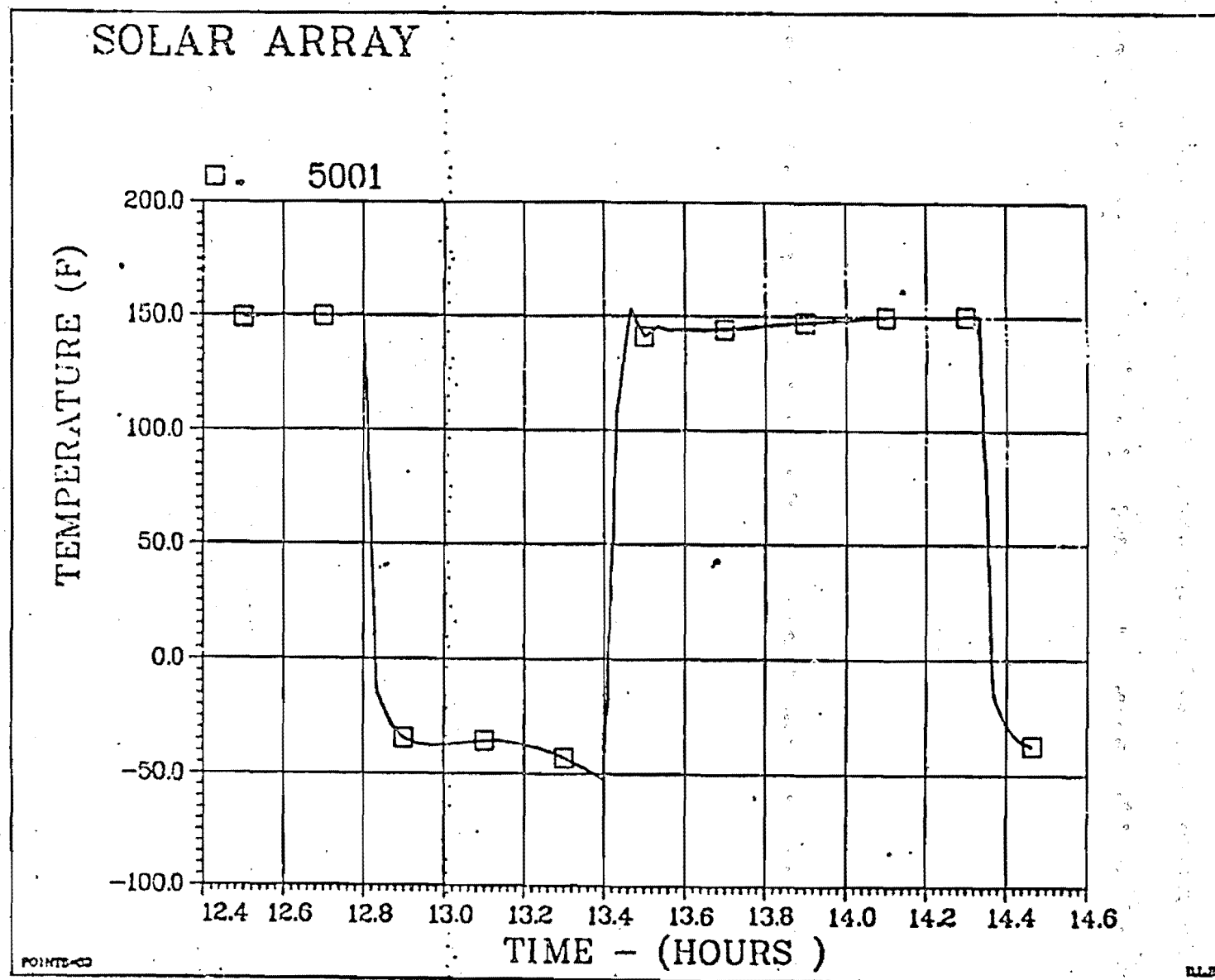


Figure 1.6 Solar Array Surface Temperature

the radiators, the average array temperature and the peak cell temperature is approximately 10°F higher. This would indicate that considerations should be taken to assure placement of radiator surfaces so their heat load and space viewing blockage would not markedly affect the temperature level of the solar arrays.

To assess the configuration sensitivity of coating degradation and insulation effectiveness, a variety of computer analyses were accomplished varying surface absorptivities and insulation conductivities. For each solar absorptivity of 0.2, 0.3, and 0.5, eight cases were set up as follows.

Case 1 - Baseline assumptions as in Tables 1.1 through 1.3

Case 2 - Internal insulation 0.5 inch thick

Case 3 - Internal insulation 0.25 inch thick

Case 4 - Internal insulation 0.05 inch thick

Case 5 - Internal insulation 0.05 inch thick, MLI conductivity increased by a factor of 2

Case 6 - Internal insulation 0.05 inch thick, MLI conductivity increased by a factor of 5

Case 7 - Internal insulation 0.05 inch thick, MLI conductivity increased by a factor of 10

Case 8 - Internal insulation 0.05 inch thick, MLI conductivity increased by a factor of 20

Results that were being compared in this analysis were shadowed module wall temperature, shadowed module heat loss rate, and sunlit module heat loss rate. These comparisons would establish a range of coating and insulation requirements for the habitable modules and assess the effects on the structure as a whole.

Figure 1.7 illustrates the shadowed module wall temperature with the various cases. It is readily apparent that increasing absorptivity would have little effect on this module because of its continued location the shadow of the solar array throughout the orbit. Cases 1 through 4 demonstrate the relatively minor role that internal insulation plays in maintaining internal wall temperatures, with a reduction in thickness of 1 inch to 0.05 inch increasing the temperature by only 1°F, out of a total internal to external temperature drop of approximately 175°F. The heat loss rate from the shadowed module, as shown in figure 1.8, confirms the relative ineffectiveness of internal insulation as the reduction in thickness by a factor of 20 increases the heat loss rate by only 1%.

Decreasing the effectiveness of external insulation, however, has a significant effect on the module wall temperature and rate of heat loss. If the dewpoint temperature were to be held in the range of 50°F, the MLI would have to be at least as effective as in Case 8, preferably with lower conductivity, as in Case 6, which is only 5 times the assumed baseline value. This would maintain the module wall well above the dewpoint temperature, preventing formation of condensation. The trade that would be involved with the more effective insulation would be the increased internal heat load that would need to be rejected by active systems, i.e., the radiators. The load which would be rejected by the active thermal control system would be the sum of the internal heat loads minus the heat which is being lost through the module walls.

Figure 1.9 depicts the heat loss from a sunlit module. It can be seen that the absorptivity characteristics markedly affect the heat loss rates. However, the difference between the rates would be less than the margin for uncertainty that would be designed into a thermal control system capable of rejecting approximately 20 times that amount of internal heat load. Therefore, the well-insulated modules would appear to be relatively insensitive to the properties of the thermal coatings. The active

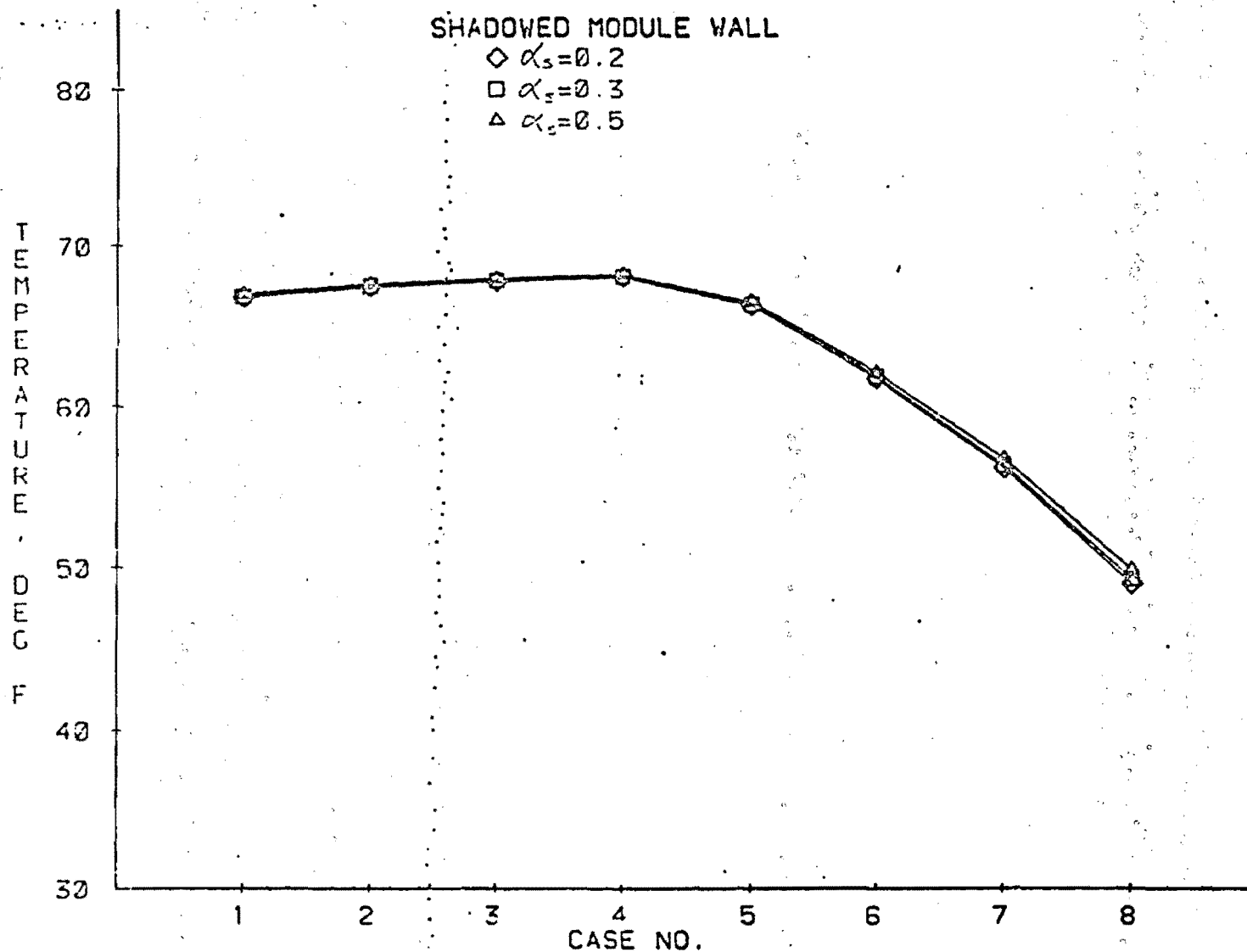


FIGURE 1.7 Shadowed Module Wall Temperature With Varying Surface Absorptivity And Decreasing Insulation Effectiveness.

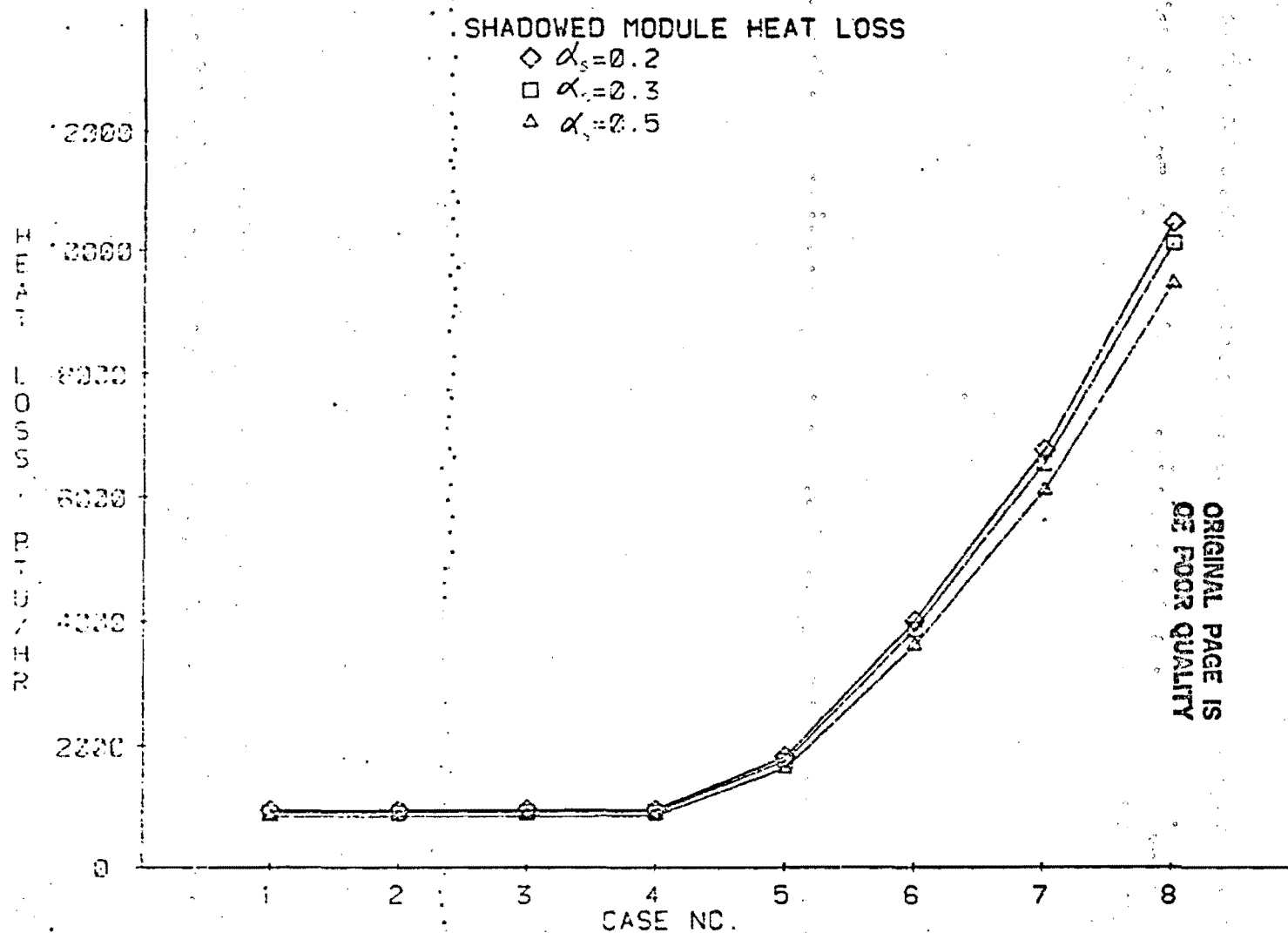


Figure 1.8 Shadowed Module Heat Loss Rate With Varying Surface Absorptivity And Decreasing Insulation Effectiveness

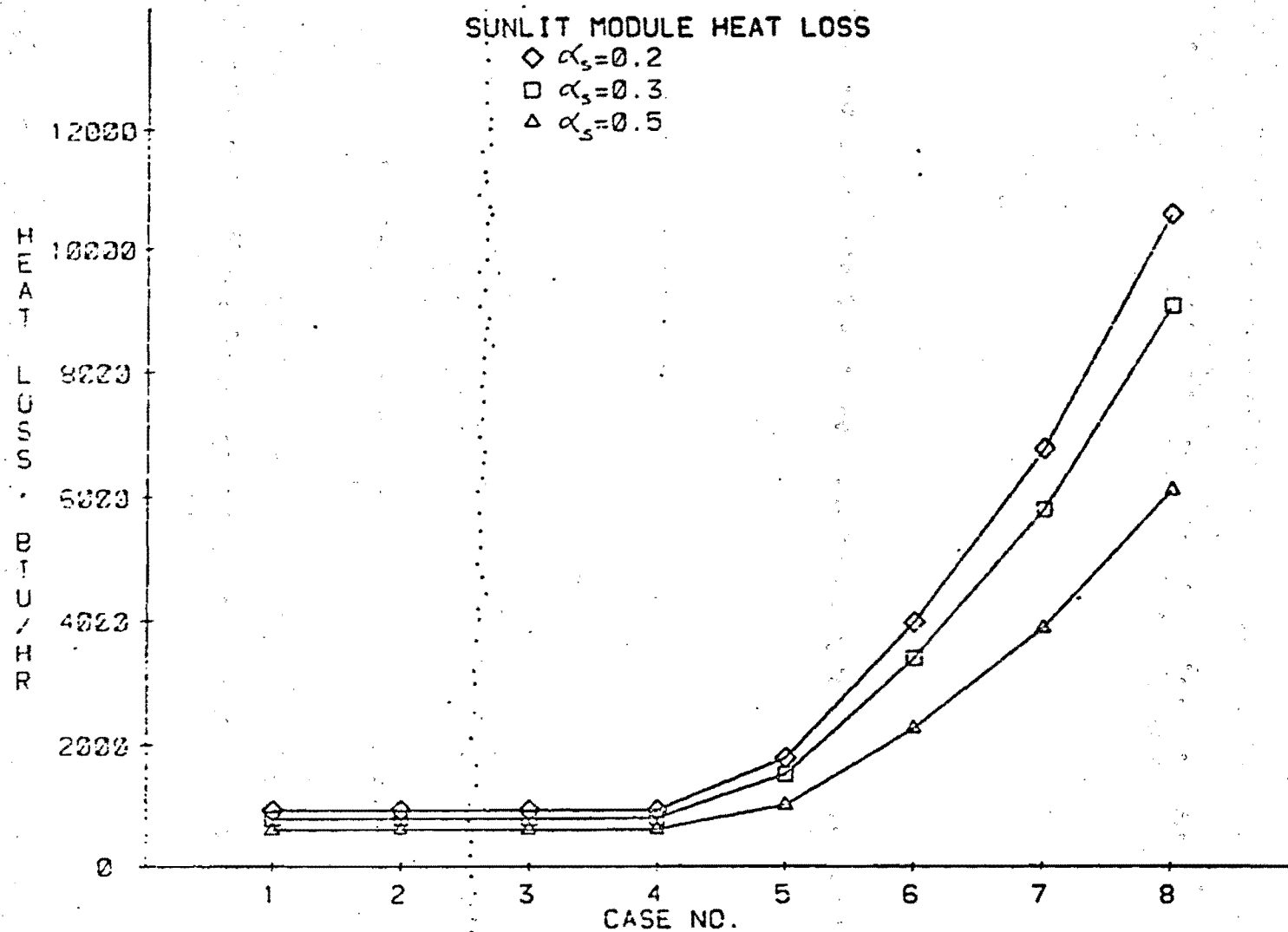


Figure 1.9 Sunlit Module Heat Loss Rate With Varying Surface Absorptivity And Decreasing Insulation Effectiveness

thermal control system would subsequently be sized to reject virtually all of the predicted internally generated heat load.

Temperatures shown in figure 1.10 reflect the effect of the higher absorptivity of 0.5 on the surfaces of the configuration, holding other material properties as baseline. Thermal gradients are more pronounced, with a temperature difference on one sunlit module being 160°F. Gradients within the truss structure are less than with the 0.2 absorptivity due to generally warmer surface temperatures radiating to the structure. Tunnel air is also warmer, though still far below a minimum dewpoint temperature, with the shadowed tunnel being -11°F and a sunlit tunnel being 35°F. The tunnel air temperatures are not significantly affected (by less than 5°F) by variations in insulation performance due to the proportional increase in heat lost and heat gained by the volume. This might imply tailoring of the surface coatings and insulation placement to enhance heat retention in the tunnels.

1.2.4 Conclusions

Results of the thermal analysis on the triangular configuration have demonstrated a number of points.

- 1) There is an inherent insensitivity of the habitation modules to thermal coatings when high performance external insulation is used.
- 2) Internal insulation is of relatively little thermal control value.
- 3) External MLI should have a conduction effectivity of approximately 0.00053 BTU/hr ft²F (effective emissivity of 0.01) as determined by the analysis.
- 4) Tunnels will probably require customized thermal treatment for passive internal temperature maintenance.
- 5) Radiator placement is important to ease affects on solar arrays.

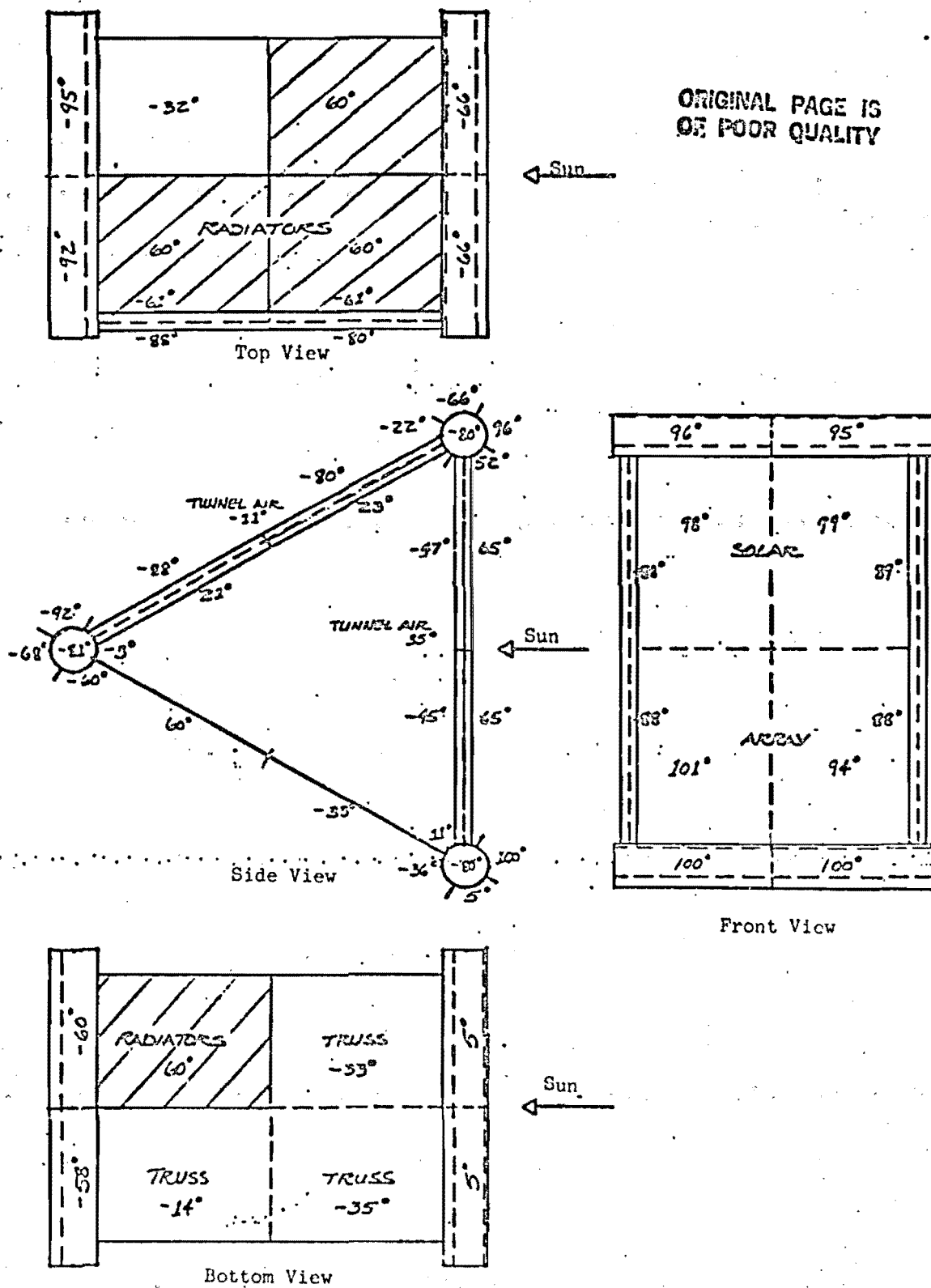


Figure 1.10 Surface Temperatures ($^{\circ}\text{F}$); $\alpha_s = 0.5$

- 6) Structural thermal gradients are relatively insignificant.
- 7) Appropriate insulation sizing and coating selection alone will not significantly reduce active thermal control requirements.

These results would indicate that exotic module surface coatings which exhibit low absorptivities and high emissivities for long durations would not be a fundamental requirement of the proposed configuration. This would possibly enable more durable types of coatings to be utilized at a lower initial build-up and replacement cost. There would, however, be some requirement for thermally selective coatings for the tunnels to increase their heat absorption capabilities and decrease heat rejection. When done together with proper insulation design, the problem should not be difficult. This is an area that will require more analysis.

Because of the demonstrated ineffectiveness of an internal insulation, there is no thermal justification for its use. However, it may be desirable to utilize a thin layer of insulation material for sound dampening or condensation absorption.

The approximate conductivity of the external multiple layer insulation is required to be as given in Table 1.4. The number of layers that would be used to attain this type of performance and the material of which the insulation is comprised will be the subject of a future study.

Due to the complex profile of solar cells and solar array matrices, thorough thermal analysis was not attempted. However, temperatures that were extracted from the analysis were judged to be a close approximation of actual performance levels. Greater modeling detail of this area is required in future iterations. Preliminary results indicate that radiator placement could influence sunlight conversion

Table 1.4

Recommended MLI

Conductivity Effectiveness

Temperature °F	Btu/Hr Ft ² °F K
-400	0.00038
- 10	0.00038
35	0.00043
80	0.00053
125	0.00090
170	0.00155
215	0.00380

efficiency because the blockage of the array backside radiation to space, raising cell temperatures. No significant problems are anticipated at this level of analysis, but further evaluation is necessary. Included in this evaluation should be the assessment of the thermal impact that would occur with the subsequent addition of subsystem hardware to the truss structure, creating greater blockage of the view to space.

Greater modeling detail is also required of the truss structure to more effectively evaluate thermal gradients that may occur through the truss matrix. Initial results using equivalent flat plate assumptions indicate that thermal gradients are not large enough to create significant stress problems. Thermal cycling that would occur behind the solar array during the orbit could possibly be a concern.

Active thermal control systems will be sized to handle virtually all of the module internal heat loads if more effective means, other than insulation sizing and coating selection, are not employed to passively reject thermal energy. More sophisticated methods of heat rejection, as analytically demonstrated in references 5 and 6, can be accomplished utilizing semi-passive thermal energy transport techniques. This would include the use of heat pipes mounted to the pressure vessel wall to distribute the internal heat load to the structure, maintaining required wall temperatures with low insulation levels. Another possibility would be the incorporation of thermally activated louvers into the micrometeoroid shield to open the pressure vessel surface to space viewing, increasing the heat rejection capability. Such enhancements of the structural thermal energy management scheme would reduce the size of the required active thermal control system, increasing overall efficiency. Therefore, it is recommended that future iterations include a preliminary analysis of such capabilities.

1.3 Radiator Concepts

Preferable radiator placement in the triangular configuration would be on the trusswork which is not supporting solar cells. This arrangement was chosen instead of an integral radiator/micrometeoroid shield because of increased radiator efficiency in the shadowed area and comparatively easy replaceability when degradation warrants. Assuming the orientation of the configuration is with the long side of the solar array roughly north and south, the upper truss area would have less incident flux because of the orbit inclination. Therefore, placement of radiators on this surface would be more favorable.

At the recommendation of NASA JSC Crew Systems Division representatives, heat pipes were chosen as the baseline radiator element because of the technology advancements in the field which have enhanced their performance and dependability. It is also thought that long term performance would be better than conventional fluid loop radiators because of the segmentation that is inherent in the design. Should a segment of a heat pipe array become damaged or degraded, total heat rejection performance will be affected by only a small percentage. Fluid loop radiators would, however, lose a large percentage of their heat rejection capability when damaged because of the larger radiator area serviced by a single fluid loop. Design heat rejection capabilities of heat pipes are also significantly higher (by approximately 50%) than conventional radiators, so smaller surface areas would be required to reject a specified load.

1.4 Possible Design Refinements

1.4.1 Structurally Enclosed Modules

A variation of the baseline triangular configuration arose during the

analysis. The proposed variation is to move the habitation modules internal to the truss structure. Some benefits of this configuration change would be the following

- 1) A more thermally benign environment for the modules.
- 2) Placement of the micrometeoroid shield on external surface of truss structure to enhance bumper shielding distance.
- 3) Easily replaceable optical surfaces for module temperature adjustment.

To assess this possible design delta for another iteration on the space station configuration, changes were made to the baseline thermal math models. These changes entailed placing the modules and tunnels internal to the planar surfaces which model the trusswork. Figure 1.11 illustrates the configuration change. As shown, the radiators are placed at the apices of the triangle to serve the double function of micrometeoroid shielding and heat rejection. These surfaces replace the stand-off bumper shields modeled in the previously described baseline configuration. This is not a proposed iteration, but merely an analytical tool to assess the thermal impact of such a design change.

1.4.2 Thermal Comparison with Baseline

Using the same assumptions of material properties and locations as the baseline configuration, except for the relocation of the micrometeoroid shield and trusswork, TRASYS and SINDA analyses were accomplished. The results of these analyses are shown in the temperature distribution in figure 1.12. As shown, module surface temperatures are less severe except on the ends, where the benefits of the radiator shielding are not present. Tunnel air temperature also does not benefit from the enclosure because of the large view of space by the tunnel surface out of the ends of the structure.

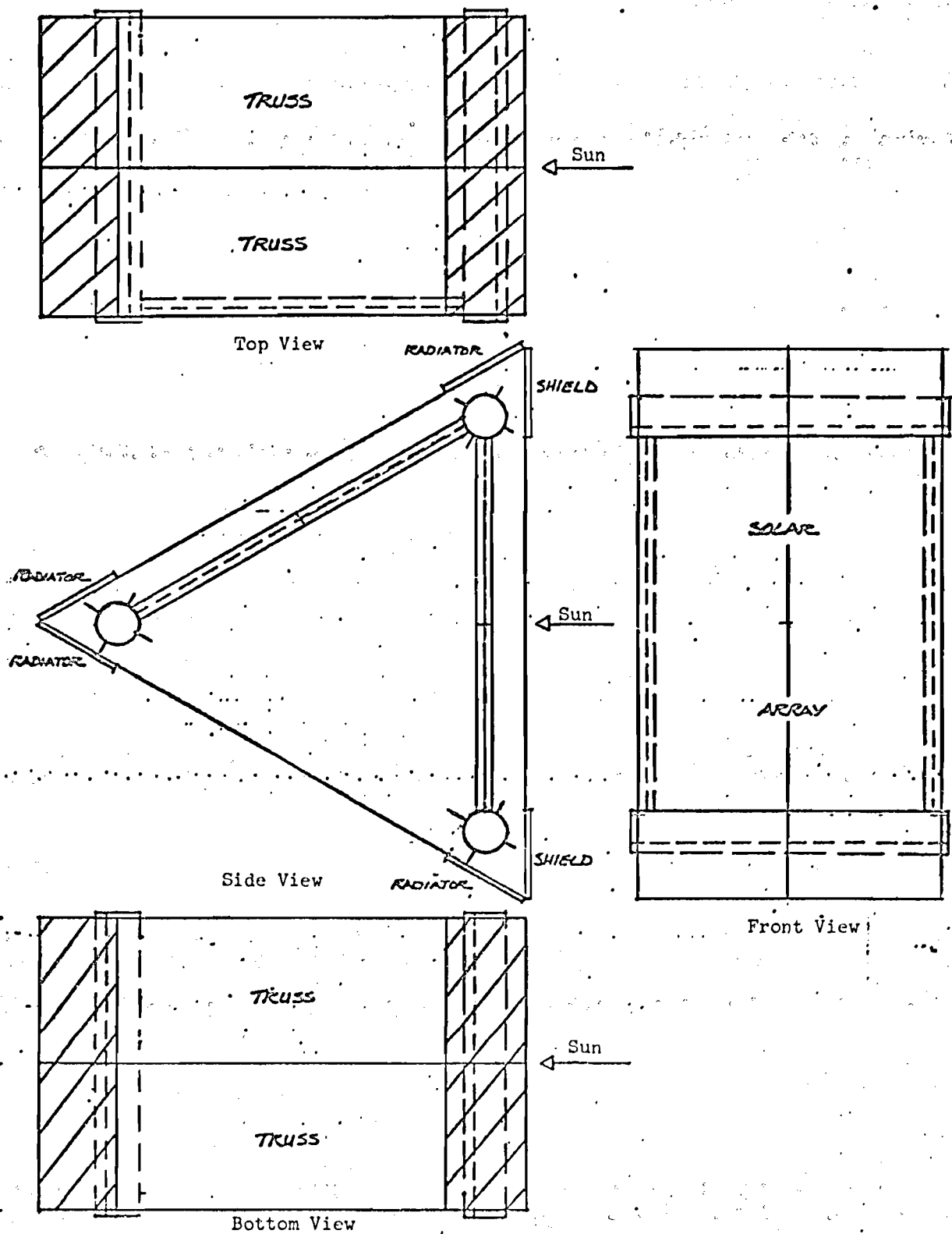


Figure 1.11 Structurally Enclosed Configuration

ORIGINAL PAGE IS
OF POOR QUALITY

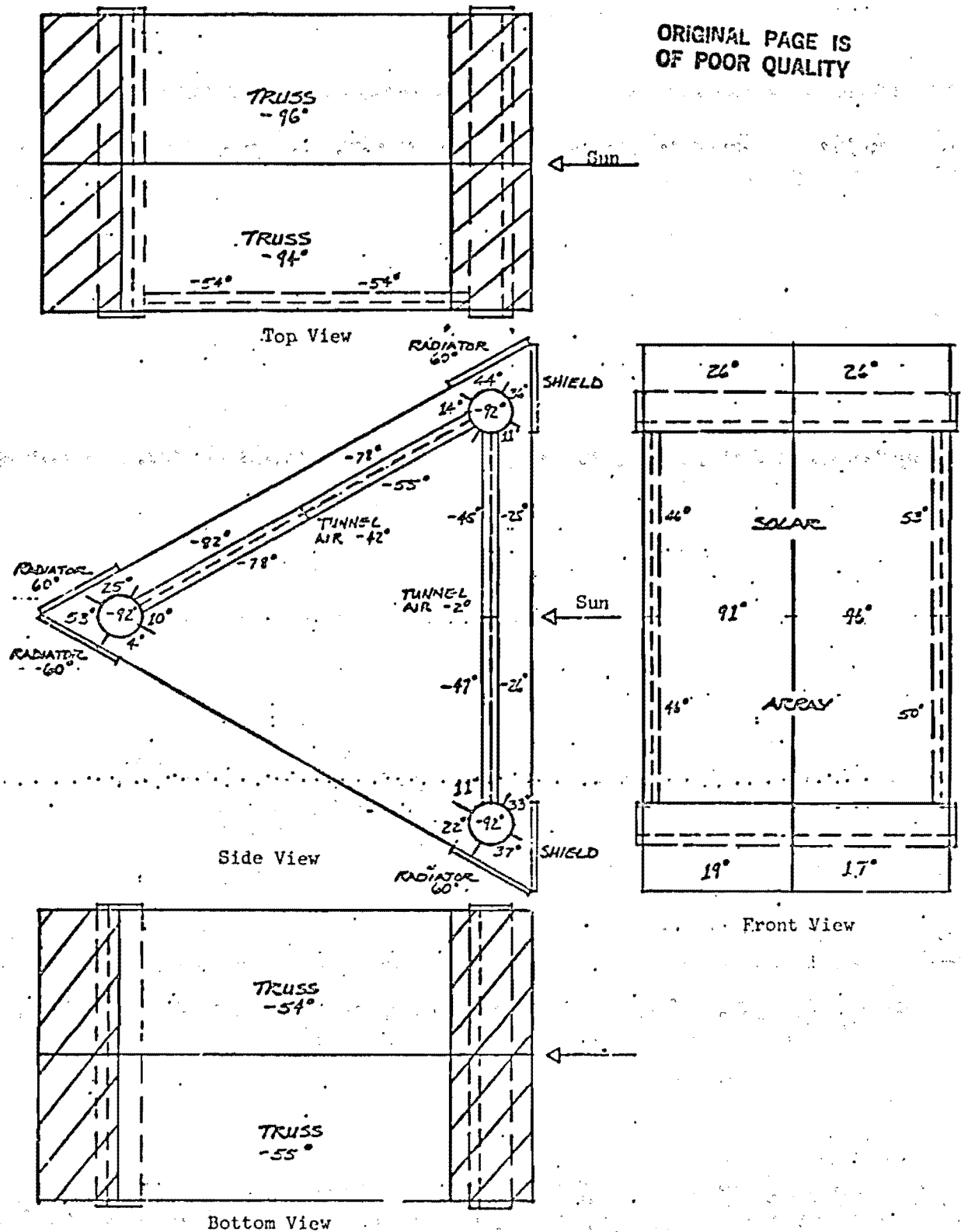


Figure 1.12 Surface Temperatures ($^{\circ}\text{F}$) of Enclosed Configuration;
 $\alpha_s = 0.2$

Figures 1.13 and 1.14 compare the shadowed module wall temperature and heat loss, respectively, between the baseline and enclosed systems as internal and external insulations are degraded. It is evident that circumferential wall temperatures remain warmer when enclosed by the radiator shielding and are less sensitive to a decrease in insulation effectiveness. It is assumed, although not analytically substantiated, that the modules would also be less sensitive to thermal coating degradation.

Heat loss rates are significantly decreased, which implies a greater heat rejection load for the radiators. However, the lower outgoing flux level would provide a margin for maintaining shirt sleeve temperatures internally should equipment, which generates a large portion of the heat load, be powered down.

The thermal benefits of the structurally enclosed triangular system are present, although they are not profound. Enclosure of the modules and tunnels, as currently configured, would not be driven primarily by thermal concerns. It should be noted that larger temperature and heat loss deltas, between enclosed and open systems, would occur if the modules were somewhat clustered.

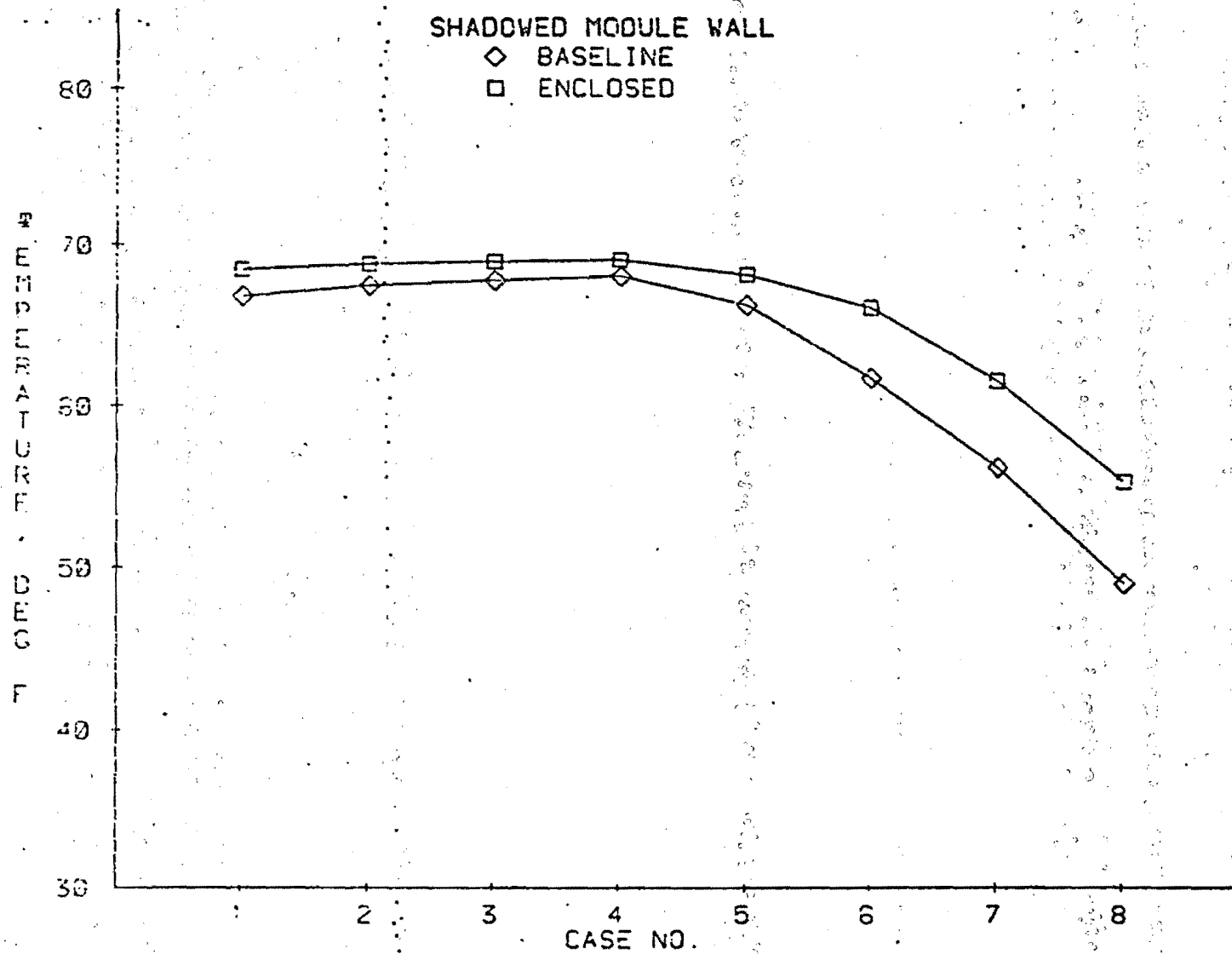


Figure 1.13 Shadowed Module Wall Temperature Baseline Vs. Enclosed Configuration With Decreasing Insulation Effectiveness

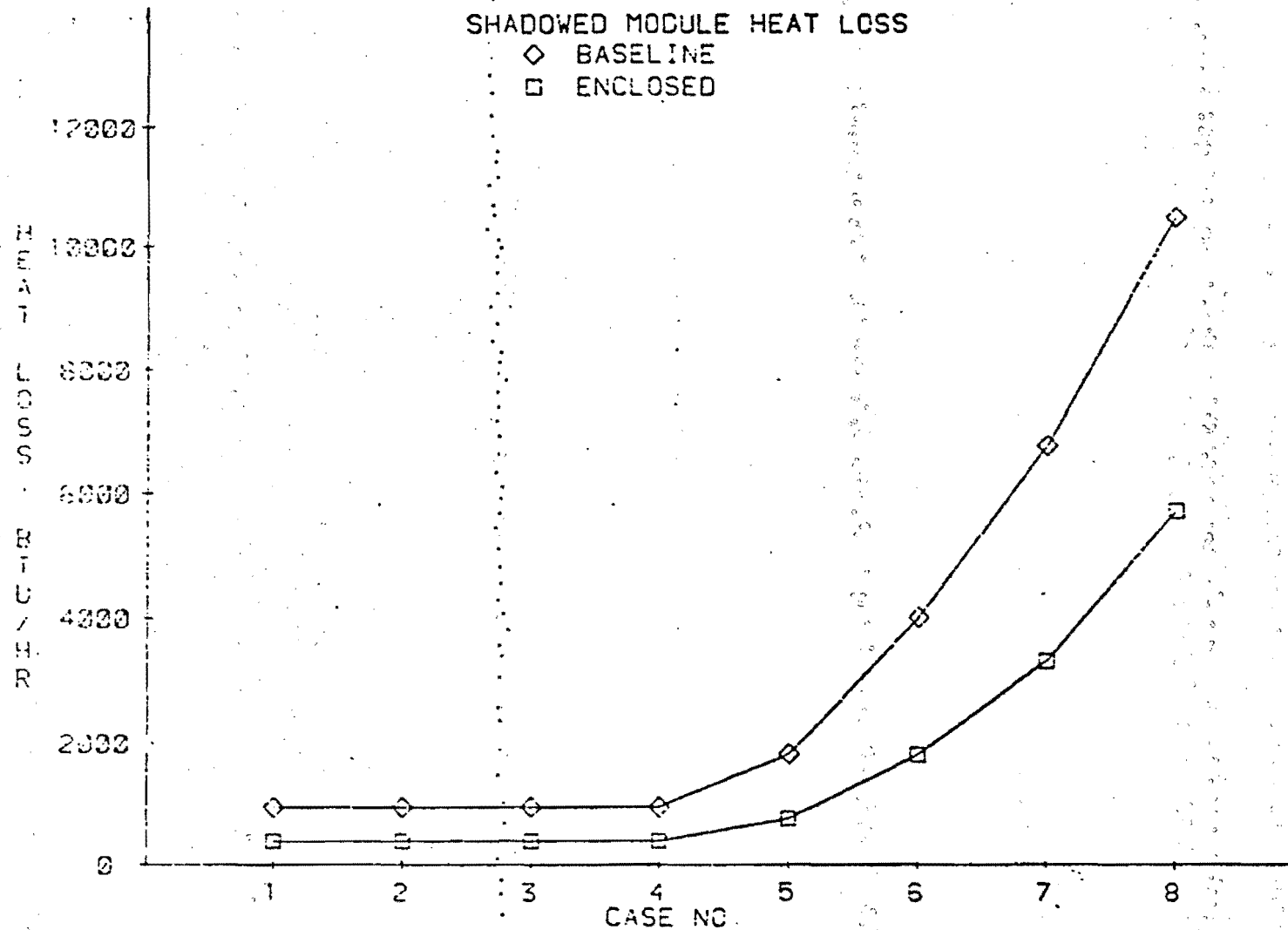


Figure 1.14 Shadowed Module Heat Loss Rate Baseline Vs. Enclosed Configuration With Decreasing Insulation Effectiveness.

References

1. Space Shuttle Program Thermodynamic Design Data Book, Thermal Control System, Book I, Rockwell International, SD73-SH-0226, February 1981.
2. Spacecraft Thermal Control Design Data, Volume 2, Polytechnic University of Madrid, ESA (TST-02), October 1979.
3. Space Operation Center System Analysis, Final Report, Boeing Aerospace Company, D180-26495-3, July 1981.
4. Sunlight to Electricity, Joseph A. Merrigan, MIT Press, 1975.
5. Space Station Thermal Control Systems Study Final Report Vols. 1 and 2, Grumman Aerospace Corporation, NASA Contract NAS9-10436, March 1971.
6. Long Life, High Reliability Thermal Control Systems Study Final Report, General Electric, NASA-CR-123956, August 1972.

2.0 Space Station On-Orbit Dynamic Analysis

2.1 Objective

The objective for this section is to determine the control requirements for Space Station operations including attitude control and orbit maintenance as a function of the natural on-orbit dynamic environment. The dynamic environments simulated included gravity gradient torques, aerodynamic drag, and aerodynamic torques. System requirements for the baseline configuration were determined for parametric variations of altitude and mass properties.

2.2 Introduction

The Space Station will require two forms of control power to maintain an indefinite orbit lifetime. Control methods are required to (1) offset the altitude losses because of atmospheric drag and, (2) efficiently maintain the desired Space Station solar inertial attitude. The Space Station by nature of current Shuttle delivery capability will be restricted to low earth orbit altitudes <230 nmi (see figure 2.1). At these low altitudes, aerodynamic drag is an important factor in orbit maintenance and attitude control. It is highly desirable to restrict the lowest operational orbital altitude to one in which at least 90 days of free altitude decay remain before a catastrophic reentry occurs. This period would allow for several STS revisit opportunities and subsequent orbit safeing maneuvers, or repair to orbit maintenance equipment.

ORIGINAL PAGE IS
OF POOR QUALITY

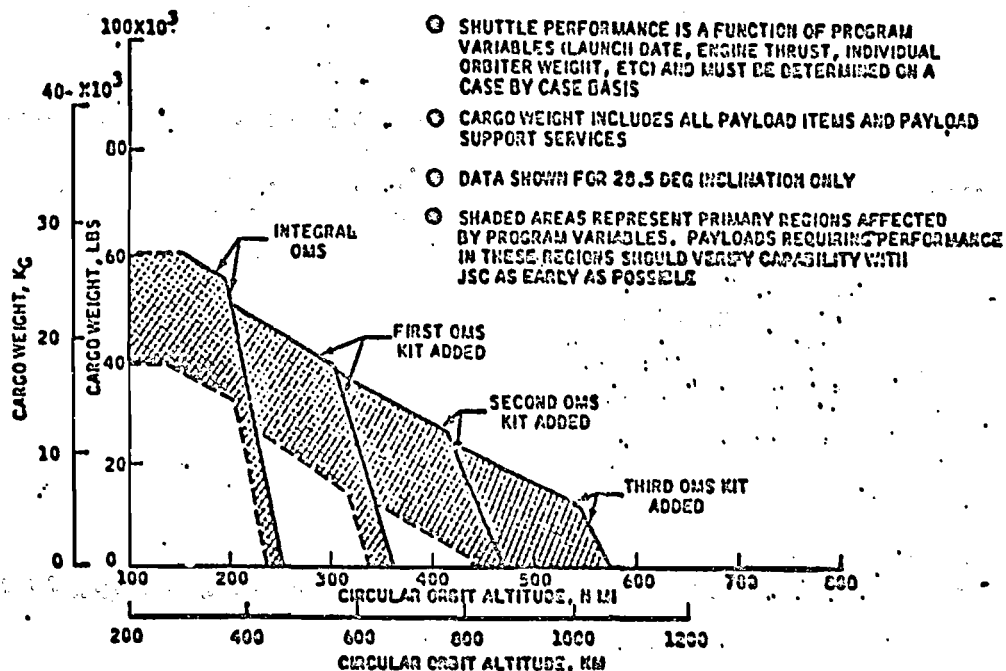


Figure 2-1 Near Term Cargo Weight vs Circular Orbital Altitude

For the case of advanced spacecraft such as the proposed Space Station, attitude control has typically been a major problem. The source of previous control difficulty has been centered on the requirement to control a highly flexible vehicle. Designs that exhibit cantilevered solar panels cause particular problems because of the low frequencies of the flex modes. If a classical control strategy is used, the flex modes are filtered out of the sensed vehicle response. This technique, unfortunately, has an adverse effect on the attitude control performance of the vehicle. In addition, the closed loop stability of the flex modes is not

guaranteed for highly flexible appendages. For highly flexible structures the control system must not only account for attitude control, but also must exhibit vibration control features.

The baseline configuration for this study minimizes the attitude control problem which is inherent in many proposed Space Station configurations. The flex modes of this configuration are relatively high (analysis indicates >5.4 Hz) and therefore can be filtered out of the sensed vehicle response. This allows rigid body control below the flex frequency bandwidth with acceptable vehicle rate and attitude performance. Furthermore, the behavior of the vehicle can be accurately predicted due to the simplicity of the structural configuration leading to a minimization of control model errors. The control system also benefits from the baseline concept since most activity is centralized at the system center of mass. Here, changes in the interior configuration will minimize the impact on rotational inertias.

2.3 Orbital Altitudes Analysis

A general purpose computer program was written to investigate the parameters affecting orbital altitude. This program addresses the contribution of five major natural phenomenon which disturb the upper atmosphere causing density fluctuations in the 100-300 nmi. Energy equations are used to predict orbit altitude.

2.3.1 Atmosphere Model

The five atmospheric variations most relevant in the dynamics modeling of the upper atmosphere are listed in order of importance as follows (1) variations with the 11-year solar cycle, (2) variations with short term solar flux and sunspot activity, (3) the diurnal variation, (4) variation with geomagnetic activity, and (5) the semi-annual variation. Solar flux related variations may produce a 10-fold density fluctuation. This surpasses a nominal density model by a factor of 3.

The current model accounts for the 11-year solar sun-cycle, day/night cycles and the disturbing effects of geomagnetic storms. Predictions of solar activity are projected into the year 1993. The next occurrence of a solar maximum occurs in 1990. The solar model is based on best fit statistical data.

2.3.2 STS Payload Performance

.....The Space Station operational altitudes are limited by the orbiter cargo delivery capability. Higher Space Station operational altitudes require less orbit maintenance energy and reduce the concern about reentry. Figure 2-1 gives the cargo weight (payload items plus payload support services) as a function of circular orbit altitude for delivery flights from Kennedy Space Center (KSC). This figure was obtained from JSC 07700 Vol. XIV Revision G. Only near term capability is presented, since long term capability is not defined sufficiently to provide adequate data for generalized performance plots. Cargo weight capability drops off

sharply at the 200 nmi altitude without the addition of OMS kits. OMS kits have not been funded for the orbiter. At the present orbiter delivery altitudes, aerodynamic drag becomes the prime design driver for operations and orbit maintenance equipment.

2.3.3 Orbit Decay Time

In preliminary studies, a nominal density profile was used (data obtained from "U.S. Standard Atmosphere 1962") to determine aerodrag at the respective altitude. Energy which is dissipated because of the frictional aerodrag loss is integrated each orbit and subtracted from the total energy, yielding an altitude history, thus, predicting free decay time. Current work indicates that a nominal density profile is not sufficiently accurate in the prediction of a long term altitude history, since the solar flux related variations produce large density fluctuations.

The free orbit decay time histories for the lightest and heaviest Space Station design configurations (designated #1 and #6 respectively) were determined for an initial insertion altitude of 230 nmi. Design configurations 2 through 5 fall within the band established for configurations 1 and 6. The summary results of this investigation are shown in figure 2-2. The results also reflect both nominal and worst case solar sun-cycle atmospheric densities.

ORIGINAL PAGE IS
OF POOR QUALITY

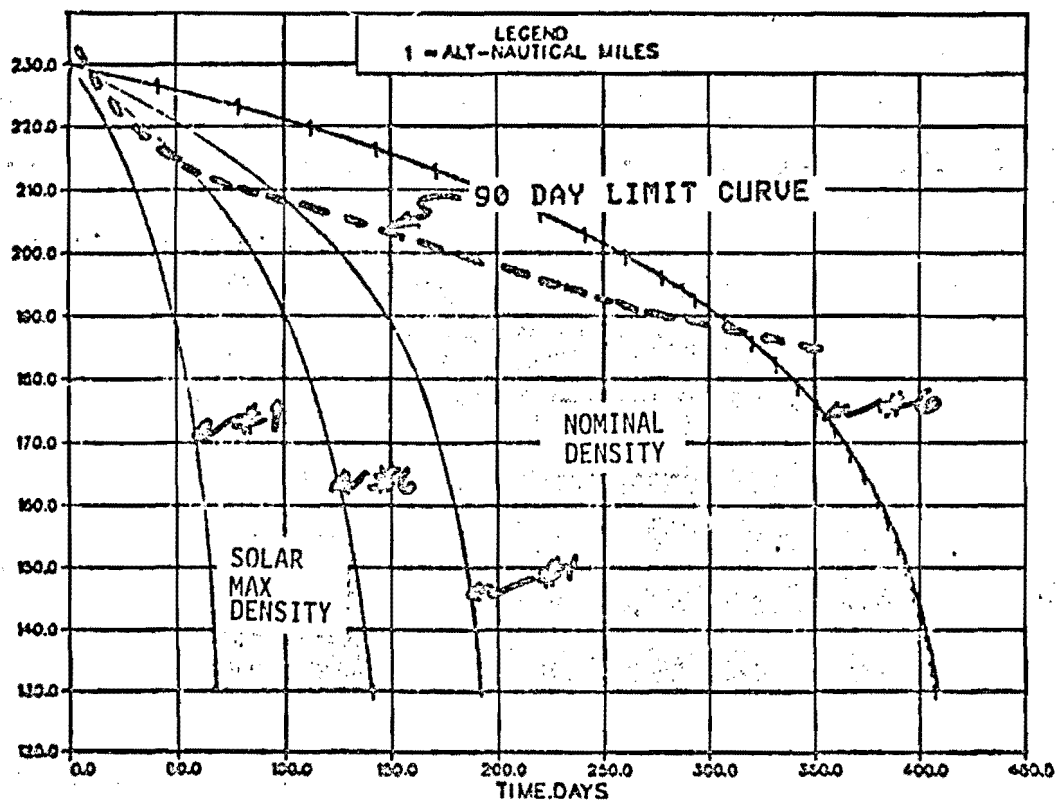


Figure 2-2 Space Station Altitude Decay Time Histories

The results shown in figure 2-2 reveal that for an orbit insertion of 220 nmi and for a nominal atmospheric density, Space Station configuration 1 will reenter in approximately 140 days, whereas, configuration 6 which is much heavier will reenter in 300 days. Backing up 90 days from the reentry time, to allow time for contingency rescue operations, configuration 1 must not fly below 208 nmi and configuration 6 must not fly below 187 nmi, for nominal atmospheric density. For a worst case atmospheric density, configuration 1 must not fly below approximately 240 nmi and configuration 6 must not fly below 215 nmi. These altitudes limit STS cargo capability for supply to the Space Station as seen in

Figure 2-1. Thus, to guarantee a free decay time of 90 days for a revisit and orbit safeing maneuvers, an orbit maintenance methodology must be incorporated into the design of the Space Station. Emergency decay time can be increased by feathering the Space Station to a minimum drag attitude at the sacrifice of power generation. The solar power generation would be reduced by 50%, whereas the average drag force would be reduced by 66.6%.

2.3.4 Orbit Maintenance Methodology

Normal altitude can be maintained by several methods including (1) drag offset thrusting, (2) periodic reboosting utilizing the Hohmann minimum energy orbit transfer method, and (3) constant thrust to spiral out and free decay to STS revisit altitude. Each of the last two methods are designed to extend the coast period to agree with STS visit frequency.

Drag offset thrusting can be accomplished with conventional chemical engines or with electric propulsion engines such as Ion engines. The Ion engines use approximately 1/10 the fuel weight of chemical engines, but require a large amount of electrical energy, approximately 14 kw per .1 lbs. thrust. The offset thrust engines must be located on booms cantilevered from the Space Station, and rotated at orbit rate such that the engines fire tangential to the orbit. The required thrust level is very small, approximately 0.1 lbs., thus simplifying the design of the support booms.

The amount of fuel per year required to maintain the Space Station at altitude using a chemical engine with ISP of 400 seconds is shown in figure 2-3. To maintain an altitude of 200 nmi, would require approximately 12,480 lbs. per year. The Ion engines would require only 1248 lbs. per year.

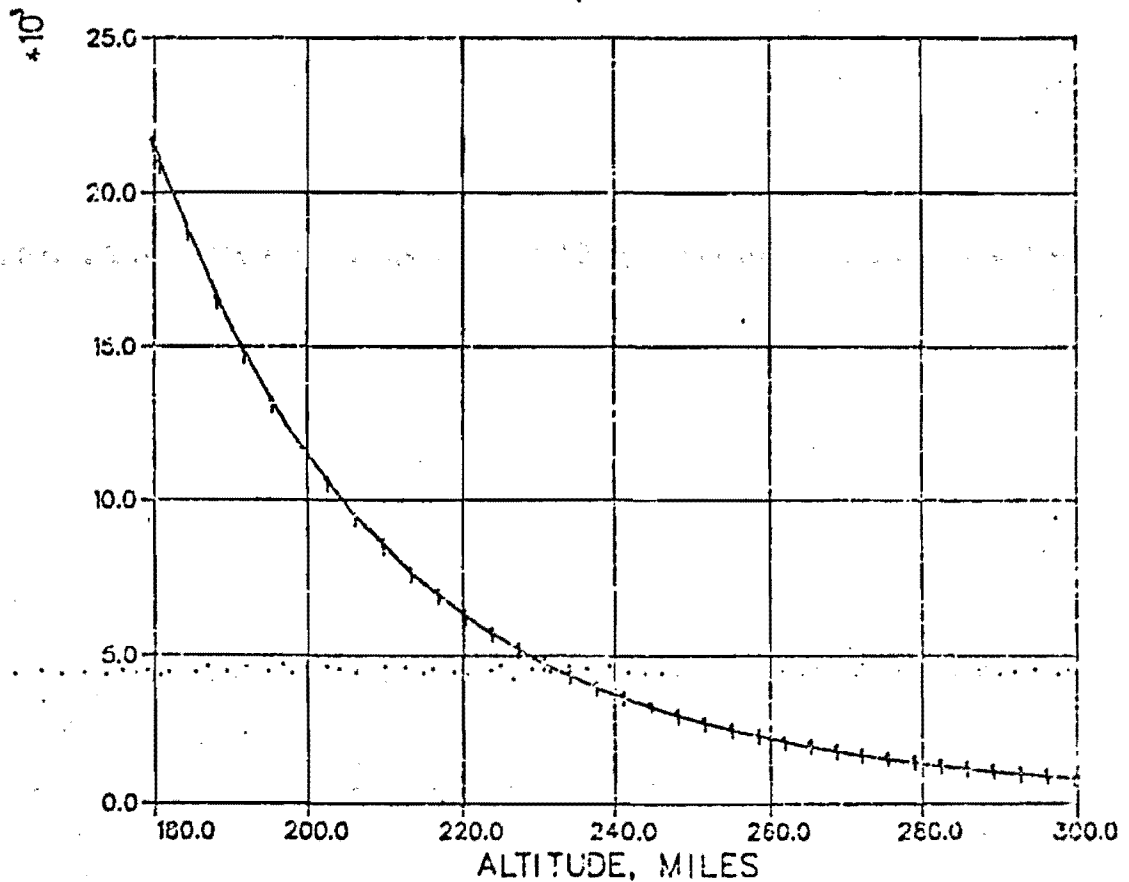


Figure 2-3 Fuel Weight Per Week to Maintain Space Station at Altitude with an ISP of 400 Sec and Nominal Aero

Another method of orbit maintenance makes use of periodic reboost utilizing the Hohmann minimum energy transfer method. This method would involve choosing an altitude range based on the expected

Orbiter revisit frequency. Suppose for configuration 6 that a minimum altitude of 200 nmi is desired and that the Orbiter can revisit in 90 days. The required upper altitude for nominal aerodynamic density from figure 2-2 is approximately 213 nmi. The amount of chemical engine fuel required for this transfer is 2482 lbs. If this orbit revisit frequency is maintained throughout the year, then 10,065 lbs. of fuel would be expended per year. This method is slightly more efficient than the constant thrust method because the Space Station is flying at a higher average altitude with less drag force. However, Hohmann reorbit burns cause load transients for the Space Station that do not occur for the constant drag alleviation burn. Also, it would not be practical to use the fuel efficient ion engines for the Hohmann transfer method because of their low thrust level.

Constant thrusting ion engines could be used to spiral the Space Station to a higher orbit where they would be then turned off and the Space Station allowed to decay down to the STS revisit altitude. This method would be the most efficient for fuel weight, but would require large amounts of electric power. A trade study is necessary to see the overall program impact of this approach.

2.4 Attitude Control Analysis

A general purpose computer simulation (SS Dynamics) was developed to predict the on-orbit dynamics of the Space Station. The program initializes with the Space Station on-orbit and calculates the time histories of altitude and attitude as a function of the dynamic

environments encountered. The simulation computes altitude losses and the control torque time histories necessary to maintain the Space Station in a solar inertial attitude. Mass and aerodynamic properties for the Space Station are computed within the initialization phase of the program as a function of the Space Station's individual components.

Rigid body equations of motion were formulated for the Space Station using Newton's second law of motion and Euler's moment equations. The equations of motion are solved using a variable step Runge-Kutta integration routine. The analysis coordinate systems and Space Station solar inertial attitude are shown in figure 2-4. Coordinates subscripted with "I" indicate inertially fixed coordinates; coordinates subscripted with "SP" indicate Space Station principle body fixed coordinates; and coordinates subscripted with "O" indicate orbit rate rotating coordinates.

2.4.1 Disturbance Torques

The Space Station will be subjected to environmental forces and torques including aerodynamic drag and torques, gravitational forces and torques, solar radiation torques, and earth magnetic torques. The latter two environments were not included in the analysis since they were several orders of magnitudes smaller than the aerodynamic and gravitational torques.

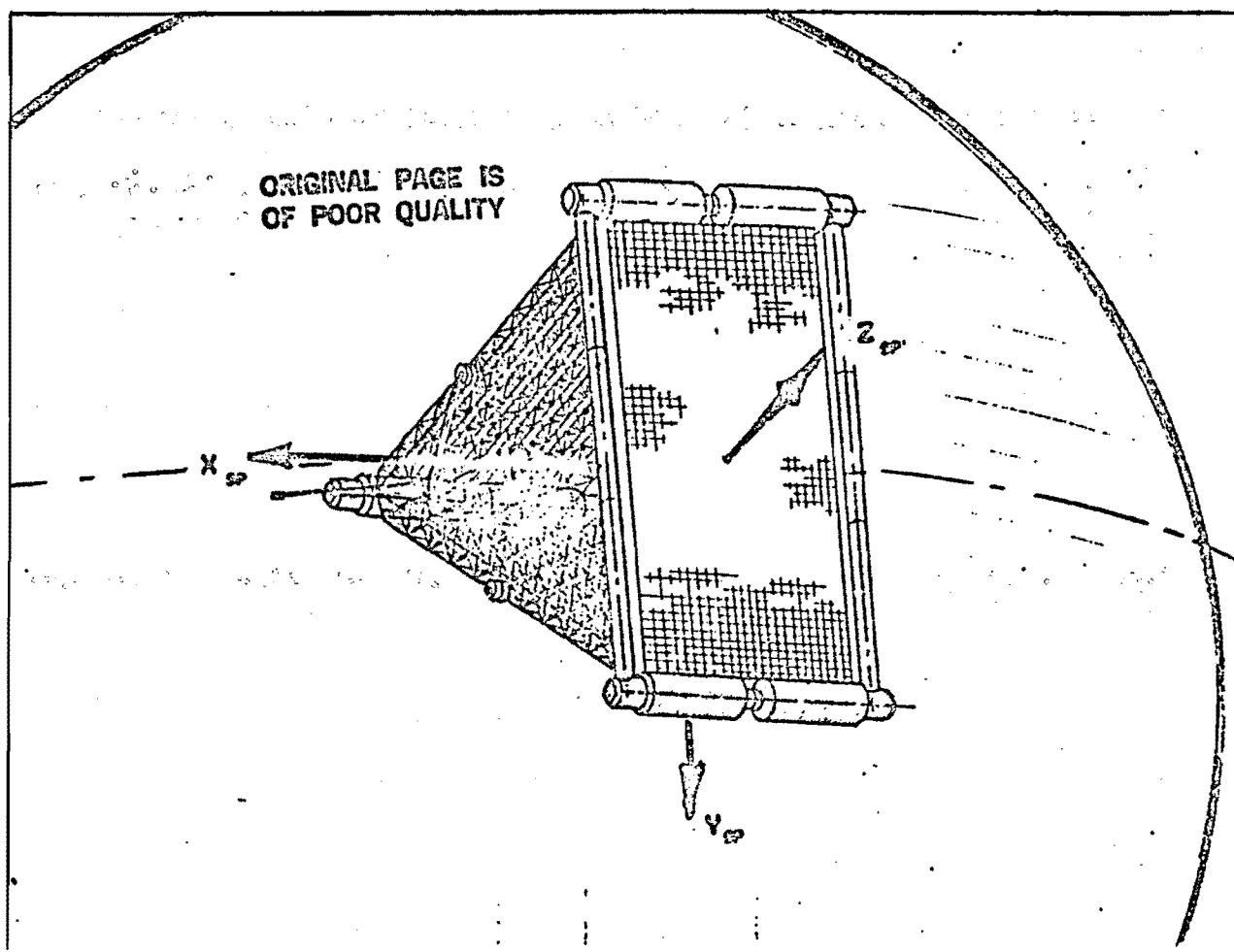


Figure 2-4 Space Station Coordinate Systems and Space Station Solar Inertial Attitude Configuration

2.4.1.1 Aerodynamic Torque

At altitudes in the range of 100-300 nmi or more the atmospheric density depends not only on altitude but also on the degree of solar activity. At this altitude range the Space Station is said to be in the "free molecular flow" regime. Molecular particles that impact the Space Station will either adhere, thereby imparting all its relative momentum, or may be reemitted after impact.

In this study, only the projection of the area normal to the orbital velocity, vector was considered. The aerodynamic drag force is defined as:

$$\overline{FAERO} = Q * S * CD * V / |V|$$

where S = Projected Area

CD = Coefficient of Drag

Q = Dynamic Pressure

V = Space Station CM Velocity

* = Multiplication

A Station which is geometrically symmetric about its center of mass will not experience any aerodynamic torque. To minimize the drag, the Space Station is flown with its X-axes in the orbit plane (see figure 2-4). In addition, the aerodynamic torques about the Space Station Y and Z axes will be cyclic in nature, since the Space Station flies a solar inertial altitude. The aerodynamic torque is defined as:

$$\overline{TAERO} = \overline{R} \times \overline{FAERO}$$

where R = Position Vector from CG of Space Station to the Center of Pressure.

The aerodynamic torque on the Space Station is not very large at altitudes of 200 nmi or greater. The aerodynamic torque for configuration 1 at 200 nmi is shown in figure 2-5. The peak torques in the body coordinate system are less than 2.0 ft-lbs. There is a small component of X-torque due to CM offset.

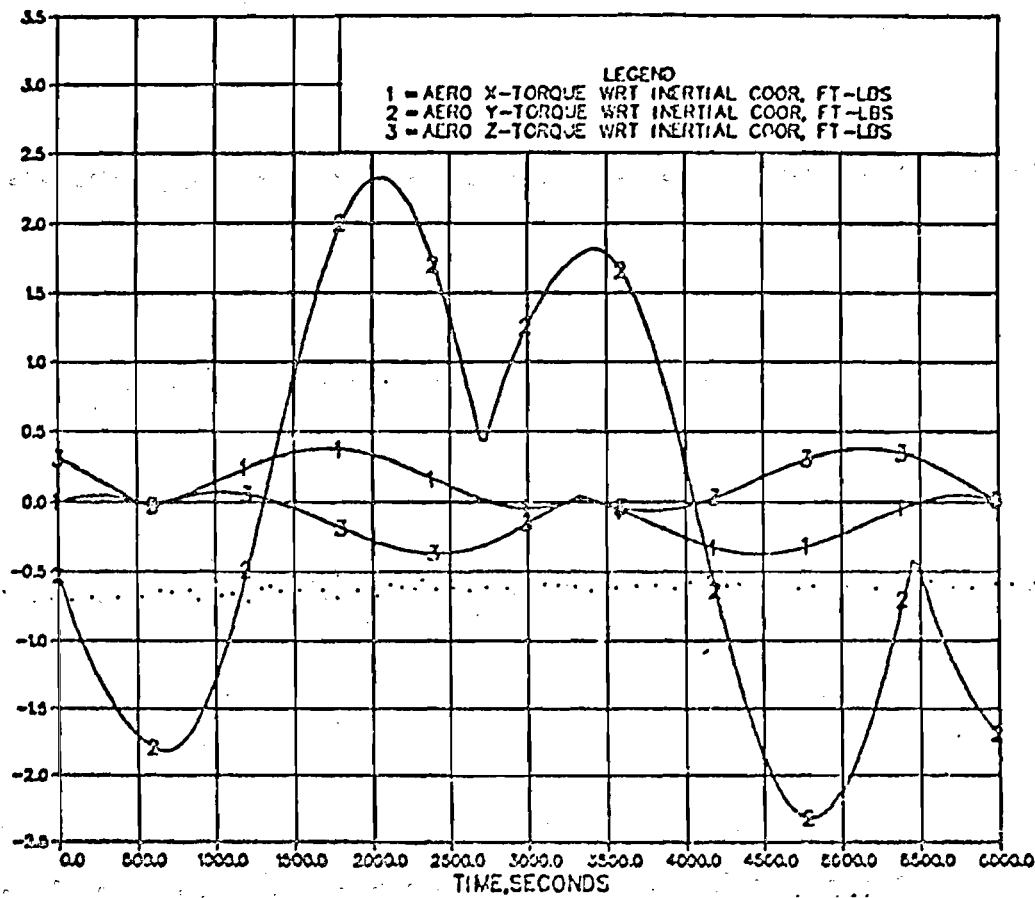


Figure 2-5 Aerodynamic Torque for Configuration 1 at 200 NM Altitude

2.4.1.2 Gravity Gradient Torque

Gravity Gradient torques may act on any vehicle whose inertias about its principle axes differ from each other. The general form of gravity vector gradient torque equation used in this analysis is

$$\overline{TGRAV} = 3*OMEG**2*\overline{UR} \times \underline{\underline{I}} \cdot \overline{UR}$$

where OMEG = Orbital Rate of Space Station

$\underline{\underline{I}}$ = Inertial Dyadic of Space Station

\overline{UR} = Normalized Space Station Position Vector

The Space Station will orbit with its principle Y-axes perpendicular to the orbit plane. This will result in a zero torque about the Space Station X and Z principle axes and a cyclic torque about the Y axes. To maintain the principle Y-axes perpendicular to the orbit plane and the solar array perpendicular to the sun, a mass properties management system will have been enforced to account for the sun Beta angular misalignments. The gravity gradient torque equations expressed with respect to the SP coordinate system (figure 2-4) reduce to the following when the equations of motion are referred to the principle axes

$$TGRAV (1) = 0$$

$$TGRAV (2) = -3/2*OMEG**2*(I3-I1)*SIN(2*TH)$$

$$TGRAV (3) = 0$$

where TH = Angle between Space Station Z axes and Local Vertical

I1 = Principle Inertia About X axes

I3 = Principle Inertia About Z axes

With the proper management of the mass properties, the quantity (I3-I1) can be minimized, thus relieving the peak torque requirements of a control moment gyro (CMG) system.

The peak torque and momentum storage requirement caused by the gravity gradient environment on the studied Space Station design configurations are 40.5 ft-lbs. and 39,500 ft-lbs-sec., respectively. Mass property management has not been performed for these configurations to reduce the disturbance torques.

2.4.2 Attitude Control Assessment

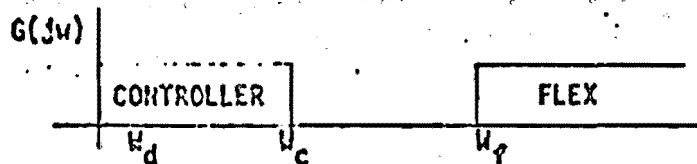
The highly flexible structure that typified previous Space Station proposals presented severe problems to flight control system designers. Space Station configurations that have large extended solar arrays present a twofold challenge to the control system. First, the arrays, when deployed in this fashion, have low frequency cantilevered beam modes (not to mention flexibility in the solar cell membranes themselves). Second, the extended arrays increase the system rotational inertia on which any control authority must act. The first problem, flexibility, is a structural stability issue. The control system must be designed such that structure modal resonance is avoided. This can be done at a very large cost to overall system performance (i.e., simple maneuvers may take days to accomplish), and/or the cost of a distributed control system. The second problem, inertia, further defeats performance by reducing the system angular acceleration achievable through the applied control torque.

The above problems result directly from the solar arrays.

Another aspect of the control problem deals with Space Station geometry and mass property changes during nominal operation modes. The control system must adapt to these discrete changes to ensure maneuver performance. Again, previous Space Stations have exhibited operational modes that produce major changes in overall system configuration. These changes result in significant mass and geometry changes as seen by the controller.

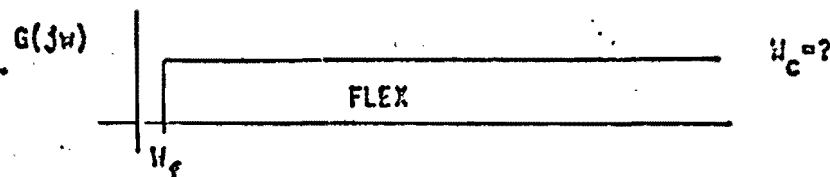
The problems of control for the Space Station have expensive solutions in cost and performance. As a preliminary guideline for the development of the Space Station proposed herein, the minimization of these control problems was a goal of high priority. To accomplish this objective, the flex frequency spectrum must be raised significantly to achieve desired separation between the flex and controller passband. Further, a configuration was sought that was relatively insensitive to operational activities. The configuration that resulted from these (and other) design guidelines is the triangular design embodied in this report. For the proposed Station the flex spectrum begins at approximately 5.4 Hz. The controller passband can now be placed below this frequency and still provide impressive maneuvering performance (see figure 2.4.2-1). Also, the enclosed configuration focuses all operational activity in the central area which is always near the center of mass of the system. Large masses (i.e., an Orbiter) can be placed here with minimal impact on system rotational inertias. Clearly, this configuration achieves the goal of minimizing the control problems of

FUNDAMENTAL PROBLEM:



CONTROL DESIGNERS DESIRE $w_c < w_f$

PREVIOUS SPACE STATIONS HAVE BEEN CHARACTERIZED BY:



FLEX INSTABILITY CAN RESULT FROM $w_f < w_c$

(SITUATION GENERALLY CAUSED BY FLEXIBLE SOLAR ARRAYS)

w_c = MAX CONTROL FREQ.

w_f = MIN FLEX FREQ.

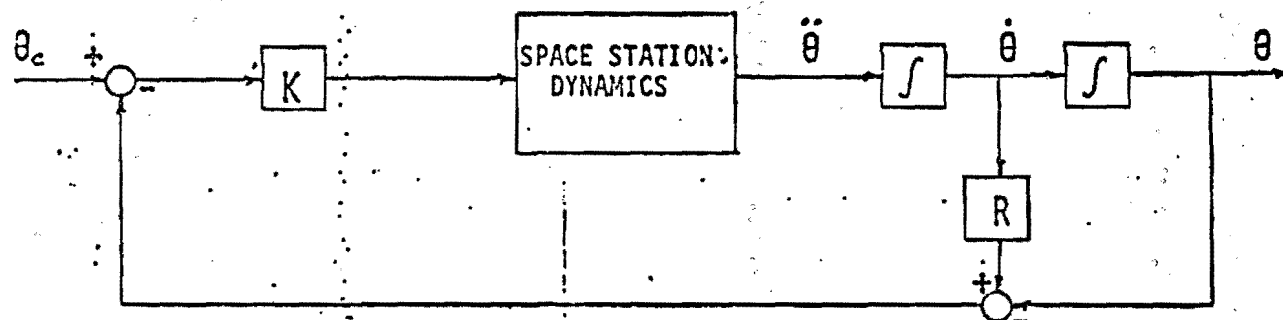
w_d = DISTURBANCE FREQ.

FIGURE 2.4.2-1, CONTROLLER BANDWIDTH BELOW STRUCTURAL FLEX SPECTRUM

the Space Station. Most important, these advantages have also produced many operational benefits so the solution to the control problem has not been achieved at the sacrifice of the primary mission objective, space operations.

Two classical methods are used to design control systems; each with their respective emphasis. The time domain, state-space methods used in optimal (or modern) control theory emphasizes the performance of the vehicle. The frequency domain analysis is used when stability issues are a concern of high priority. For the operational Space Station, performance requirements are low compared to other space vehicles while system stability is an important control objective. Hence, the frequency domain design and analysis techniques were used. The control system design is applied to maneuver about one principle axis to characterize performance parameters. The flowchart of the rate and position feedback system is included for review (see figure 2.4.2-2). Classical techniques were used to size system loop gains and control the overall maneuvering characteristics. A 45° attitude change maneuver was selected for response analysis.

A model of the vehicle disturbance environment was determined to quantify the cyclic and secular (non-cyclic) torques. Also, for the proposed Station, solar inertial pointing is a necessary maneuvering requirement (approximately $0.06^\circ/\text{sec}$). After examining the character of the environment, the control system effector selection was made. Because of the predominant cyclic



FREQUENCY DOMAIN DESIGN USING POSITION AND RATE FEEDBACK

FIGURE 2.4.2-2, CONTROL SYSTEM BLOCK DIAGRAM USING RATE AND POSITION FEEDBACK

nature of the disturbance torques a momentum management scheme was devised using CMG's (control moment gyro's) and RCS (reaction control system). The CMG's are ideal for the cyclic torque management, but the noncyclic disturbances will accumulate momentum in the CMG's until the storage limit (saturation) is achieved. To desaturate the CMG's a cancelling momentum vector must be applied by the RCS system. The described system, is the means by which the vehicle holds a solar inertial attitude. The CMG's will require in excess of 40,000 ft-lb-sec while the peak torque requirements (as discussed later) should be in the 1000 ft-lb class. A vendor search was conducted to verify the feasibility of these CMG requirements and a candidate cluster of CMG's was located. The reader may note that the Skylab CMG's were capable of 160 ft-lb of peak torque with 2300 ft-lb-sec of momentum storage.

To study the maneuvering capabilities of the Station, a commanded 45° angular displacement was imposed. To accomplish this maneuver, RCS firings were examined as a candidate effector system. This technique produced adequate performance, but the step impulse of the RCS jet firings causes higher frequency excitation (see figure 2.4.2-3). As we have seen on the Orbiter, RCS firings during operational periods can result in resonance in the flex spectrum. In other words, the forcing function has a higher frequency content as well as timed low frequency pulses based on the phase plane switching lines (rate limits and attitude deadbands). A maneuvering scenario that utilized only CMG's circumvented the excitation problems of the

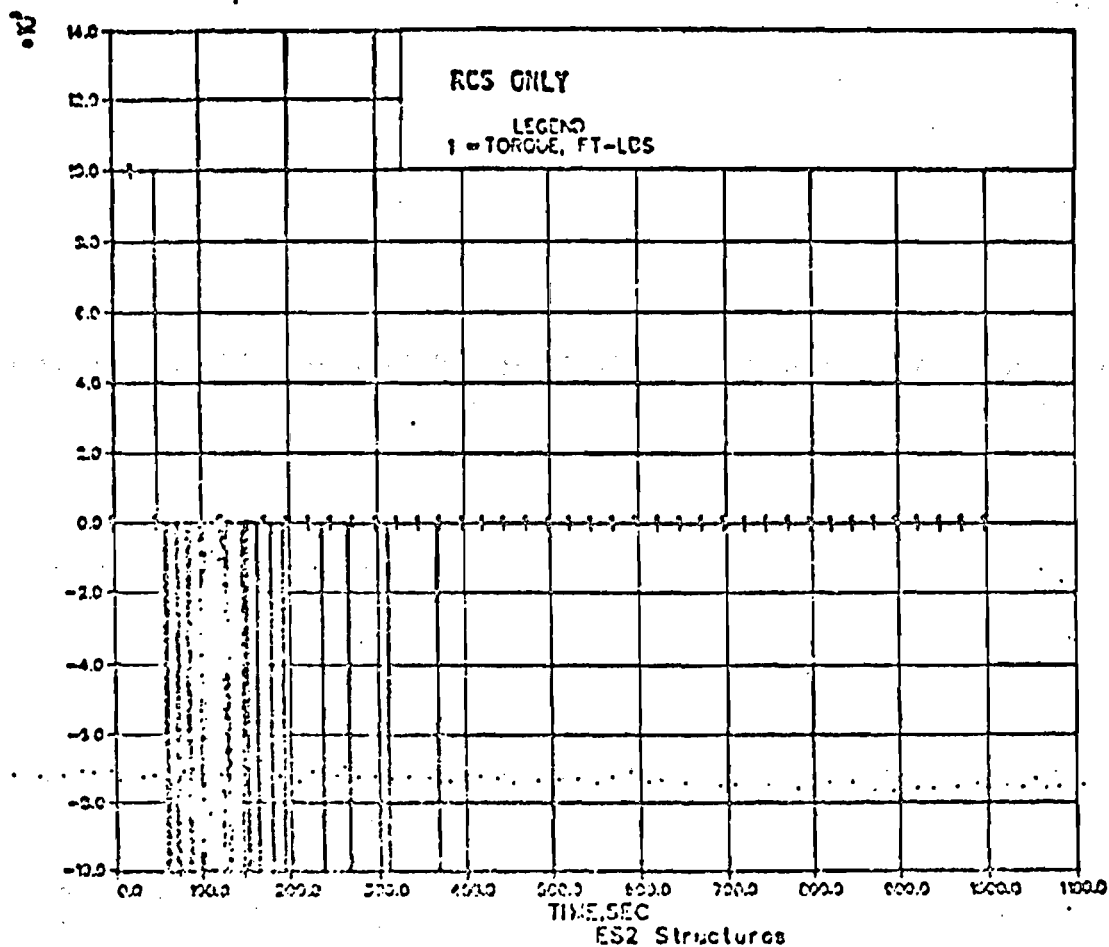


FIGURE 2.4.2-3, RCS JET FIRINGS, ILLUSTRATING HIGH FREQUENCY CONTENT OF CONTROL EFFECTOR INPUT.

RCS (see Figures 2.4.2-4 and 2.4.2-5), but could not achieve adequate performance at acceptable peak torque and secular momentum levels. Certainly, a large enough CMG system to accomplish attitude hold and maneuvering is possible, but only when accompanied by a severe weight penalty.

A method of maneuvering the vehicle using a combined RCS and CMG authority was researched. This system uses the RCS for coarse attitude changes and then transfers authority to the CMG's for fine tuning and holding a specified attitude. This technique uses the RCS torque capability which is easily available and the benign nature of the CMG's for fine attitude management. This technique synergistically applies the benefits of both systems. The resonant pulsing character of the RCS in the vicinity of the desired attitude is traded for the smooth torqueing character of the CMG's. Also, the peak torque required of the CMG's for maneuvering has been significantly reduced. The attitude time history is shown in Figure 2.4.2-6.

Controller torque levels applied to the vehicle were varied from 1000 ft-lb to 100,000 ft-lb. The value that produced adequate performance time histories as well as afforded sufficient closed loop frequency separation between controller and flex passbands was 10,000 ft-lb of peak torque. The RCS, when located at the vertices of the triangle, are sized to 100 lb. thrust to yield the desired torque level.

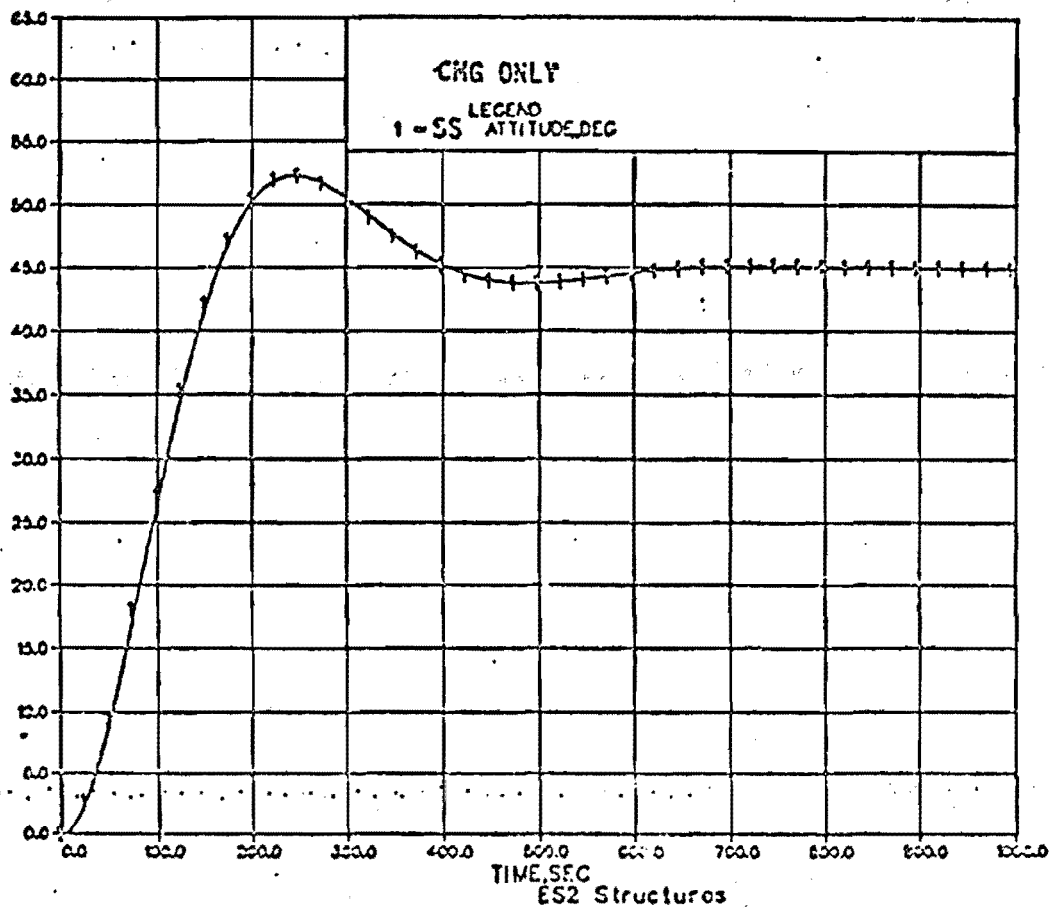


FIGURE 2.4.2-4, ATTITUDE RESPONSE OF SPACE STATION TO COMMANDED 45° MANUEVER USING CMG'S ONLY

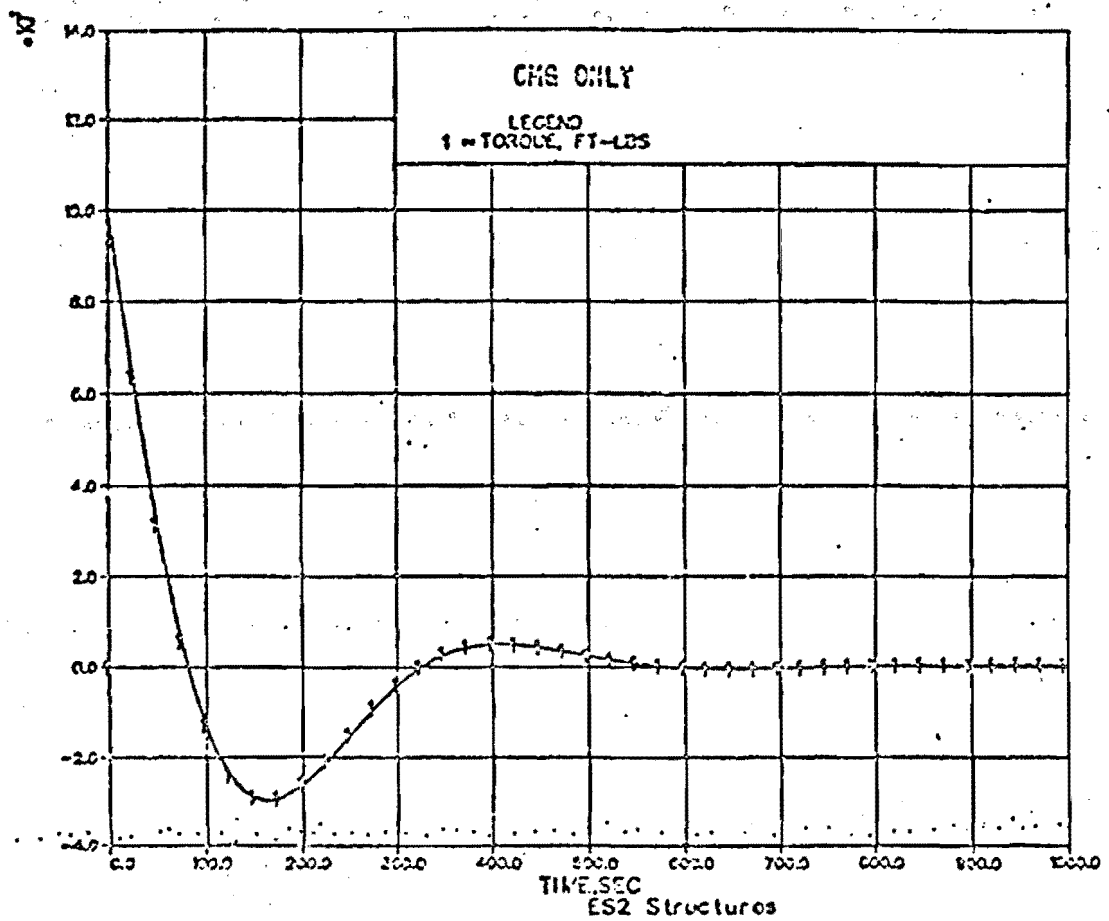


FIGURE 2.4.2-5, TORQUE HISTORY OF CMG'S DURING 45° MANUEVER

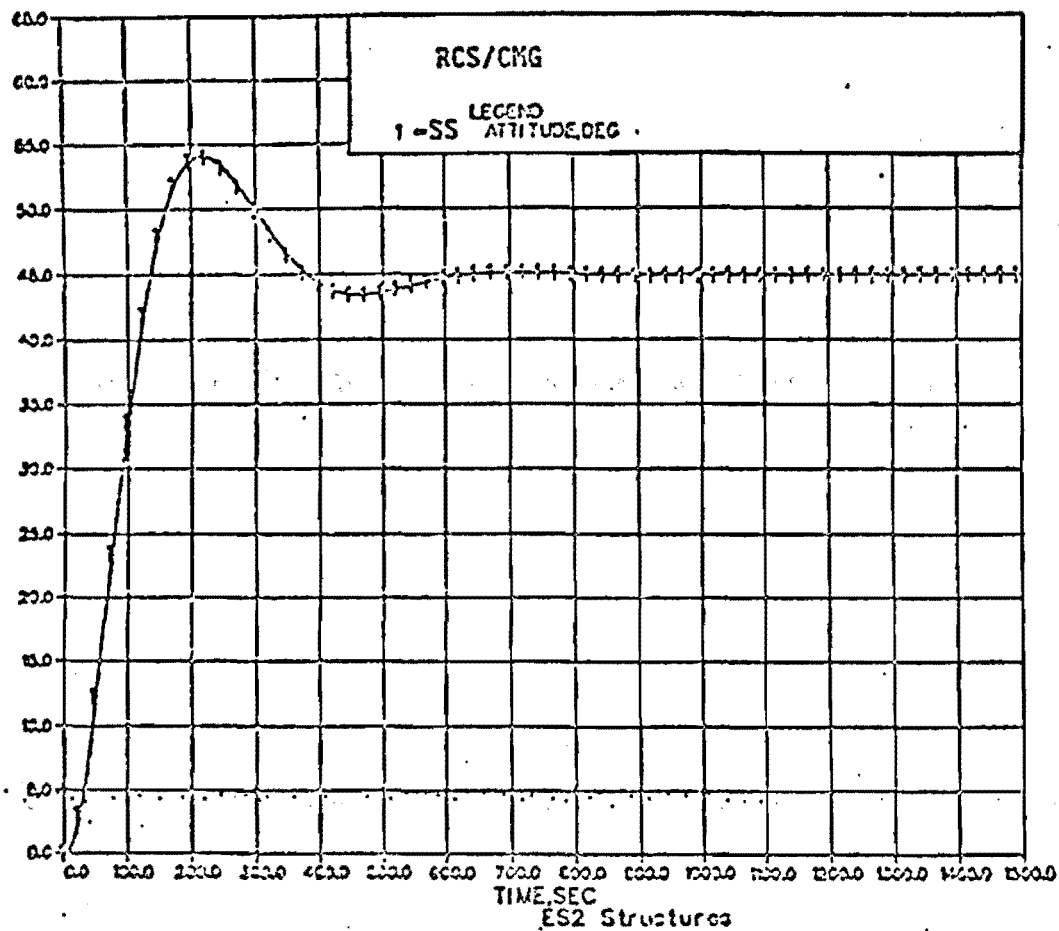


FIGURE 2.4.2-6, ATTITUDE RESPONSE OF SPACE TO COMMANDED 45° MANUEVER
USING A HYBRID RCS/CMG EFFECTOR SYSTEM

With the control system intact, the closed loop frequency response of the system must be analyzed to verify the necessary separation between the controller bandpass and the flex spectrum of the vehicle. The controller bandwidth limit was defined at -3dB in the frequency domain. In figure 2.4.2-7 the closed loop response is compared to the flex frequencies of the vehicle. The controller limit is two decades below the first flex modal frequency. The response curve is located in the frequency domain as an inverse function of system inertia (increase in inertia lowers the frequency response) and a direct function of control torque (increased torque leads to higher frequency response). The amount of separation between control and flex is dictated by the slope of the response curve. If the absolute value of the slope is low (curve appears close to horizontal) more separation is required. The response curve in figure 2.4.2-7 has a steep frequency response and therefore can be moved closer to the flex spectrum without significant modal resonance problems. The separation in this system (two decades) allows for flexibilities encountered during operations (i.e., moving large masses by a remote manipulator system). If maneuvering requirements are increased, the control torque can be increased to 100,000 ft-lb (1000 lb. RCS thruster at the apexes) and the Space Station will exhibit performance qualities similar to flying space vehicles. With appropriate modifications, the Space Station can be transformed into an interplanetary type vehicle. The advantages of this robust structure allow for an impressive growth scenario in both size and performance.

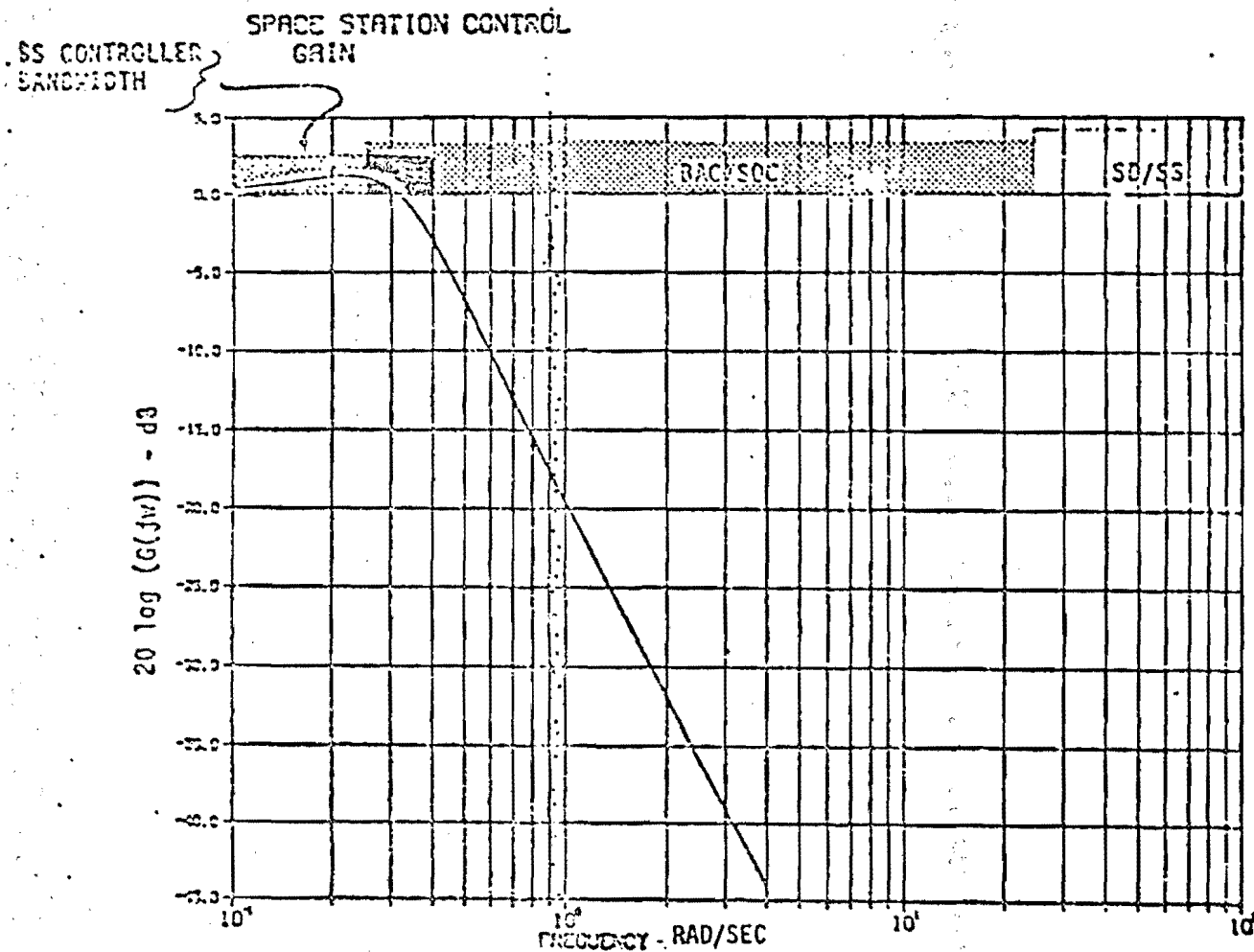


FIGURE 2.4.2-7, SPACE STATION CLOSED LOOP FREQUENCY RESPONSE TO VERIFY SEPARATION FROM STRUCTURAL FLEX FREQUENCIES. NOTE: BOEING SPACE OPERATION CENTER FLEX SPECTRUM SHOWN FOR COMPARISON.

The attitude control system survey included magnetic torque bars and electric Ion engines. The torque bars, used for CMG desaturation, were considered too cumbersome and low in torquing capability. The electric Ion engine has many desirable properties (i.e., high ISP, throttling), but requires large power supply (approximately 14 kw/engine/.1 lb thrust) and yields low thrust levels. If maneuver requirements are dramatically reduced a further look at these and similar devices is warranted.

2.5 Conclusion

This investigation of the Space Station on-orbit dynamics as a function of the natural dynamic environment surrounding the earth has quantified several potential problem areas and identified potential solutions. The foremost problem is a function of the terminal altitude that the STS can achieve with a sizeable payload, (less than 220 nmi). At these low altitudes, aerodynamic drag reduces the free decay orbit lifetime so drastically that the design of a fail safe orbit maintenance system becomes a high priority item. Inherent in an orbit maintenance system at low altitudes are increased propulsion consumables. This problem will be significantly reduced if the STS can deliver cargo to an altitude of approximately 300 nmi. At this altitude using nominal drag, configuration 1 would reenter in 1350 days and configuration 6 in 2870 days (see figure 2-6), as compared to 140 and 300 days, respectively for the 220 nmi orbit.

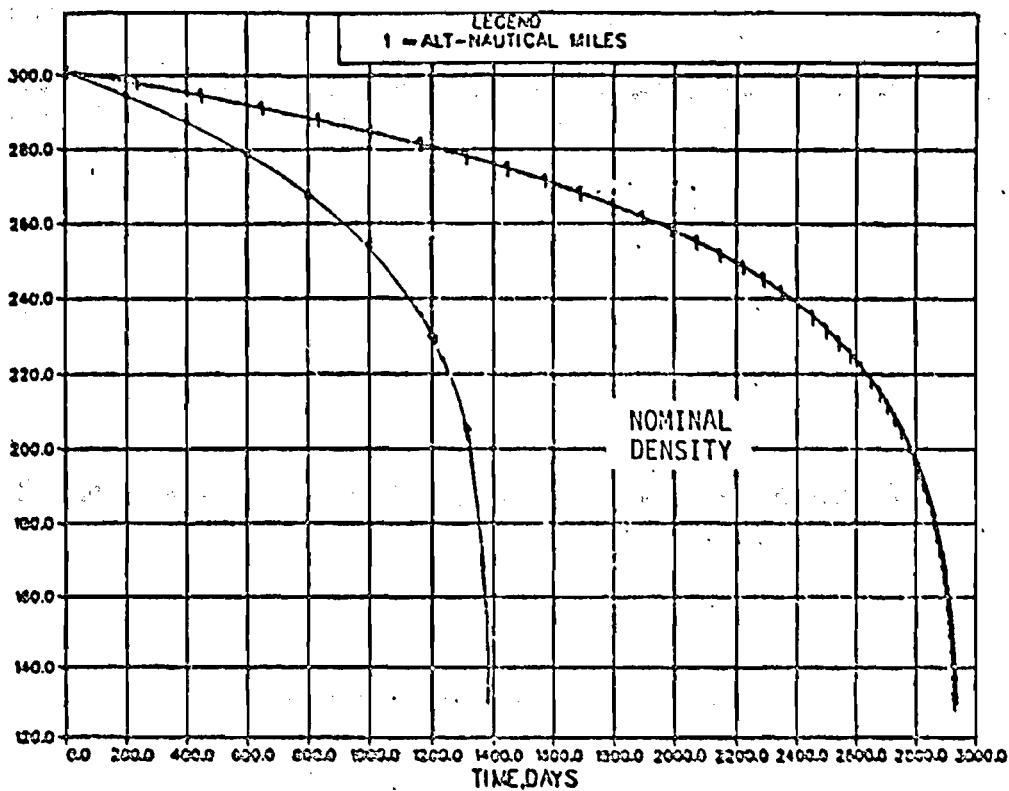


Figure 2-6 - Space Station Altitude Decay Time History for 300 NM

Recent predictions of STS payload capability by the Systems Engineering Division show that the use of a direct insertion mode will allow for delivery of 60,000 lb. payloads to a 300 NM altitude (see Figure 2-7).

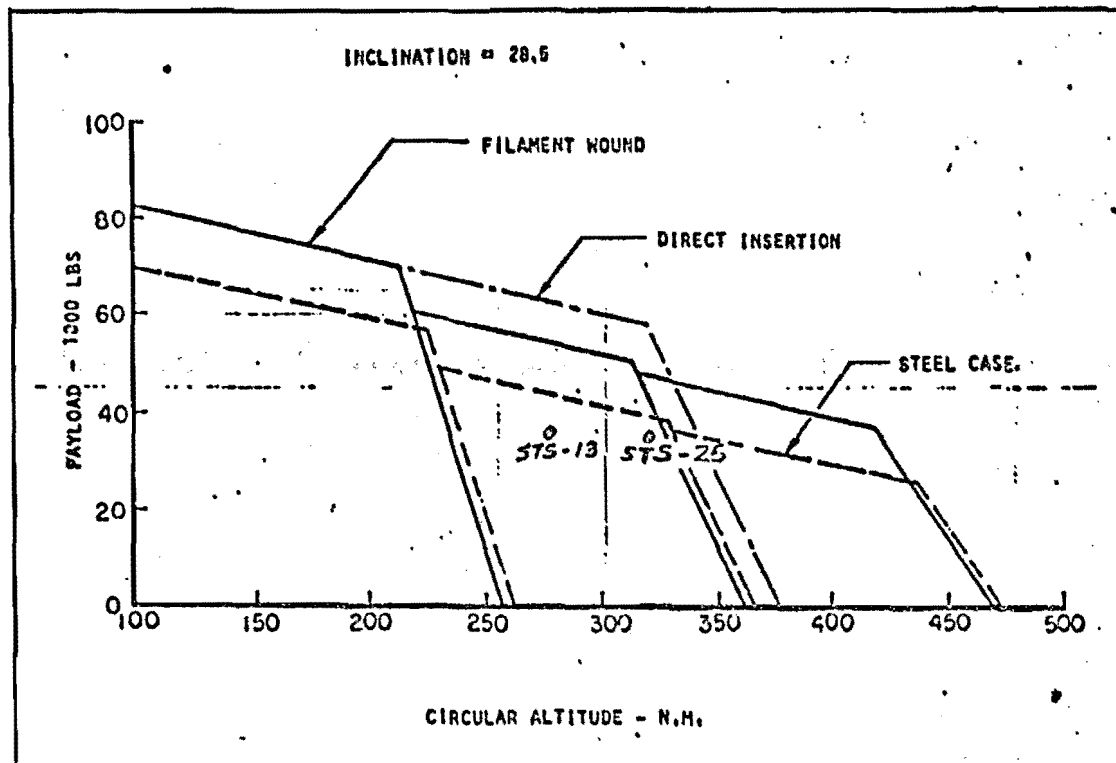


Figure 2-7 Orbiter Payload Capability/Systems Engineering Division

At this altitude, an Ion drag alleviation system would only need to supply a thrust of .01 lbs. This size engine requires only 1.4 kw of electric power, and 125 lbs of fuel per year.

Based on a detailed study of the on-orbit dynamics of the Space Station, a solar inertial attitude hold mode for the Space Station is realizable, if a mass properties management system is enforced. The environmental forces and torques are predominated by the gravity gradient torque. This torque becomes cyclic about the Y-axes, if the X and Z principles axes of the Space Station fly in the orbit plane. The aerodynamic torques are much smaller than the gravity gradient torque and are cyclic. Thus, a CMG system can efficiently maintain the desired Space Station attitude. A method of maneuvering the Space Station using a hybrid RCS/CMG control system offers many advantages and is recommended.

3.1 DEPLOYABLE TRUSS

3.1.1 Introduction

The structural concept for the Triangular Space Station incorporates three large multi-purpose trusses to form the sides of the equilateral triangle. Not only will these trusses form the basic foundation for the Space Station construction, but they will also provide large planar areas that can serve as work and storage platforms and support for the solar arrays and various manned modules.

This section provides the rationale and analysis required to support the feasibility of constructing these large trusses for the Space Station environment.

3.1.2 Truss Requirements

The basic requirements identified for the trusses of the Space Station are

- a. Form a planar surface approximately 72' x 125' for the attachment and display of the station solar array.
- b. Serve as a support structure for mounting radiators, plumbing, electrical wiring, payloads, and manned modules.
- c. Serve as a work platform for construction of orbital transfer vehicles and repair of large satellites.

d. Be automatically deployable from the shuttle cargo bay to minimize EVA for construction.

e. Have a service life of 10 years or more.

Specific structural requirements for the truss that were identified as being important from other studies of large space structures include:

a. Have a relatively high natural frequency.

b. Have adequate strength and stiffness properties for temperatures between -250°F and +350°F.

c. Have a low coefficient of thermal expansion.

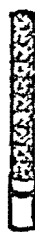

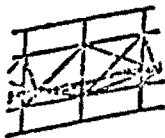
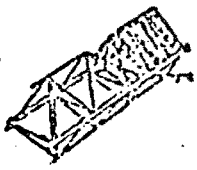


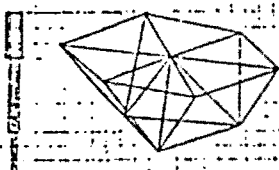
d. Have a low weight for launch to orbit transport.

e. Have a packaging characteristic that will observe the shuttle payload bay requirements.

3.1.3 Truss Concept Study

Review of the existing literature indicated that there are many studies concentrating on space structures that can be used for constructing large space antennas and platforms. Reference 1 contains several papers presented at the NASA Langley Third Annual Technical Review in November 1981, concerning large space systems technology. Several of these papers were used to establish the concept for the Space Station study. Table 3.1.1 shows a summary of deployable beam and platform systems development from reference 2 that have emerged as being more mature concepts with respect to actual working models. Also shown

TABLE 3.1.1 DEPLOYABLE CONCEPT SUMMARY

CONCEPT	DEVELOPMENT STATUS	MATERIALS
<p>CONTINUOUS LONGERON MAST</p> 	SPACE-PROVEN, WITH INSTALLATION OF SMALL ELECTRICAL LINES	FUTURE USE OF LOW CTE COULD BE PROBLEM
<p>ARTICULATED LONGERON MAST</p> 	DEMONSTRATION MODELS WITHOUT PREINSTALLED UTILITIES	FUTURE DESIGN COULD USE LOW CTE MATERIALS
<p>EXTENSIBLE SUPPORT STRUCTURE FOR SEASAT</p> 	SPACE-PROVEN, BUT WITHOUT UTILITIES INSTALLATION—5 FT x 33 FT LONG	TITANIUM, BUT CAN BE LOW CTE
<p>DIPLOID-SHAPED BEAM</p> 	DEMONSTRATED AUTOMATIC DEPLOYMENT OF FIVE-BAY STRUCTURE—SMALL UTILITIES INCLUDED—MODEL 5 x 7.5 FT CROSS-SECTION	LOW CTE MATERIAL WITH ALUMINUM FITTINGS
<p>DOUBLE-CELL, DOUBLE-FOLD TRUSS</p> 	DEMONSTRATED DEPLOYMENT IN AISC BUOYANCY TANK WITH 4 WIRE BUNDLES—EXTERNALLY APPLIED FORCES—SIZE, 3 M x 3 M x 6 M LONG	ALUMINUM, BUT CAN EMPLOY LOW CTE MATERIALS
<p>BOX TRUSS WITH X-BRACING</p> 	DEMONSTRATION MODEL WITHOUT UTILITIES	LOW CTE MATERIAL
<p>TETRAPATRUS</p> 	DEMONSTRATION JOINT MODEL WITHOUT UTILITIES	LOW CTE MATERIAL

in this table is the Tetratruss Concept proposed from references 3 and 4.

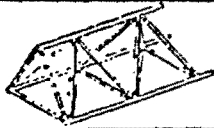

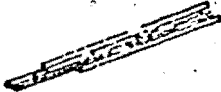

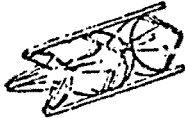

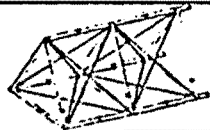


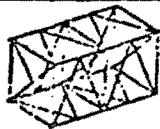





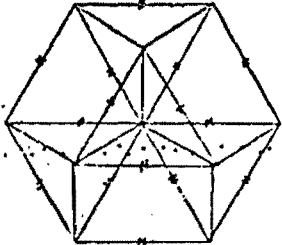



Table 3.1.2 shows a summary of the deployable designs from references 2 and 3 which were considered to meet the Space Station basic requirements. All designs will fold to fit in the payload bay and be deployable in space. However, some will require EVA and some will require additional flights to deliver the entire Space Station frame structure.

The first two designs from this table 3.1.2 are limited by their length. The longitudinal members do not fold and their total length will be limited to the length of the payload bay. Since this length is less than the required 72 foot minimum dimension of the planar area, the truss would have to be cut in half and packaged into two sections 36 feet long. The six truss halves required for the total Space Station structure will then fit into the payload bay and can be delivered in one mission. However, an extra EVA will be required to rejoin the severed halves.

The third design is limited to a single beam configuration by its folding characteristics. A total planar surface cannot be constructed on the ground and deployed in space. The total planar surface will have to be constructed of individual beams. Using, for example, 10.41 foot long by 2.0 inch diameter

ORIGINAL PAGE IS
OF POOR QUALITY

TABLE 3.1.2 DEPLOYABLE TRUSS DESIGNS

Type	Deployed	Partially Deployed	Packaged
Warren Truss - Transverse Fold ①			
Cable Cross-Braced - Transverse Fold ②			
Cable Cross-Braced - Transverse and Longitudinal Fold ③			
K Brace - Longitudinal Fold ④			
K Brace - Longitudinal Fold ⑤			
TETRAPRUS - Transverse Fold ⑥	 		

tubular members, it is possible to package the required 21 beams for a complete Space Station structure in the payload bay and deliver them to orbit in one launch. However, several EVA's will be required to connect the beams together to form the required surface.

The fourth and fifth designs are limited to a longitudinal fold which will allow for packaging, but not allow a sufficient number of beams to be launched at one time to erect the complete Space Station framework. Using the 10.41 foot by 2.0 inch diameter tubular member example, only eight beams can be packaged in the payload bay at one time. The Space Station framework will require a total of 21 beams, so a minimum of three flights will be required. Additional EVA's will be required to connect the beams together to form the necessary planar area.

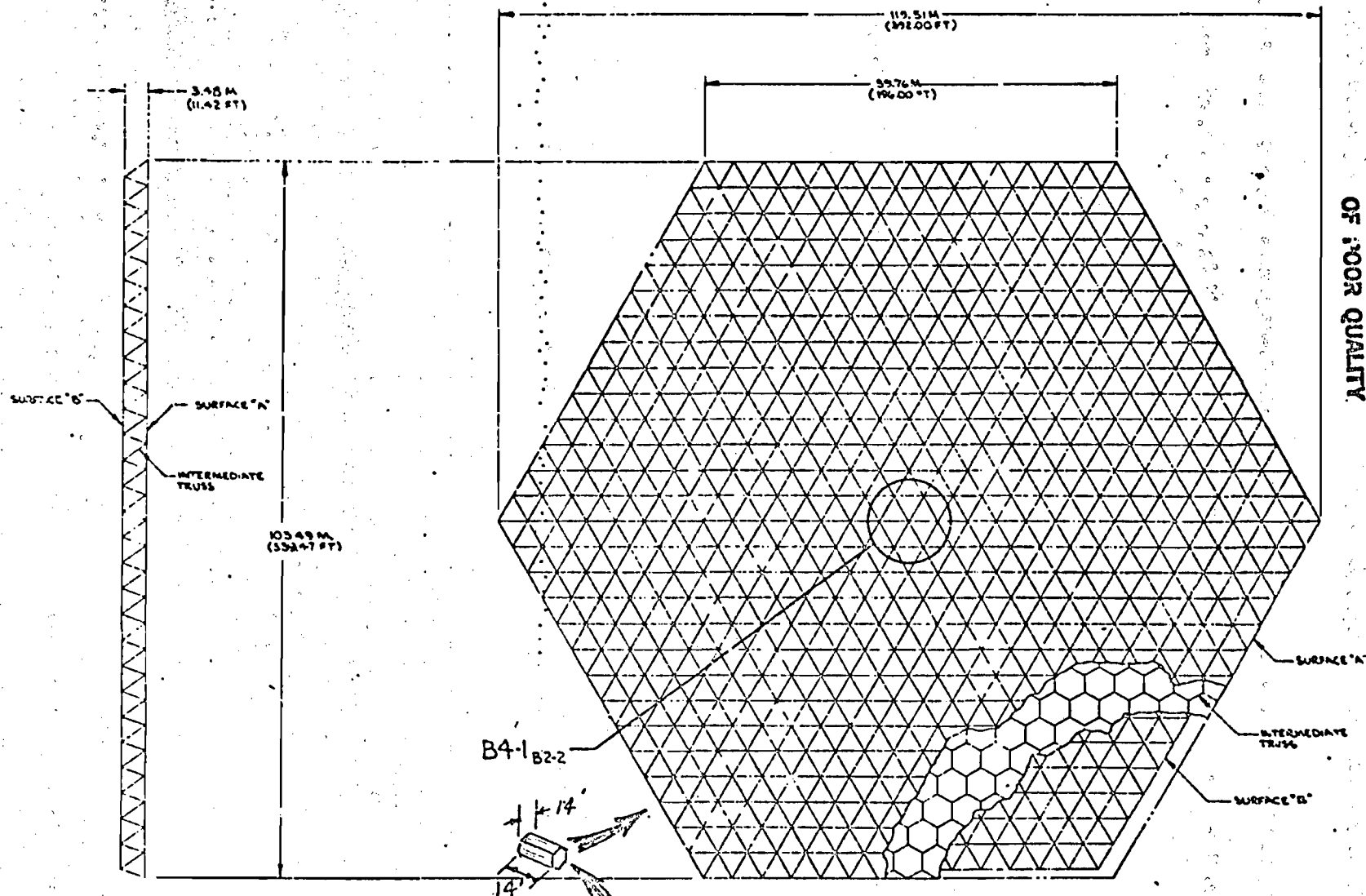
The sixth design is the only configuration that will allow packaging and deployment without an EVA to construct the necessary planar area. Using the same member dimensions, the three planar trusses required for the total Space Station framework can be packaged in the payload bay and delivered in one flight. In addition to meeting the minimum EVA for construction requirement, the Tetratruss concept is also the only redundant structure of the group so that there will be alternate load paths in case a member is accidentally damaged. This is a great advantage from a structures and life point of view.

Figure 3.1.1 shows the packaging and deployment capabilities of the Tetratruss concept from reference 3. The particular size of planar truss shown in this figure was the maximum planar area that could be packaged in the payload bay diameter and be deployed in orbit without an EVA. It can be seen that a very large planar area can be packaged using this concept.

It does not appear that there would be any restrictions on any of the designs of table 3.1.2 with respect to the materials used for the truss members. Therefore, all truss concepts could meet the specific structural requirements. The main difference between the designs of table 3.1.2 would be the number of launches and EVAs required to construct the framework. Designs four and five could be eliminated because they will require several launches to get the total Space Station framework to orbit. All the other designs except the Tetratruss will require extra EVAs to construct the sides of the triangular Space Station. As an additional advantage, the Tetratruss has a highly redundant structural arrangement and as shown by reference 2, has effective stiffness properties that are of isotropic nature for analysis purposes. Therefore, in this study the Tetratruss concept was selected for the Space Station framework.

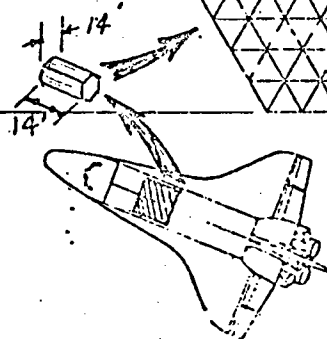
3.1.4. Truss Loading

Preliminary structural design loads that have been identified for the Space Station framework members include

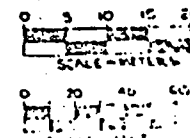


ORIGINAL PAGE IS
OF POOR QUALITY

FIGURE 3.1.1
TETRATRUSSE CONCEPT



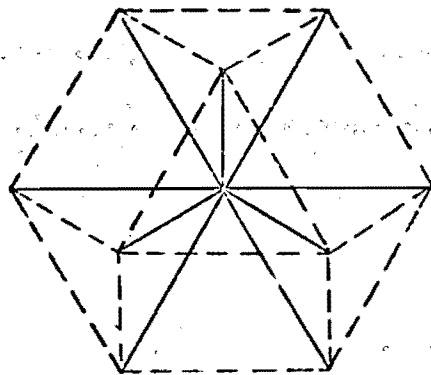
14 RING CONFIGURATION
4.27 M (14.00 FT) STRUTS
5250 TYPICAL MEMBERS



equipment and payload docking, thermal, dynamic, gravity gradient, and orbital transfer. Frame loading conditions for mission events such as ignition, liftoff, and ascent were not considered to be applicable for individual member design since the frame will be in a packaged state and assumed to be adequately supported in the shuttle payload bay. This detail will be refined in a later report.

It was assumed for this study that equipment and payload docking loads would present the critical member design condition. Since the Tetratruss configuration is a statically indeterminant structure, a computer model was generated to determine the individual member loads. Figure 3.1.2 shows a finite element model of one module of the Tetratruss configuration having an estimated 1000 pound limit vertical load and 500 pound limit lateral load applied to a typical frame node point. Solution of this problem shows that the maximum member limit load is ± 491 pounds.

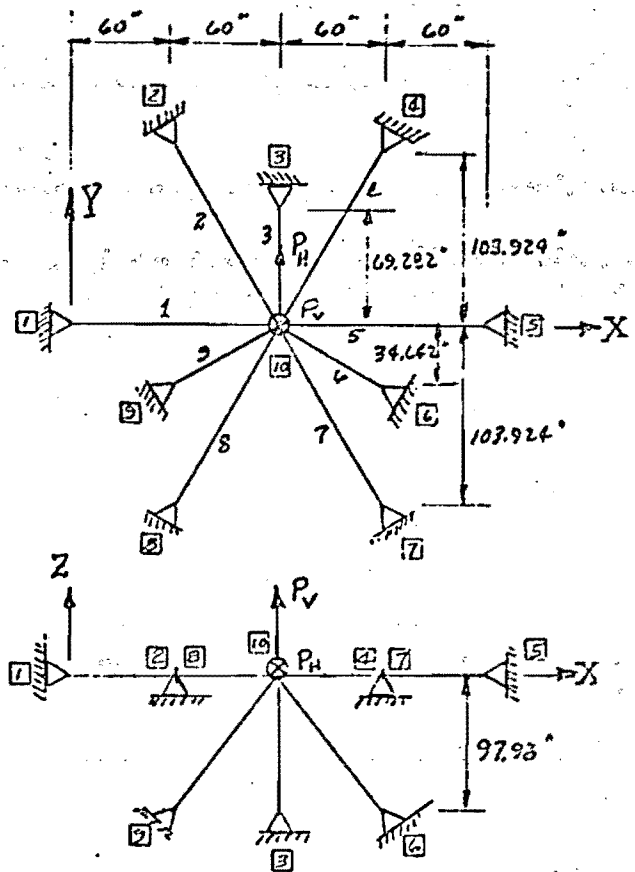
Thermal loads in the frame members can be minimized by a careful selection of member materials having a low coefficient of thermal expansion. Preliminary thermal analysis of the Space Station from Section 1.0 indicates that the critical frame in the system is the one that supports the solar array. This analysis shows that the frame will have a temperature cycle from 150° to 200°F as the station rotates about the earth. It does not appear



TETRATRUS MODULE

LET

$$\begin{aligned} P_H &= 500 \# \\ P_V &= 1000 \# \\ L &= 10' = 120" \\ A &= 2" \text{OD} \times .025" \text{THK} = .157 \text{ in}^2 \\ E &= 20 \times 10^6 \text{ PSI} \\ \nu &= .3 \end{aligned}$$



NODE	X	Y	Z
1	0	0	0
2	60	103.924	0
3	120	69.282	-97.98
4	180	103.924	0
5	240	0	0
6	180	-34.642	-97.98
7	180	-103.924	0
8	60	-103.924	0
9	60	-34.642	-97.98
10	120	0	0

RESULTS —

DEFLECTIONS

NODE	X	Y	Z
10	0	.00546	-.01911

MEMBER FORCES

MEMB. NO.	FORCE
1	0
2	-123.72
3	-490.73
4	-123.72
5	0
6	-367.00
7	123.72
8	123.72
9	-367.00

FIGURE 3.1.2 FINITE ELEMENT LOADS MODEL

that this temperature variation will cause any significant thermal loads in the members of the 125 foot long frame regardless of the material selected. However, as the Space Station configuration and material selection matures, the effects of thermal expansion and contraction should be reevaluated.

Frame member load resulting from gravity gradient effects have been formulated in reference 5 for the Tetratruss configuration. The results of reference 5 show that for trusses less than one mile wide, the member forces, due to gravity gradient, are relatively small when compared to the other member design loads. Therefore, truss member loading due to gravity gradient effects are omitted from this study.

Dynamic loading of the individual frame members have not been assessed at this time because of a detailed definition of the Space Station. This particular analysis will require use of a dynamic computer code and definition of a forcing function. Because of the large dynamic model and computer time that would be required to obtain a solution, it was decided that this phase of the Space Station study would be deferred. An assessment of the member dynamic loads and frame frequencies will be presented later. For the preliminary analysis, the proposed 1000 pound vertical and 500 pound lateral loads will be assumed to be sufficient to include dynamic effects.

Orbital transfer, control, and reboost loads in the individual frame members have also been investigated in reference 5 for the Tetratruss configuration. The model used for the reference 5 study considered thrusting the frame structure at its edge to produce only inplane frame loading. The propulsion considered was Ion engines producing .001 pounds of thrust per engine. The conclusions reached in reference 5 is that the member loads produced by this model are insignificant. However, as the Space Station design and propulsion requirements become better defined, this loading should be reconsidered.

Therefore, the maximum member loading condition established for the truss occurs for docking and equipment stowage and shows a magnitude of ± 491 pounds. For purposes of this study and inclusion of uncertainties, a limit design load of ± 500 pounds will be used for member sizing and analysis. It has also been assumed that the trusses can be manufactured economically if all the members are identical. This assumption will incur a weight penalty for the members showing a lower load in Figure 3.1.2 but will add conservatism to the system for the other loads that were considered negligible.

3.1.5 Truss Materials Study

The basic requirements for structural materials used in large space structures are usually high stiffness, low density, adequate strength at operating temperature and loads, low

coefficient of thermal expansion, and a service life of 10 years or more.

High stiffness of the frame is not only required to enhance the dynamic characteristic of the system so that it will not respond to low frequency vibration, but also to provide bending and axial rigidity to the station. Low density materials are primarily required to provide a light packaged structure for transportation to orbit as well as a high natural frequency.

The material must also have adequate strength at its operating temperature to react the design loads. However, the analysis shown in section 1.0 shows that the Space Station truss has an apparent maximum operating temperature of only 150°F. It does not appear that this temperature will cause any significant degradation of material strength properties. As a result, this material requirement will be insignificant for the material comparison.

Because of the large size of the truss framework, it appears desirable to keep the material coefficient of thermal expansion as low as possible to minimize the thermal distortion of the Space Station. The truss frame facing the sun will expand because of its warmer temperature while the two frames shielded by the solar array will be cooler and contract. The station will then warp and no longer form a symmetrical cross section. This

may not be a real problem for the Space Station; however, a low coefficient of thermal expansion will still be considered to be an important parameter for the material selection until this effect can be adequately evaluated.

Table 3.1.3 shows a comparison of various selected materials that could be used in the manufacture of the truss members. The best candidate materials that will fulfill the stated requirements are those that exhibit the highest stiffness to density ratio and have the lowest coefficient of thermal expansion. The graphite/epoxy composites and the graphite/aluminum tubing of Table 3.1.3 appear to be the best choices. A final selection between these two candidates will be based on their relative cost and ability to meet the service life requirement.

The graphite/epoxy composites have been in development for a long time and have proven themselves in various areas of aerospace products as both primary and secondary structures. The Space Shuttle OMS Pods and payload bay doors are made of graphite/epoxy composites and have been certified for a 10-year service life. In addition, the manufacturing and repair procedures have been established and proven. Several papers have been presented in reference 1 concerning radiation and other space environment

TABLE 3.1.3 MATERIAL PROPERTIES @ 150°

PROP.	ALUM (TUBING)	GR/EP (TAPE)	GR/EP (FABRIC)	GR/AL* (TUBING)	B/AL* (TUBING)	B/EP
E (PSI)	10.3 $\times 10^6$	28-75 $\times 10^6$	10-33 $\times 10^6$	53 $\times 10^6$	30 $\times 10^6$	31.5 $\times 10^6$
F _{TU} (KSI)	61.4	200-400	77-200	92	161	180
F _{cy} (KSI)	41.1	200	48	100	343	295
F _{su} (KSI)	38.2	5.5	6.6	—	6.9	12.3
α (in/in/°F)	13 $\times 10^{-6}$	-2 to 3 $\times 10^{-6}$	-2 to 3 $\times 10^{-6}$.5 $\times 10^{-6}$	4 $\times 10^{-6}$	20 $\times 10^{-6}$
ν	.33	.3	.3	.3	.25	—
ρ (#/in ³)	.10	.055	.055	.086	.095	.078

* MATERIAL PROPERTIES AT ROOM TEMPERATURE

effects on the graphite/epoxy composites and none appear to indicate any degradation of properties that would affect the Space Station life requirement.

The graphite/aluminum metal-matrix composite is also attractive for space applications from the standpoint that these composites should inherently have a 10-year or better life. However, this composite is still in the technology development stage, and it is expected that the cost of this material would be greater than graphite/epoxy. A complete investigation covering the life and cost of both graphite/epoxy and graphite/aluminum should be conducted prior to the final design. In addition, other materials such as graphite/polimide should be evaluated.

Based on this limited materials study, it is recommended that the graphite/epoxy material be used for the baseline design.

3.1.6. Space Station Frame Geometry

From preliminary layouts of the triangular Space Station configuration, it was determined that the overall dimensions of the truss frame should be approximately 72' x 125'. To construct a planar surface using the Tetratruss concept, it is required that all truss members have identical lengths. Therefore, one of the overall frame dimensions must be held constant while the member length is varied to meet the other

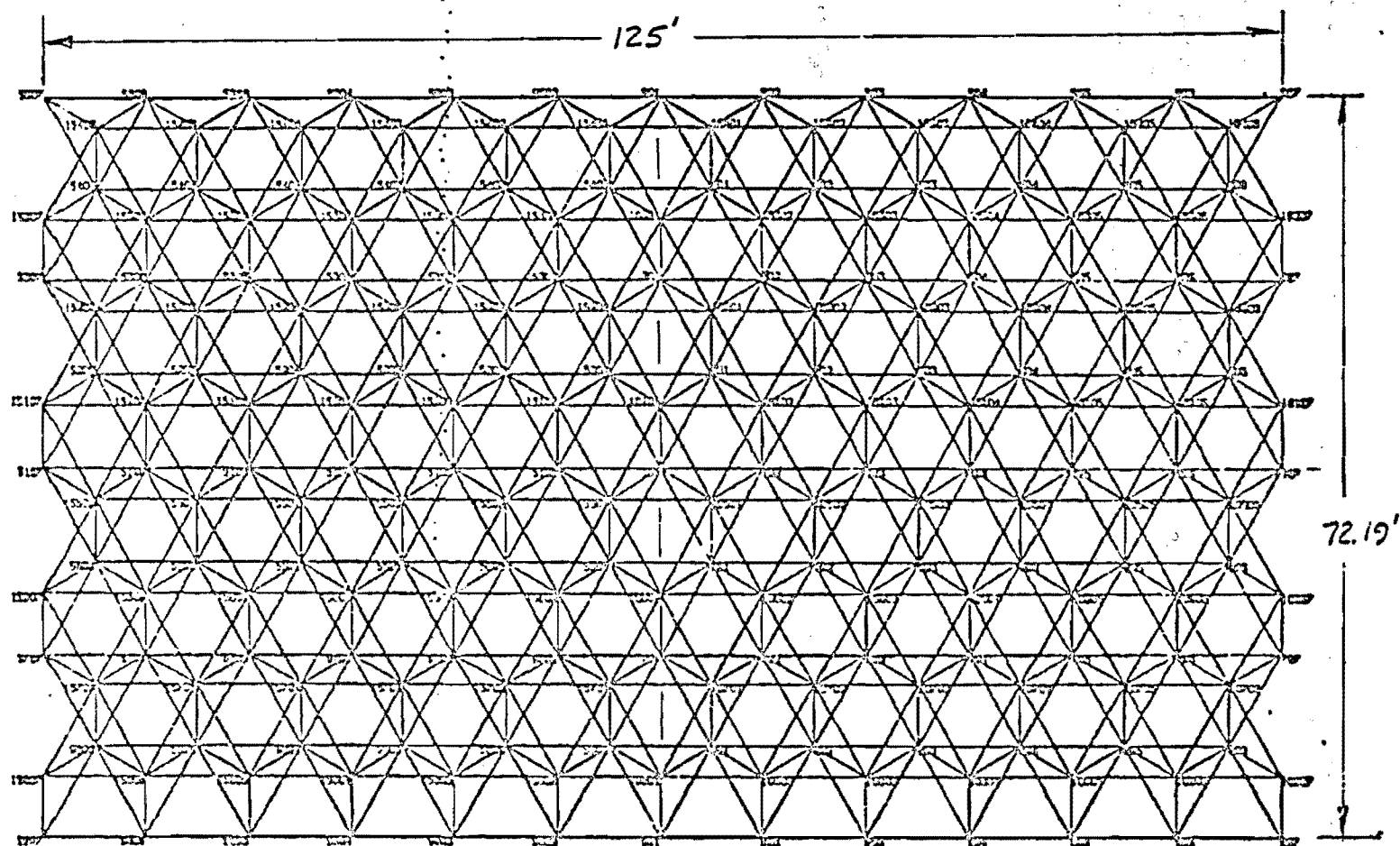
overall dimension. Holding the 125' frame length constant and allowing the member length to be as long as possible to reduce the number of members required, the study resulted in a frame that has a 72.19-foot width instead of 72 feet, and a member length of 10.41 feet. Figure 3.1.2 shows a computer generated plan view of the proposed Tetratruss frame. Strength integrity of the 10.41-foot long member must now be established.

3.1.7 Truss Member Sizing and Weight Analysis

The limit design load for the truss member was established as ± 500 pounds in Section 3.1.4. Using an ultimate factor of safety of 1.4 for structural integrity requirements, the design load becomes ± 700 pounds. The member will be sized for the following failure modes:

- a. Column buckling
- b. Strut compression
- c. Strut tension
- d. Strut bending due to handling loads

Reference 3 presented a Tetratruss member sizing exercise very similar to the study that will be presented herein. Therefore, this analysis will take advantage of the work that has already been done. From reference 2, the truss member design was a 2.0-inch diameter tube with a .025-inch wall thickness. This study will also use the 2.0-inch diameter tube but will establish



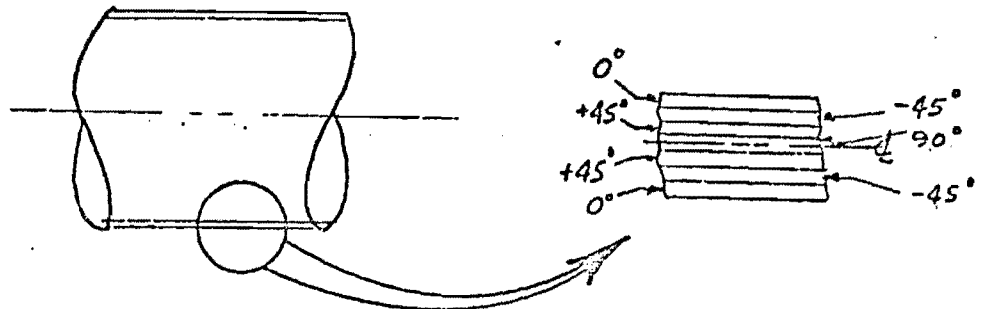
NO. OF NODE POINTS = 213
NO. OF MEMBERS = 848

MEMBER LENGTH = 10.41'
BEAM DEPTH = 8.51'

FIGURE 3.1.2 PLAN VIEW OF TRUSS

the necessary number of graphite/epoxy plies for a wall thickness that will be required to produce positive margins of safety for the loading and failure modes presented above.

Manufacturing of the tubing from composites will require that the material be laid up in a balanced fiber orientation. This will prevent the tubing from becoming warped during the cure cycle. Using a unidirectional ply tape, a tube having seven plies consisting of two plies at 0° , four plies at $\pm 45^\circ$, and one at 90° will constitute a balanced lay-up. The balanced configuration is shown in the following sketch.



This composition will consist of 58%, $\pm 45^\circ$ plies, 29%, 0° plies, and 13%, 90° plies. From figure 3.1.3 this lay-up will have a coefficient of thermal expansion of $.5 \times 10^{-6}$ in/in/ $^\circ\text{F}$. Also, the seven plies of tape will constitute a composite thickness of .035-inches.

HIGH-MODULUS GRAPHITE/EPOXY REFERENCE 6

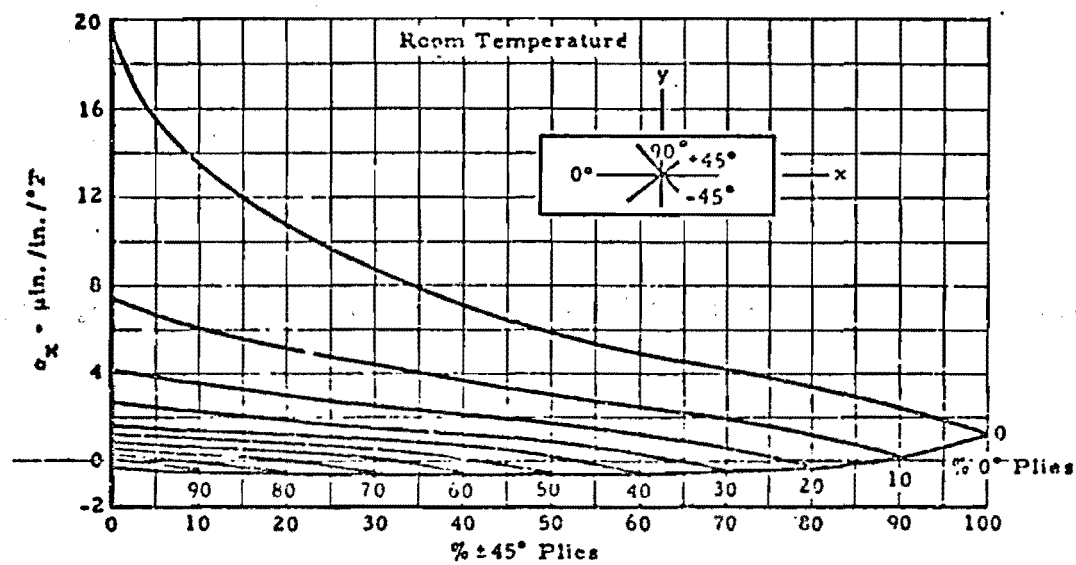


FIGURE 3.1.3 COEFFICIENT OF THERMAL EXPANSION FOR GR/EP COMPOSITE

ORIGINAL PAGE IS
OF POOR QUALITY

For column buckling

Assume a pin ended column, $L = 10.41' = 125''$, $P = .7071''$

$$L/P = 125/.7071 = 177$$

$$\sigma_{cr} = \frac{\pi^2 E}{(L/P)^2} = \frac{(\pi)^2 (29 \times 10^6)}{(177)^2}$$

$$\sigma_{cr} = 8821 \text{ psi}$$

For strut compression $A = \pi D t = (\pi)(2)(.035) = .22 \text{ in}^2$

$$\sigma_c = \frac{P}{A} = \frac{700}{.22}$$

$$\sigma_c = 3182 \text{ psi}$$

Material allowable from table 3.1.3 is 200 KSI. Thus, the margin of safety is high for compression. Margin of safety for column buckling is

$$M.S. = \frac{8821}{3182} - 1 = \underline{\underline{+1.77}}$$

For strut tension

$$\sigma_T = \sigma_c = 3182 \text{ psi}$$

From table 3.1.3, the minimum tensile allowable is 200 KSI. The margin of safety for tension is high.

For strut bending due to handling loads

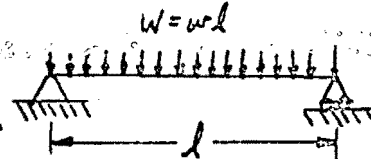
The strut must be checked for failure due to bending under its own weight during the truss construction in a lg environment. Assume a pin ended beam.

$$W = wL = APL$$

$$W = (.22)(.056)(125) = 1.54^{\text{K}}$$

$$M_{\text{MAX}} = \frac{WL}{8} = \frac{(1.54)(125)}{8}$$

$$M_{\text{MAX}} = 24.06 \text{ IN} \cdot \text{K}$$



$$I = \frac{\pi D^3 t}{8} = \frac{(\pi)(2)^3 (.035)}{8}$$

$$I = .11 \text{ in}^4$$

Bending stress

$$\sigma_E = \frac{MR}{I} = \frac{(24.06)(1)}{.11}$$

$$\sigma_E = 219 \text{ PSI}$$

Wall crippling allowable for bending

$$\sigma_{\text{ALLOW}} = \frac{2\sigma E}{\sqrt{2(1-\nu^2)}} \frac{t}{D}$$

where

$$\nu = 1 - .731 [1 - e^{-\phi}]$$

$$\phi = \frac{\pi}{16} \sqrt{\frac{D}{2t}}$$

$$e = 2.71828$$

$$\phi = \frac{\pi}{16} \sqrt{\frac{2}{(2)(.035)}} = .33408$$

$$\nu = 1 - (.731) [1 - e^{-.33408}] = .792$$

$$\sigma_{\text{ALLOW}} = \frac{(2)(.792)(28 \times 10^6)(.035)}{\sqrt{(3)(.91)} (2)}$$

$$\sigma_{\text{ALLOW}} = 470000 \text{ PSI}$$

The margin of safety is high for this failure mode.

Analysis of the seven-ply configuration shows that the minimum margin of safety for ultimate loading is +1.77 and that the critical failure mode is column buckling. A smaller margin of safety could be calculated for a thinner wall tube, but in order to keep a balanced lay-up, the coefficient of thermal expansion from figure 3.1.3 would either increase or become negative.

Using the member dimensions noted above and the density of .056#/in³ for graphite/epoxy composite, a single tube that is 10.41 feet long will weigh 1.54 pounds. The computer generated figure 3.1.2 indicates that there are 848 members in the Tetratruss frame.

Weight of one frame = (848) (1.54) = 1306#

Assume a 20% weight increase for member end fittings and foldable joints.

Frame weight = (1.2) (1306) = 1567#

Total weight of Tetratruss frames for the Space Station configuration:

Total weight = (1567) (3) = 4701#

Natural frequencies of the truss structure were determined from the NASTRAN computer code for three particular cases of a simply supported truss loaded by its own member weight, loaded by its member weight plus the distributed mass of the solar cells, and loaded by its own member weight plus the mass of an OTV attached to one corner of the truss. Figures 3.1.4 (a) through

3.1.4 (c) show the first, second, and third mode shapes of the frame with the distributed mass of the solar cells and the calculated natural frequencies for these mode shapes. A summary of the lowest natural frequencies for the three-load cases is shown in table 3.1.4.

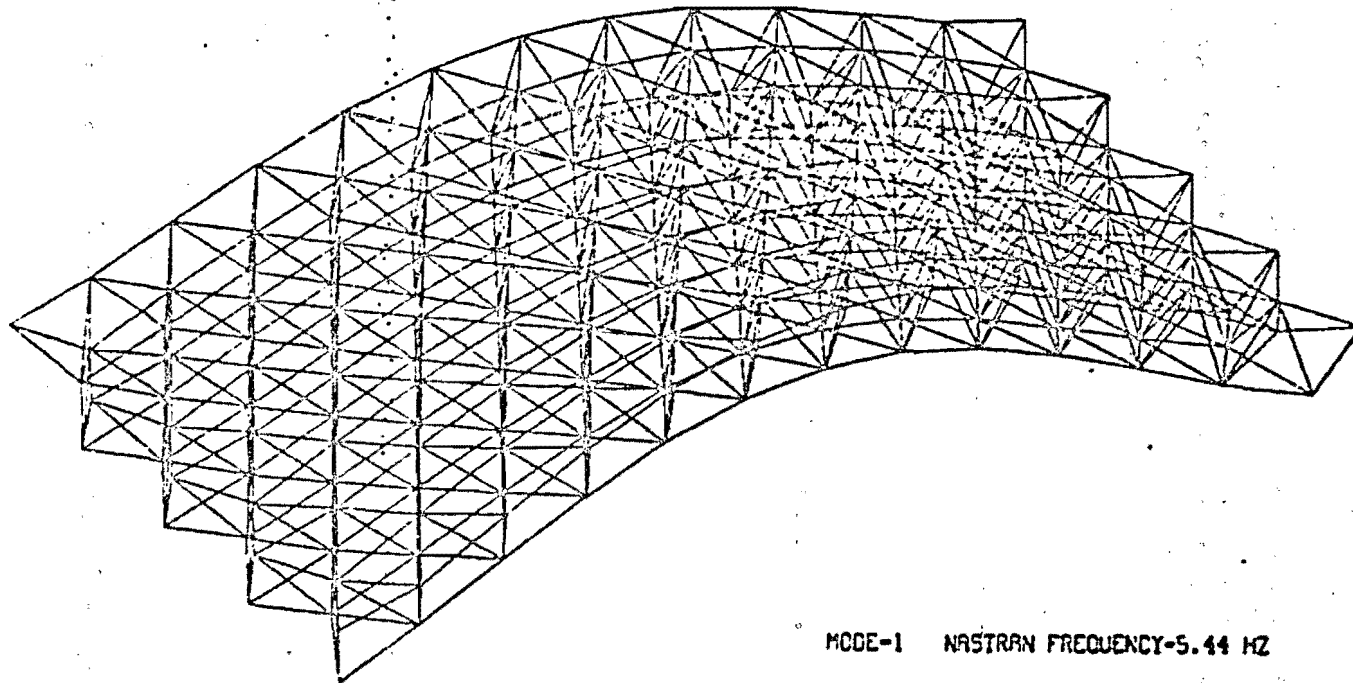
TABLE 3.1.4 Summary of Frame Natural Frequencies

FRAME CONDITION	NATURAL FREQUENCY
UNLOADED FRAME	9.78 H _z
FRAME WITH SOLAR ARRAY	5.44 H _z
FRAME WITH OTV MOUNTED AT CORNER	7.95 H _z

3.1.8 Payload Packaging Analysis

Reference 3 and 4 show schemes on folding the large Tetratruss frame for packaging. However, reference 3 gives specific emphasis for packaging the large planar area in the shuttle payload bay. This scheme is shown in a partially deployed position in table 3.1.2 and indicates that the upper and lower members are hinged at their mid-length and made to lie against

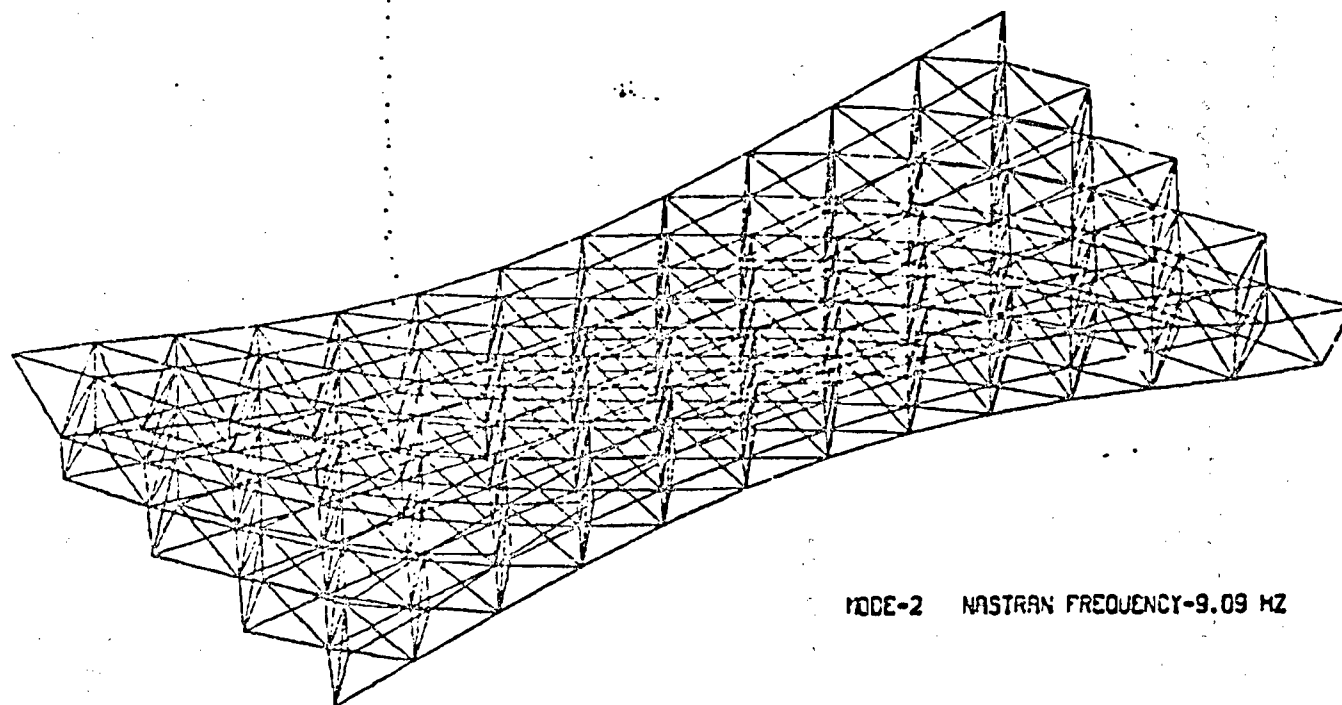
STRUCTURE'S DIVISION SPACE STATION CONFIGURATION
SOLAR CELL PANELS --- SUPPORT ALONG 866 BOUNDARY



MODE-1 NASTRAN FREQUENCY=5.44 HZ

FIGURE 3.1.4(a) FIRST MODE SIMPLY SUPPORTED TRUSS
WITH DISTRIBUTED SOLAR CELL MASS

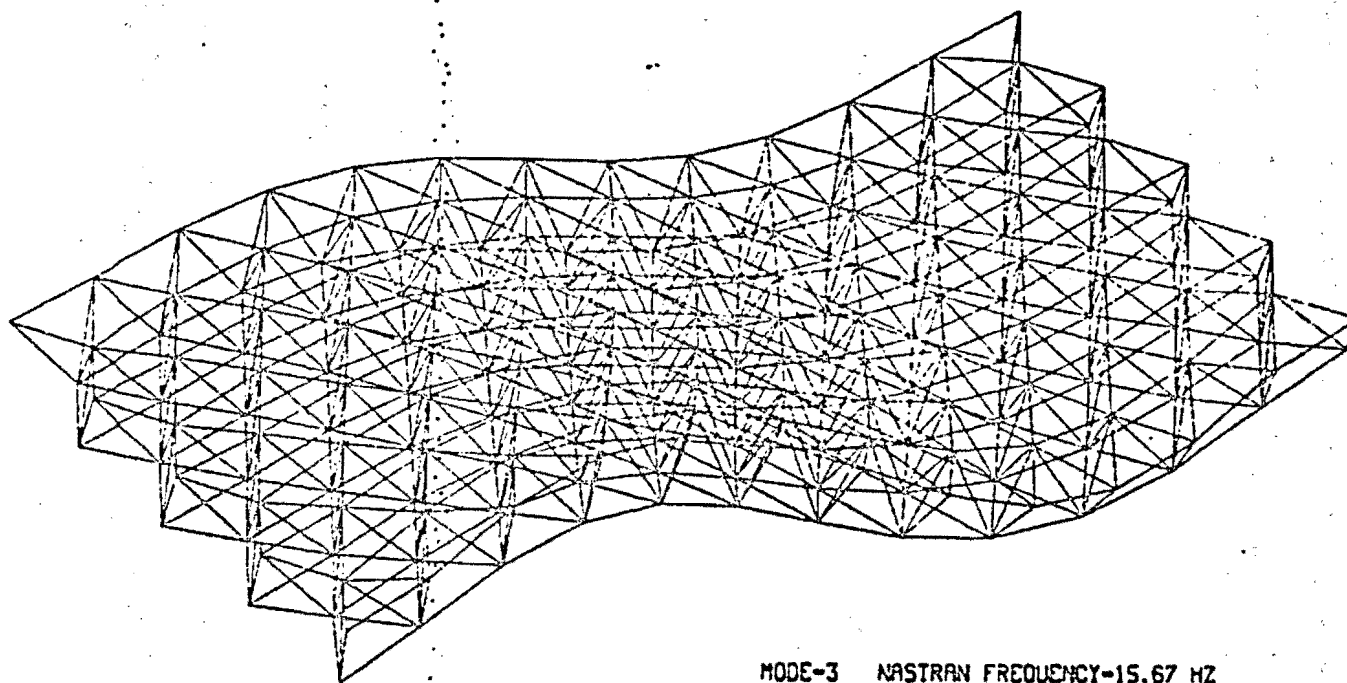
STRUCTURE'S DIVISION SPACE STATION CONFIGURATION
SOLAR CELL PANELS --- SUPPORT ALONG 866 BOUNDARY



MODE-2 NASTRAN FREQUENCY-9.09 HZ

FIGURE 3.1.4(b) SECOND MODE SIMPLY SUPPORTED TRUSS
WITH DISTRIBUTED SOLAR CELL MASS

STRUCTURE'S DIVISION SPACE STATION CONFIGURATION
SOLAR CELL PANELS --- SUPPORT ALONG 866 BOUNDARY



MODE-3 NASTRAN FREQUENCY-15.67 HZ

FIGURE 3.1.4(c) THIRD MODE SIMPLY SUPPORTED TRUSS
WITH DISTRIBUTED SOLAR CELL MASS

each other when the truss is fully collapsed. In this manner, the whole truss is a tightly compacted bundle of tubes for packaging.

The dimensions of the packaged truss are then a function of the tube diameters. Figure 3.1.5 shows a plan view of the upper surface of the truss. In the folded configuration, there will be two tube diameters on every line connecting a node point and one tube diameter for every node point. For the deployed 125-foot direction, there are a maximum of 12 lines connecting node points and 13 node points.

Packaged 125 ft. length = $(2)(2)(12) + (2)(13) = 74' = 6.2'$. For the 72.19-foot direction, there are eight lines connecting node points along a 60° diagonal and nine node points.

Packaged 72.19' length = $[(2)(2)(8) + (2)(9)] \sin 60^\circ = 43.3' = 3.6'$

The lower surface packaged dimensions will be slightly smaller since

there are fewer members. From Figure 3.1.6 the packaged sizes are

Packaged 125' length = $(2)(2)(12) + (2)(13) = 74' = 6.2'$

Packaged 72.19' length = $[(2)(2)(7) + (2)(8)] \sin 60^\circ = 38.1' = 3.2'$

From the partially deployed view of the Tetratruss in table 3.1.2, it can be seen that the packaging concept requires that the upper surface members fold downward and the lower surface members fold upward. Since these members are folded in half, half the member

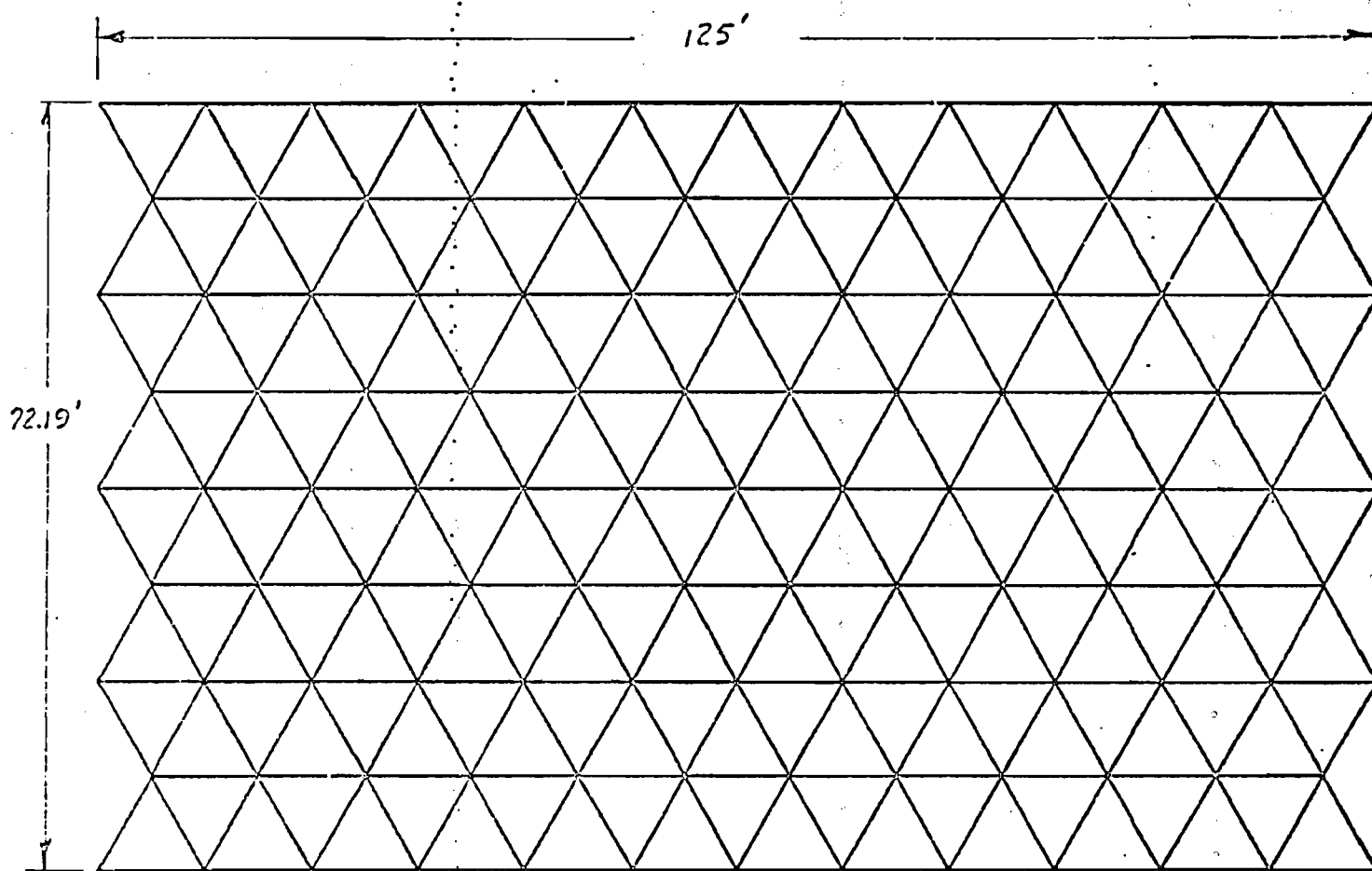


FIGURE 3.1.5 UPPER SURFACE OF TETRATRUSSE FRAME

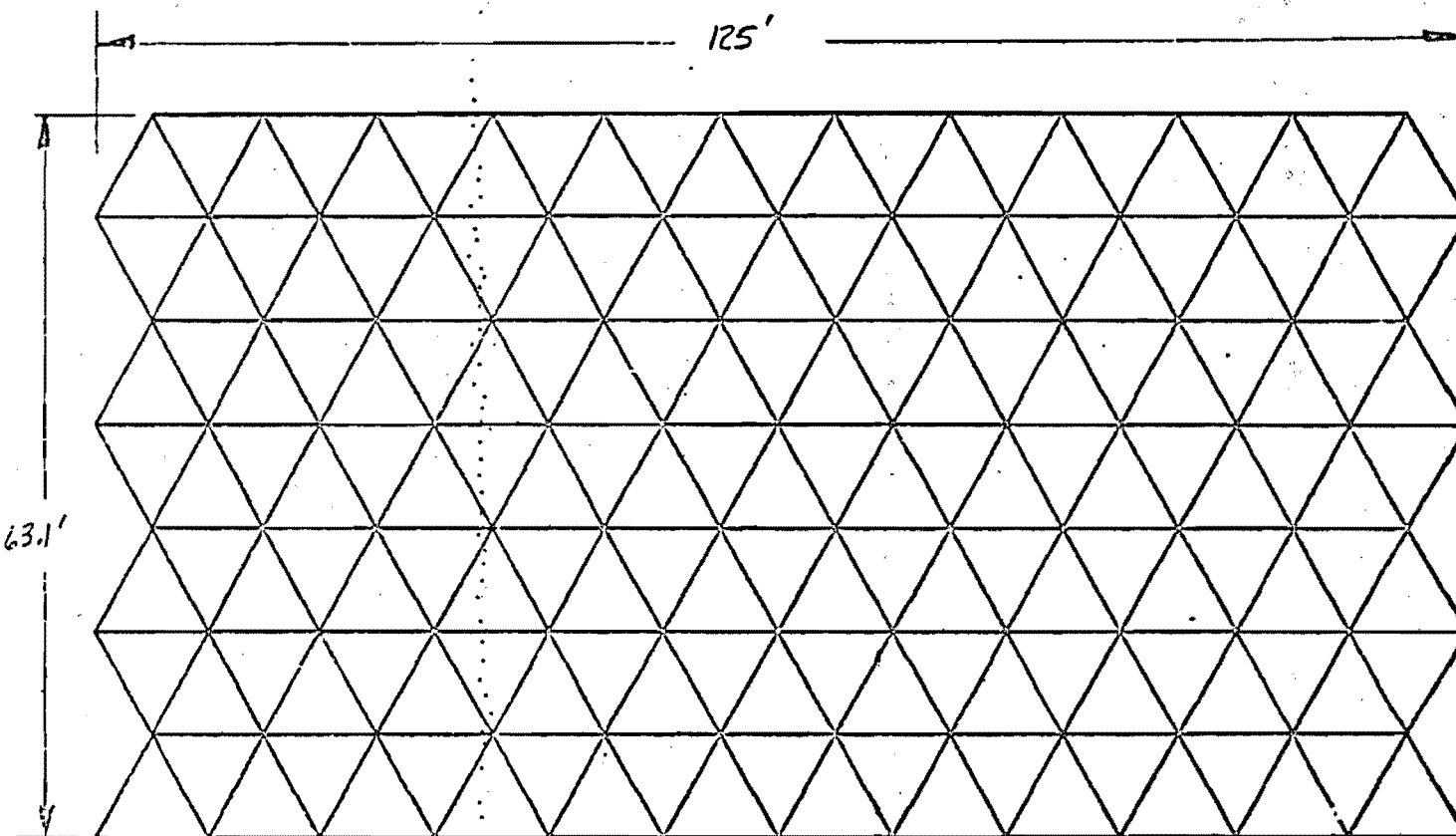
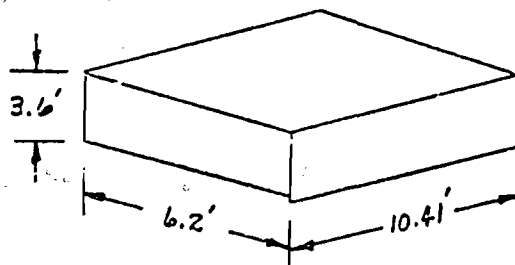


FIGURE 3.1.6 LOWER SURFACE OF TETRATRUSSE FRAME

length from both upper and lower surfaces will fold against a full length diagonal member. The diagonal members of the truss do not fold. There should not be any interference between the upper and lower folded members since they are rotated 30° from each other. Therefore, the total packaged length of the truss is the length of the diagonal member. The maximum packaged dimensions for a single truss are shown in the following sketch

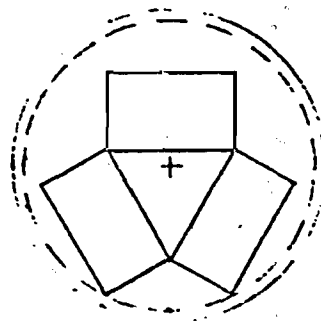
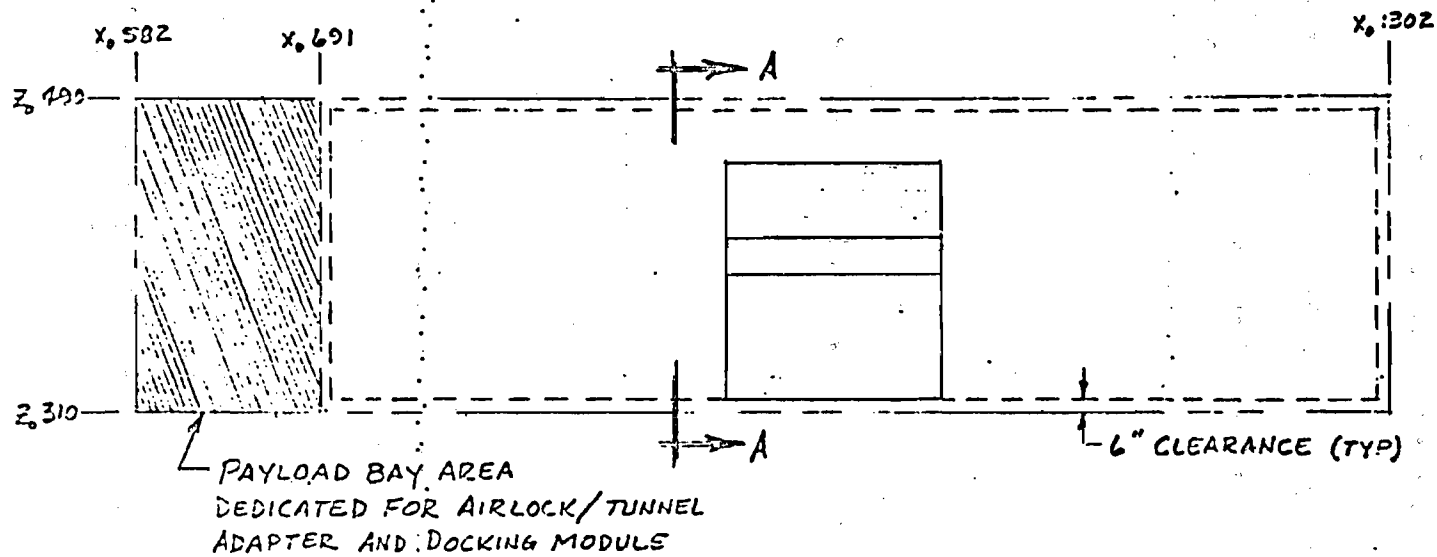


The three required Space Station trusses will fit in the shuttle cargo bay with room for other equipment as shown by the proposed scheme of figure 3.1.7.

3.1.9 Deployable Joint and Fitting Study

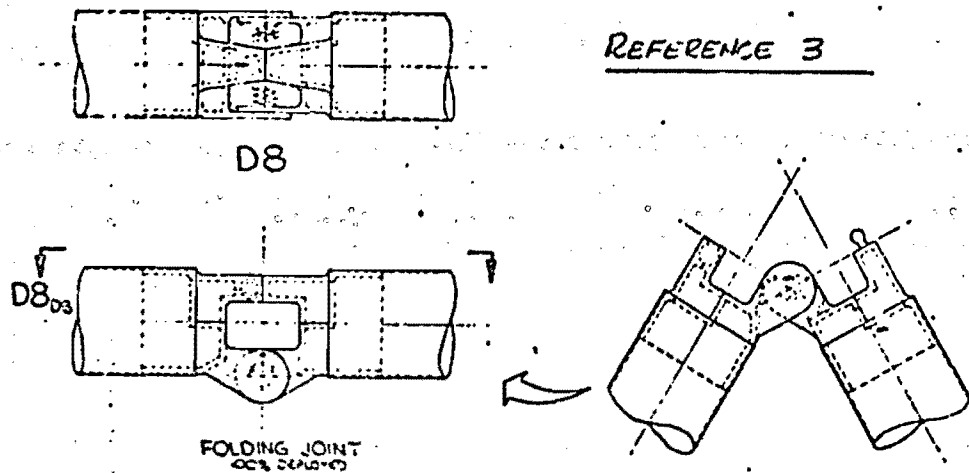
References 3, 4, and 7 present concepts for the deployable joint and fitting designs that will allow compact packaging of the Tetratruss frame. The basic requirements for the deployable joint are that it allows compact folding, automatic and reliable deployment in a space environment, and provide a rigid member when fully deployed.

Figure 3.1.8 shows the foldable joint concepts presented by references 3 and 4. The joints discussed in

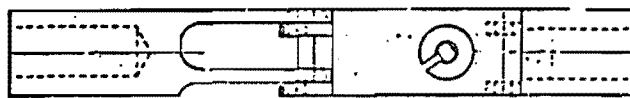


SEC A-A

FIGURE 3.1.7 TRUSS PACKAGING SCHEME FOR TRANSPORT



ORIGINAL PAGE IS
OF POOR QUALITY



REFERENCE 4

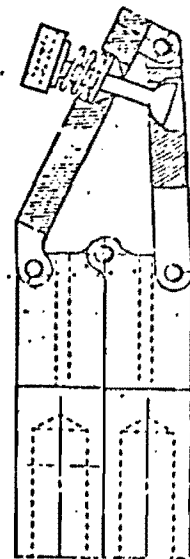
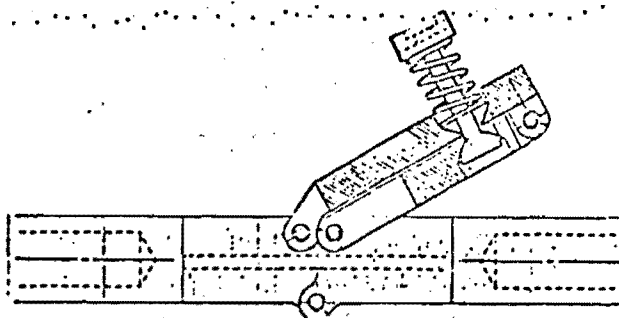
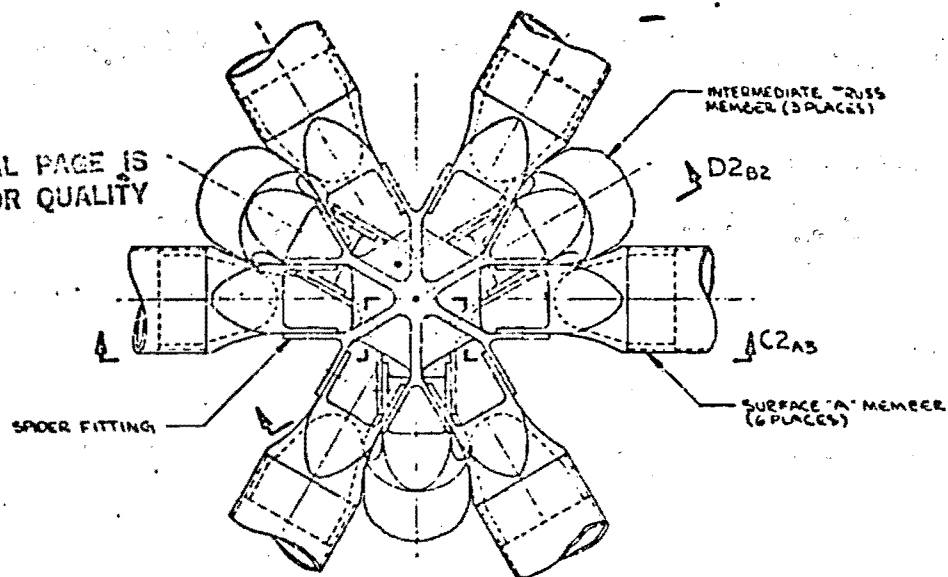


FIGURE 3.1.8 FOLDABLE MID JOINT CONCEPTS

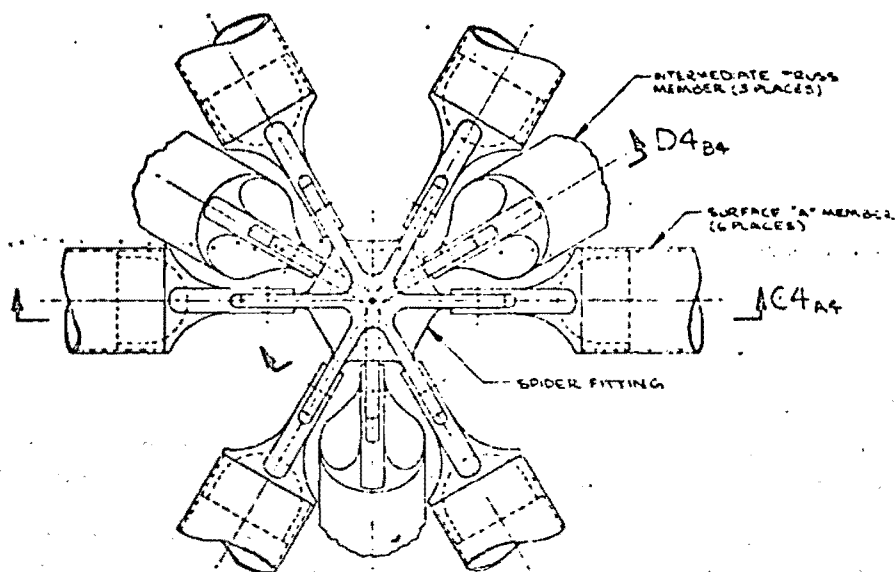
Reference 3 depicts a spring loaded "cabinet door" ball and socket locking mechanism. This concept envisions the socket side of the hinge as a capsule, containing an adhesive that would be ruptured on contact allowing the material to cure and firmly hold the ball in a locked position. This idea would indeed produce a rigid joint but probably produce an undesirable cloud of adhesive spray particles in the space environment. It appears possible to improve on this design and provide a locking mechanism that is not dependant upon an adhesive for rigidity. The joint of reference 4 shows a spring loaded scissors mechanism that will deploy the joint and hold the member in an extended position. It appears that it would require a substantial tensile load in the member to open the spring loaded scissors joint once it has been deployed; however, the joint is not totally rigid. This particular design is a refinement of a design used on the SEASAT synthetic aperture radar extendable support structure. The main refinement is a reduction of the packaged hinge into a cross sectional area no larger than the members to which it is attached.

Figure 3.1.9 and 3.1.10 show central node fittings as proposed by reference 3 and 4, respectively. An additional requirement for this fitting is to have the ability to secure payloads and equipment. The fittings of figure 3.1.9 seem to be the best suited for this requirement as the center of the fitting provides an unobstructed and adequate area for the addition of male or female docking hardware. Also, reference 3 indicates that

ORIGINAL PAGE IS
OF POOR QUALITY



IB3-2
PLAN VIEW
WIDE MOUTH SPIDER FITTING
(SCALE 1/1)



3B3-2
PLAN VIEW
PIN JOINT SPIDER FITTING
(SCALE 1/1)

FIGURE 3.1.9 CENTRAL NODE FITTING (REF 3)

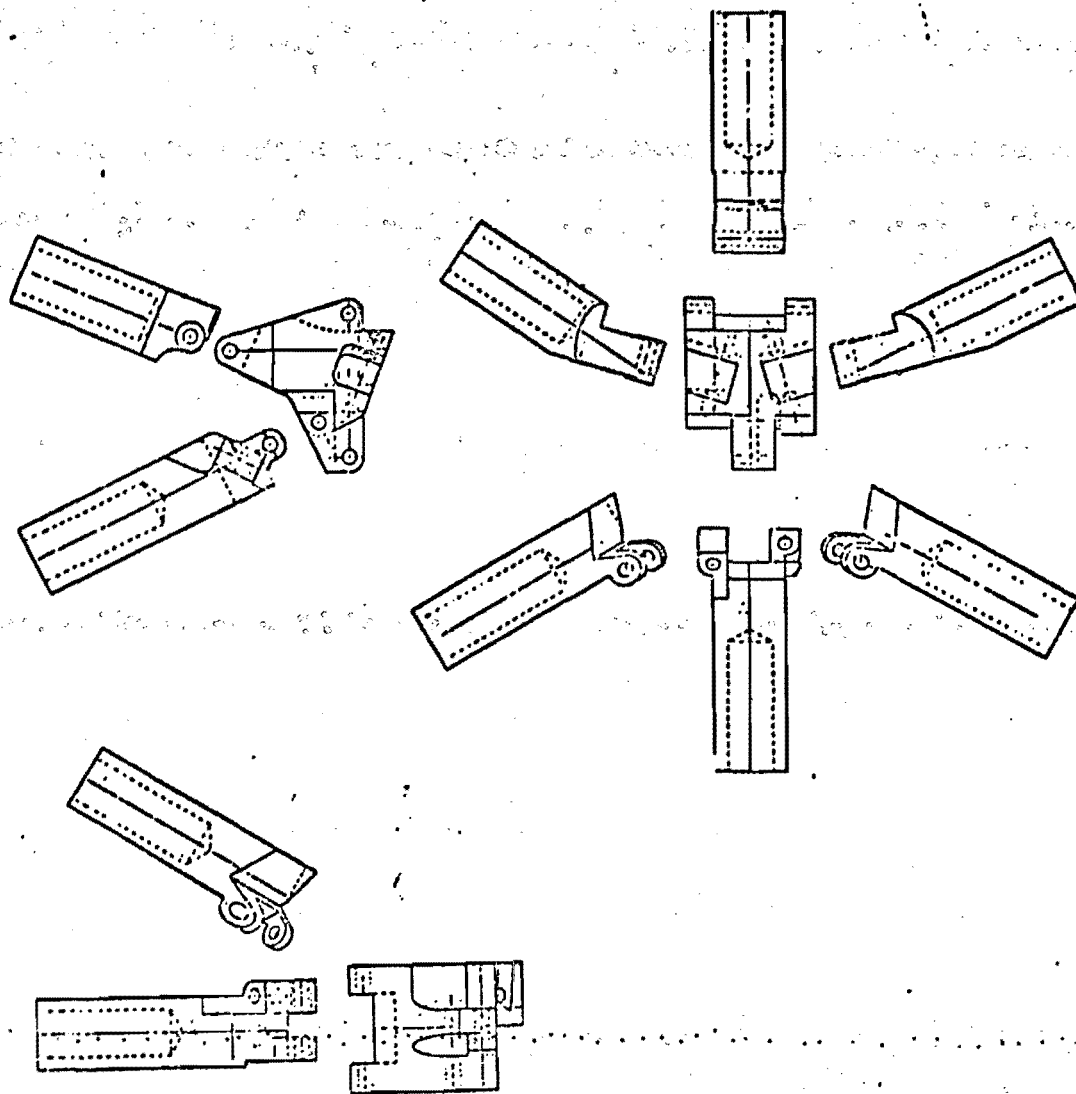


FIGURE 3.1.10 CENTRAL NODE FITTING (REF 4)

these clustered fittings have been manufactured for testing from injection molded graphite reinforced thermoplastic materials indicating a low cost approach to the design. The fitting of figure 3.1.10 indicates a very busy and costly concept requiring complicated machining not only for the node fitting itself but also for the member end fittings. It would appear that a node fitting concept chosen from figure 3.1.9 would be more desirable for the Space Station.

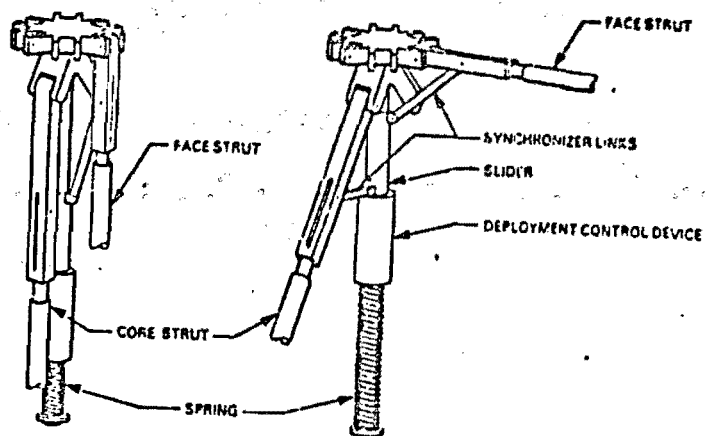
Figure 3.1.11 shows an umbrella-type truss deployment scheme from reference 7. This approach would provide the spring energy at the truss node fittings so that the deployment springs at the member hinge joints depicted in figure 3.1.8 could be eliminated and replaced with positive mechanical locks.

3.1.10 Space Deployment Concept

Deployment of the Space Station truss framework can be accomplished in two phases. The first phase consists of removing the packaged truss scheme depicted in figure 3.1.7 from the payload and rotating the three trusses forward 90° as shown in figure 3.1.12. The three common frame corners shown in figure 3.1.12 (a) (which are also frame edge node joints), are hinged by a ball-and-socket joint to allow the forward rotation. As the frames are rotated, the other frame edge node joints will lock into place by a mechanism similar to an automobile hood or trunk latch, one frame side containing pins and the other frame side

STOWED

DEPLOYED



STOWED

PARTIALLY DEPLOYED

DEPLOYED

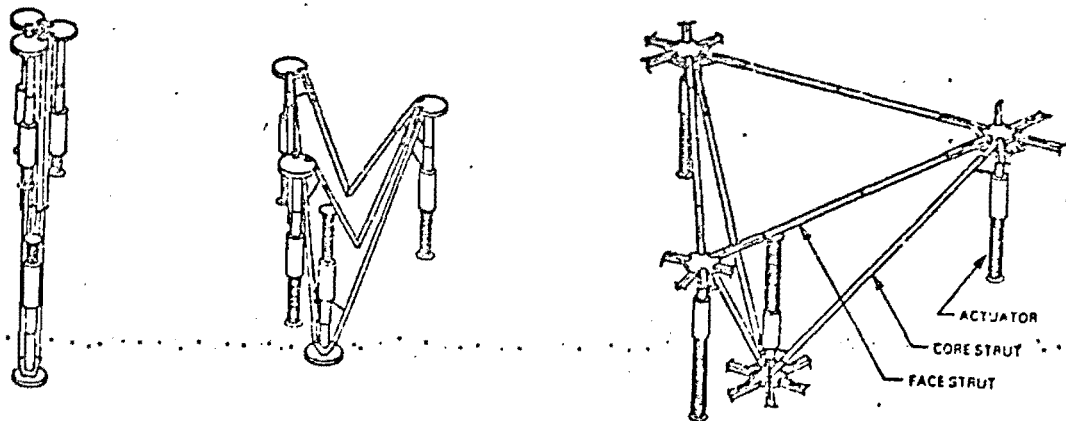


FIGURE 3.1.11 TRUSS DEPLOYMENT MECHANISM
(REF 7)

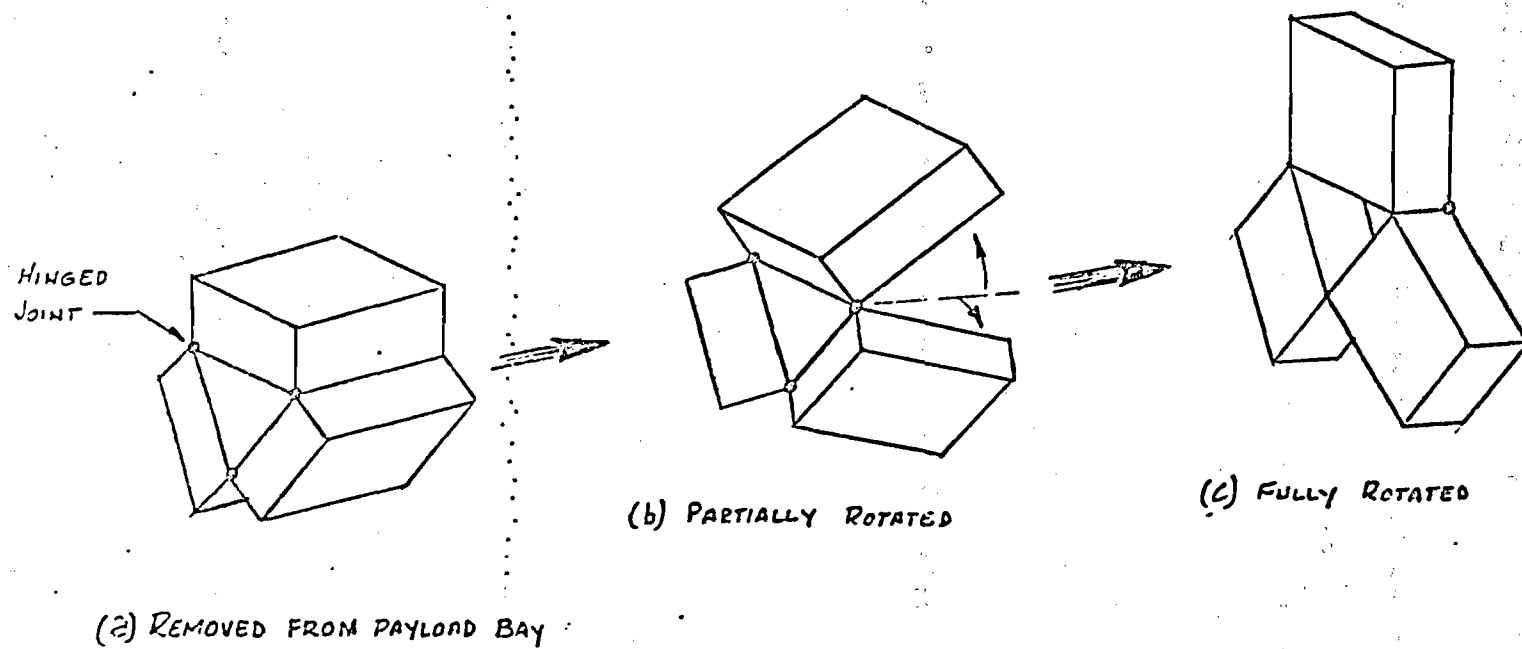


FIGURE 3.1.12 TRUSS DEPLOYMENT FROM THE ORBITER PAYLOAD BAY

contains the latching hooks. It is anticipated that this phase of the deployment will require astronaut assistance since an automatic rotating system would impose an unnecessary weight penalty to the payload.

The second phase of the deployment scheme is shown in figure 3.1.13 where the truss work is extended. The frames will expand outward as well as longitudinally. Because of the simultaneous double translation of the frames, it is not expected that the trusses can be deployed sequentially. This is the critical phase of the deployment scheme that requires that all members of the truss unfold at the same time to prevent binding. In addition, the energy contained in the deployment mechanisms must be attenuated toward the end of the deployment cycle to damp inertia loads in the joints. It is expected that the only astronaut assistance that would be required for this phase is the final inspection of the frames for damage and complete deployment. As stated earlier, the Tetratruss concept is a highly redundant structure so that the damage incurred by any strut member or joint... will not cause a complete loss of the structure. It should also be pointed out that the truss is repairable.

The expandable Tetratruss concept is feasible for the Space Station frame structure; however, only limited models of the concept have been built. The technology of the large planar truss is available but needs to be proven, particularly with the

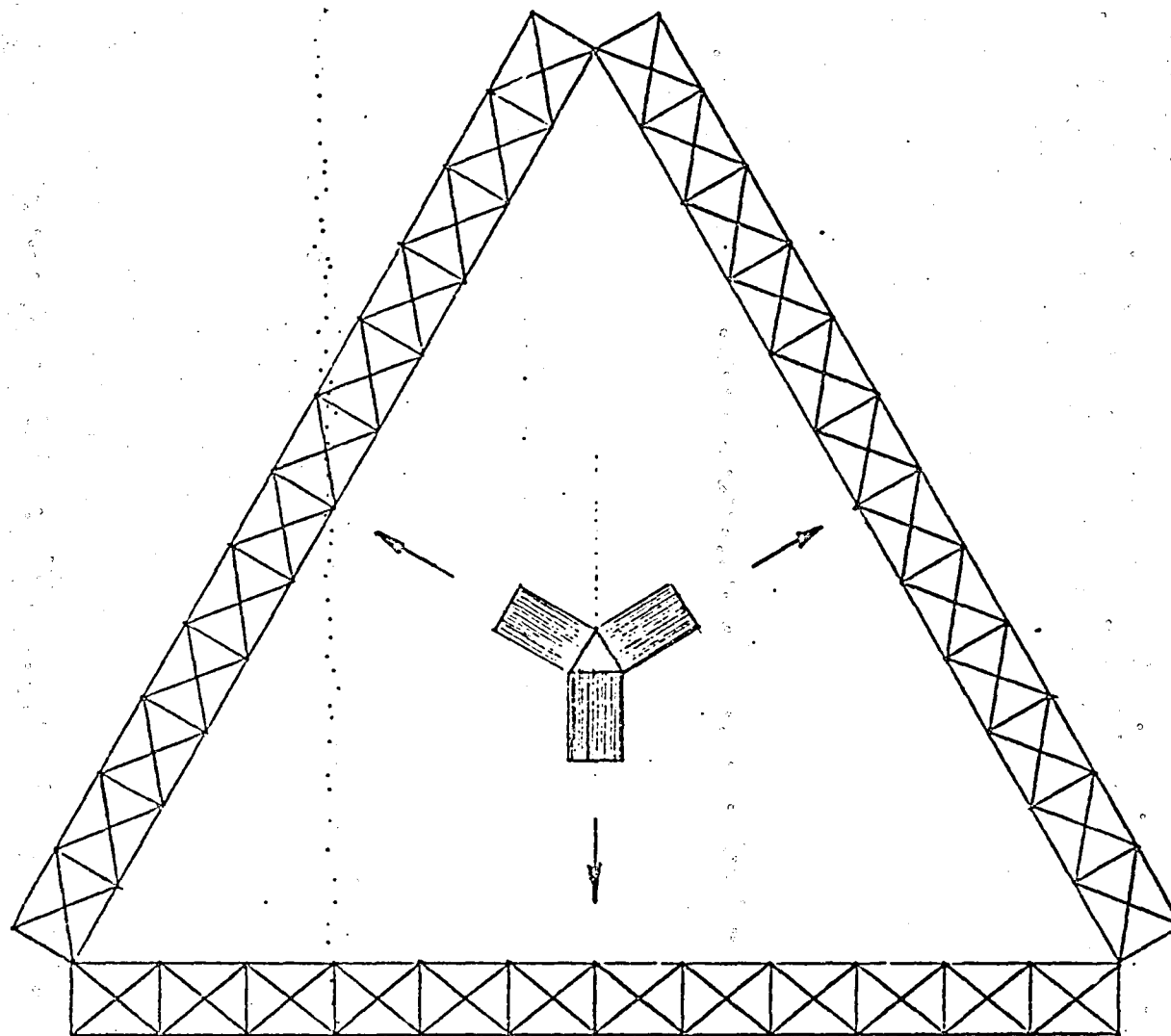


FIGURE 3.1.13 ORBITING SPACE STATION FRAME
STRUCTURE DEPLOYMENT

mechanisms involved. Therefore, the concept needs to be evaluated with respect to building a large planar truss and testing the deployment characteristics in the near zero-g environment of a water tank.

3.1.11 Conclusions and Recommendations

Analysis and rationale have been presented in this section that support the feasibility of constructing the large planar framework to meet the requirements of the proposed Space Station. Based on this concept and analysis, it was found that these large frames do not necessarily have the same stringent requirements imposed on them that some of the industry reports used for their concepts. For example, the reports indicate that the frames are primarily used for support of solar arrays and antennas suspended by long structural booms which would inherently be critical for dynamic and thermal loading. The present concept not only provides a well secured substructure for the solar array but also provides planar area for work platforms and storage support. Consequently, the dynamic requirement to form a stable surface is only with respect to coupling with other dynamic systems of the space station. Preliminary thermal analysis of the space station has shown that the maximum expected temperature is only 150°F which is almost negligible as far as degradation of frame material properties is concerned, and with the proper choice of composite material composition and lay-up direction, the resulting thermal deflections can be considered negligible.

Investigation of frame concepts proposed by industry shows that the only scheme available for the automatic deployment of a large planar area without a great amount of astronaut assistance is the Tetratruss design which was baselined for this study. Evaluation of all the reported concepts indicated that a minimum EVA requirement was the only real separator for the design as all concepts could be made to serve the Space Station purpose. However, some would require several launches to transport the total Space Station framework to orbit. In addition, the Tetratruss concept was the only design that offered a structurally redundant system that could allow severe damage to the truss members without losing the system.

The critical design load conditions for the Tetratruss Space Station concept considered payload docking, thermal, dynamic, gravity gradient, and orbital transfer. It was determined from these conditions that payload docking and dynamic loads were the most critical for the individual frame members. An analysis was made of a typical Tetratruss node joint using an assumed combined limit docking and dynamic loading of 1000 pounds normal and 500 pounds lateral to the node. Since the structure is statically indeterminate, a computer solution was obtained which showed that the maximum member design load is 491 pounds limit in tension or compression. This figure was rounded up to ± 500 pounds for the member sizing analysis. A safety factor of 1.4 was used for ultimate sizing. For economy of manufacturing, all truss

members are proposed to be identical. This will impose a weight penalty for those members showing a lower design load, but adds conservatism to the redundant structure.

Comparison of various materials that could be used in the manufacture the truss members revealed that those best suited to meet the proposed requirements were the graphite/epoxy and graphite/aluminum composites. The most important parameter for this comparison study was the low coefficient of thermal expansion which allowed negligible thermal displacements. Material strength at operating conditions, while not all that important at the estimated temperatures and relatively low member loads, was also included as selection criteria along with the high stiffness needed for a high natural frequency. Graphite/epoxy composite was selected over the graphite/aluminum composite primarily due to the expected cost of materials and manufacture. A detailed analysis of cost comparisons will have to be performed later.

Final sizing and analysis showed that the typical frame member is a 2.0-inch diameter tube with a .035-inch wall thickness and is 10.41 feet long. The critical failure mode is column buckling and shows a positive ultimate margin of safety of 1.77. The 2.0-inch diameter tube is made of 7 plies of graphite/epoxy tape for a balanced ply lay-up having a very low coefficient of thermal expansion. Using the density of .056 pounds/cubic inch for the composite, the weight of one tube is

1.54 pounds. The computer analysis indicates that there are 848 members per frame, therefore, the total weight of the Space Station framework is 4701 pounds which includes a 20% factor for the additional weight of member end fittings and node joints. Calculations for the frame natural frequency shows that the lowest frequency is 5.44 hertz and occurs for the condition of frame memberweight plus the distributed mass of the solar cells. This frequency is substantially higher than other Space Station concepts reviewed in the literature.

It has been shown in the preceding sections that the Tetratruss concept can be collapsed after its construction on the ground for storage in the shuttle cargo bay and deployed in space with a minimum EVA. The success of this concept is its dependability and reliability of the frame joints to deploy once the framework is in place outside the cargo bay. Figures 3.1.8, 3.1.9, and 3.1.11 depict joints and deployment mechanisms from the literature that are feasible; however, development of these mechanisms on larger scale models needs to be completed.

Therefore, it is recommended that a program be developed and initiated to fabricate several foldable joint designs and incorporate these designs into a subscale Space Station framework structure for evaluation of the most reliable and dependable performance.

3.1.12 References

1. NASA Conference Publication 2215 Part 1, Large Space Systems Technology 1981, Third Annual Review at NASA Langley Research Center, Hampton, VA, Nov. 16-19, 1981.
2. Jewell, R. E., "Deployable Platform Systems Development," Paper Presented in Reference 1, Page 219.
3. Large Space Erectable Structures, Final Report Contract NAS9-14914, April 1977, NASA Johnson Space Center.
4. Hedgepeth, John M., "Sequential Deployment of Truss Structures," Paper Presented in Reference 1, Page 179.
5. Mikulas, Jr., M. M., Bush, H. G., and Card, M. F., "Structural Stiffness, Strength, and Dynamic Characteristics of Large Tetrahedral Space Truss Structures," NASA TMW-74001, March 1977.
6. Advanced Composites Design Guide, Air Force Flight Dynamic Laboratory, Wright-Patterson Air Force Base, Ohio, Vol. 1, Design, Third Edition (Second Revision) January 1973, Chapter 1.2, Page 1.2.2.
7. "Large Space Programs," Presentation to NASA JSC Structures Division by R. R. Johnson of Lockheed Missiles and Space Company, Inc. on August 9, 1982.
8. Stebbins, Frederick J., "Characterization of Compression Elements of Large Space Structures," Johnson Space Center Structures Branch Report, ES2-81-1, August 1978.
9. Leissa, Arthur W., "Vibration of Plates," NASA SP-160, 1969.

3.2 Handling Equipment

During the normal everyday operations of the Space Station, it is necessary to move equipment, modules, pressure vessels fuel tanks, and other spacecraft components from one location to another. This requires handling equipment which would either be remotely operated or manned. In either case, the requirements are somewhat different from ground handling equipment such as cranes, forklifts, etc. Ground equipment must be designed for lifting objectives under one-G force field and then transporting those objects. Handling equipment for orbital operations need only to transport objects and then to position those objects to secure them. In the present Space Station configuration, the handling equipment should have a reach of about 100 feet and should have the capability of operating either on the inside or the outside of the station. A manipulator similar to the Shuttle Remote Manipulator System (RMS), but twice the size, is evaluated as a station RMS. These station manipulators will be attached to the edge of the Tetratruss midway between the apex modules. The dynamic effect of handling a 187 KIP payload was determined for this configuration including the loads and stresses at the base of the RMS.

3.2.1 Requirements (Goals)

- A) Two manned manipulators
 - o Handling OTV etc.
 - o Rescue Of one crew from an immobilized unit by the other unit
- B) Each manned manipulator should be capable of easy inside to outside conversion
- C) Each manned manipulator should be capable of reaching the base of the other (for rescue)
- D) Crew in each manipulator can operate in shirt sleeve environment
- E) Crew should be capable of EVA from manipulator
- F) Each manipulator shall be capable of docking with the
 - o Space Station module
 - o Orbiter
 - o The other manipulator
- G) Capability for one manipulator unit to relocate the other manipulator
- H) The manipulator chamber shall have sufficient gas storage to resupply chamber at least once
- I) The payload bay stowage should be based on minimum Orbiter flights
 - o Both manned manipulators should be launched in one mission without docking airlock in payload bay
 - o One manned manipulator should be able to be stowed with docking airlock in the payload bay

3.2.2 The Manipulator Concept

Two types of manipulator systems are considered

A. Manned Manipulator System - This system would have a manned capsule attached to the end of an articulated boom as shown in Figures 3.2-1 through 3.2-4. This capsule would be pressurized and would have its own life support equipment to provide a shirt sleeve environment for the operator. It would have the necessary controls so that it could be translated in any direction and would have the necessary pitch, yaw, and roll controls. Attached to this capsule would be a pair of manipulator arms operated by the man inside the capsule. This capsule would also have a standard docking port for personnel transfer (module to module, shuttle to module).

B. Remote Manipulator System - This system would be similar in design operation to that of the Shuttle RMS. The end of the manipulator could have an end effector, work platform, or grappling arms. It would be operated from within the Space Station module by direct vision and/or closed circuit TV.

There are advantages and disadvantages to either system. However, they both can use the same basic manipulator arms. This manipulator arm could be a specially designed arm based on the reach requirements and payload stowage, or it could be a scaled-up version of the Shuttle RMS.

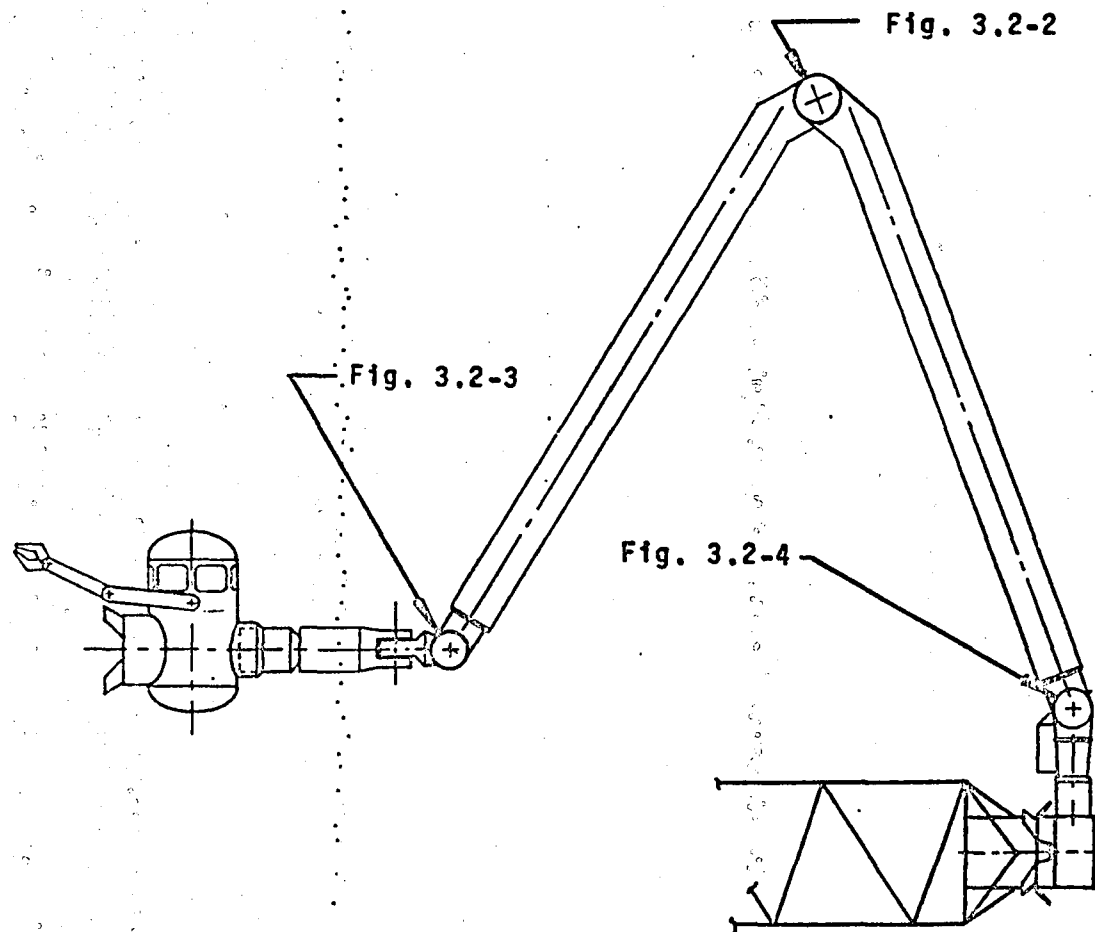


Fig. 3.2-1. Space Station Manipulator Concept.

ORIGINAL PAGE 19
OF POOR QUALITY

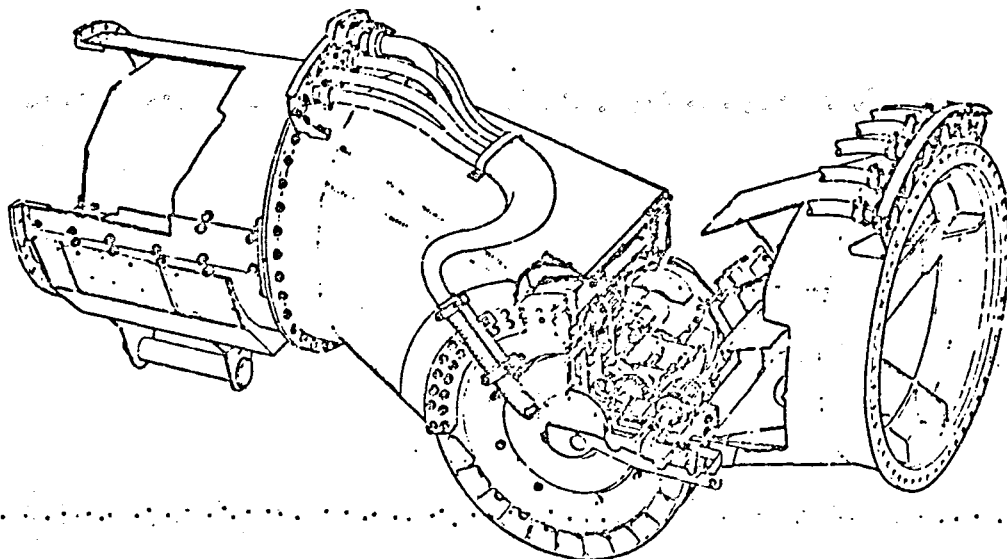


FIGURE 3.2-2 MANIPULATOR ELBOW JOINT

7075 - T73
ALUMINUM
FORWARD
ELECTRONICS
COMPARTMENT

GEARBOX
(TYPICAL)
CUSTOM 455
STEEL

7075 - T73
ALUMINUM
PITCH/YAW
TRANSITION

ROLL JOINT
7075 - T73
ALUMINUM

7075 - T73
ALUMINUM
TRANSITION
PIECES

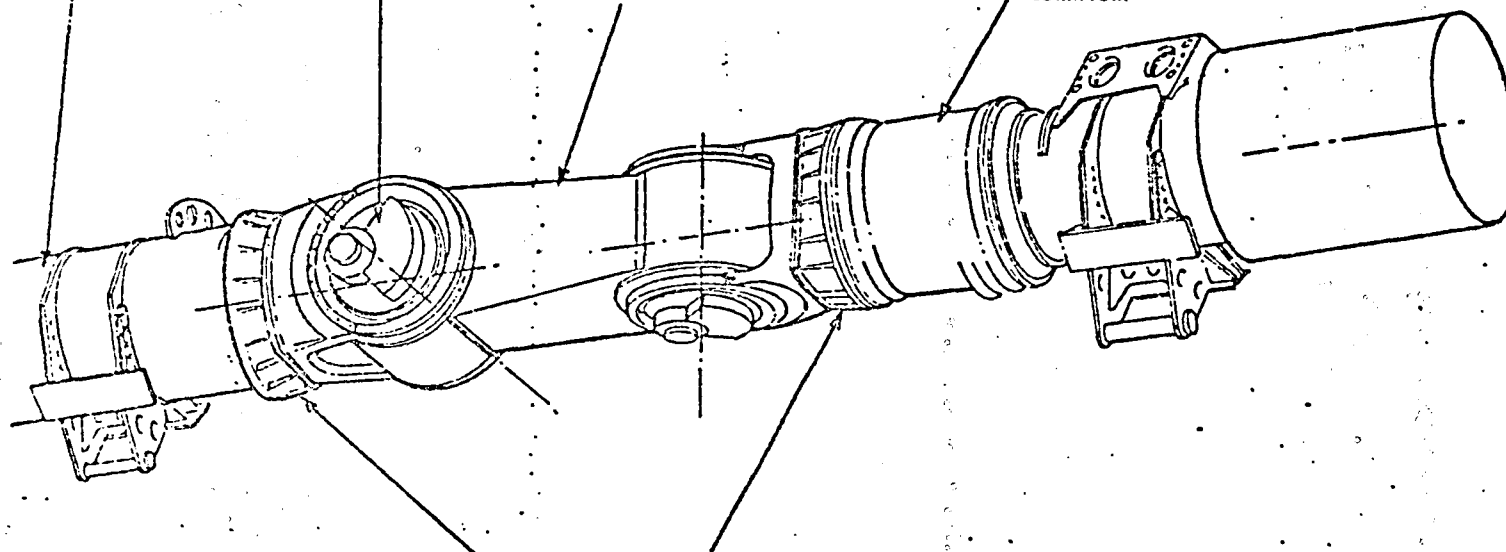


FIGURE 3.2-3 MANIPULATOR WRIST JOINTS

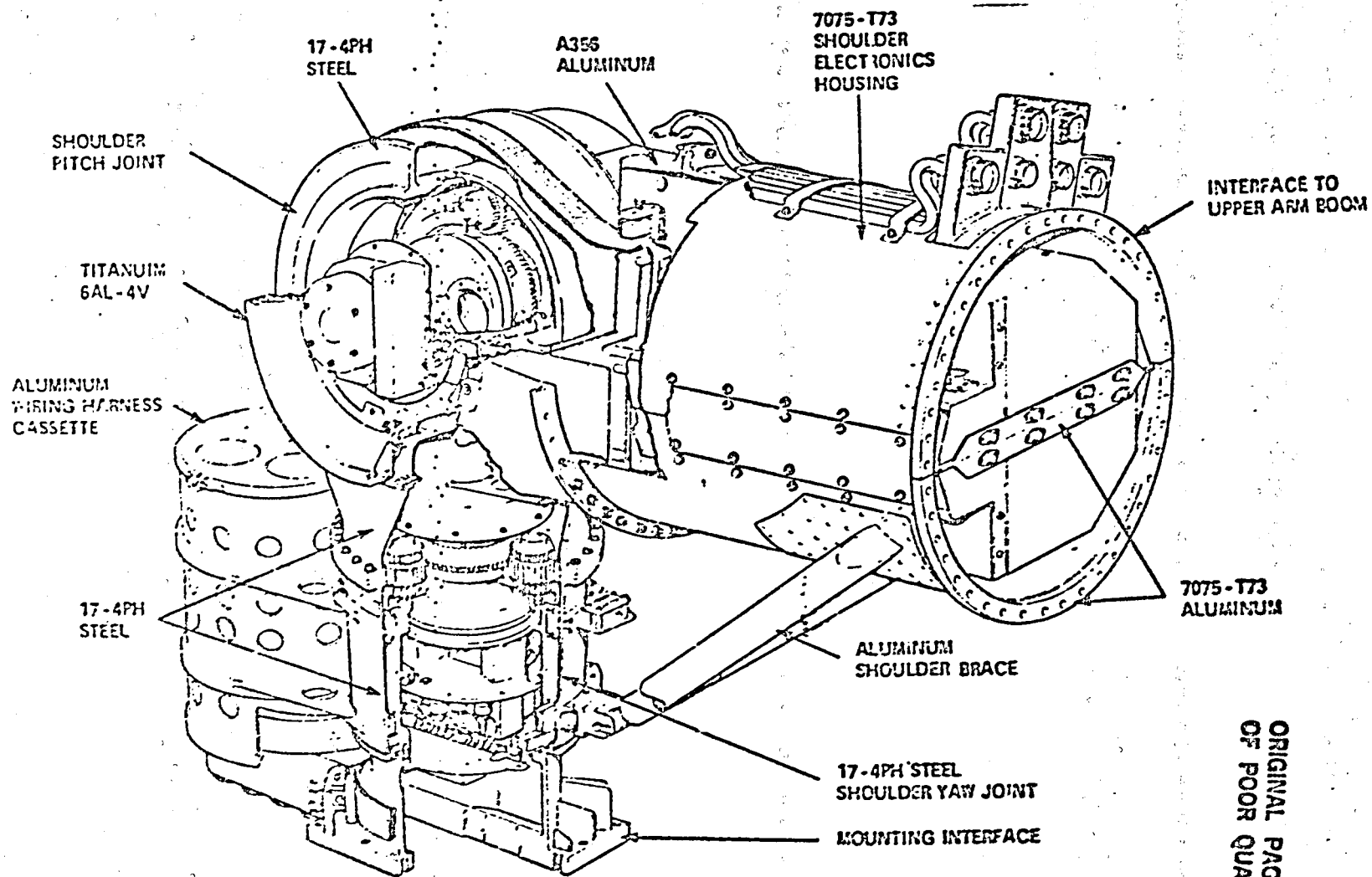
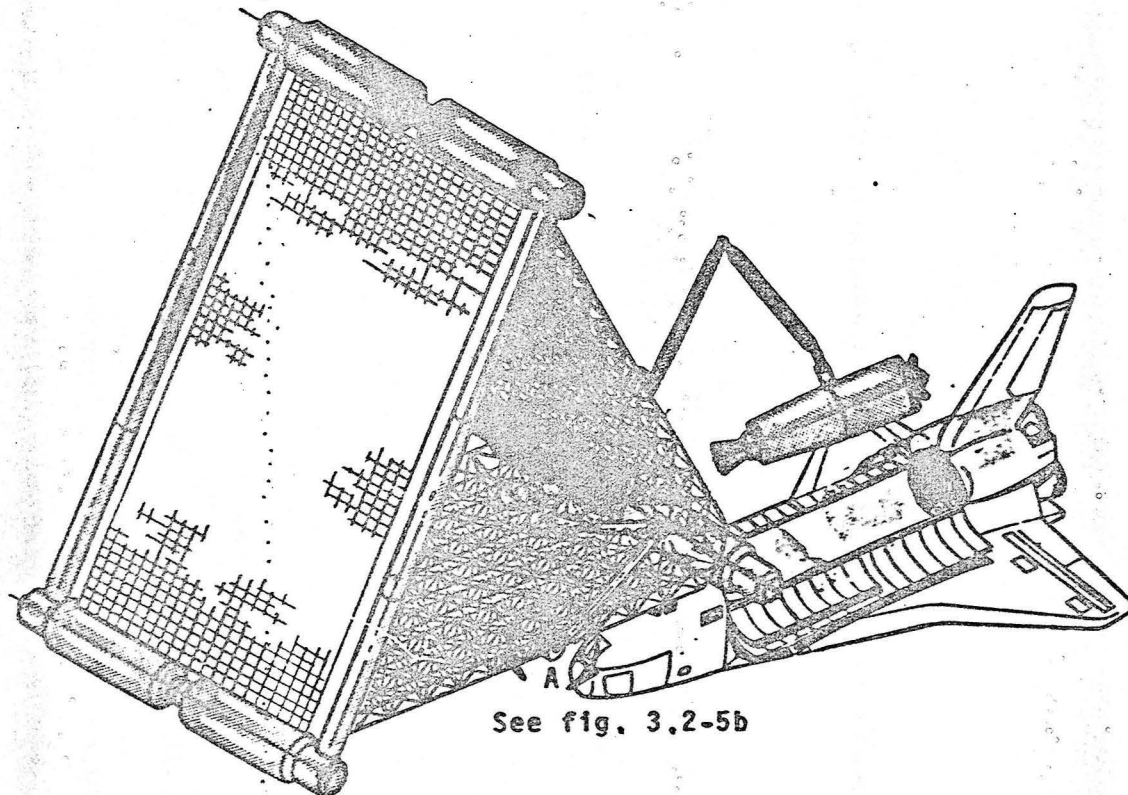


FIGURE 3.2-4 MANIPULATOR SHOULDER JOINT

ORIGINAL PAGE IS
OF POOR QUALITY

3.2.3 Loads And Stresses

The purpose of this section is not to show a thorough stress analysis of the manipulator system, but to evaluate the effect that the manipulator tip loads would have on the attachment to the Space Station structure. It is anticipated that these manipulators would be fastened on the edge of the tetratruss structure as shown in figure 3.2-5, midway between the modules. This location is the best for reach capability but the worst for structural loads and deflections. If this tetratruss is too flexible, the RMS response time will be too long; if the loads are too large, the tetratruss individual members may be too weak in Euler column buckling. The local members adjacent to the base attach structure of the manipulator can be increased in size. This section will evaluate the amount of local redesign required to insure strength integrity of the tetratruss structure and related it to the maximum excursion velocities which load the system.



See fig. 3.2-5b

Figure 3.2-5a. Space Station Showing Typical Locations of Manipulator Systems.

ORIGINAL PAGE IS
OF POOR QUALITY

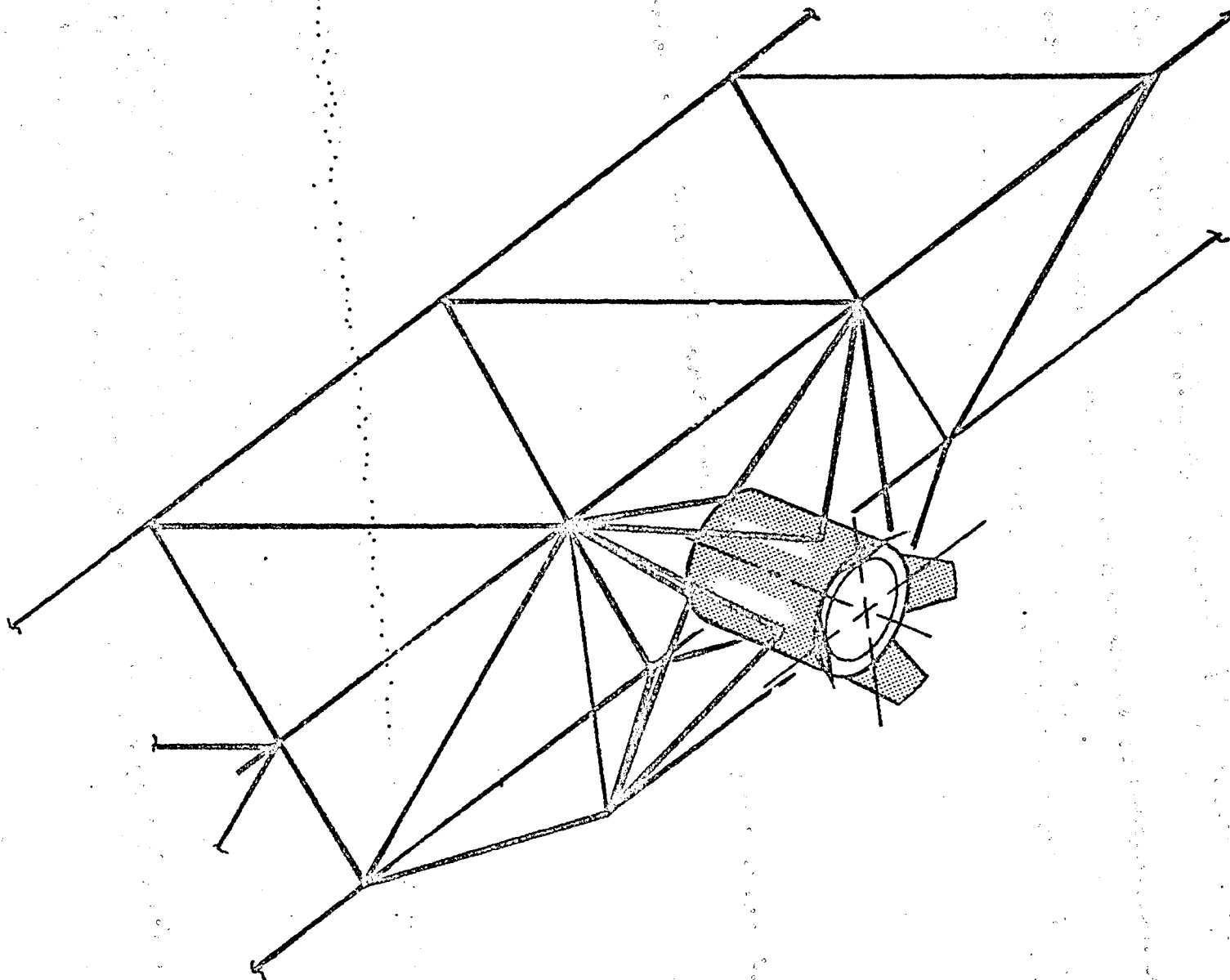


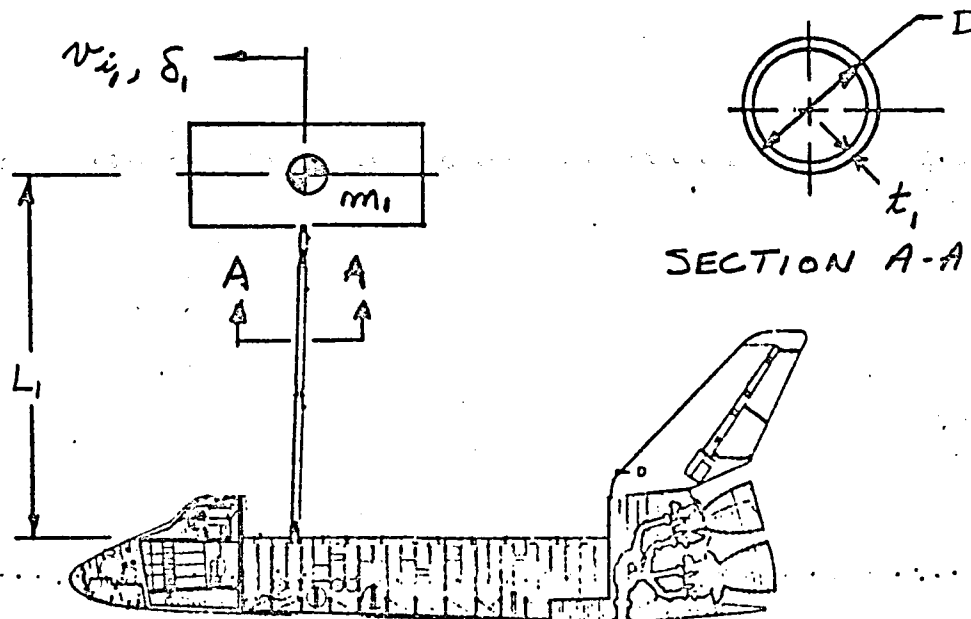
Figure 3.2-5b. Detail A, Base Attachment of Manipulator System.

PREPARED BY CJ WESSELSKI	NASA - Lyndon B. Johnson Space Center	PAGE NO. <u> </u> OF <u> </u>
CHECKED BY	STRESS ANALYSIS REPORT	REPORT NO.
DATE 8-17-82	TITLE	MODEL NO.
		DES NO.

REF.

3.2.3.1 OPERATIONAL STRESSES

SHUTTLE RMS CRITERIA AND DESIGN



FOR THE SHUTTLE, THESE VALUES APPLY:

$$L_1 = 57 \text{ FT}$$

$$D_1 = 15 \text{ IN}$$

$$t_1 = .05 \text{ IN}$$

IN AN EMERGENCY, BRAKES MAY BE APPLIED AT ALL JOINTS WITH THE ARM HANDLING A $m_1 = 32,000 \text{ lb}$ PAYLOAD AT A MAXIMUM VELOCITY OF $v_{1i} = .2 \text{ FT/SEC.}$

PREPARED BY C. J. WESSELSKI	NASA - Lyndon B. Johnson Space Center	PAGE NO. _____ OF _____
CHECKED BY	STRESS ANALYSIS REPORT	REPORT NO.
DATE 8/17/82	TITLE	MODEL NO.
		DES. NO.

REF.

3.2.3.1 OPERATIONAL STRESSES (CONT'D)

FOR THESE CONDITIONS, THE STOPPING DISTANCE, S_1 SHOULD BE LESS THAN 2.0 FEET. WHEN THE FLEXIBILITY OF THE ARMS AND JOINTS ARE CONSIDERED, THE TIP LOAD AT THE RMS END EFFECTOR IS $F_1 = 55$ LB.

SPACE STATION RMS CRITERIA AND DESIGN

REFER TO FIGURE 3.2-5 FOR A DYNAMIC MODEL. THIS TIME, FOR DESIGN LOADS, ASSUME THAT THE SHUTTLE IS AT THE END OF A MANIPULATOR ARM THAT IS SIMILAR TO THE BASELINE RMS EXCEPT THAT IT IS BIGGER. BASED ON A LAYOUT OF THE MANIPULATOR STOWED IN THE PAYLOAD, THE GEOMETRIC SCALE IS ABOUT 2.0.

ASSUME THEN A SCALE FACTOR = 2.0 ON ALL THE DIMENSIONS. ASSUME THAT THE BOOM MATERIAL IS GRAPHITE EPOXY, THE SAME AS FOR THE SHUTTLE RMS. SINCE THE MODULUS IS ONE-TO-ONE, IT IS DESIRED THAT THE STRESSES ALSO BE ONE-TO-ONE. TO OBTAIN THIS CORRELATION, THE MAXIMUM TIP FORCE MUST BE CHOSEN.

PREPARED BY CTWESSELSKI	NASA - Lyndon B. Johnson Space Center	PAGE NO. 67
ORIGINATED BY	STRESS ANALYSIS REPORT	REPORT NO.
DATE 8-18-82	TITLE	REVISION NO.
		FIG. NO.

REF.

3.2.3.1 OPERATIONAL STRESSES (CONT)

ORIGINAL PAGE IS
OF POOR QUALITY

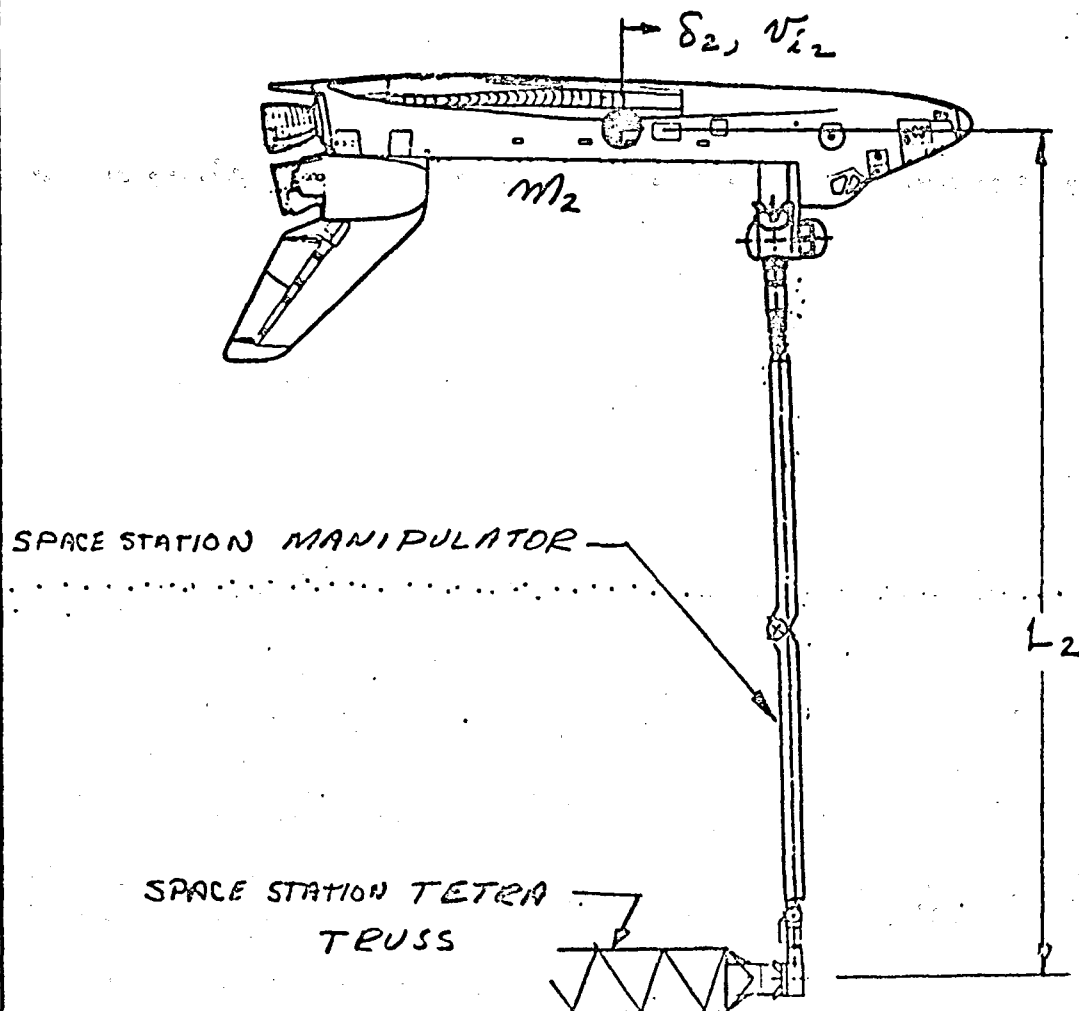


FIG 3.2-6. SPACE STATION MANIPULATOR DYNAMIC MODEL

PREPARED BY CJ WESSELSKI	NASA - Lyndon B. Johnson Space Center	PAGE NO. _____ OF _____
CHECKED BY	STRESS ANALYSIS REPORT	REPORT NO.
DATE 8-17-82	TITLE	REVISION NO.
		REVISION NO.

REF.

3.2.3.1 OPERATIONAL STRESSES (CONT)

FOR $\sigma_1 = \sigma_2$

THEN $\sigma_1 = \frac{M_1 C_1}{I_1} = \frac{M_2 C_2}{I_2}$

$\therefore \frac{M_2}{M_1} = \frac{I_2}{I_1} \frac{C_1}{C_2}$

LET THE MOMENTS BE

$M_1 = F_1 L_1, \quad M_2 = F_2 L_2$

AND $I_1 = \frac{\pi D_1^3 t_1}{8}, \quad I_2 = \frac{\pi D_2^3 t_2}{8}$

$\therefore \frac{F_2 L_2}{F_1 L_1} = \frac{\frac{\pi D_2^3 t_2}{8}}{\frac{\pi D_1^3 t_1}{8}} \frac{D_1/2}{D_2/2}$

$= \frac{D_2^2}{D_1^2} \frac{t_2}{t_1}$

AND $\frac{F_2}{F_1} = \frac{D_2^2}{D_1^2} \frac{t_2}{t_1} \frac{L_1}{L_2}$

$= 2^2 (2) \frac{1}{2} = 4.0$

SINCE THE MAX. TIP FORCE FOR THE SHUTTLE RMS IS 55 LB

$F_2 = 4 (55) = \underline{220 \text{ LB}}$

PREPARED BY CJ WESSELSKI	NASA - Lyndon B. Johnson Space Center	PAGE NO. _____ OF _____
CHECKED BY	STRESS ANALYSIS REPORT	REPORT NO.
DATE 8-17-82	TITLE	MODEL NO.
		TEST NO.

REF.

3.2.3.1 OPERATIONAL STRESSES (CONT)

OTHER VALUES FOR THE SPACE STATION
MANIPULATOR ARE

$$m_2 = 187,000 \text{ lb (ORBITER MASS)}$$

$$L_2 = 114 \text{ FT}$$

$$D_2 = 30 \text{ IN}$$

$$t_2 = 0.10 \text{ IN}$$

THE RELATIONSHIP BETWEEN THE
VELOCITY AND STOPPING DISTANCE
WILL NOW BE FOUND.

$$KE = \frac{1}{2} m_2 v_{i2}^2$$

FOR A CANTILEVER BEAM

$$U = \frac{F_L \delta_L}{2}$$

EQUATING U to KE WE HAVE

$$\frac{F_L \delta_L}{2} = \frac{m_2 v_{i2}^2}{2}$$

PREPARED BY CJ Wesselski	NASA - Lyndon B. Johnson Space Center	PAGE NO. 1 OF 1
DESIGNED BY	STRESS ANALYSIS REPORT	REPORT NO.
DATE 8-17-82	TITLE	BASE NO.
		ISS NO.

REF.

3.2.3.1 (CONT)

THEREFORE

$$\delta_2 = \frac{m_2 \dot{u}_{i2}^2}{F_2}$$

A FEW VALUES ARE TABULATED:

δ_2 , FT	\dot{u}_{i2} , FT/SEC
.5	.14
1.0	.19
1.5	.24
2.0	.28

OVERALL APPROACH

1. ASSUME GEOMETRIC SCALE FACTOR = 2.0
2. ASSUME BOOM STRESS OF SPACE STATION RMS TO BE SAME AS SHUTTLE RMS.
3. DETERMINE OVERALL SPRING RATE OF BOOM, JOINTS AND TETRATRUS.
4. DETERMINE EXCURSION VELOCITY BASED ON BRAKE SEIZURE.
5. DETERMINE TETRATRUS MEMBER LOADS & CHECK FOR STRENGTH & STABILITY.

PREPARED BY CTWESSELSKI	NASA - Lyndon B. Johnson Space Center	PAGE NO. <u> </u> OF <u> </u>
CHECKED BY	STRESS ANALYSIS REPORT	REPORT NO.
DATE 8-24-82	TITLE	ISSUED TO
		ISSUED BY

REF.

3.2.3.1.1 STIFFNESSES

3.2.3.1.1.1 SHOULDER JOINT

FOR THE ORBITER RMS

$$K_{ST} = 7.87 \times 10^5 \text{ FT-LB/RAD}$$

FOR THE SPACE STATION RMS WHICH IS TWICE AS BIG, USE A SCALE FACTOR OF 2.0 ON LENGTH AND A FACTOR OF 4.0 ON FORCE.

$$K_{ST} = 7.87 \times 10^5 (2)(4)$$

$$= 63 \times 10^5 \text{ FT-LB/RAD}$$

$$= 756 \times 10^6 \text{ IN-LB/RAD}$$

3.2.3.1.1.2 ELBOW JOINT

FOR THE ORBITER RMS

$$K_{EJ} = 7.36 \times 10^5 \text{ FT-LB/RAD}$$

AS BEFORE

$$K_{EJ} = 7.36 \times 10^5 \times 8$$

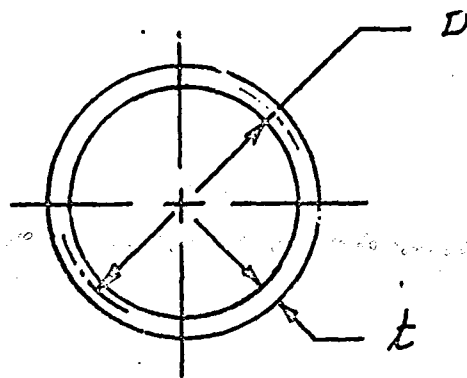
$$= 59 \text{ FT-LB/RAD}$$

$$= 708 \text{ IN-LB/RAD}$$

PREPARED BY CJ WESSELSKI	NASA - Lyndon B. Johnson Space Center	PAGE NO. _____ OF _____
DESIGNED BY	STRESS ANALYSIS REPORT	REPORT NO.
DATE 8-24-82	TITLE	FIGURE NO.
		TABLE NO.

REP.

3.2.3.1.1.3 BOOM



FOR THE SPACE STATION BOOM

$$D = 30 \text{ IN}$$

$$t = .10 \text{ IN}$$

$$E = 20 \cdot 10^6 \text{ lb/IN}^2$$

$$\therefore I = \frac{\pi D^3 t}{8} = \frac{\pi 30^3 (.10)}{8}$$

$$= 1060 \text{ IN}^3$$

$$\text{AND } EI = (1060) 20 \cdot 10^6$$

$$= \underline{2.1 \cdot 10^6 \text{ lb-IN}^2}$$

PREPARED BY CJ WESSELSKI	NASA - Lyndon B. Johnson Space Center	PAGE NO. _____ OF _____
CHECKED BY	STRESS ANALYSIS REPORT	REPORT NO.
DATE 8-24-82	TITLE	MODEL NO.
		DWG NO.

REF.

3.2.3.1.1.4 TETRATRUS

PLATE STIFFNESS

AS SHOWN IN FIG 3.2-7 THE TETRA-
TRUSS IS MADE FROM EQUAL ELEMENTS.
THE OVERALL PLATE STIFFNESS IS

$$D = \frac{\sqrt{3}}{4} E_c A_c l$$

WHERE E_c = MODULUS OF ELASTICITY OF
COLUMN MEMBERS

A_c = CROSS SECTIONAL AREA

l = LENGTH OF MEMBERS

FOR THESE VALUES:

$$E_c = 28 \times 10^6 \text{ PSI}$$

$$l = 10.41 \text{ FT} = 125 \text{ IN}$$

$$t_c = .025 \text{ IN}$$

$$d_c = 2.0 \text{ IN}$$

$$A_c = \pi d_c t_c = \pi (2.0) (.025) = .157 \text{ IN}^2$$

$$D = \frac{\sqrt{3}}{4} 28 \times 10^6 (.157) (124.9) = 169.8 \times 10^6 \text{ IN-LB}$$

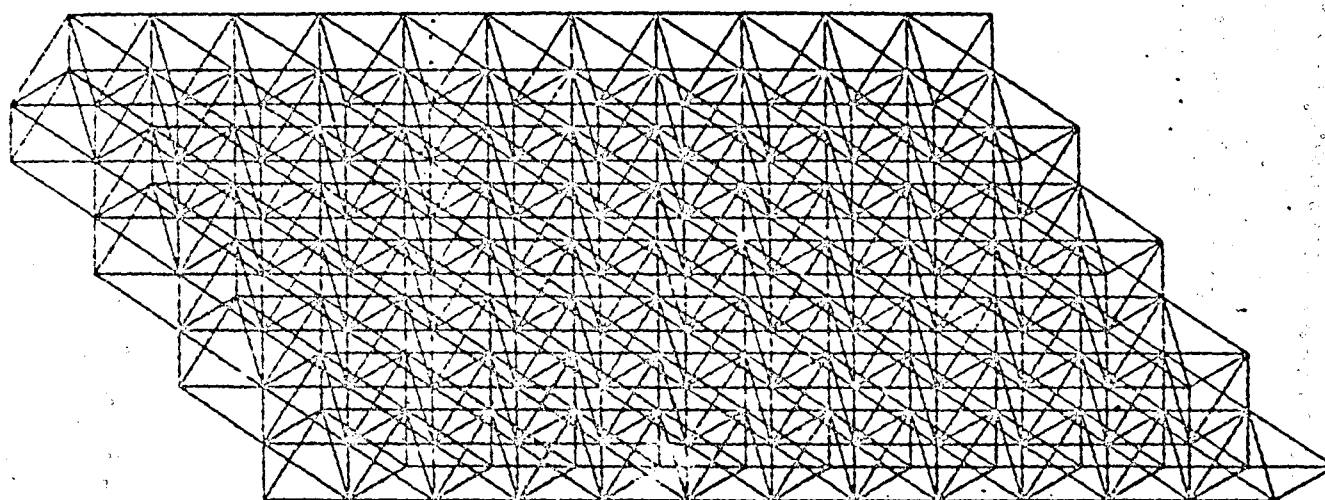


Fig. 3.2-7. Orthographic View of Tetra-truss.

PREPARED BY C J WESSELSKI	NASA - Lyndon B. Johnson Space Center	PAGE NO. 67
CHECKED BY	STRESS ANALYSIS REPORT	REPORT NO.
DATE 8-25-82	TITLE	REVISION NO.
		REV NO.

REF.

3.2.3.1.1.4 (CONT)

EQUIVALENT MODULUS

ASSUME THAT THE TETRAPOSS IS AN ISOTROPIC PLATE. CALCULATE THE EQUIVALENT MODULUS OF ELASTICITY. THE RELATIONSHIP OF PLATE STIFFNESS AND MODULUS AND THICKNESS, h , IS

$$D = \frac{E h^3}{12(1-\nu^2)}$$

ASSUME $\nu = 0$, THEN WITH $h = 102.1$ IN,

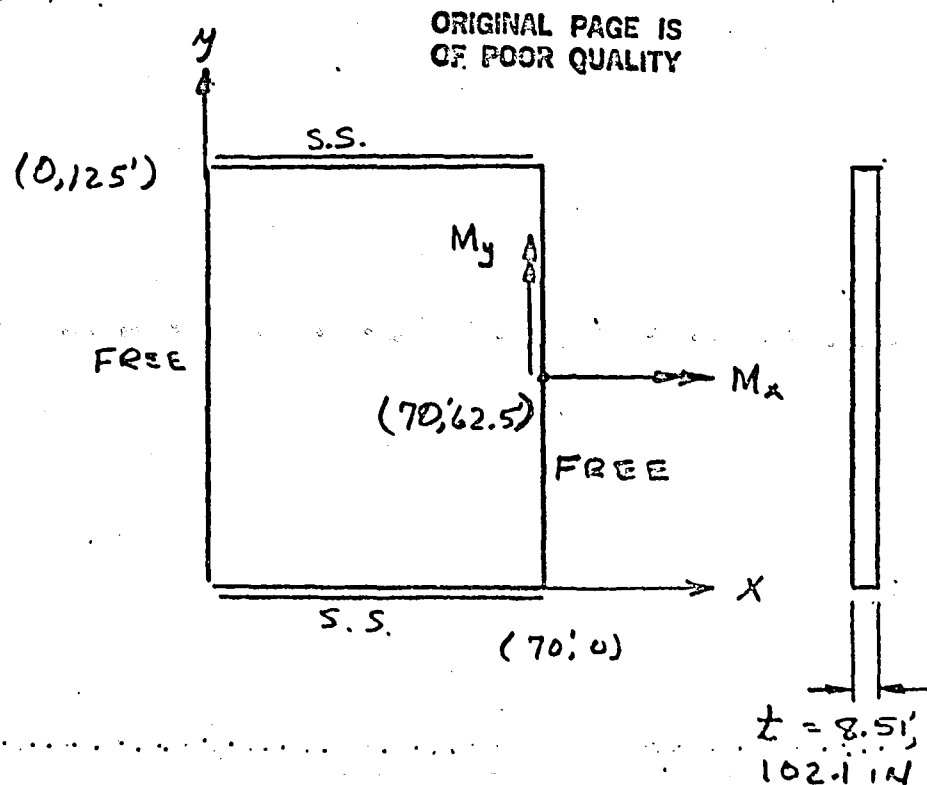
$$E = \frac{12 D}{h^3}$$

$$= \frac{12 (169.8) 10^6}{(102.1)^3} = 1914 \text{ PSI}$$

PREPARED BY C J WESSELSKI	NASA - Lyndon B. Johnson Space Center	PAGE NO. _____ OF _____
CHECKED BY	STRESS ANALYSIS REPORT	REPORT NO.
DATE 8-25-82	TITLE	MODEL NO.
		TEST NO.

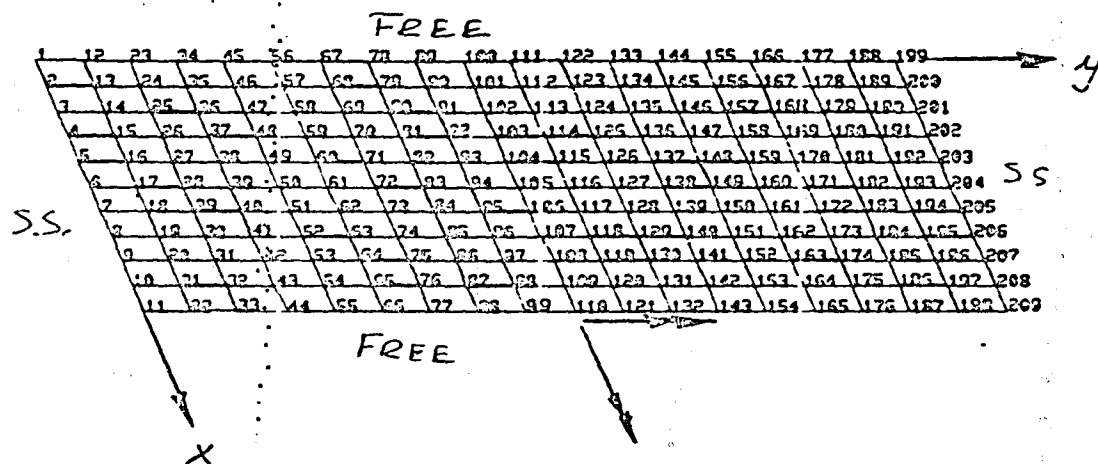
REF.

3.2.3.1.1.4 (CONT)



ASSUME THAT THE ABOVE ISOTROPIC PLATE ADEQUATELY SIMULATES THE TETRATRUS. THE TOP AND BOTTOM EDGES ARE ATTACHED TO THE CORNER MODULUS AND SIMPLE SUPPORTS ARE ASSUMED. THE LOAD IS APPLIED TO ONE OF THE FREE EDGES MIDSPAN ($X = 70'$, $Y = 62.5'$) FOR EACH OF THE MOMENTS, M_x , M_y . THE SPRING RATE, IN-IB/RAD, IS TO BE DETERMINED.

PREPARED BY C J WESSELSKI	NASA - Lyndon B. Johnson Space Center	PAGE NO. _____ OF _____
CHECKED BY	STRESS ANALYSIS REPORT	REPORT NO.
DATE 8-25-82	TITLE	FIG. NO.
		FIG. NO.
REF.	<p><u>3.2.3.1.1.4 (CONT)</u></p> <p>THE PLATE WAS MODELED AS SHOWN IN FIG 3.2-7. THE DEFLECTED SHAPES ARE SHOWN IN FIGURES 3.2-8 AND 3.2-9.</p> <p>THE VALUES OF THE SPRING RATES ARE</p> <p>$K_{\theta y} = 145 \cdot 10^6 \text{ IN-IB/RAD}$</p> <p>$K_{\theta x} = 200 \cdot 10^6 \text{ IN-IB/RAD}$</p>	



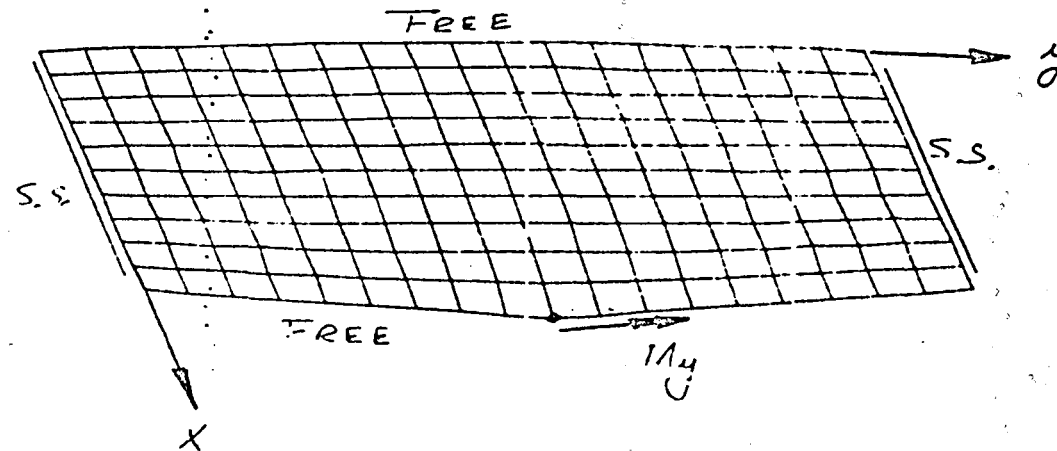
SPEC - FLAT PLATE -
3.1

0 249
SCALE

Fig. 3.2-8. Isotropic Finite Element Model of Tetra-truss.

MY AT CENTER OF FREE EDGE

ID=2/1/1



ORIGINAL PAGE IS
OF POOR QUALITY

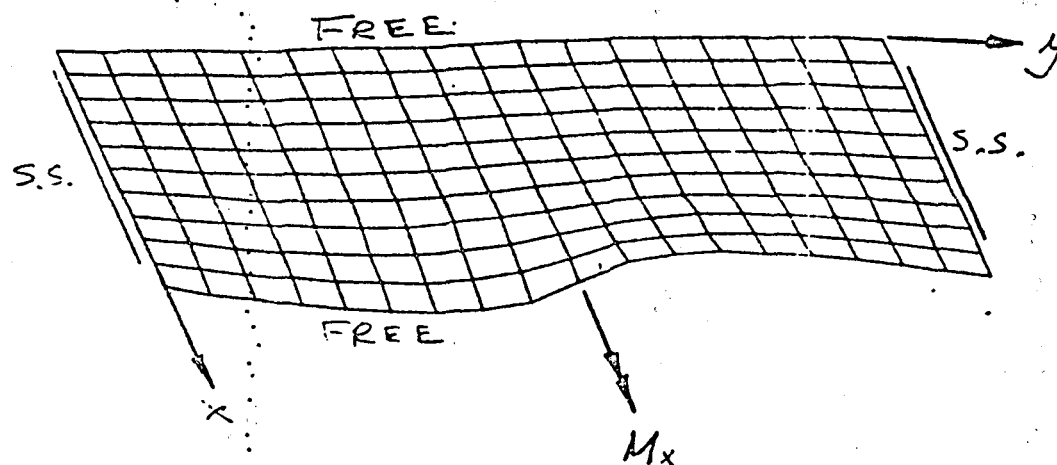
SPEC - FLAT PLATE -
3.1

0 254
SCALE

Fig. 3.2-9a. Deflected Shape Under M_y Load.

MX AT CENTER OF FREE EDGE

ID=1/1/1



SPEC
3.1

- FLAT PLATE -

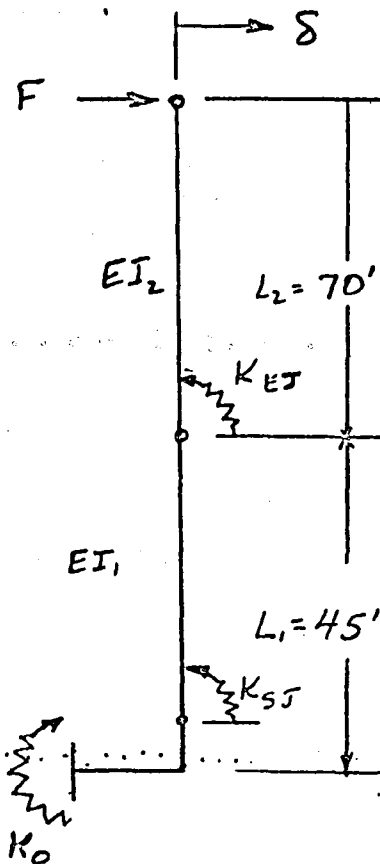
0 264
SCALE

Fig. 3.2-9b Deflected Shape Under M_x Load.

PREPARED BY CJ WESSELSKI	NASA - Lyndon B. Johnson Space Center	PAGE NO. 8F
CHECKED BY	STRESS ANALYSIS REPORT	REPORT NO.
DATE 8/23/82	TITLE	PROJECT NO.
		WORK NO.

REF.

3.2.3.1.1.5 TOTAL STIFFNESS



THE TOTAL DEFLECTION UNDER THE LOAD F IS

$$\delta = \frac{F(L_1 + L_2)^2}{K_0} + \frac{F L_2^2}{K_{EJ}} + \frac{F L^3}{3 EI_1} + \frac{F(L_1 + L_2)^2}{K_{SJ}}$$

PREPARED BY C J Wesselski	NASA - Lyndon B. Johnson Space Center	PAGE 19. OF
DESIGNED BY	STRESS ANALYSIS REPORT	REPORT NO.
DATE 8/23/82	TITLE	MODEL NO.
		UNIT NO.
REF.	<p><u>3.2.3.1.1.5 (CONT)</u></p> <p>FOR THE VALUES $L_1 = 540 \text{ IN}$ $L_2 = 840 \text{ IN}$ $EI_1 = 2.12 \cdot 10^{10} \text{ lb-IN}^2$ $K_0 = 145 \cdot 10^6 \text{ IN-lb/rad}$ $K_1 = 756 \cdot 10^5 \text{ IN-lb/rad}$ $K_2 = 708 \cdot 10^5 \text{ IN-lb/rad}$</p> $\frac{\delta}{F} = \frac{(540 + 840)^2}{145 \cdot 10^6} + \frac{840^2}{708 \cdot 10^5} + \frac{1380^3}{3(2.12) \cdot 10^{10}}$ $+ \frac{(540 + 840)^2}{756 \cdot 10^5} = .013 + .010 + .041$ $+ .025$ $= .089 \text{ in/lb}$ <p>FOR A LOAD, F, OF 220 lb</p> $\delta = 220 (.089) = \underline{\underline{19.6 \text{ IN}}}$	

PREPARED BY CJ WESSELSKI	NASA - Lyndon B. Johnson Space Center	PAGE NO. _____ OF _____
CHECKED BY	STRESS ANALYSIS REPORT	REPORT NO.
DATE 8-24-82	TITLE	REVISION NO.
		DESIGN NO.

REF.

3.2.3.1.2 MAXIMUM VELOCITY

AS GIVEN IN SECTION 3.2.3.1, THE TIP DEFLECTION, LOAD, MASS AND VELOCITY ARE RELATED AS FOLLOWS

$$\delta_2 = \frac{m_2 v_{i2}^2}{F_2}$$

$$\text{OR } v_{i2} = \left[\frac{\delta_2 F_2}{m_2} \right]^{1/2}$$

$$\text{FOR } F_2 = 220 \text{ lb}$$

$$m_2 = 187,000 \text{ lb}$$

$$\delta_2 = 19.6 \text{ in}$$

$$v_{i2} = \left[\frac{19.6/12 (220) 32.2}{187,000} \right]^{1/2}$$

$$= \underline{\underline{.249 \text{ FT/SEC}}}$$

THIS MEANS THAT THE SAME CRITERIA CAN BE USED FOR THE SPACE STATION AS FOR THE SHUTTLE RMS. I.E.,

$$v_{i2} < .2 \text{ FT/SEC}$$

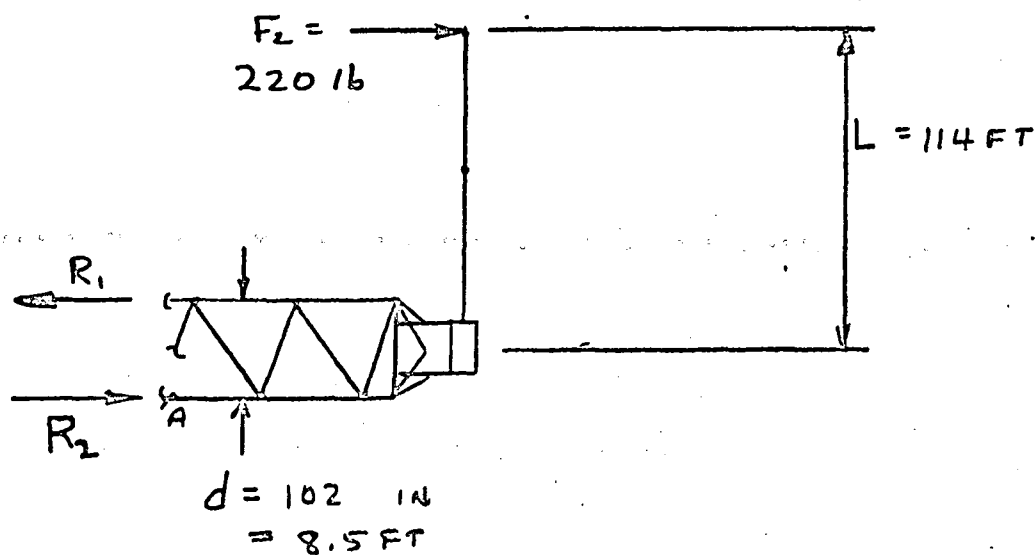
$$S_2 < 2 \text{ FT}$$

153

PREPARED BY	NASA - Lyndon B. Johnson Space Center	PAGE NO. _____ OF _____
CHECKED BY		REPORT NO. _____
DATE	TITLE	MODEL NO. _____
		TEST NO. _____

REF.

3.2.3.1.3 TETRA TRUSS MEMBER LOADS AND STRESSES



$$\sum \bar{M}_A = 0 = 220 (114 + 4.25) - R_1 8.5$$

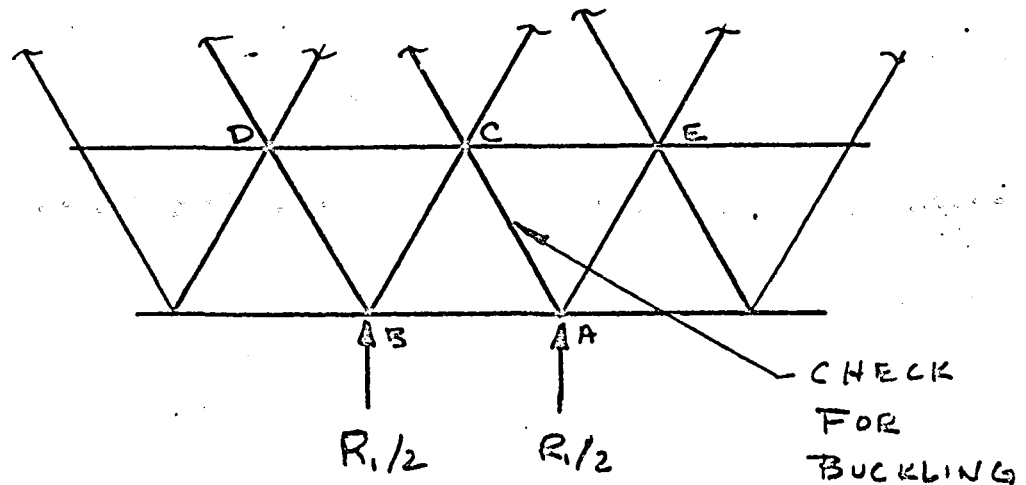
$$R_1 = \frac{220 (119.25)}{8.5} = \underline{\underline{3086 \text{ lb}}}$$

$$R_2 = R_1 - F_L = 3086 - 220 = \underline{\underline{2866 \text{ lb}}}$$

PREPARED BY CTWESSELSKI	NASA - Lyndon B. Johnson Space Center	PAGE NO. _____ OF _____
CHECKED BY	STRESS ANALYSIS REPORT	REPORT NO.
DATE 8-25-82	TITLE	MODEL NO.
		TEST NO.

REF.

3.2.3.1.3 CONT



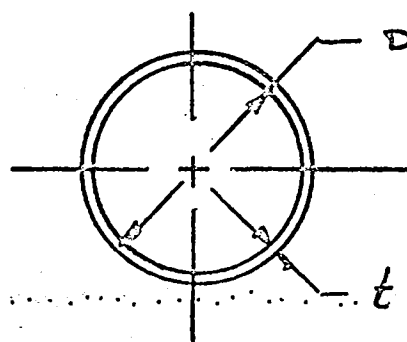
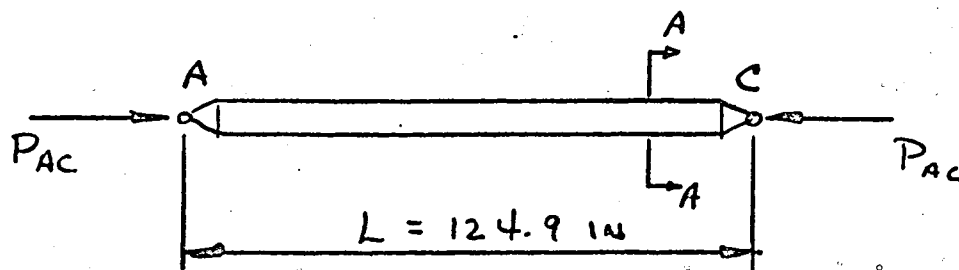
ASSUME THAT THE LOAD R_1 GETS FED
IN TO TWO NODE POINTS AS SHOWN.
THE INDIVIDUAL MEMBER LOAD (A TO C
FOR EXAMPLE) IS

$$\begin{aligned}
 P_{AC} &= \frac{R_1/2}{\cos 30^\circ} \div 2 \\
 &= \frac{3086/2}{2 \cos 30^\circ} = \underline{\underline{891.16}}
 \end{aligned}$$

PREPARED BY C J WESSELSKI	NASA - Lyndon B. Johnson Space Center	PAGE NO. 1 OF 1
DESIGNED BY	STRESS ANALYSIS REPORT	REPORT NO.
DATE 8-25-82	TITLE	REV. NO.
		REV. D.

DEF.

3.2.3.1.3 (CONT)



SECTION A-A

THE CRITICAL EULER BUCKLING LOAD IS

$$P_{CR} = \frac{\pi^2 EI}{L^2}$$

PREPARED BY C J WESSELSKI	NASA - Lyndon B. Johnson Space Center	PAGE NO. <u> </u> OF <u> </u>
CHECKED BY	STRESS ANALYSIS REPORT	REPORT NO. <u> </u>
DATE 8-25-82	TITLE	REVISION NO. <u> </u>
		DESIGN NO. <u> </u>

REF.

3.2.3.1.3 (CONT)

USE THESE VALUES

$$E = 28 \times 10^6 \text{ PSI}$$

$$D = 2.0 \text{ IN}$$

$$L = 125 \text{ IN}$$

$$t = .035 \text{ IN}$$

$$I = \frac{\pi (2.0)^2 (.035)}{8} = .11 \text{ IN}^4$$

$$P_{cr} = \frac{\pi^2 (28 \times 10^6) (.11)}{124.9^2} = 1392 \text{ lb}$$

FOR A S.F. = 1.5

$$MS = \frac{1392}{891(1.5)} - 1 = \underline{\underline{+.04}}$$

3.2.4 Manipulator Operations

When the Space Station is servicing OTV vehicles, or when the Shuttle is coming in or going out of the Space Station, or when equipment is stowed or rearranged, many manipulator operations will be necessary. Objects of various sizes and weights will have to be moved from one location to another to perform the various tasks. Different types of basic operations are described in the following sections.

3.2.4.1 OTV Handling

A concept for handling OTV and component parts is shown in figure 3.2-10. In these operations, heavy mass items such as fuel tanks will have to be moved about and assembled to one another. These operations can be greatly facilitated by a manned manipulator since some EVA may be necessary. The manned capsule provides a station from which local EVA is performed.

3.2.4.2 Moving Base of Manned Manipulators

Depending on the task, the manipulators may need the capability of reaching any object on the Space Station configuration, inside or outside. However, if two manipulators are used, not all areas are accessible. It would be desirable if one or both manipulators could change their base location. There are practical problems associated with this desired capability. The main problem is the umbilical power, feed and cooling lines that would have to be disconnected and reconnected. Unless there is a self contained power

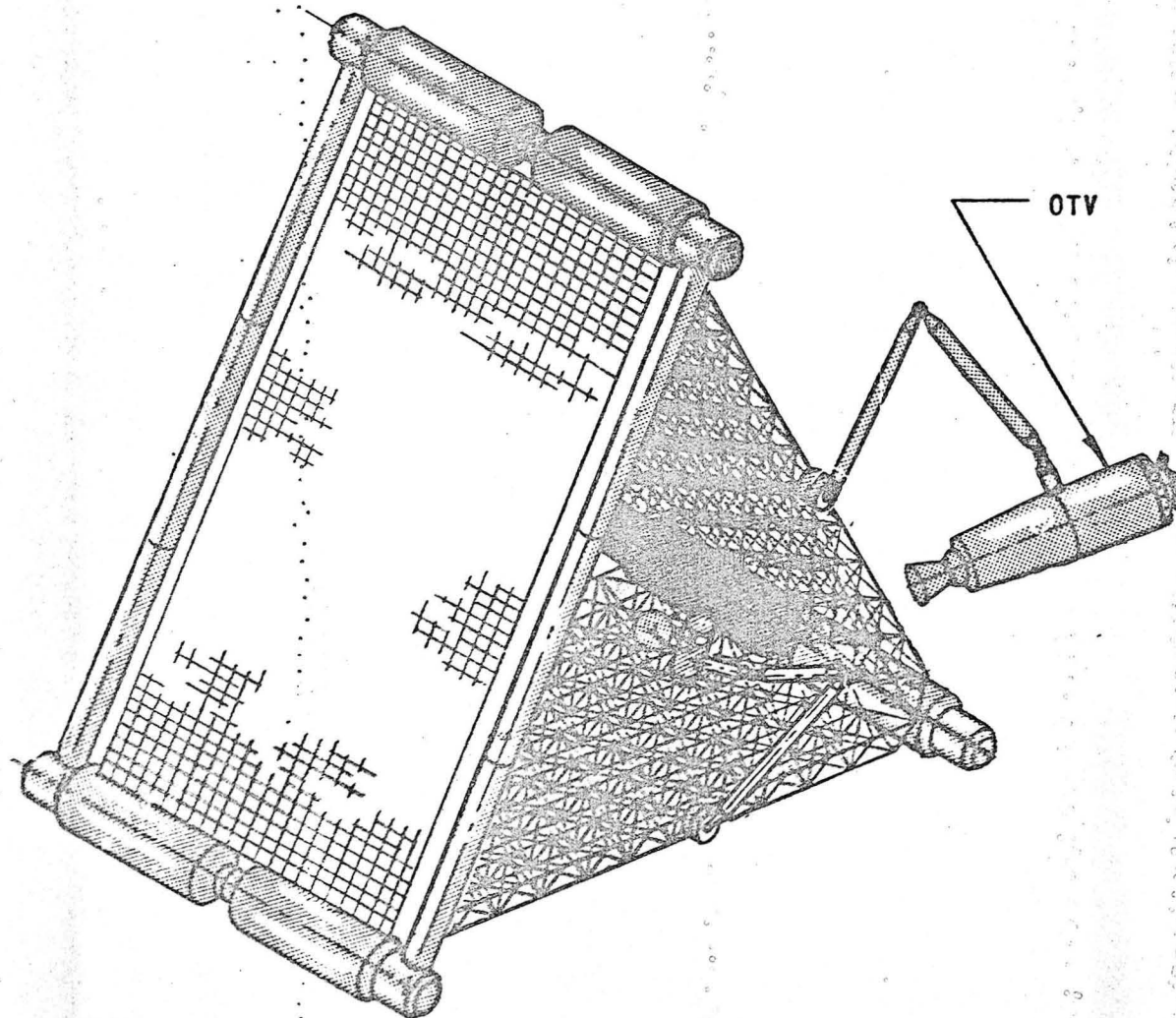


Fig. 3.2-10. OTV (Orbital Transfer Vehicle) Handling.

ORIGINAL PAGE IS
OF POOR QUALITY

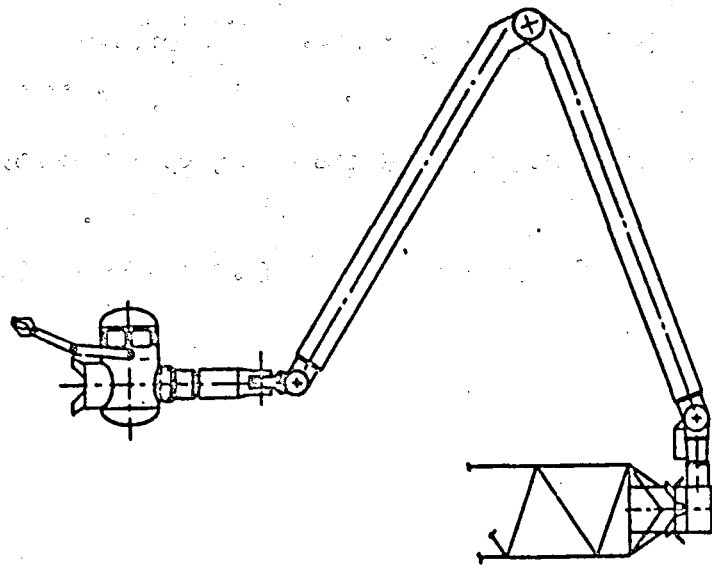
supply, one manipulator could not relocate itself since it would be inactive as soon as the umbilical is disconnected. The only practical way is for one manipulator to relocate the other one and even that would be hard to achieve because of the umbilical, which would need an automatic disconnect and reconnect feature.

3.2.4.3 Inside and Outside Conversion

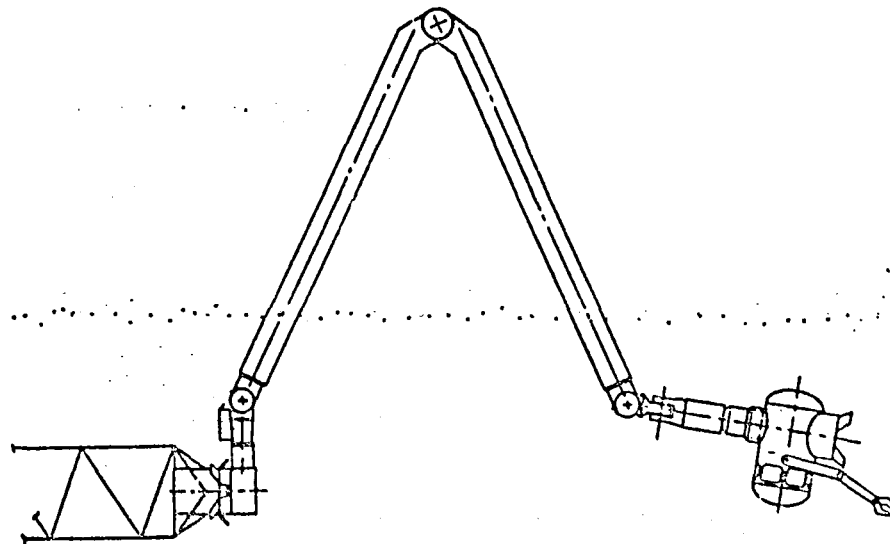
With the manipulator working from the base located midspan on the edge of the Tetratruss, it would be highly desirable for the manipulator to operate on either side of the tetratruss. This can be achieved by a turntable rotation feature at the base as shown in figure 3.2.11. In effect, this permits the manipulator to reach twice as much area as one designed to work on one side only.

3.2.4.4 Shuttle Docking

One of the main functions of the manipulators is to dock with the Shuttle for berthing and station keeping and to extract payloads from its payload bay. In figure 3.2-12 is shown a docking operation where the Orbiter is kept some distance away from the Space Station. In this case, the other manipulator can be used for extracting a payload. The disadvantage of this is the difficulty of crew transfer. Conceivably, after the payload is extracted, the second manipulator can grapple some fixed part of the Orbiter and the first manipulator can be used for crew transfer. In another concept, as shown in figure 3.2-13, the Shuttle can be docked to some part of

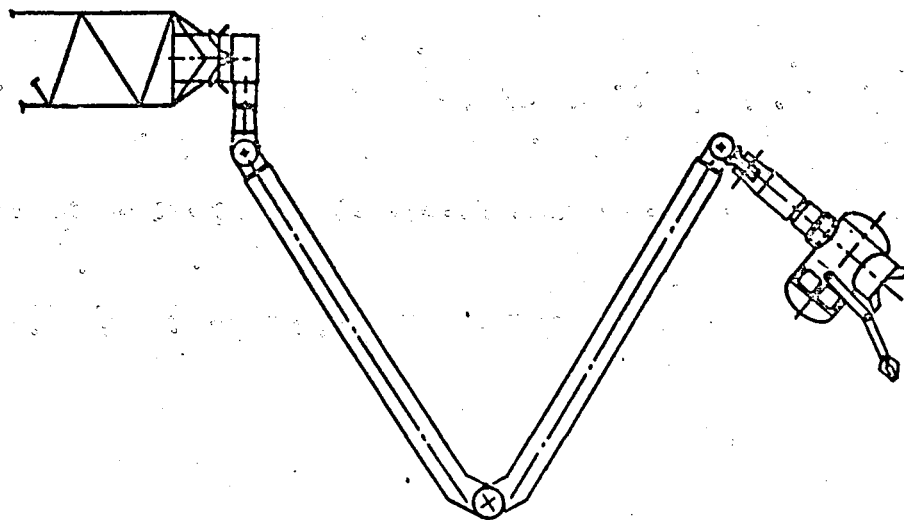


Step 1

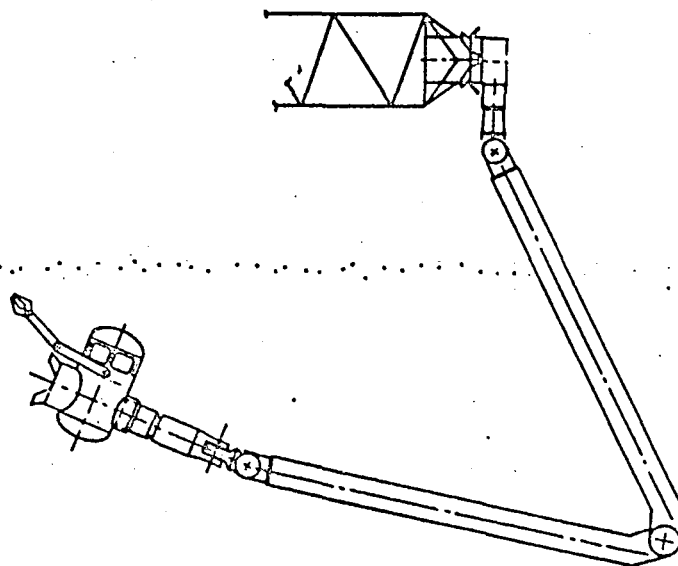


Step 2

Fig 3.2-11a. Inside and Outside Conversion, Steps 1 and 2.



Step 3



Step 4

Fig 3.2-11b. Inside and Outside Conversion, Steps 3 and 4.

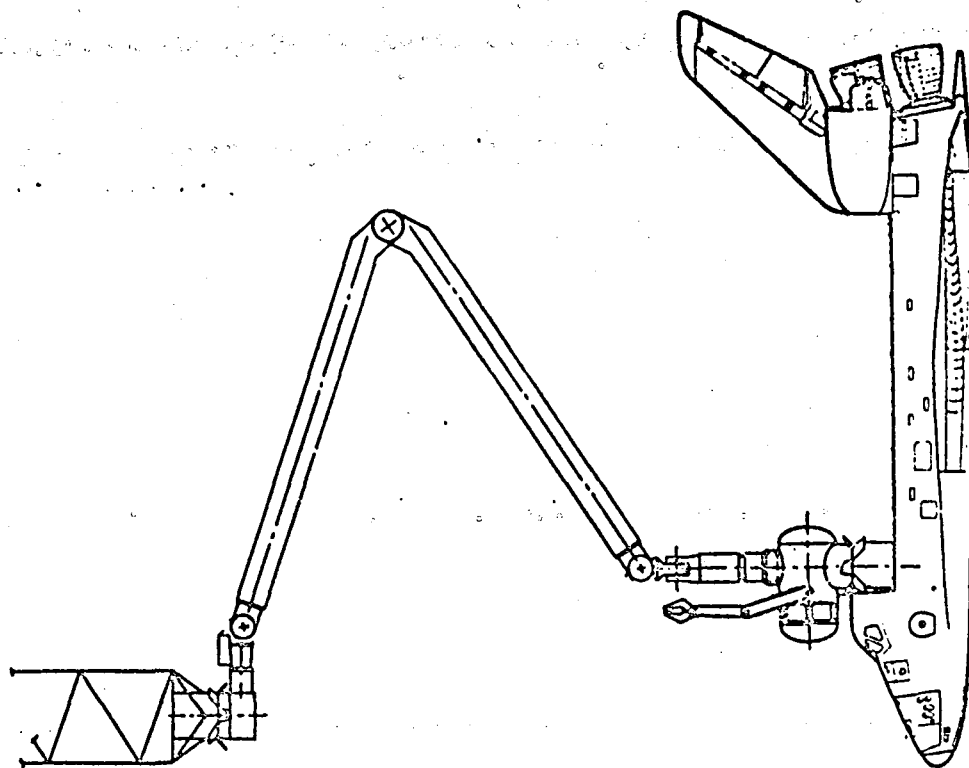
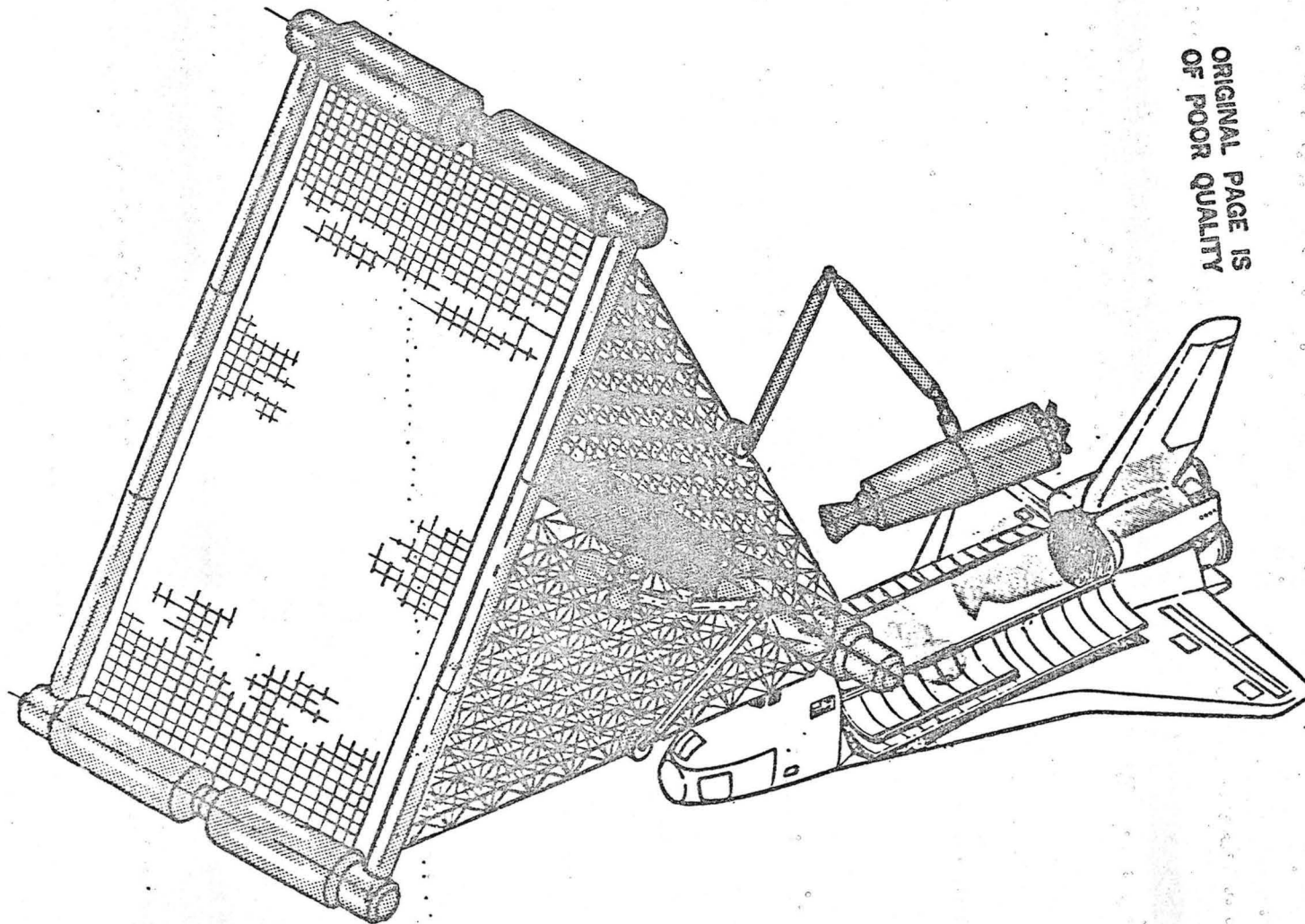


Fig. 3.2-12. Shuttle Docking.



ORIGINAL PAGE IS
OF POOR QUALITY

Fig. 3.2-13. Shuttle to Space Station Docking, Manipulator System Operation.

the Space Station and one of the manipulators can be used for extracting the payload. This too would have certain disadvantages such as the requirement for additional docking ports on the station modules.

3.2.5 Stowage of the Manipulator

Our primary concern is how the manipulators can be stowed in the payload and transported to the Space Station. It is also highly desired that both manipulators be taken up in one flight. One concept for stowing the manipulators is shown in figure 3.2-14. Initially during Space Station buildup, the manipulators can be flown up and the Shuttle RMS can be used for extracting them from the payload bay and installing them on their respective bases. Note that the turntable base is not packaged with the manipulators and would have to be flown prior to this flight and installed into place.

ORIGINAL PAGE IS
OF POOR QUALITY

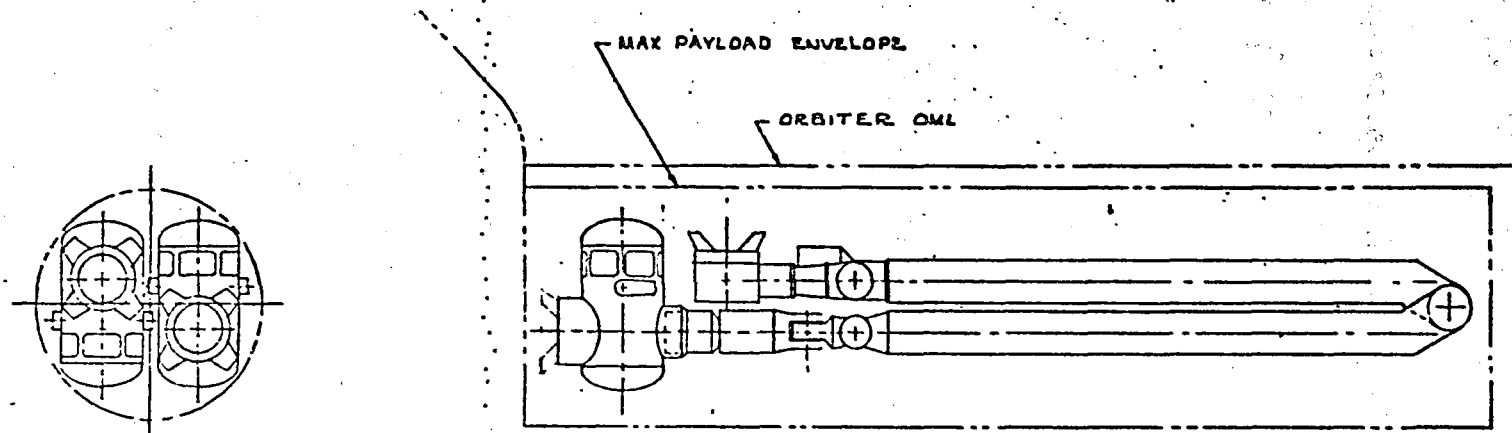


Figure 3.2-14. Manipulator Stowage in Payload Bay.

3.2.6 Conclusion

A manipulator system is conceived that will be used for handling a large variety of equipment, modules, or the Orbiter. This manipulator can be either remotely operated or manned. It is based on the current Orbiter RMS design and is scaled up to handle large masses such as the Orbiter. For this large mass, it is feasible to design this Space Station manipulator end to have an excursion velocity of 0.20 ft/sec and a stopping distance of less than two feet with minimal structural beef-up near the base attach point. For smaller masses, the excursion velocity can be greater. It is also feasible to package two manipulator systems, without their bases, in the payload bay assuming the full length can be utilized.

References

1. NASA TMX-74001, "Structural Stiffness, Strength, and Dynamic Characteristics of Large Tetrahedral Space Truss Structures" March 1977.

3.3 Holddown Attachments

3.3.1 Introduction

Space Station potential uses include maintenance and servicing of a large variety of Orbital Transfer Vehicles (OTV), satellites and the Shuttle Orbiter. The servicing tasks are expected to be extensive, involving numerous components and processes. The typical servicing activities will include

- a. Propellant and oxidizer loading (transfer)
- b. Checkout and refurbishment of OTV and satellites
- c. Orbiter payload unloading and loading
- d. Berthing and stowing of items on Space Station
- e. Assembly of OTV and satellites from subunits
- f. Launch and deployment of OTV and satellites

The performance of these tasks will involve the attachment and securing of a diverse variety of hardware to the Space Station. For the station concept of this study, the majority of the items are attached to the expandable trusses that comprise the three sides of the station. The proposed design of the trusses is a tetrahedral deployable design. The trusses are made of graphite/epoxy tubular members with special fittings at the nodal points. The attachment of the various items to the trusses is made at the nodal points except for the attachment of low mass items, such as cable and tubing runs, which could be attached anywhere on the truss members.

The imposed loads on the holddown attachments are relatively low, in that the accelerations of attached OTV, satellites, and other items, because of station maneuvers, are minimal when compared to ascent and descent loading for typical orbiter missions.

The truss nodal points have the tentative requirement to resist a 1000-lbs. normal load and two 500-lbs. orthogonal shear loads with respect to the plane of the truss. The holddown attachments will have the same tentative loading criteria as the truss nodal points, i.e., to resist a 1000-lbs. normal load and two 500-lbs. orthogonal shear loads with respect to the plane of the truss.

The proposed holddown attachments will perform the following

- a. Attachment of OTV to station
- b. Attachment of Orbiter to station
- c. Attachment of ancilliary equipment to station
 1. Propellant/oxidizer tanks
 2. Gas storage tanks
 3. Cable runs
 4. Tubing runs
- d. Attachment of satellites to station

The scope of this section includes the various holddown attachments that were considered with preliminary design concepts, analyses, and sizing information.

3.3.2. Attachment Interfaces

3.3.2.1 Attachment at Truss Nodal Points

The holddown attachments to the Tetratruss system will be interfaced primarily at the nodal points utilizing the truss fittings that form the interconnection between truss diagonals. The preliminary concept selected for the truss fittings utilizes a nonmetallic, molded design. The diagonals are attached to the periphery of the fitting by means of bolt through integral lugs that are molded with the fittings. In the center of the fitting, there is an unobstructed boss that may be utilized as an attach point for holddown devices. A titanium or aluminum insert would be installed in the center of the boss at the time of manufacture. The insert would have a hole (1/4" diameter to 3/8" diameter) for holddown device attach pins. The truss fittings and the holddown device fittings are fastened to each other with EVA compatible quick-release pins. Figure 3.3-1 depicts the attachment configuration.

3.3.2.2 Attachment to Truss Diagonals

The attachment of low mass miscellaneous items, such as cable and tubing runs, does not have to be restricted

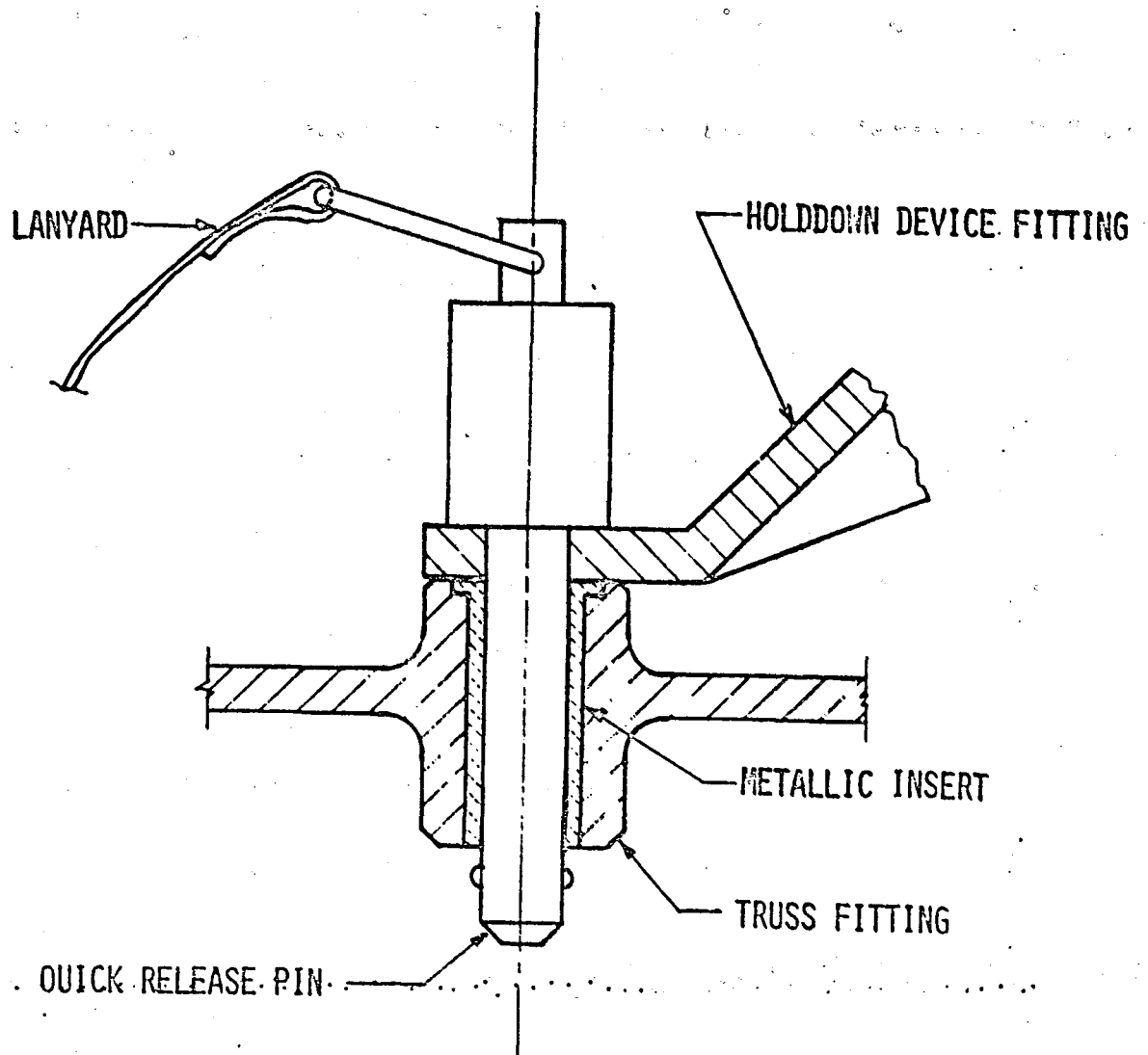


FIG. 3.3-1 ATTACHMENT AT TRUSS NODAL
POINTS

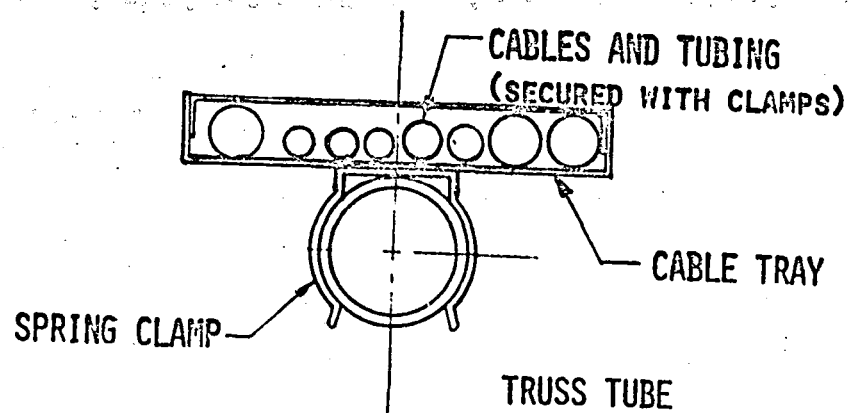
to the truss nodal points. These items may be connected to the tetratruss diagonals at any arbitrary location due to the low loads that they induce into the truss members.

The cable or tubing trays are fastened to the truss member with a push on type spring or latch mechanism that will be attached by EVA. Figure 3.3-2 illustrates two alternate attachment concepts.

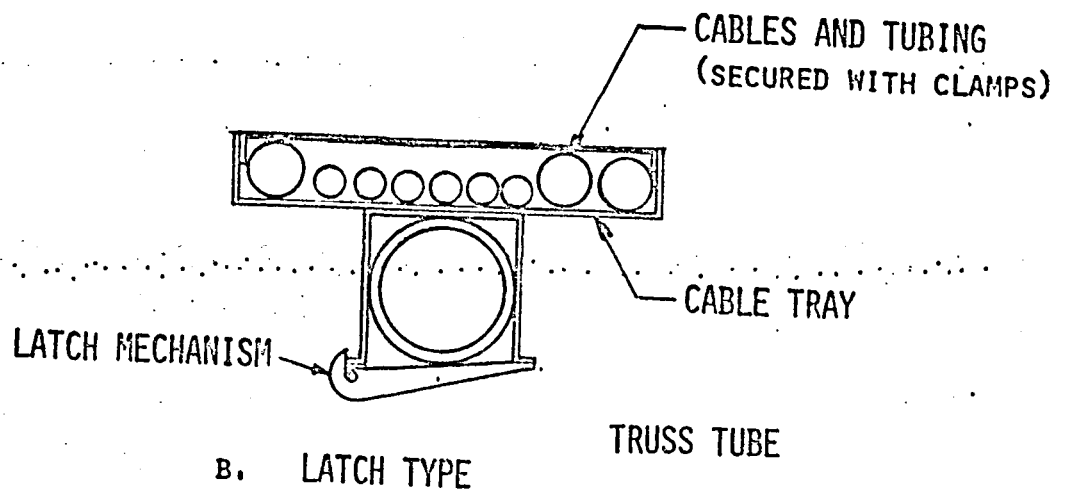
3.3.3 OTV Holddown Attachments

Since OTV are in the preliminary concept stage, there are no firm requirements and configuration definitions. Various groups within government and industry are performing tradeoff studies to arrive at OTV requirements. Because of the lack of indefinite OTV definition, the requirements for the tie-downs were derived from Shuttle payload restrictions. The Shuttle capabilities are fixed, thus, the mass and size characteristics for OTV subunits will not exceed Orbiter limits when they arrive at the station. On orbit assembly and propellant and oxidizer weight could increase the final "launch" weight and length of an OTV considerably.

All OTV stages, payloads and associated equipment will be transported to orbit in the orbiter payload bay. It is therefore reasonable to expect that all OTV components will have trunnion attachments for payload bay stowage, grapple fixtures



A. SPRING TYPE



B. LATCH TYPE

FIG.3.3-2 ATTACHMENT AT TRUSS DIAGONALS.

RMS handling, and possibly attachment devices for interfacing to currently contemplated handling mechanisms such as Handling and Positioning Aid (HPA) and Payload Installation and Deployment Actuator (PIDA). The onorbit holddown attachments should be designed to utilize fixtures on OTV that will serve other functions as well, thus, deleting the need for specialized fixtures dedicated only for onorbit stowage.

The holddown attachments should meet the following requirements

a. Stowage and transportation of holddown attachment to orbit in orbiter payload bay.

b. Deployment and securing of holddown attachment by station manipulator on EVA.

c. Stowage and release of OTV with remotely actuated latching mechanisms.

d. Ability to place and secure at any location on truss to meet various OTV servicing requirements. This is also a requirement for the truss.

3.3.3.1 OTV Trunnion Attach with Tripods

The Orbiter transported OTV will most likely use a 5 point trunnion attach method in the payload bay. This would mean the use of four longeron trunnions and one keel trunnion. The longeron trunnions could be utilized to secure the OTV to the tetratruss on the Space Station. For this configuration, at each

longeron trunnion there is a tripod support (see figure 3.3-3). The tripod members are graphite/epoxy tubular members. The attachment of the tripods to the truss nodal points are made with quick release pins as shown in section 3.3.2.1 (see figure 3.3-1). The attachment of the OTV to the tripod can be accomplished by means of capture latches that would mate automatically when an OTV trunnion is berthed to them. The trunnion latches have a remotely actuated release mechanism that is operated by means of an electrical solenoid or motor. The lightweight longeron fitting might be utilized for this application.

The preliminary sizing for the tripod members is based on a calculated 5000 lbs. normal load to the plane of the truss per tripod. This was obtained assuming that the OTV impact is taken by two tripods. For this load, the loads in the tripod members are in the range of 2000 to 2500 lbs. The tripod member lengths are 8 to 12-ft. This results in a member size similar to the truss diagonals; i.e., a graphite/epoxy tube of about 2" diameter with about .049-wall thickness. The reactions normal to the truss at the truss nodal points range from 1300 to 2300 lbs. Thus, the quick release pins could be from 3/8 to 1/2 diameter and be more than adequate from the strength stand point. It is possible that EVA requirements may very well dictate a larger pin diameter for the quick release pins.

The layout of the members for the Tetratruss is a

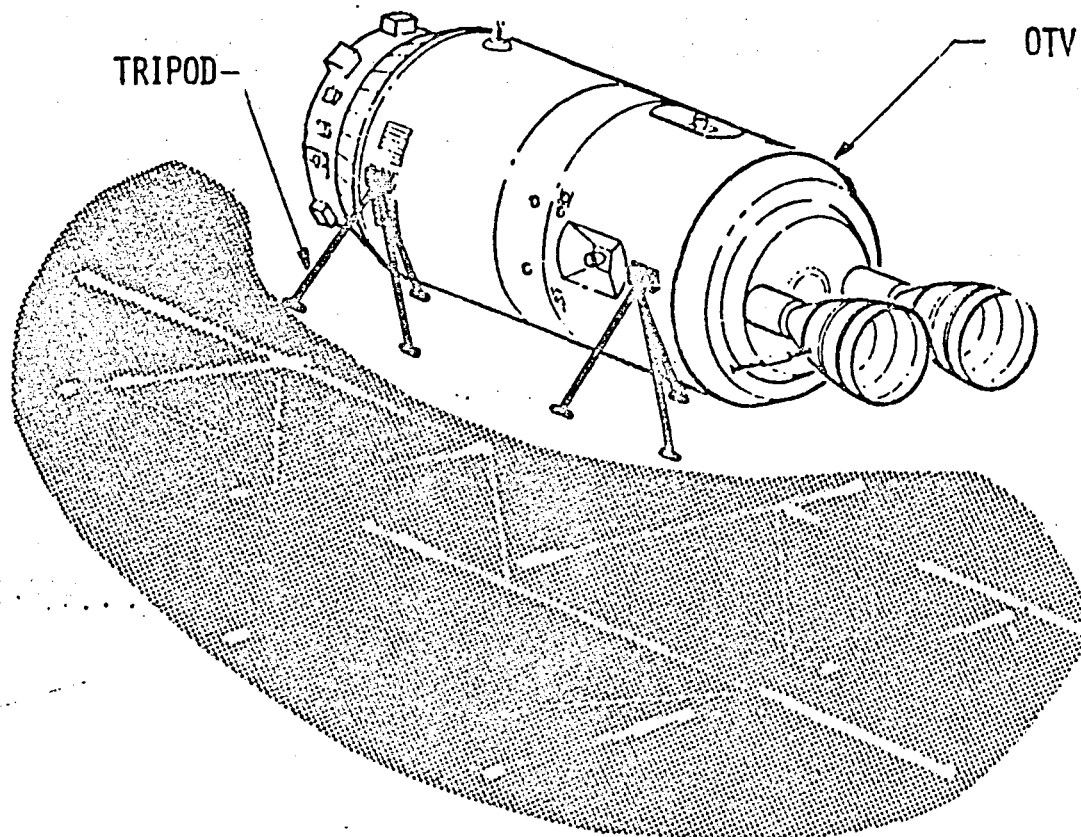


FIG.3.3-3 VIEW OF OTV TRIPOD SUPPORT

uniform pattern of equilateral triangles with a 10.4-ft. nodal dimension. Figure 3.3-4 shows a plan view of the truss, with an outline of an OTV and four tripods. For the depicted configuration the trunnion spacing on the OTV would have to be 18.04 ft. to permit the use of similar tripods. If the trunnion spacing is something other than multiples of 9.02 ft, then the tripods would be different for forward and aft trunnions of the OTV.

3.3.2 Handling Fixture Attach

All expected OTV designs will incorporate some form of permanent handling fixtures as part of the OTV structure. These may be grapple fixtures for handling by RMS, PIDA fixtures for deployment by PIDA, or passive HPA fixtures for manipulation by HPA.

It is conceivable that these fixtures may be utilized for on-orbit stowage and retention of various OTV components. In order to satisfy the requirement that all significant loads be applied to the tetra-truss at the nodal points, the use of PIDA-HPA type devices requires the employment of a low tripod that would serve as a load path to the truss nodal fittings. Figure 3.3-5 depicts a possible configuration for a PIDA/tripod attachment device. Generically this concept would be the same regardless of the type of fixture that was used (PIDA, HPA, etc). They all share the inherent drawbacks that

- a. The mass of the OTV is cantilevered from the plane of the truss and the lateral loads are resisted only by the moment

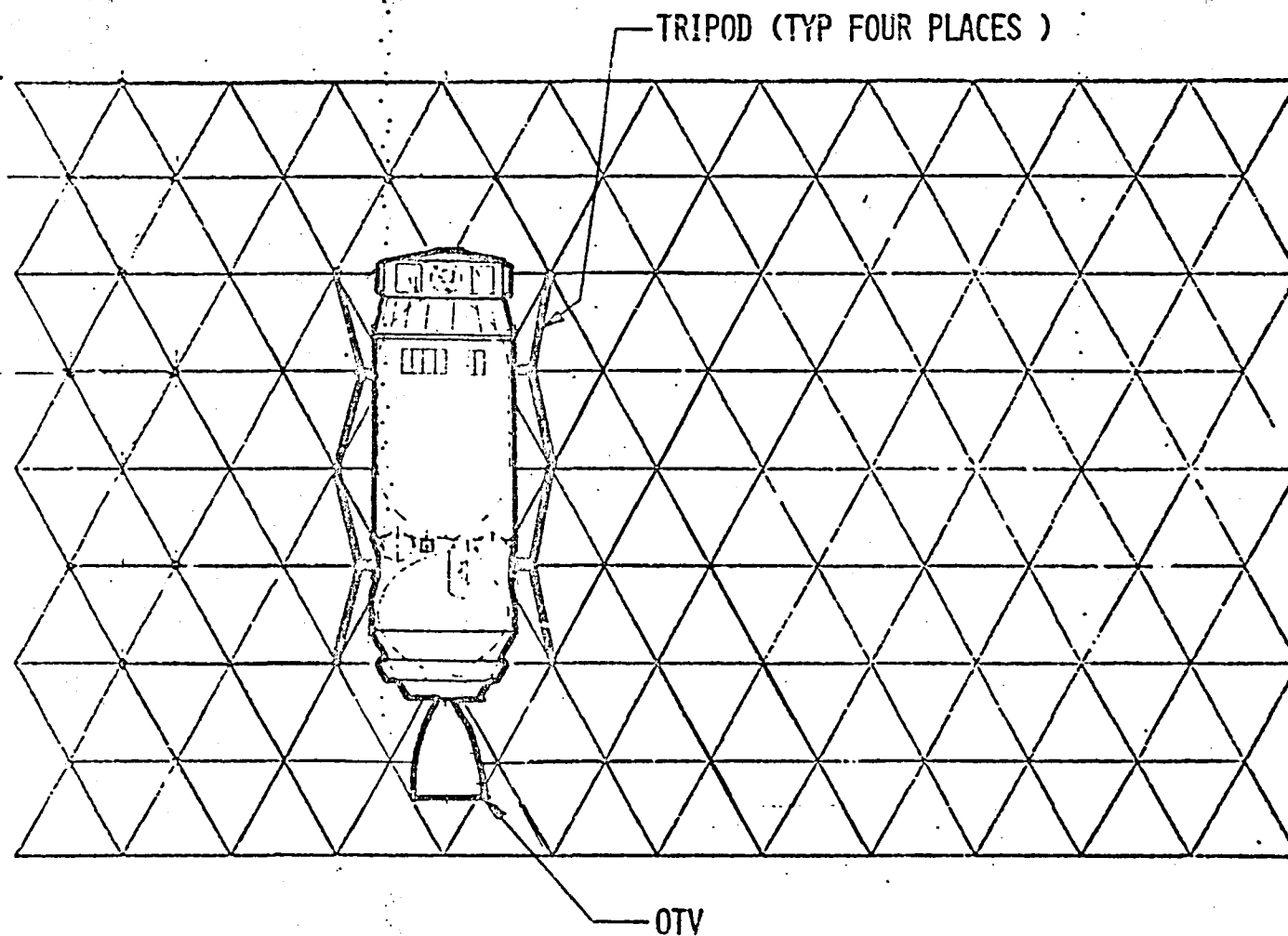


FIG. 3.3-4 VIEW OF OTV AND TRIPODS ON TETRATRUS

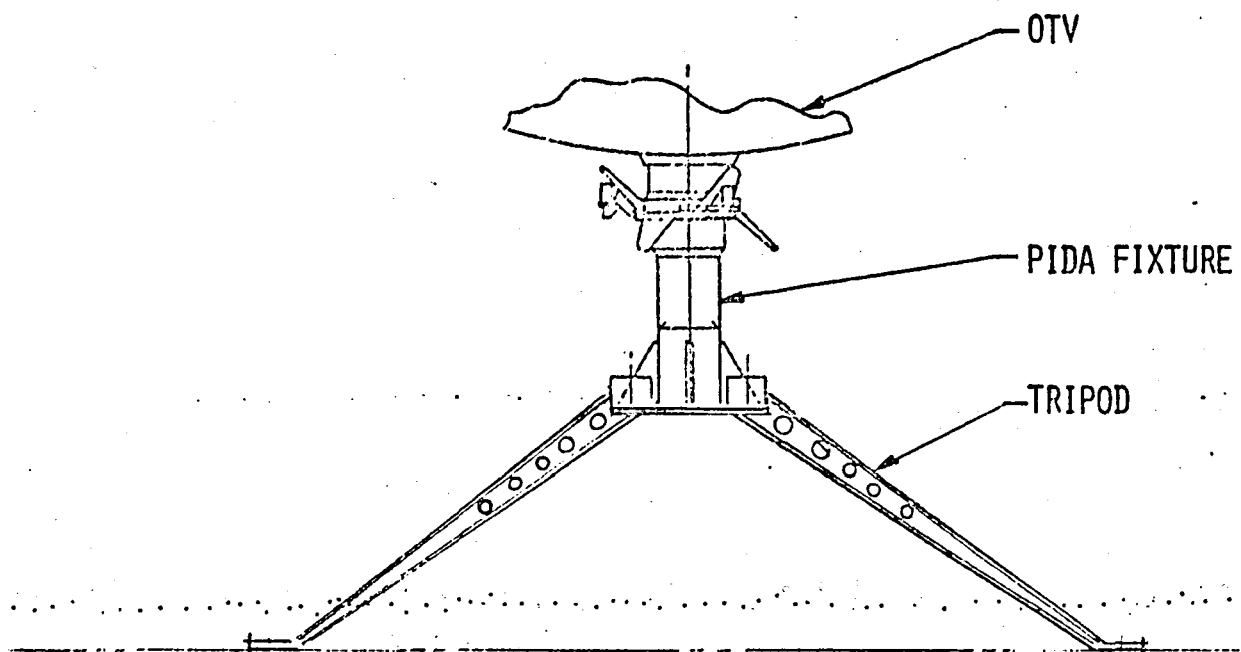


FIG. 3.3-5 VIEW OF PIDA/TRIPOD ATTACHMENT FOR OTV

capability of the PIDA/HPA type fixture.

b. The loads from the OTV are transferred into fewer nodal points of the tetratruss than with the trunnion attach method.

c. The PIDA/HPA type mechanisms are inherently complex and require further development to demonstrate long term reliability when exposed to onorbit environments.

The use of this type of attachment for OTV berthing to the space station is not recommended due to the drawbacks cited herein.

It is conceivable that later designs and inventions may make this type of attachments more desirable; however, further consideration is deferred at this time.

3.3.3.3 OTV Berthing Fixture Attach

On some previous concepts, various OTV stages and payloads are depicted with interstage attachment devices that strongly resemble Orbiter type docking units. In those configurations OTV are shown berthing to the Space Station, to payloads, and to other stages by means of the docking unit.

The use of such a concept is very inefficient from the structural point of view. The diameter of the docking unit is considerably smaller than the diameter of the OTV. Thus, any bending moments imposed on the docking unit will result in high

strength requirements which means more weight. If those bending moments were taken out thru some skirt attach scheme along the periphery of the OTV then considerable weight savings could result.

The docking units are also quite complex mechanically, which might result in long term maintenance problems.

It would be a desirable requirement to minimize the number of docking units for the space station and OTV's. The benefits of such action would be weight and cost savings, as well as increased life for the Space Station.

For the reasons cited herein Orbiter-type berthing and docking units are not recommended for OTV propulsion stages or unmanned payloads.

3.3.4 Orbiter Berthing to Station

In the course of routine station operations the orbiter will visit the station on a regular basis. The typical visit will include the following

- a. Approach to station
- b. Station keep prior to berthing
- c. Berth to station
- d. Stay berthed to station for duration of visit
- e. Deberth from station
- f. Separate from station in preparation for deorbit
- g. Deorbit

The activities during the visit will be highly variable, however, generically they will involve the transfer of

- a. Personnel
- b. Payloads
- c. Propellants/oxidizers/fluids/gases
- d. Consumables

A successful berthing system will be adaptable to all possible Orbiter-station interactions including provisions for resisting all berthing interface forces and moments.

3.3.4.1 Orbiter Berthing with Baseline Docking Tunnel

The baseline orbiter docking module is defined in MCR 5546. In that proposed concept, the docking module is located at the forward end of the payload bay. The tunnel is attached to the hatch located in the crew cabin aft bulkhead. The docking interface is at Zo515. The docking module support structure attaches to the longerons and the keel with standard payload fittings. Figure 3.3-6 depicts the docking module concept:

The docking system mechanism is similar in concept to Apollo Soyuz Test Project (ASTP) with active and passive docking units, where "active" refers to the docking unit with attenuator supported standoff ring which engages and latches the other docking unit on initial contact. It is anticipated that in this concept the Orbiter docking module will be the active one and the Space Station docking interfaces will be passive.

ORIGINAL PAGE IS
OF POOR QUALITY

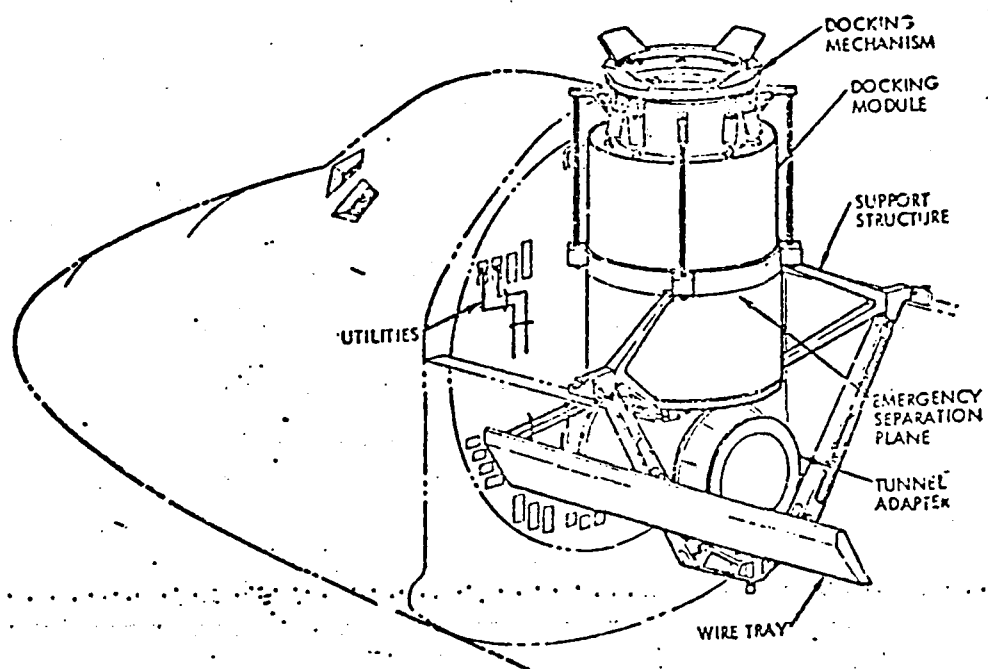


FIG. 3.3-6 ORBITER DOCKING MODULE CONCEPT.

The Orbiter docking module has the following preliminary design requirements.

a. Docking requirements

<u>Mission</u>	<u>Weight</u>
Normal payload docking	65,000 lbs
Orbiter/orbiter docking	Orbiter weight
Orbiter/station docking	Orbiter + payload weight

b. Contact conditions

Parameter

Rel. contact velocity (-Z)*		.05 fps min 0.5 fps max
	(X,Y)	0 to + .1 fps max
Relative ang. vel.	(3 axes)	+ 1.0 deg/sec about any axes
Relative lateral displacement	(X,Y)	0 + .5 ft.
Relative angular (pitch & roll) misalignment		0 + 5 deg about each axis
Relative rotational (yaw) misalignment		0 + 7 deg

* Parameters in Orbiter coordinate system

The docking module concept for Orbiter-to-station berthing is achievable, however, it has a drawback. Considerable payload bay volume must be sacrificed to accommodate the docking module. The docking module would have to fly on every mission, thus, the net effect would be the reduction of available payload bay length by approximately 70-80 inches.

The station concept described in this document has spare berthing ports available on all modules except on the logistics module. It is feasible to berth the Orbiter to any unoccupied berthing port. Figure 3.3-7 shows one option for orbiter berthing. The orientation of the Orbiter with respect to the station would be a function of the particular task to be performed i.e., payload unloading, crew transfer, etc.

The handling devices (cherry pickers) are described in section 3.2. One concept involves a manned operators module that has a berthing port which enables the handling device to serve as a means of berthing the Orbiter. One of the handling devices would berth with the Orbiter docking module, while the other handling device would be utilized to remove or install payloads from the payload bay. Configuration and operational details of the handling devices are described in detail in section 3.2.

3.3.4.2 Alternate Orbiter Berthing Concepts

The present configuration of the Orbiter limits the methods of berthing to that of the docking module concept.

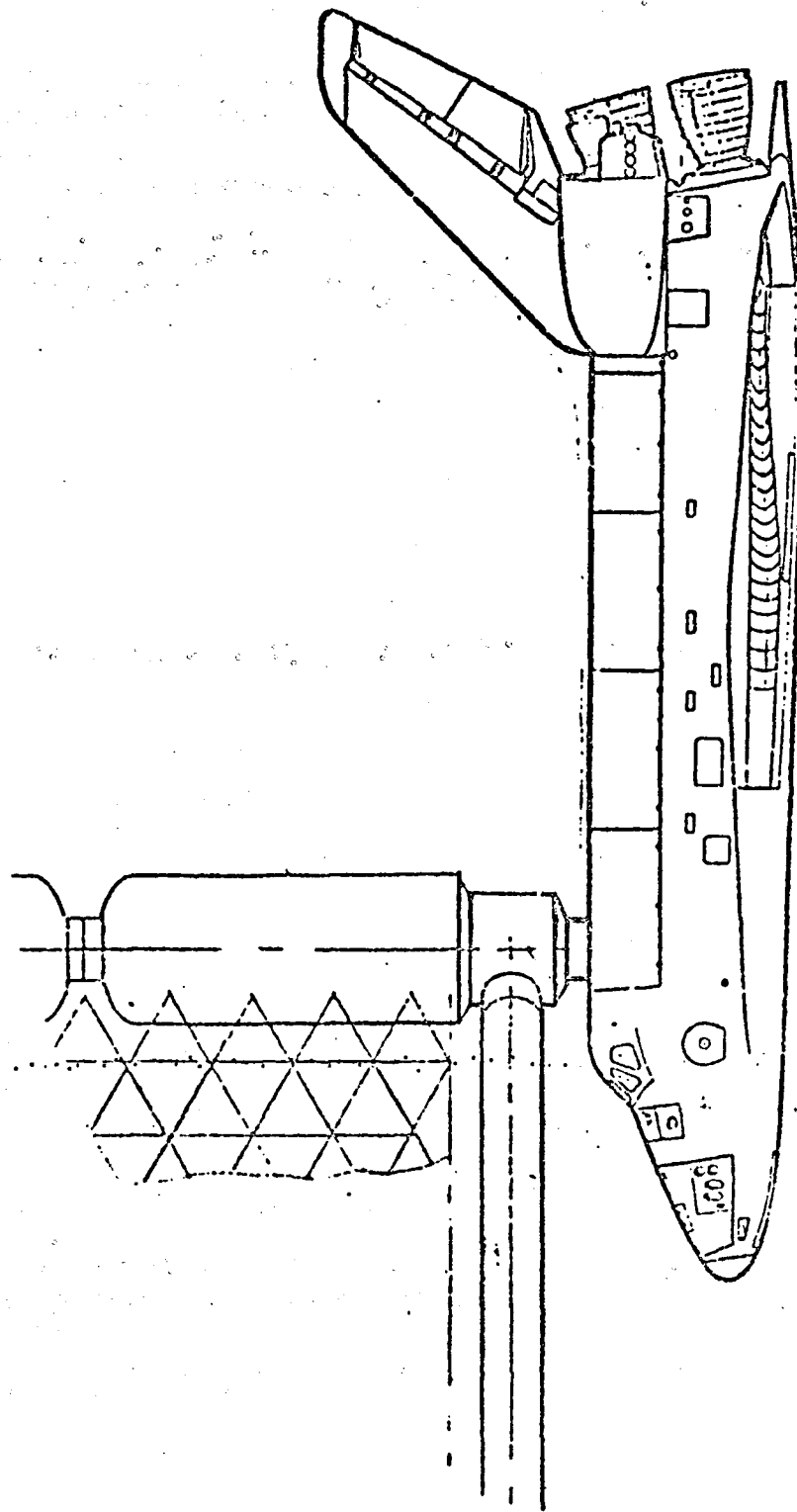


FIG. 3.3-7 VIEW OF ORBITER BERTHING AT APEX OF STATION

However, with modifications to the Orbiter it would be possible to develop alternate means of berthing to the Space Station. Whether the costs can be justified, is a function of the required payload bay length. If a potential customer would have a payload that required the full payload bay length for a high value cargo, then an extensive modification to the orbiter might be economically feasible.

Alternate concepts have been discussed where the Orbiter would be attached to the station utilizing special new design fittings, or existing attachments such as forward and aft ET attachments. Generally, they all required Orbiter modifications; they were in high heat areas, thus, tile damage was likely from routine attachment operations; they were at points that would be hard to reach from the trusses on the station. One concept is depicted in figure 3.3-8. It is expected that development of station mating equipment will be costly, however, program requirements may justify the required funding levels.

3.3.5 Attachment of Ancilliary Equipment to Station

3.3.5.1 Storage Tank Attachment

The servicing of OTV will involve the use of considerable amount of ancilliary equipment. It is expected that propellant and oxidizer tanks will be rather large with storage capacities in the 30-80K lbs. range. This precludes their integration to the station as part of a module. Storage tanks of this size will have to be mounted onto one of the Tetratrusses.

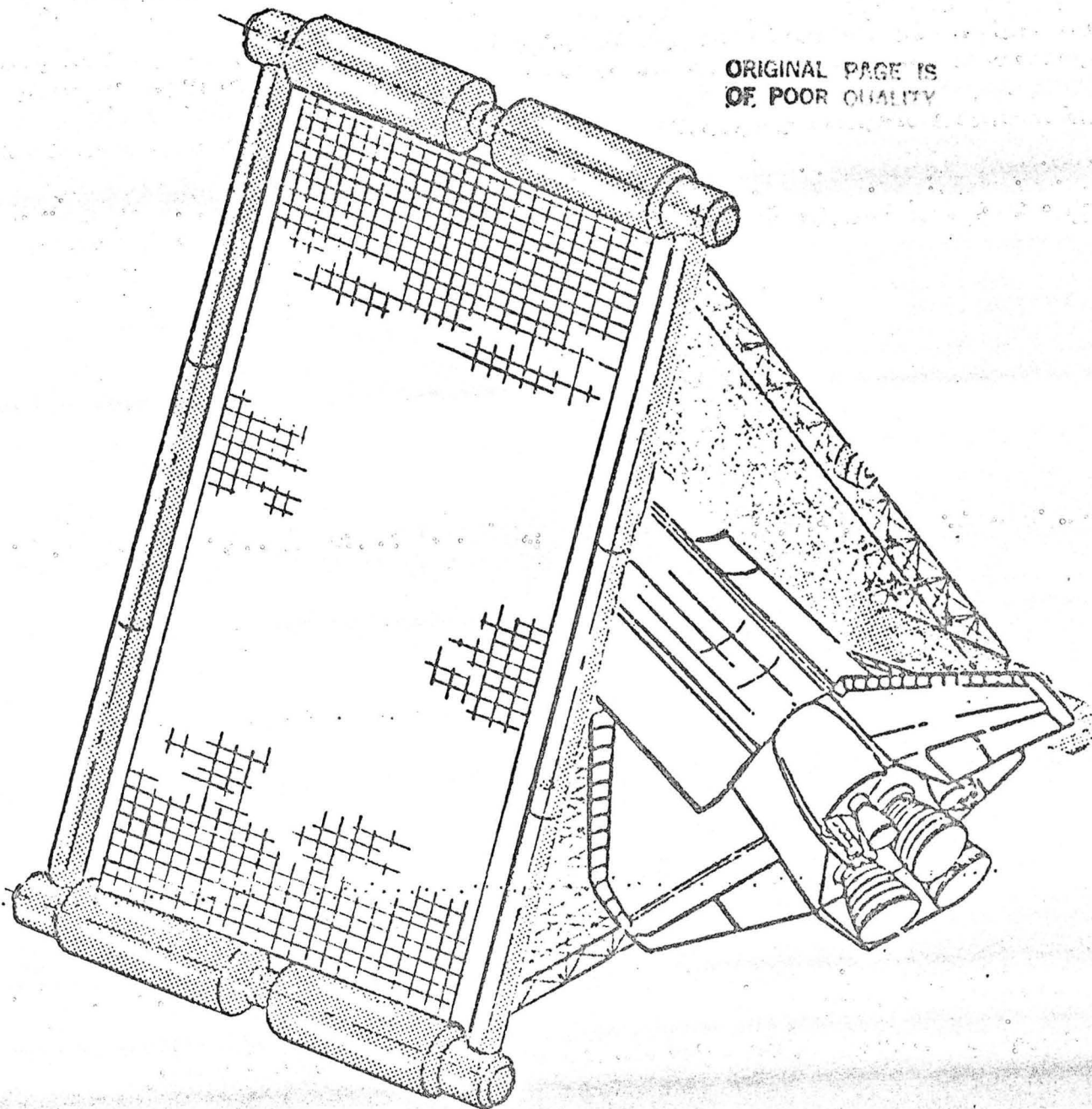


FIG. 3.3-8 VIEW OF ORBITER BERTHED WITHIN STATION

The large storage tanks will be transported to the station in the Orbiter. Likely they will have a four-or five-point trunnion attachment configuration for payload bay transport. Thus, the attachment method that is planned for OTV would also be feasible for the storage tanks. The trunnion attachment with tripod (see section 3.3.3.1) will be utilized for securing the storage tanks to the Tetratruss. Description of the tripod attachment scheme will not be repeated here since it is identical to the OTV attachment.

The OTV servicing function also includes the need for smaller tanks. Some of these are for gas storage, whereas, others for liquids. Because of their size, these smaller tanks could be located anywhere on the station. However, there is requirement to minimize tubing and cable runs. Thus, it would be a decided advantage to locate all storage tanks in close proximity to one another. This would result in shorter tubing and cable runs and perhaps simpler umbilical connections.

For this station concept the OTV servicing tank farm is located on the inside plane of one of the Tetratrusses close to the apex. The tankfarm includes a deployable, nonthrusting boom for purge and vent operations. There is a cable and tubing tray run to the closest service module and one to the OTV service area.

3.3.5.2 Tubing and Cable Tray Attachment

The tetratruss inside plane areas are the planned locations for the OTV servicing activities. The outside planes are the locations for the solar arrays, the radiator panels and the various communications and radar antennas.

The various components that comprise the total function of the station will be interconnected by a number of electrical, data, and antenna cables and tubing runs for multiple fluids and gases.

The tubing and cable runs have to be deployed, attached to the Tetratruss and interconnected to the various components before station operation may begin.

The configuration selected for this Space Station concept is a foldout type cable/tubing tray that is attached to the tubular members of the Tetratruss. The cable trays are transported to orbit in 40-foot sections. The sections contain all the required cables and tubing, and are hinged together at the ends. Flexible joints are provided for the tubing runs. Umbilicals are attached to the cabletrays at the ends of tubing runs. The cable trays are transported to orbit in the folded configuration and stowed in the Orbiter payload bay. They are deployed on orbit with the RMS and attached to the tetratruss. The attachment interface is described in section 3.3.2.2. After the installation of cable

trays and all mating components the umbilicals are deployed and mated. With subsequent purge, fill, and checkout activity the cable and tubing tray installation is completed.

3.3.6 Attachment of Satellites to Station

The satellite servicing function for the Space Station will encompass the retrieval, store, servicing, and deployment of various satellites. The projected traffic model to year 2000 includes a diverse variety of satellites. They range from communications satellites destined for GEO, to space telescopes, LDEF.

The satellites are expected to be unique in spite of present efforts underway to standardize satellite design. Thus, the attachment and stowage problem for satellites on the space station is expected to be formidable.

Where possible, Orbiter transport cradles, trunnion fittings, and grapple fixtures may be utilized for the attachment of the satellites to the station. This method however may not be feasible when the satellite has large appendages (such as solar panels, radiators).

In general, ICD requirements between satellites and the Space Station will have to be developed on a case-by-case basis. Thus, attachment hardware for Space Station berthing will have to be developed simultaneously with the satellite. Because of the lack of requirements and definition, further consideration is deferred.

3.4 Module Design

3.4.1 Introduction

The basic modular element of the Space Station is envisioned to be a large cylindrical pressure vessel that can be transported to the orbiting station in the Shuttle cargo bay. A sketch of this concept is shown in figure 3.4.1. The cylindrical vessel will have end domes that contain docking ports and windows. It is also envisioned that this module will be designed so that it can serve as a universal shell and frame element that can be used for multiple functions. This type of design will lead to a mass production of modules from an assembly line and minimize the cost of a Shuttle launched Space Station. The module function (crew quarters, medical service, galley, laboratory, etc.) would define the interior support equipment.

The study conducted in this section will present a universal module design concept that can be transported in the Shuttle cargo bay.

3.4.2 Module Design Requirements

The following list specify general requirements that have been identified for the Space Station module.

A. The module should have a ten year service life with a possible refurbishment every three years.

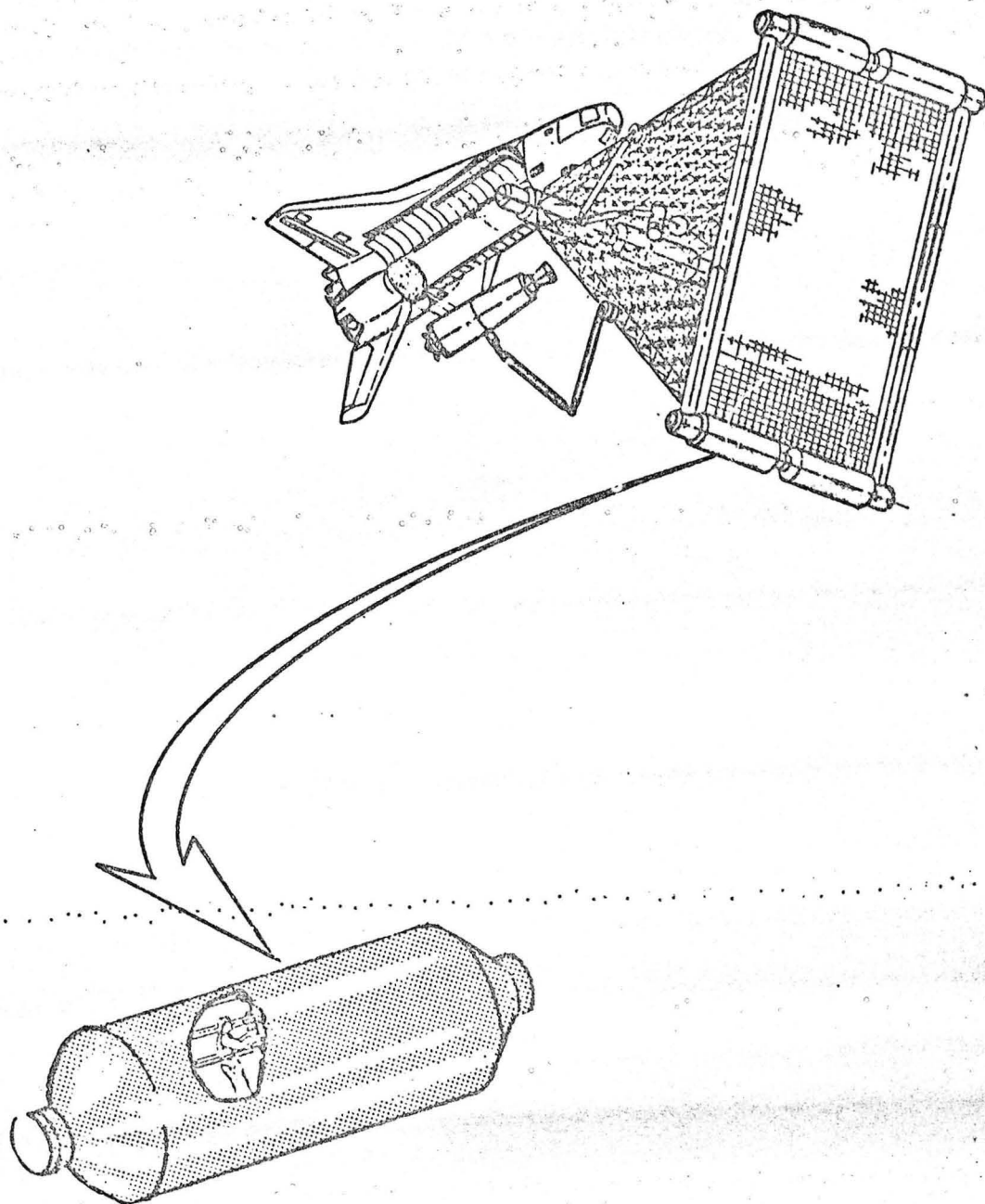


FIGURE 3.4.1 SPACE STATION MODULE ELEMENT

B. Factors of safety

1. Ultimate factor of safety = 2.0 for internal pressure.
2. Ultimate factor of safety = 1.4 for inertia loads.

C. Module size to utilize maximum Shuttle cargo space without violating the Shuttle requirements.

D. Provide a shirt sleeve environment at 14.7 psia.

E. Provide adequate internal attachment structure for module function configuration.

F. Lightweight structural design.

G. Module internal volume to remain "clean" for maximum module function configuration.

H. Probability of no meteoroid penetration for ten years of .9.

I. Provide structural capability for docking to other modules and to the Space Shuttle.

J. Provide vehicle viewing ports and umbilical panels.

The design service life of the Space Station will be ten years. The 2219 aluminum proposed for the module structure will have no problem meeting this criteria for sustained loads. The other parameters that will affect the life of the module will be fatigue stress cycling because of thermal and internal pressure changes and onorbit external loads. It is expected that these effects will be negligible for the module service life.

The maximum module size that will fit into the Orbiter payload bay without infringing on the Orbiter's clearance envelope is shown in figure 3.4.2. The module size shown is 14 feet in diameter and 49.917 feet long. However, because of possible deployment problems with this module, it was decided to reduce the module length for this study to 46 feet.

A shirt sleeve environment for the module will require thermal conditioning and a 14.7 psia atmosphere. The thermal conditioning will require thermal insulation and radiators. The module structure will have to provide attachments for the insulation. The expandable truss structure will provide support for the radiators.

It is envisioned that the module ring frames will provide ample attachment area for the internal configuration of the module. Since the module CG limits, as dictated by the Space Shuttle System Payload Accommodations, reference 1, indicates that the Z-CG will lie below the centerline of the module, it is anticipated that the larger mass items will be located beneath the module floor on pallets attached to the ring frame flanges. The configuration above the floor is anticipated to be a "peg board" type structure attached to the ring frame flanges that will allow any combination of equipment mounting and compartment bulkhead installations. Details of the different internal configurations required for an operational Space Station have not been defined.

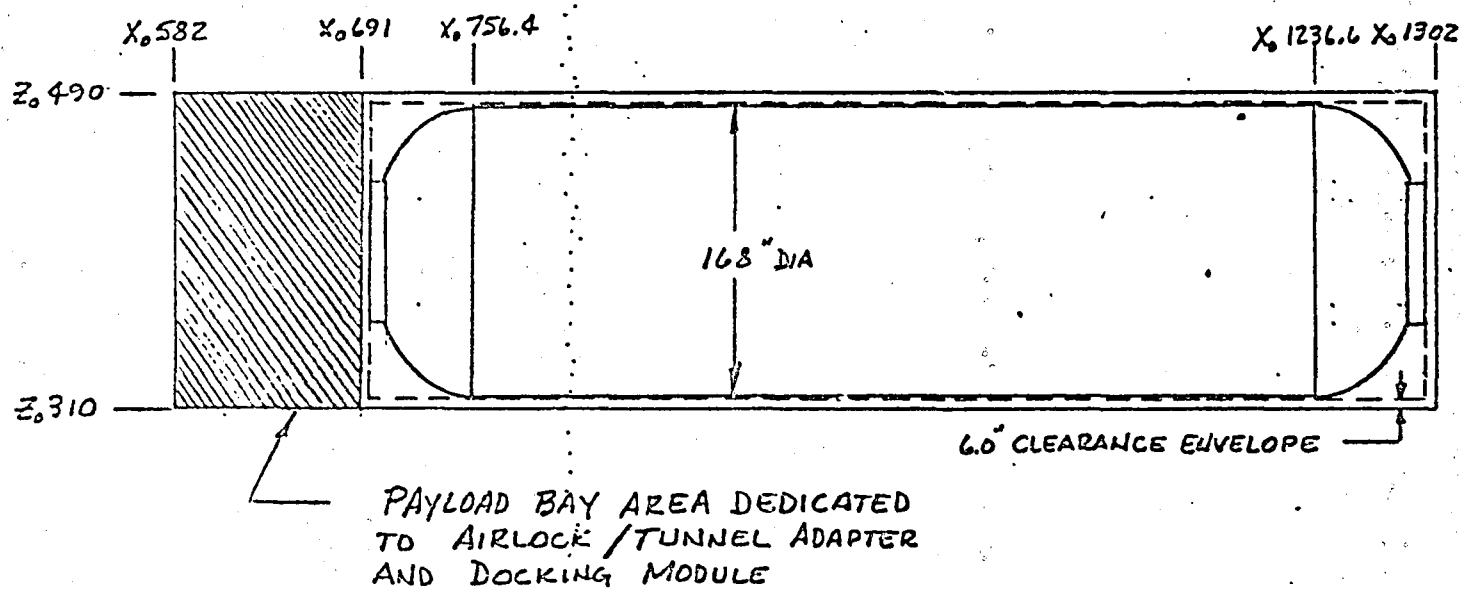


FIGURE 3.4.2 OML DIMENSIONS FOR MODULE ELEMENT

The universal module primary load carrying structure must be as light as possible to allow for growth in the equipment required for any module function that may be required. This requires a high-strength-to-weight material that can be easily and economically formed into the structural shapes needed for the design. Section 3.4.6 is devoted to this requirement and goes into considerable detail involving cost and manufacture. A module weight of 40,000 pounds was used for the sizing and weight analysis in this feasibility study; however, the module does not need to be restricted to this weight.

To have a module that will serve any given function efficiently, the primary load carrying structure should be clear of the interior space, giving abundant work or storage area. In this study, the primary load carrying structure is considered to be an integrally stiffened skin with ring frames. The skin will resist the pressure loads and also be stiffened by stringers equally spaced along the outer circumference to resist body bending and axial loads from the Shuttle flight environment. The placement of the stringers on the outer surface of the skin will not only produce a "clean" internal volume, but will also produce a more efficient section to preclude general instability of the module from the large axial forces during ascent. The ring frames will be located in the interior of the module and serve a double purpose to reduce the overall column length of the module for buckling considerations, and also to provide attachment locations for internal equipment and bulkhead partitions. In general, the

ring frames are usually heavier than required for buckling considerations; therefore, the additional material they possess can be used for the attachments.

Design of a manned modular element for the space environment should certainly include protection for meteoroid and debris impact. The exposed surface area and ten year service life will require a certain amount of protection for the crew and equipment even with the anticipated low earth orbit of the Space Station. The approach used for this study includes a meteoroid shield that will be separated from the module pressure skin by nonheat conducting standoffs attached to the longeron. Therefore, the shield and pressure skin will form the meteoroid barrier. Because of the lack of a definition of the probability of having a penetration, it has been assumed for this study that there will be a 90% probability of no penetrations for the ten-year service life of the module.

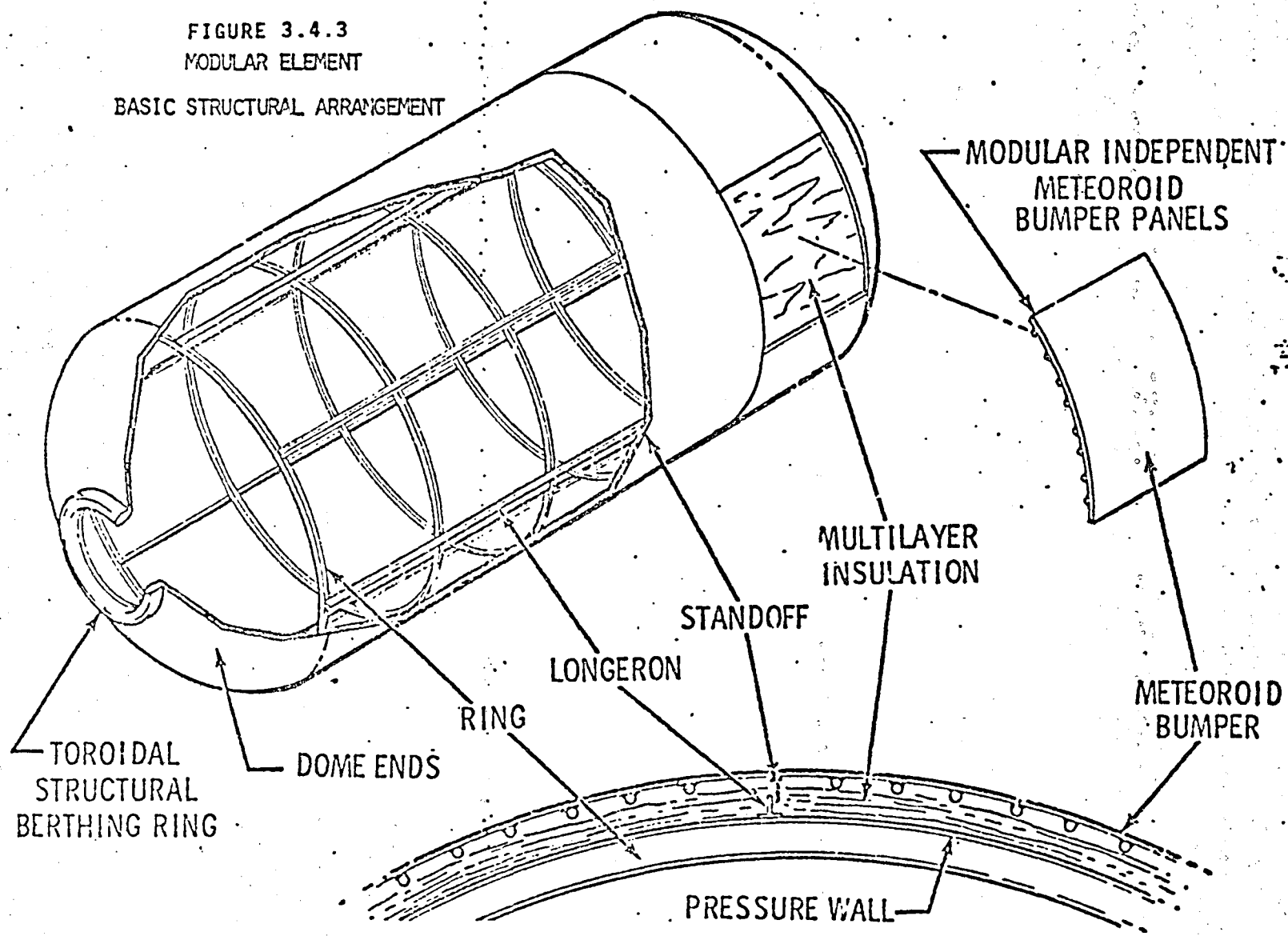
Versatility of the module will require that docking ports be provided for mating to other modules as well as the Shuttle. To provide entrance and egress at two locations in the module, two docking ports will be provided, one at each end at the module dome apex. This would also be an ideal location for viewing ports.

3.4.3 Module Configuration

The configuration baseline chosen for this study is shown in Figure 3.4.3 and is an all welded aluminum, integrally stiffened cylinder with double curvature domes. The inside radius of the module was reduced to 80 inches to allow an additional 4 inches for the meteoroid shield. From a study presented in a later section, the baseline double curvature end closure was chosen to be the Cassinian dome which will be shown to have several advantages over the other dome shapes. A 80-inch diameter docking hatch has been included at each dome apex which will provide a 60-inch wide passageway for cargo and equipment. Each hatch has also been equipped with a centrally located window.

3.4.3.1 Module Skin Thickness - The thickness required in the cylindrical portion, using 2219 aluminum to resist the internal pressure of 29.4 psi (ultimate) is .0392-inch. The basic thickness required in the Cassinian dome area is .032-inch (see reference 2; $m = .19$, $n = 1.67$, $r = 0$, $a = 80$ inches, $F_{tu} = 60,000$ psi). Theoretically, the Cassinian dome under consideration will experience no discontinuity stresses at the dome/cylinder interface if the thicknesses of each are equal. A basic thickness of .040-inch is recommended to resist the internal pressure; however, thickness of .060-inch will be required to meet the meteoroid protection criteria.

FIGURE 3.4.3
MODULAR ELEMENT
BASIC STRUCTURAL ARRANGEMENT



Ring and Longitudinal Stiffener Design- Ring and stiffener spacings for the modular element were selected to provide adequate attachment points for meteoroid shielding, equipment, floors, ground handling, etc. This selection resulted in nine rings spaced equidistant along the cylindrical portion of the module and 162 longitudinal stiffeners spaced equidistant around the circumference and running the entire length of the cylindrical portion of the module. Strength and buckling requirements were adequately satisfied in this functional design. This arrangement provides a light stiffened structure and also provides a versatile basic structure if design changes should be necessary.

The module rings were designed primarily to provide for attachment of internal equipment, and for handling and mounting of the module in the Shuttle payload bay. The cross section is more than adequate to carry the launch and flight loads. Typical cross sections are shown in figure 3.4.4. The dimensions for the longitudinal stiffeners were chosen to facilitate attachment for the meteoroid shielding and also to provide adequate stiffness to prevent buckling of the skin. a typical cross section is shown in figure 3.4.5.

High density mass of unidentified subsystems may cause some minor perturbation in local reinforcement of the ring frames, but it is expected that this structural weight perturbation will

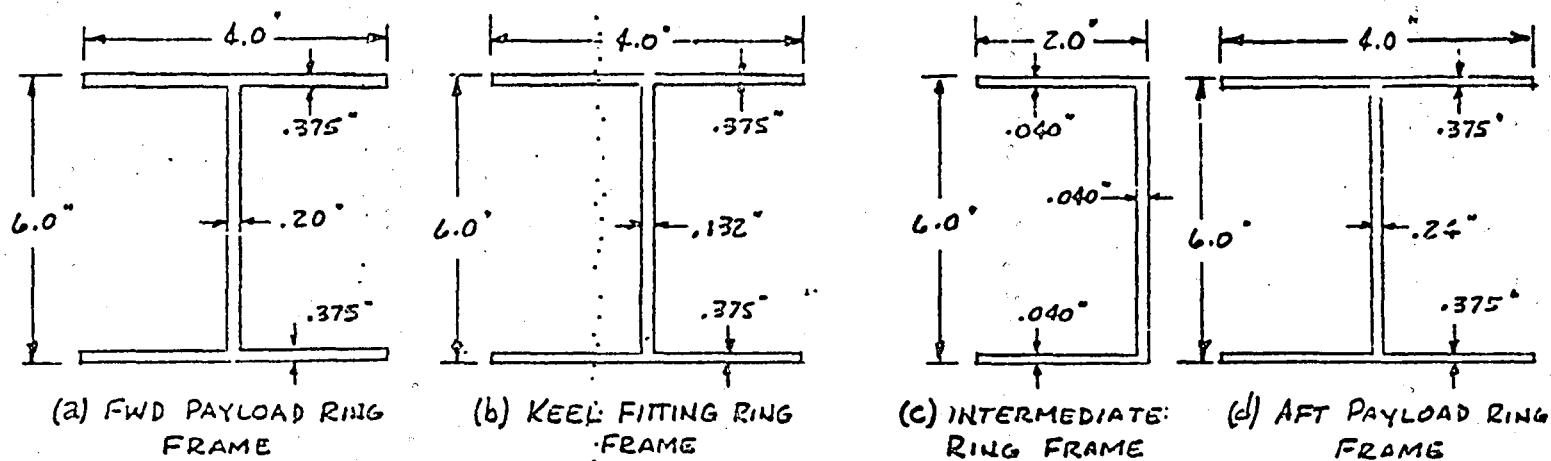


FIGURE 3.4.4 TYPICAL RING CROSS-SECTION

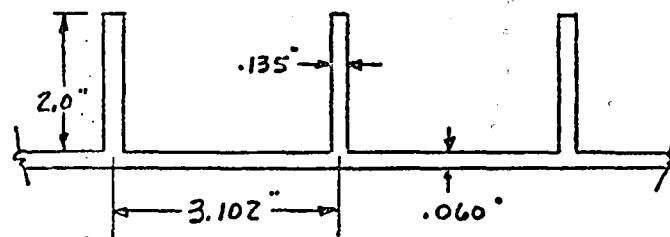
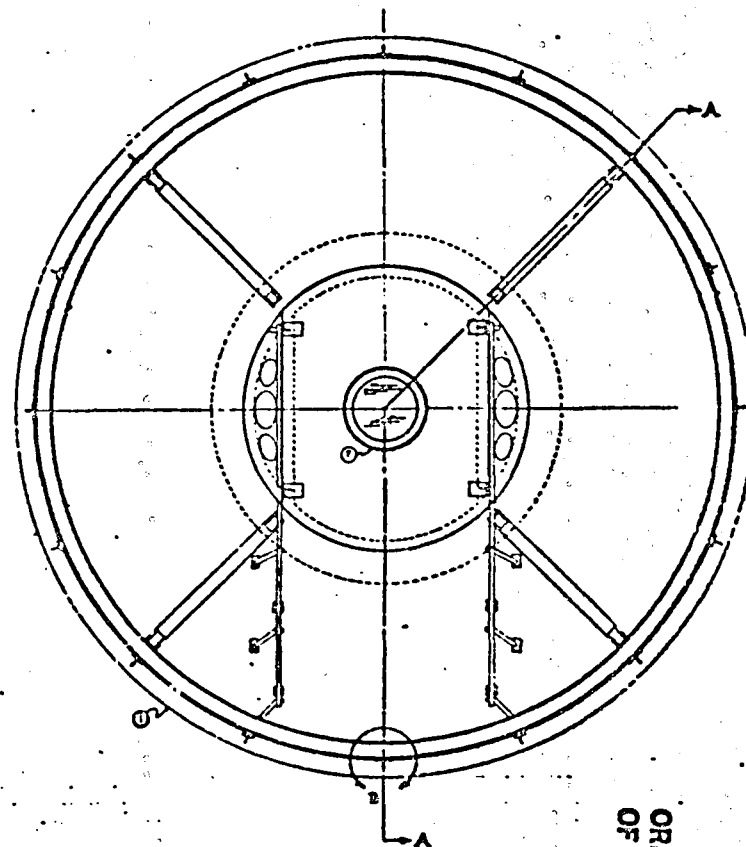
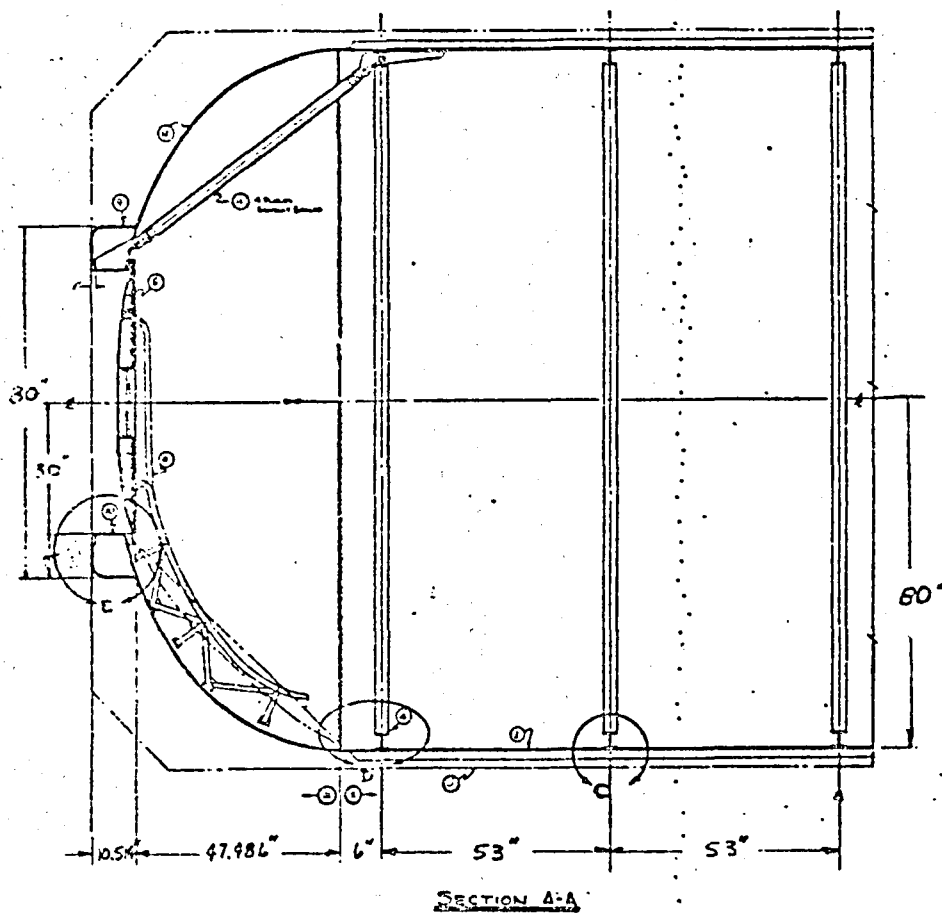


FIGURE 3.4.5 INTEGRALLY MACHINED STIFFENER CROSS-SECTION

be minimal. Floors and partitions will carry the loads due to crew and mounted equipment, but the basic design must remain "clean" in order to afford the maximum possible configuration flexibility.

3.4.3.2 End Closure Design - The Cassinian dome, chosen as the baseline end closure for this study, has an internal radius of 80 inches and an internal rise of 53.978 inches. The Cassinian curve may be used to design a wide range of shapes with a minimum of discontinuity stresses. Hemispherical and ellipsoidal domes are special cases of the Cassinian dome. The meridional curve of a Cassinian dome contains two parameters that permit much flexibility in meeting design conditions. The parameters m and n were selected to yield a minimum rise under the condition of all tensile membrane stresses during internal pressure loading ($m = 0.19$ and $n = 1.167$ -- see reference 2). The Cassinian dome end closure has the highest strength-to-weight ratio under pressure loading than any of the other configurations considered in this study.

A 60-inch diameter hatch is centrally located in each end closure as shown in figure 3.4.6. The hatch opening is bounded by a torus to provide a minimum distortion seal surface. The door of the end closure is mounted on parallel rails for sliding operations so as to minimize the encroachment into the



ORIGINAL PAGE IS
OF POOR QUALITY

FIGURE 3.4.6 SHUTTLE LAUNCHED SPACE STATION BASIC
MODULE --- CASSINI CONFIGURATION

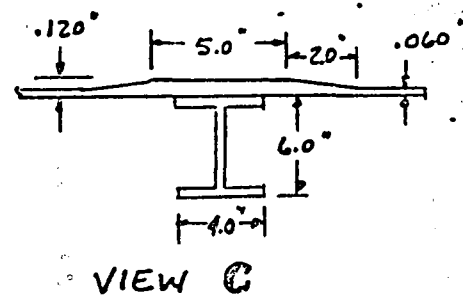
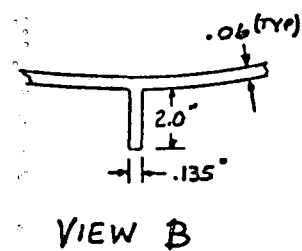
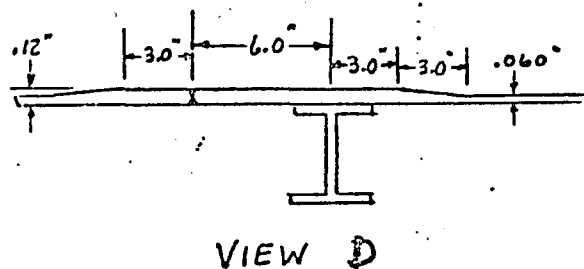
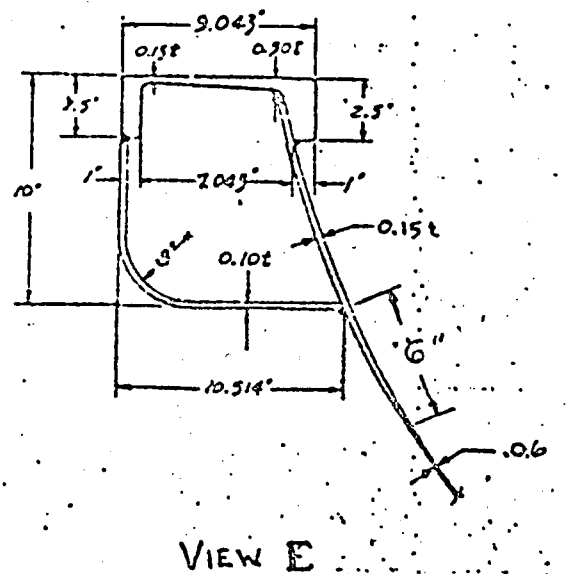


FIGURE 3.4:6 (CONTINUED)

element functional area. The door has a centrally located window. A sandwich-type, lens-shaped door was considered. A membrane-type lightweight door has been conceived as an alternate design.

Four struts connect the torus area at the door seal to fittings in the cylindrical section of the modular element. The struts are located so that the door slides along the wall between two of the struts. The four struts are not required for strength under pressure loading. As presently conceived, the inertial loading due to docking will require the strut configuration.

The struts do not seriously infringe upon the clean volume concept. However, an alternate design to accommodate the inertial loads was formulated. The alternate load path was provided by a "bird cage" structure exterior to the Cassini dome closure. This concept weighs over 400 pounds in comparison to 160 pounds for the recommended four-strut design.

3.4.3.3 Weld Joint Design - A weld land of 0.12 inch, or "2t," was used at the dome/cylinder circumferential intersection. This welded joint was analyzed in detail for stresses in the weld area because of pressure loading. Since the module is so large, it is doubtful that the joint can be conditioned after welding and would lead to a possible weak area with respect to strength and life integrity. Additional stresses in the weld because of mismatch and sinkage discontinuities, were calculated to establish manufacturing tolerances.

3.4.3.4 Supporting Analysis - Reference 3 is a computer analysis of a Cassinian dome Space Station module very similar to the design considered for this study. Of particular interest is the analysis of a torus/cassini dome area surrounding a docking hatch. This analysis not only confirmed a design which did not require the struts for pressure loading of the shell but also confirmed that the torus and shell combination possesses sufficient torsional and bending stiffness to minimize the distortion of both the inner and outer sealing surfaces of the docking interface.

Loads at the docking interface will require four struts to transfer the load to a ring frame in the cylinder of the module. The monocoque shell structure of the dome will not provide the needed load path without buckling even though it is assumed to be pressure stabilized. The following analysis was required for the strut sizing in which it was assumed that two of the four struts carry all the load.

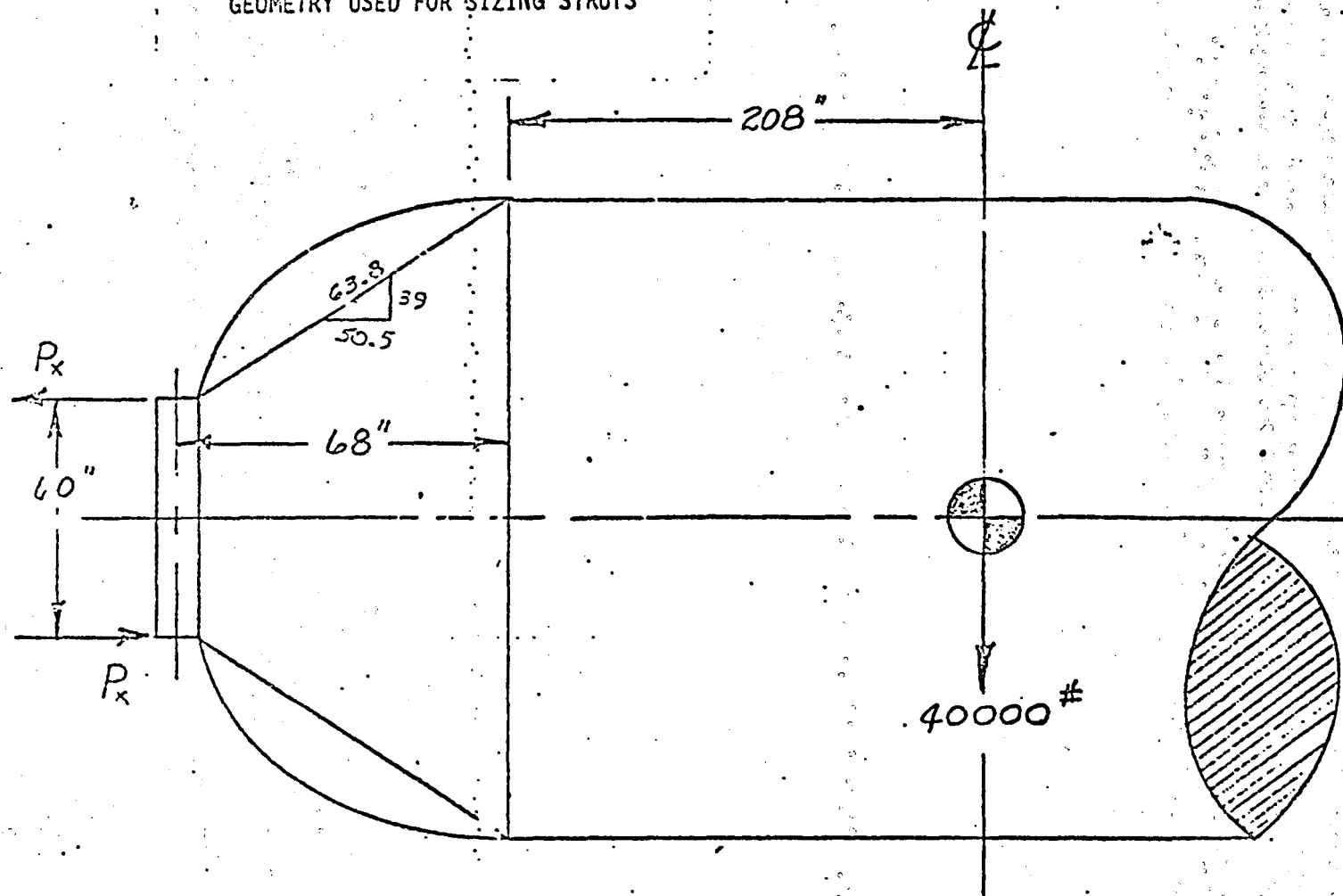
Strut Sizing - The ultimate load factor is assumed to be 1.0g. From Figure 3.4.7 the reaction couple for is

$$P_x = \frac{(40000)(1.0)(276)}{60} = 184000\#$$

The maximum tension and compression load in the strut is

$$P_x = \frac{(184000)(63.3)}{50.5} = 230638\#$$

FIGURE 3.4:7
GEOMETRY USED FOR SIZING STRUTS



Choosing an aluminum tube 2014-T6 of 6" OD x 1/4" wall thickness

$$A = 4.712 \text{ in}^2 \quad \mathcal{I} = 2.121 \text{ in}^4$$

The ultimate tension and compression stress in the tube is

$$\sigma = \frac{230638}{4.712} = 49000 \text{ psi}$$

The buckling allowable from Figure 3.4.8 for

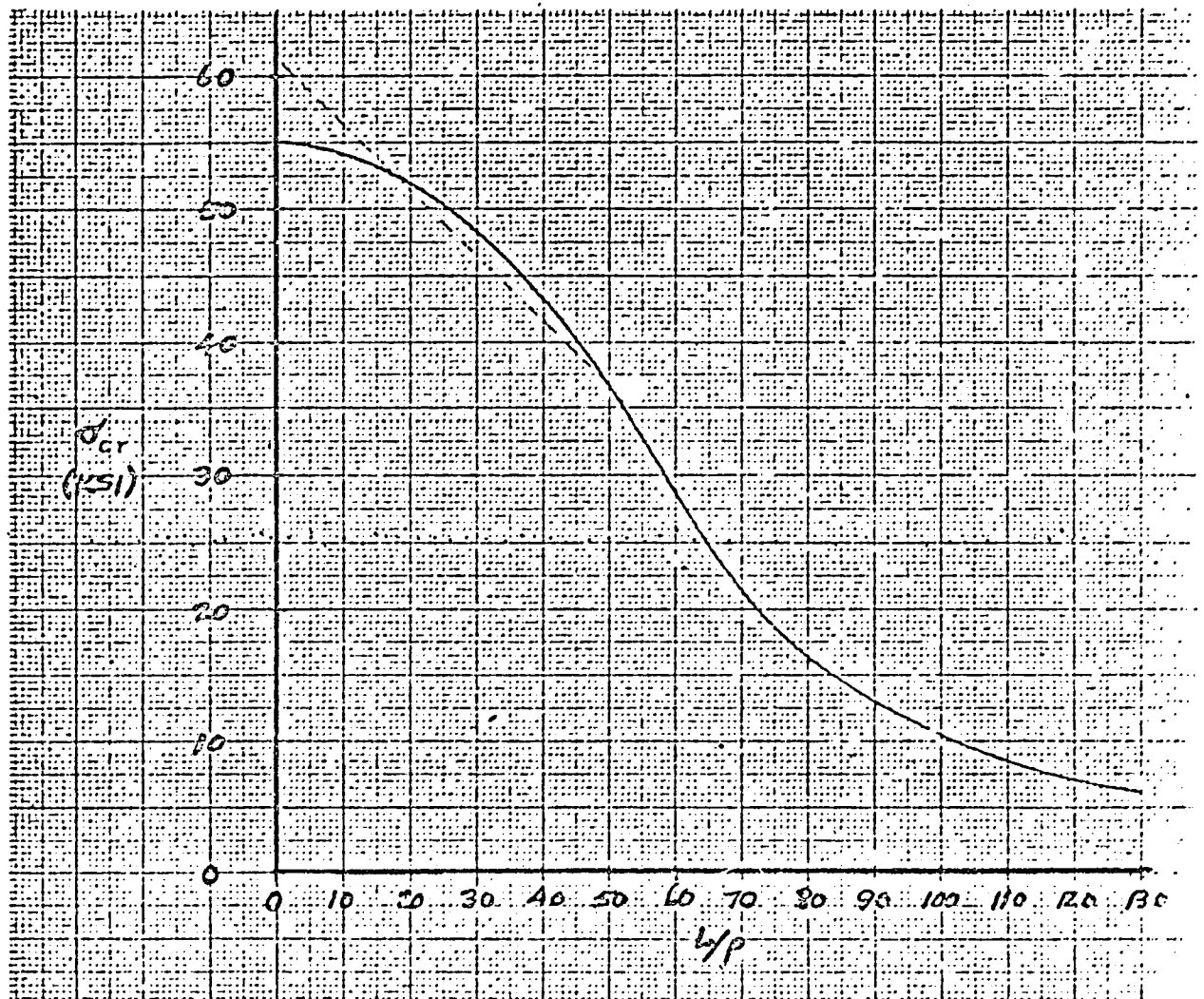
$$L/\rho = \frac{63.8}{2.121} = 30 \quad \text{is}$$

$$\sigma_{cr} = 49000 \text{ psi}$$

The weight of each tube is approximately 30 pounds. An additional 10 pounds should be added to each tube for end fittings.

ORIGINAL PAGE IS
OF POOR QUALITY

FIGURE 3.4.8
COLUMN ALLOWABLE CURVE (EULER - JOHNSON)
END FIXITY COEFFICIENT = 1.0 (PIN ENDED)
2014-T6 ALUMINUM EXTRUDED TUBING



3.4.4 Meteoroid Protection

The Space Station requirement established in this study for meteoroid protection reliability, states that the station will have a 90° probability of no penetrations for 10 years. Using the criteria of references 4 and 5, it can be seen that a single module skin thickness required to meet this requirement is over 1-inch thick. Therefore, it is recommended that the meteoroid protection system use the meteoroid bumper concept. This concept requires that an outer shield be placed around the module (usually aluminum) that will act as a meteoroid bumper. The purpose of the bumper is to slow down the meteoroid as well as break it into smaller pieces. Experiments using hypervelocity impact projectiles and aluminum targets have optimized the bumper thickness and spacing between the bumper and the pressurized shell structure that will cause the meteoroid and the impacted metal to vaporize resulting in a gaseous impact loading on the pressurized shell structure.

Using the meteoroid shield concept, the shield thickness required to meet the design requirement of 90% probability of no meteoroid penetration for 10 years is .037 inches. The required pressure shell thickness to withstand this impact without having a penetration is .080 inches for a spacing of two inches between the shield and the pressure shell, or .057 inches for a 4-inch spacing.

Because of the modular concept, a punctured module could be shut off from the rest of the station and could be repaired or replaced. Because of the replacement capability of the module concept, perhaps a probability of 90% of not having a penetration for three years would be a more reasonable goal. For this requirement, the shield thickness becomes .027 inches thick and the pressure hull would be .040 inches thick at the 4-inch spacing which happens to be the same internal pressure requirement plus a 25% increase for impact damage. However, in keeping with the original design requirement, it is recommended that the outer shield thickness be .040 inches and the pressure shell thickness be .060 inches with a 4-inch spacing between the shield and the pressure shield.

3.4.5 Module Weight

The primary structural weight has been calculated for the modular element in its "clean" condition; i.e., less floors, partitions, docking mechanisms, etc. Some of the omitted items are included in secondary structure and the remaining items are listed as subsystems. A total launch weight of 40,000 pounds was assumed. The basic skin thickness was .060 inch. The weight was accurately calculated, but some minor perturbation will occur from the detailed analysis of the structure.

The distribution of weight in a basic modular element with Cassinian dome end closures and a basic skin thickness of .060 inch is as follows.

A. Cylindrical Sidewall Assembly	4191	
B. Dome Assembly	1516	
C. Total Primary Structure		5707
D. Secondary Structure (10% of Subsystems)		3118
E. Subsystems		
Meteoroid Protection	952	
Seals	64	
Thermal Insulation	373	
Remaining Subsystems	29,786	31,175
Total Launch Weight		40,000 lbs.

The cylindrical section weight breakdown is as follows

A. Skin (t = .06)	1315
B. Rings (9)	696
C. Longerons (162)	1907
D. Mounts	35
E. Weld Lands	238
	4191 pounds

The breakdown of the weight in the Cassinian dome end closure is represented in line 1 table 3.4.1. The skin gage was assumed as .060 inch (meteoroid requirement) and not the .032 inch.

TABLE 3.4.1 END CLOSURE WEIGHT COMPARISON
FOR A 14-FOOT DIAMETER CYLINDRICAL
TANK UNDER 29.4 PSI PRESSURE

GEOMETRIC SHAPE	C O M P O N E N T S							TOTAL
	Docking Cylinder	Torus	Collar	Door	Core or Beams, Rings, etc	Skin	Weld and Weld Lands	
Cassinian Dome	128	60	34	183	160	156	37	758
Elliptic Dome	128	60	34	183	160	156	37	758
Conic Dome	128	60	34	183	215	230	37	887
Spherical Dome	128	60	34	183	160	202	37	804
Flat Sandwich	141	--	60	183	540	192	50	1166
Flat Beam/Skin/ Stringer	188	60	34	183	545	103	47	1160

required for pressure loading. The weights shown are based on detailed computer analysis of the modular element under pressure loading. The inertial loading from a docking environment has been considered for the strut analysis in a "slide rule" calculation. Thorough analysis of the module structure in an artificial g-environment is pending.

A comparison of the weights of primary structure required for various types of cylinder end closures is given in table 3.4.1. The weights were obtained from a cursory design and analysis study and are not necessarily optimum structure. The Cassinian, elliptic, and spherical domes are essentially equal in weight, but the Cassinian dome has the lowest discontinuity stresses.

3.4.6 Manufacturing Summary

3.4.6.1 Materials Selection - Aluminum alloys were selected as the primary structural materials for the Space Station module. The rationale for selection was based on the low cost, lightweight, and fabrication ease of aluminum as compared to other candidate structural materials. Two specific alloys, types 2219 and 6061, were incorporated because of their good weldability and their successful application on previous manned spaceflight programs. Past experience with these two aluminum alloys has established proven fabrication techniques and procedures which should provide flight hardware at a minimum development cost.

3.4.6.2 Fabrication Considerations - The fabrication of the Space Station module presents several problems because of its relatively large size (approximately 14-foot diameter and 46 feet long). The module is basically a cyclindrical structure capped at each end by some type of structural closure.

The fabrication of the cylindrical portion of the module can be accomplished, using existing manufacturing technology. One procedure for fabricating the cylindrical portion could be as follows

- A. Use 2" thick, 60" wide, flat plate stock, 2219-T351 aluminum alloy to make cylindrical segments.
- B. Rough machine plates to form integral longitudinal stringers.
- C. Roll or stretch form rough machined plates to proper contour (14 feet diameter).
- D. Finish machine (using chemical milling) to final membrane thickness and weld land configuration, allowing for future dimensional changes in processing.
- E. Age cylindrical segments to T851 heat treat condition.
- F. Assemble the cylindrical portion of module by welding all segments together.

The fabrication of the end closures for the module requires somewhat different manufacturing techniques, depending on the geometric shape of the closure. In this study, six types of end closures were investigated: Cassinian dome, elliptic dome, spherical dome, conic dome, flat bulkhead (beam/skin/stringer construction), and flat bulkhead (sandwich construction). The Cassinian dome was selected as the baseline design end closure for comparison with other type closures. Fabrication considerations for the end closures are included in the following sections.

3.4.6.3 Cassinian, Elliptic, and Spherical Dome Fabrication - The fabrication techniques for

the Cassinian, elliptic, and spherical dome end closures are similar. The design of these closures does not require integral stringers or similar reinforcement; therefore, relatively thin sheet stock (approximately 1/8" thick) can be used in their construction. Ideally, these domes should be fabricated from a single sheet of 2219-T851 aluminum alloy; however, the maximum capacity of existing aluminum sheet rolling mills restricts the final sheet size to approximately 10 feet wide. Twenty-foot-wide sheet stock would be required to fabricate each dome from a single sheet. The limitation on sheet stock width necessitates welding an assembly of pie-shaped dome segments. Two or more segments can be used in assembly, but only two segments would be preferred to minimize the welding requirements.

The fabrication of each dome could be done using the following procedures

A. Use 1/8" thick, 120" wide, flat sheet stock, 2219-T351 aluminum alloy to make dome segments.

B. Trim and roll segments to the approximate flat contour required.

C. Form (using explosive or hydroelastic press-forming techniques) to the exact dome contour dimensions.

D. Finish machine (using chemical milling) to final membrane thickness and weld land configuration, allowing for future dimensional changes in processing.

E. Age dome segments to T851 heat treat condition.

F. Assemble the module dome by welding the segments together.

Other methods for fabricating a one-piece of unitized dome closure were investigated, included were shear forming, spinning, and explosive forming. Of these three methods, only shear forming appears to be feasible because of limitations in the maximum width of available sheet stock. Shear forming may be used because the thicker plate material is thinned during forming, resulting in a larger diameter finished product. The problem of heat treating a 14-foot diameter dome to acceptable strength levels after shear forming requires further study.

3.4.6.4 Conic and Flat Bulkhead Dome Fabrications -

The conic and flat bulkhead dome fabrication is more complex because the design requires integral stiffeners to carry the loads. The details of the design have not been established, but previous fabrication experience can be incorporated to manufacture these domes with essentially no development work required.

The conic and flat bulkhead (beam/skin/stringer construction) can be fabricated using techniques similar to those used in the cylindrical portion of the basic modular element. The Martin-Marietta Corporation incorporated a flat bulkhead design (beam/skin/stringer) in the 15-foot diameter Subsystem Test Bed vehicle that was delivered to JSC in 1971.

The flat bulkhead (sandwich construction) was also considered in this study, primarily to obtain a fabrication cost comparison with the other domes. Its fabrication can be accomplished with proven skin and honeycomb construction techniques used on previous manned spaceflight vehicles.

3.4.6.5 Fabrication Cost Comparison -

The relative costs of six types of end closures were compared. The Cassinian dome was selected as the baseline cost reference. A breakdown of comparative costs is presented in figure 3.4.9. This cost comparison includes factors related to fabrication of the end

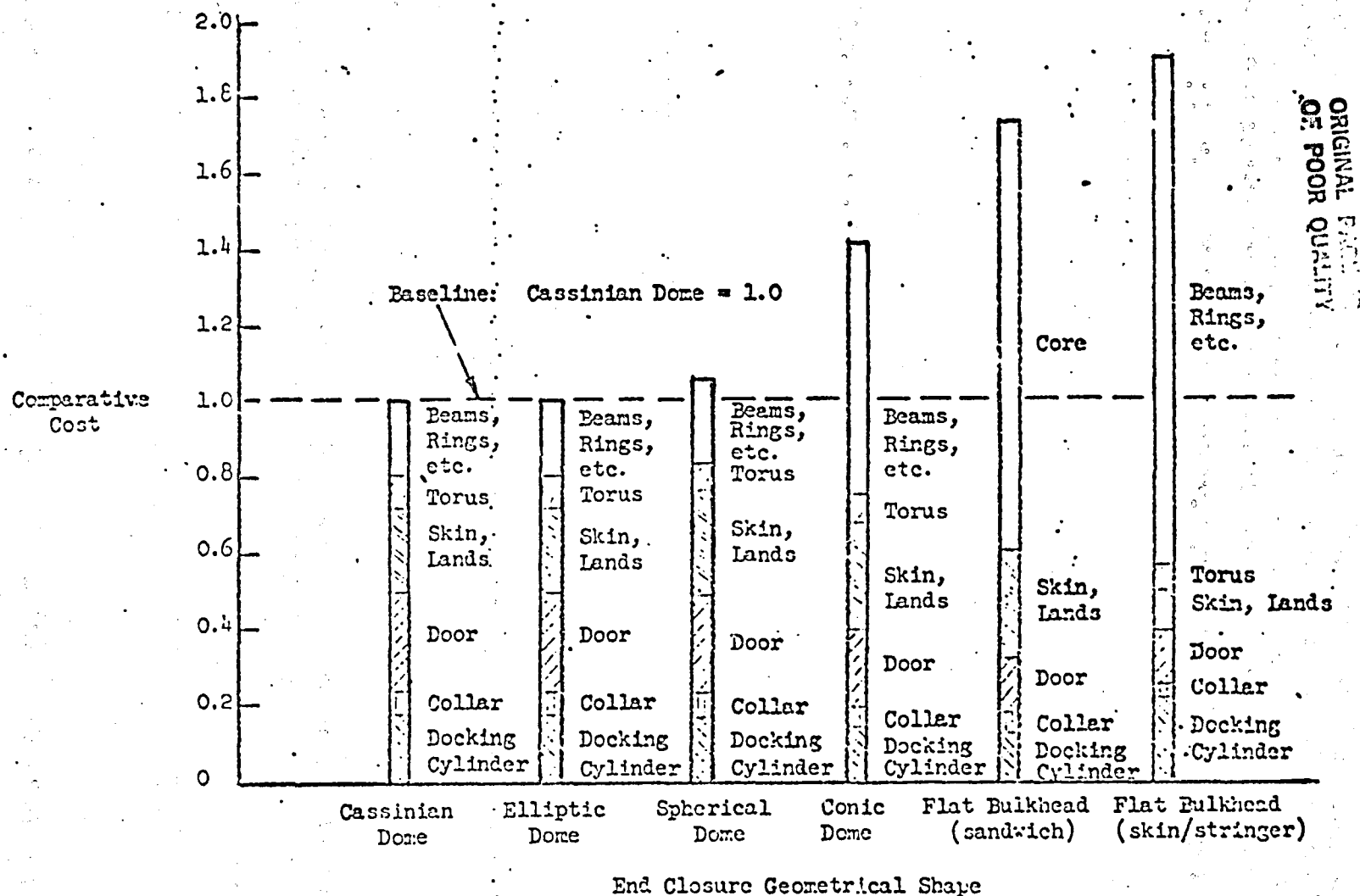


FIGURE 3.4.9 Fabrication Cost Comparison For Six End Closures Proposed for 14 Ft. Diameter, 45 Ft. Long Space Station Module

closures only. The cylindrical portion of the module was assumed to be the same for each dome shape, although longer cylinders will be required for the two flat bulkhead designs to maintain a constant module overall length.

The primary factors evaluated in developing relative costs of the various domes included fabrication techniques and complexity, materials availability and costs, design weight, and previous costing experience. Perhaps the most significant cost factor was design weight because weight is indirectly related to the load-carrying efficiency of the dome structure. As a result, the Cassinian dome proved to be the least costly of the six domes evaluated. The gradual transition of the cylindrical portion of the module to the Cassinian dome closure minimizes structural discontinuities which require heavy reinforcement of the load-carrying members with a resulting increase in weight.

3.4.6.6 Fabrication Summary and Recommendations - The possible manufacturing procedures for fabricating the cylindrical portion and the various end closures for the Space Station module were reviewed and evaluated. For least cost, the curved dome end bulkheads (Cassinian, elliptic, and spherical) were favored because of a more efficient load-carrying design. The fabrication of the curved domes was limited, however, to segmented and welded assemblies because of present aluminum alloy sheet width rolling mill capacities.

The following additional tasks are recommended to investigate other areas, not included in the present design, for further reduction of fabrication costs

A. Explosive forming or spinning of unitized domes, using welded sheet stock.

B. Shear forming of unitized domes, using thick plate stock.

C. Assembly of external or internal structural stringers and rings, using adhesive systems and/or mechanical fasteners.

D. Evaluation of other candidate alloys in more detail, such as nonheat treatable aluminum alloys and maraging alloy steels for the structural shell.

3.4.7 Tunnels

The component of the Space Station which permits a crew member to go from one module to another module (across the truss) are the three tunnels. The tunnels also satisfy the requirement for a dual escape from the modules in case of fire, and other emergencies.

Each tunnel is constructed of three telescoping sections that are .03 inches thick, four feet in diameter, with two internal layers of flexible but relatively inextensible

membrane for containing the pressure (see figure 3.4.10). The collapsed tunnels are stowed for launch in the void existing down the center of the modules. A system of pretensioned cables will react the axial load caused by internal pressure, thus, eliminating additional load on the modules.

Alternate Concept to the Tunnels

One alternate concept that was considered in place of the three tunnels is the cable car concept. Each tunnel is replaced with a pair of cylindrical capsules having docking ports on each end, drawn by cables, mounted on opposite sides of a taut cable system (see figure 3.4.11). Each habitable module will have two docking ports and a cable driven system instead of a tunnel interface.

ORIGINAL PAGE IS
OF POOR QUALITY

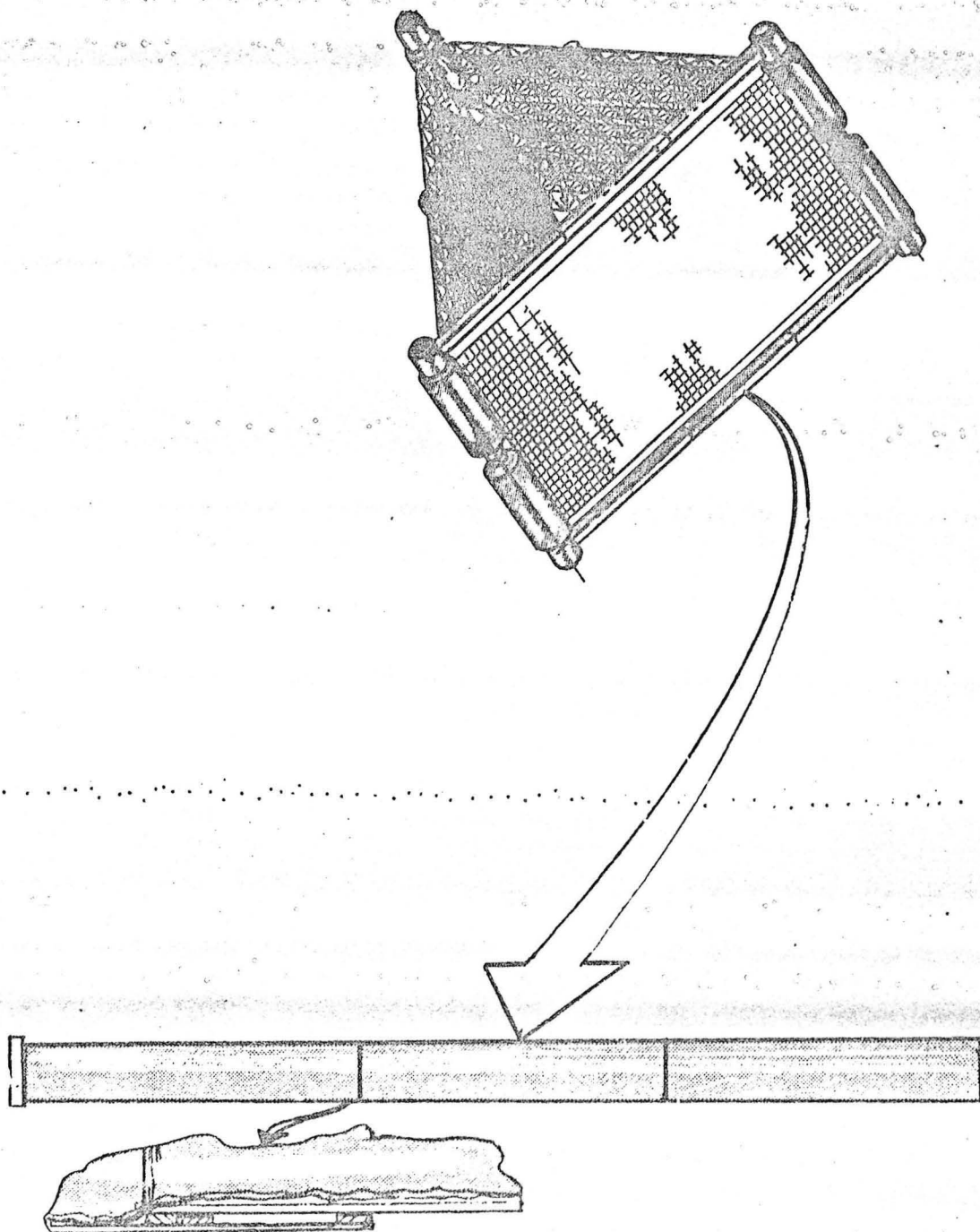
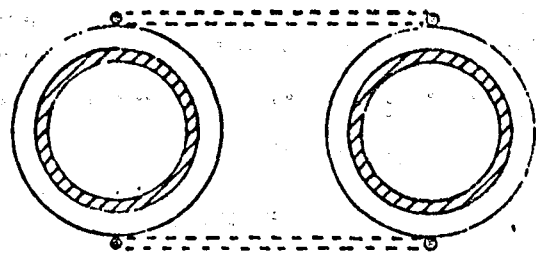


FIGURE 3.4.10

CABLE-CAR TRANSFER CONCEPT



END VIEW
BOTH CARS SHOWN

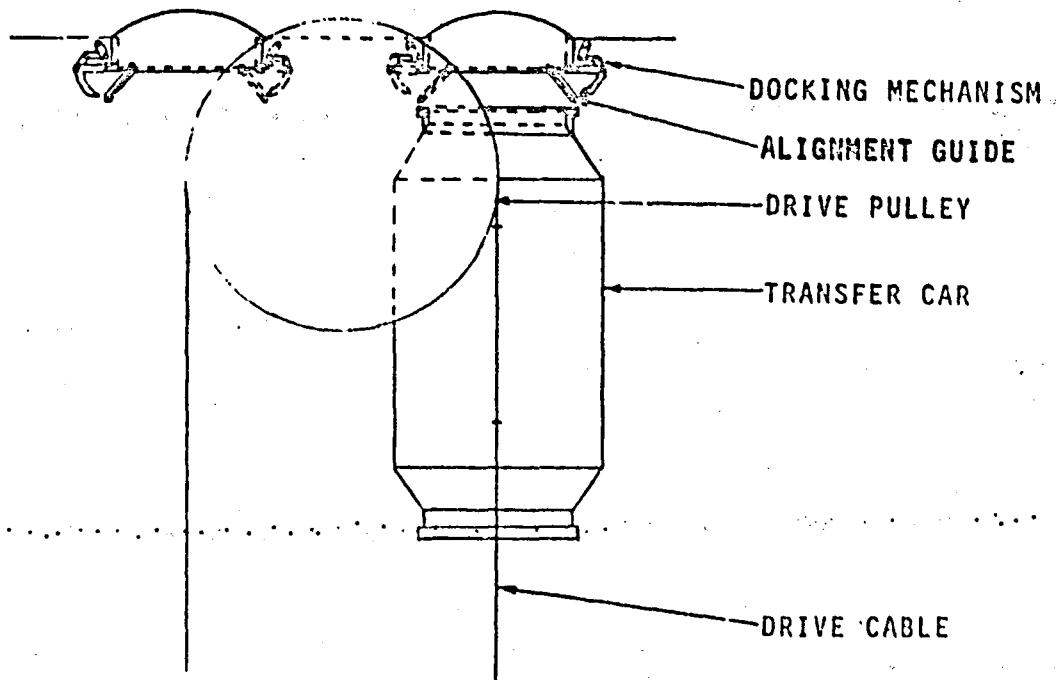


FIGURE 3.4.11

3.4.8 Conclusions and Recommendations

This section has presented analysis and rationale to establish the feasibility for the design and manufacture of a Shuttle launched Space Station module. The results of this study have determined one specific size and shape of module which may change as the Space Station configuration becomes more defined. However, this study was conducted to verify the feasibility of manufacturing a universal size module. As the Shuttle load carrying capability becomes better defined, it is recommended that a more detailed and rigorous module study be performed. It is also recommended that additional thought be given to the meteoroid penetration and debris requirement.

The Cassinian dome end closure concept is recommended for the baseline design for the following reasons

A. The shape of the dome will add a few more inches to the cylinder length resulting in a larger internal volume.

..... B. The discontinuity stresses at the juncture of the dome and cylinder are less than other dome shapes.

C. The Cassinian has the highest strength-to-weight ratio than other domes.

D. Least costly to manufacture.

It was found that all end closures examined in this study would require additional stiffening to withstand external docking loads. The concept chosen for the baseline was the addition of four tubular struts to transfer these loads from the docking ring directly to the cylinder ring frame. The arrangement of these struts was situated so that they would not interfere with head space or hatch opening and closing; however, these struts could be removed in orbit and stowed if necessary.

3.4.9 References

1. Space Shuttle System Payload Accommodations, NASA JSC 07700, Vol. XIV. Rev. G, Sept. 26, 1980, ICD 2-19001, "Shuttle Orbiter/Cargo Standard Interfaces," Attachment 1.
2. Spera, David A. and Johns, Robert H., "Theoretical Elastic Stress Distributions in Cassinian Domes," NASA TN D-1741, July 1963.
3. Martinez, J.E., and Stricklin, J.A., "Stress Analysis for a Cassinian Space Station Under Internal Pressure," Report 70-96, Aerospace Engineering Department, Texas A&M University December 1970.
4. NASA SP-8013, "Meteoroid Environmental Model-1969."
5. Kavanaugh, H. C., "Meteoroid Protection for Spacecraft," NASA Manned Spacecraft Center Internal Note No. IN-65-ES-6, May 1965.

4.0 Buildup Sequence

The order of the Space Station buildup sequence is important to minimize the number of Orbiter flights and the EVA requirements. In addition, it is desirable to have a Space Station that can be inhabited as early in the buildup as possible. The objective of this section is to define a tentative buildup sequence with the above constraints. Based on this study, a total of eight Orbiter flights is required for a fully operational station but it can be inhabited after the second flight. The buildup will be in the following sequence

Delivery Flight No. 1

The Orbiter arrives at the Space Station orbital location with the following hardware in the cargo bay

- A) Three deployable trusses
- B) Solar cells
- C) Radiators
- D) Control moment gyros (CMG)

The three deployable trusses are removed from the payload bay, joined together at the three apexes and deployed to full size. Preferably, the three trusses could be joined prior to launch, removed from the Orbiter payload bay, and deployed as a single unit.

The solar cells are deployed next. EVA will probably be required for final solar cell connections to the truss. The radiators are also deployed and connected to the outside of another panel. See figure 4.1 for the Space Station configuration after this first flight.

Following the above sequence the solar cells can be checked out and truss joints inspected prior to Orbiter return.

One advantage to the above plan deployment of the three trusses, solar cells, and radiators is that complete checkout can be accomplished prior to any modules being brought to orbit. Module delivery and connection to the trusses is expected to be less difficult than truss erection.

Delivery Flight No. 2

Flight No. 2 begins the module flights, the first of which is a combination service module - habitat module. This first module can house the first crew in a part of the module. The SM/HM could function as a "mini" Space Station until further buildup.

Deployment of the SM/HM from the payload bay is accomplished with the (RMS). The triangular truss is held by the handling and positioning aid (HPA). The SM/HM is then connected to the truss by using the Orbiter RMS to position this module into place as shown in figure 4.2.

Delivery Flight No. 1

- 3 Deployable Trusses
- Solar Panels
- Radiators
- CMG Package

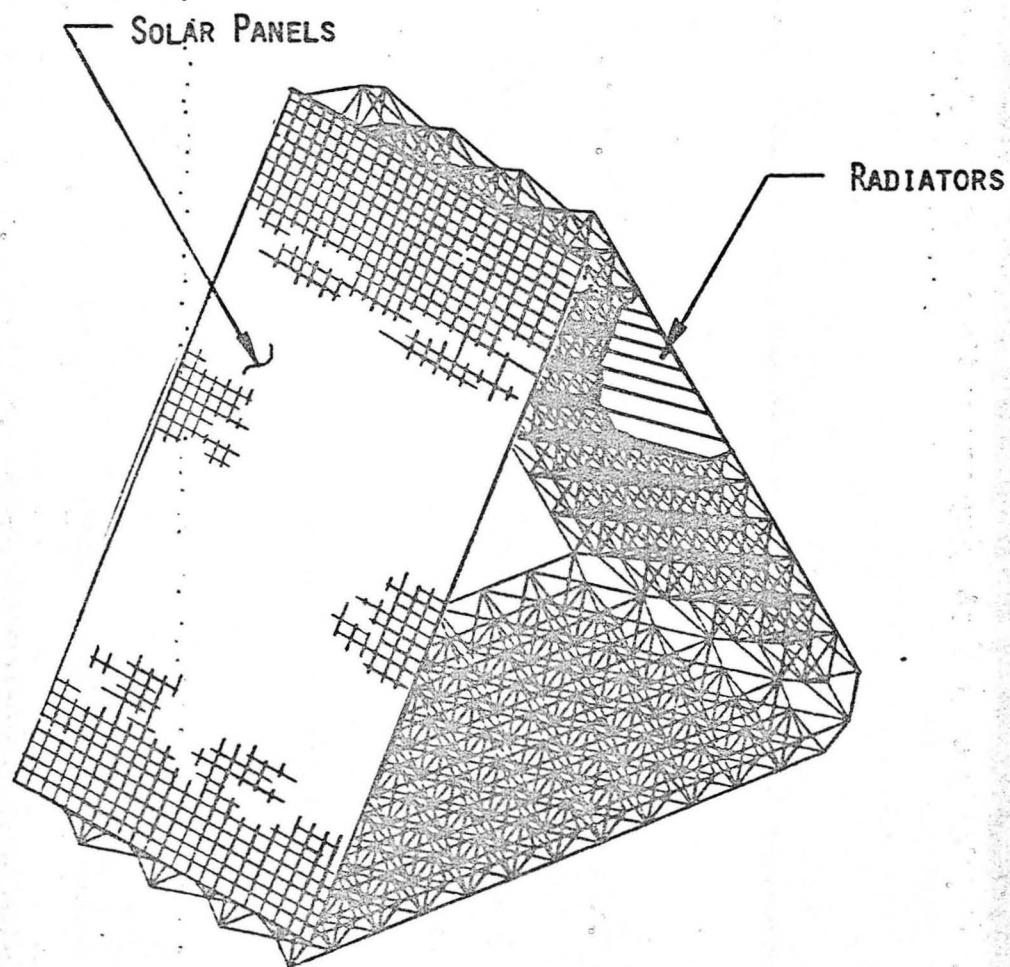


Fig. 4.1. Delivery Flight No. 1.

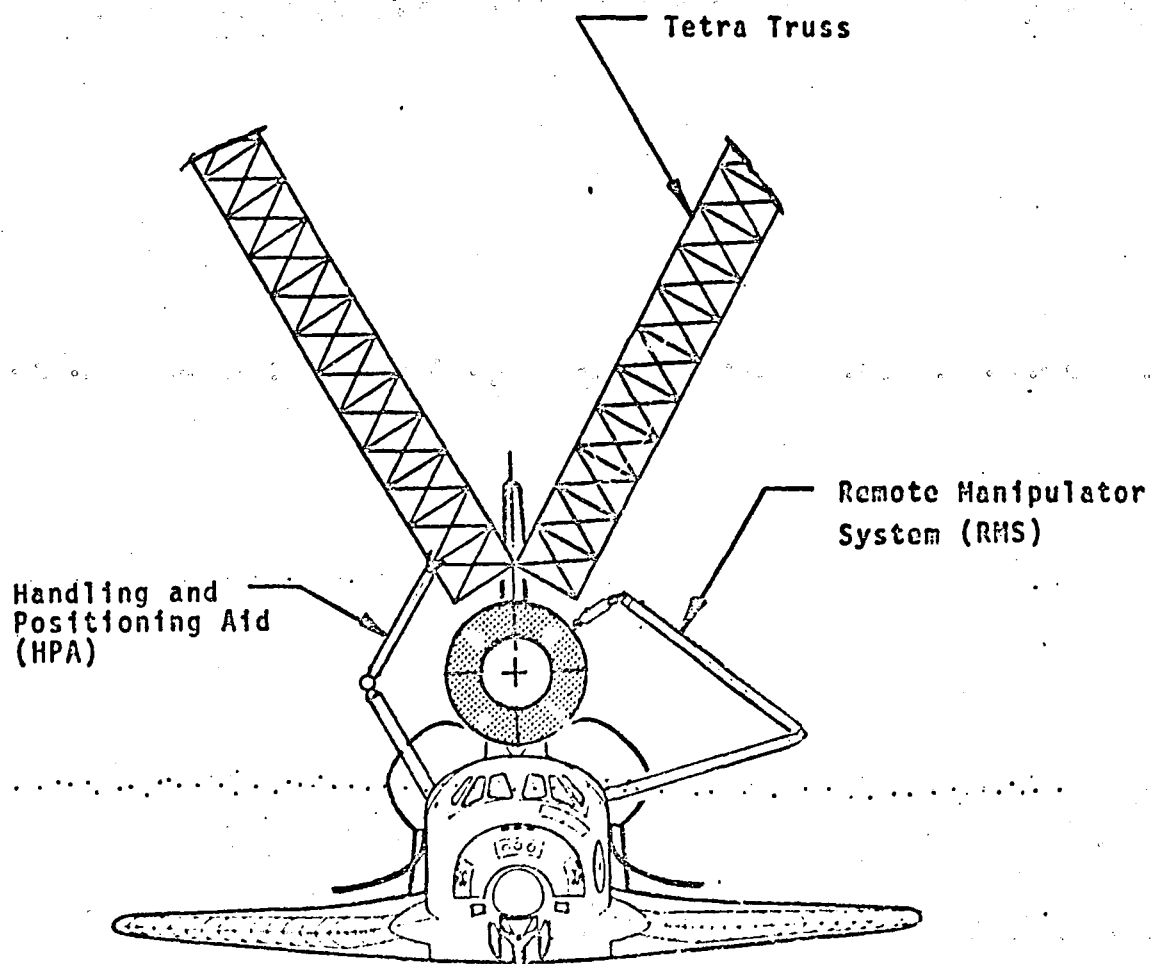


Fig. 4.2. The Positioning of a Typical Module into Place.

The truss to module joints are then locked by EVA crewmen. The solar cells are connected to the module electrical system, The ECLS system is connected and the Space Station is then functional on a small scale. See figure 4.3.

Delivery Flight No. 3

Orbiter flight No. 3 will bring a logistics module to orbit. The station will be held in position by the HPA and the logistics module will be removed from the payload bay by the RMS and attached to the truss joints by the same method used with the SM/HM. The logistics module will be berthed to the end of the SM/HM to complete a two module side of the triangle as shown in figure 4.4.

Delivery Flight No. 4

Flight No. 4 may be the optimum time to bring the manipulators to the station as shown in figure 3.2-14. Both can be carried in the payload bay, off-loaded and attached by the RMS and EVA crewmen. These manipulators will be attached to the edge of the tetratruss as shown in figure 4.5.

Delivery Flight No. 2

● Service - Habitat Module

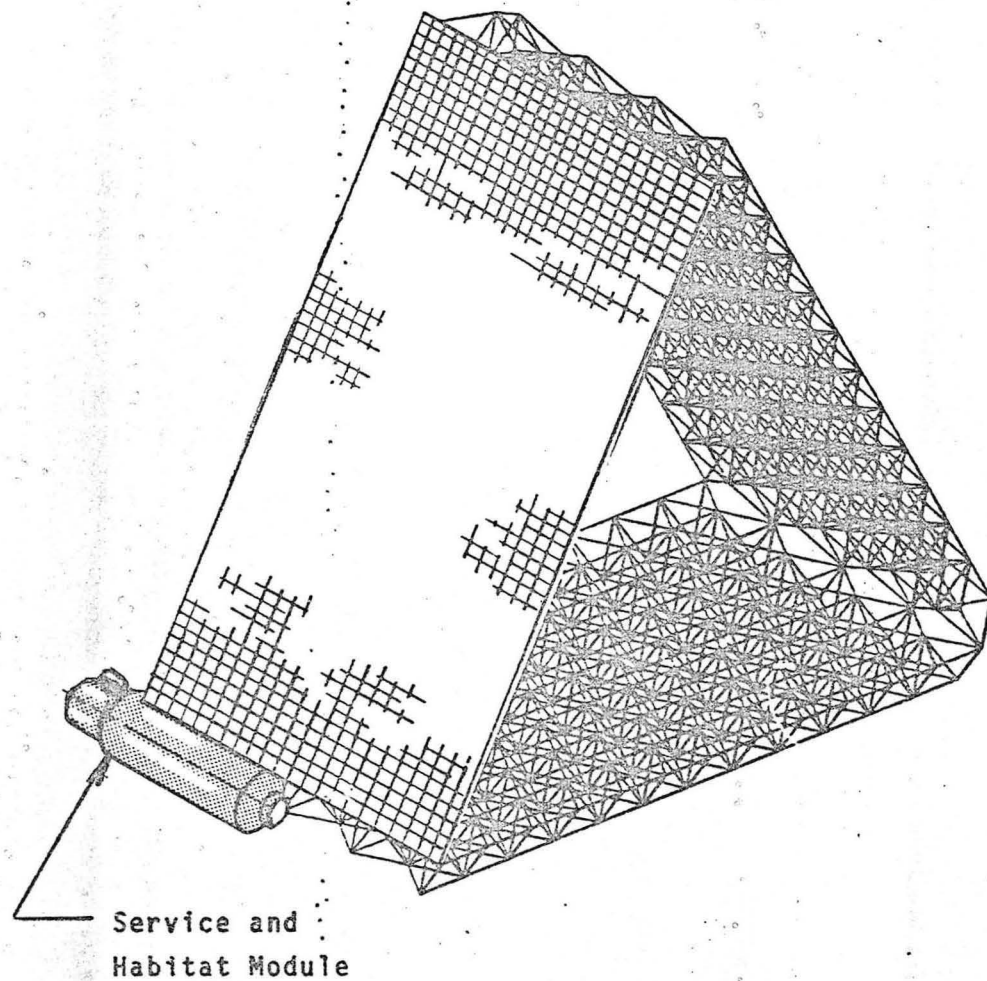


Fig. 4.3. Delivery Flight No. 2.

ORIGINAL PAGE IS
OF POOR QUALITY

Delivery Flight No. 3

● Logistics Module

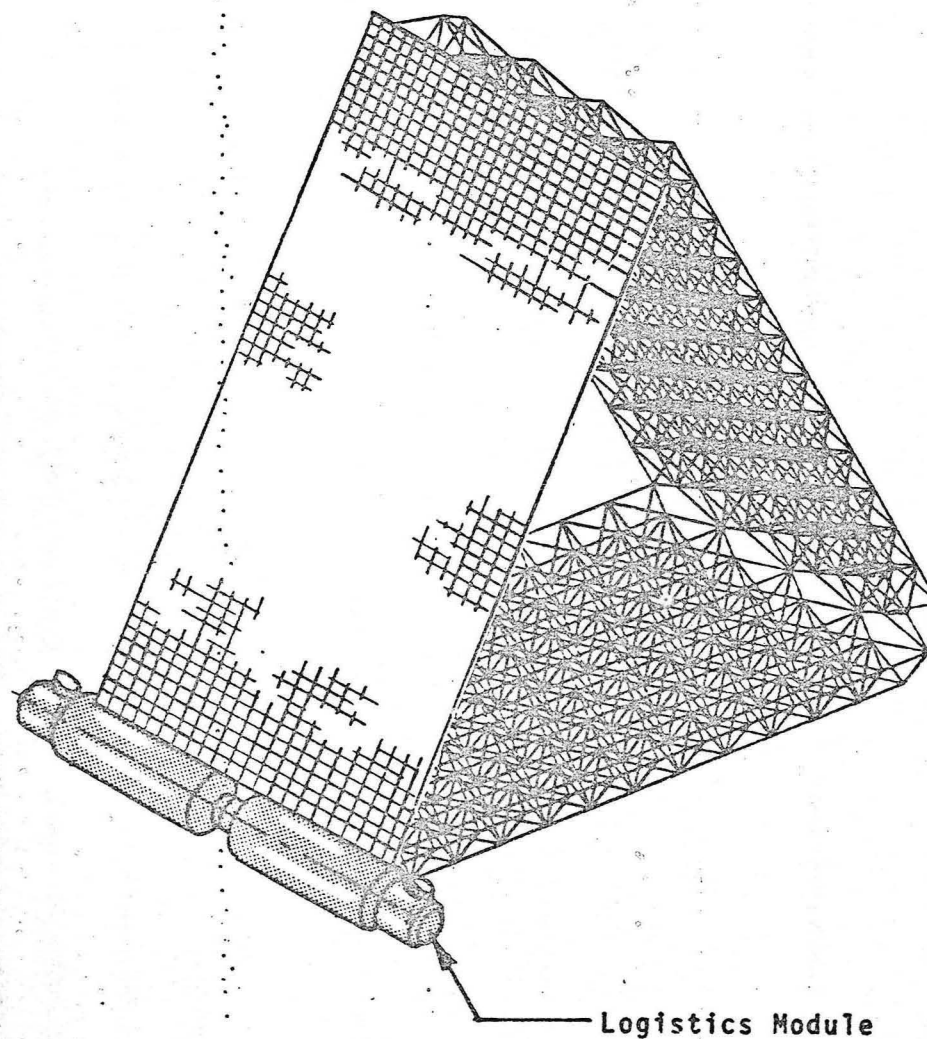


Fig. 4.4. Delivery Flight No. 3.

Delivery Flight No. 4.

• Two Manipulator Systems

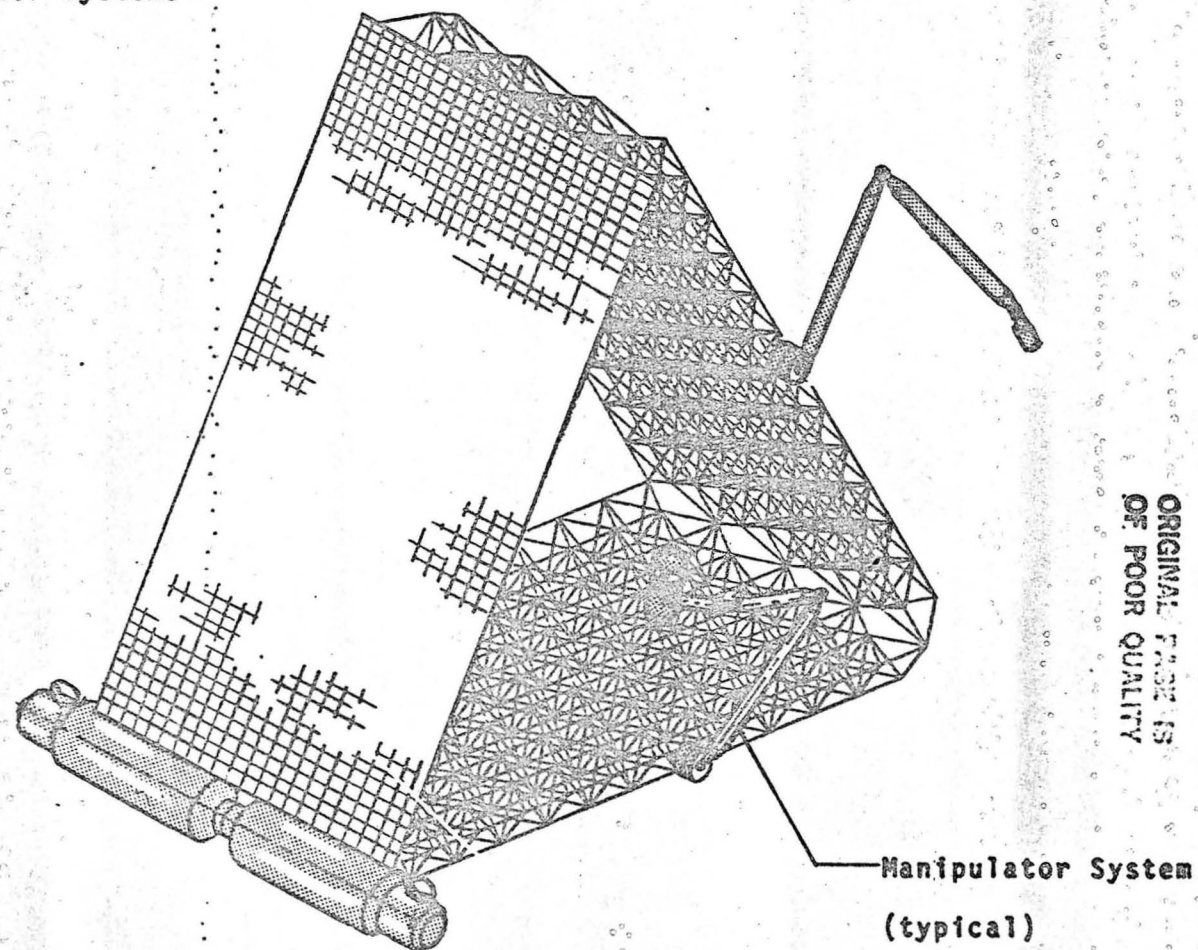


Fig. 4.5. Delivery Flight No. 4.

Delivery Flights 5,6,7, and 8

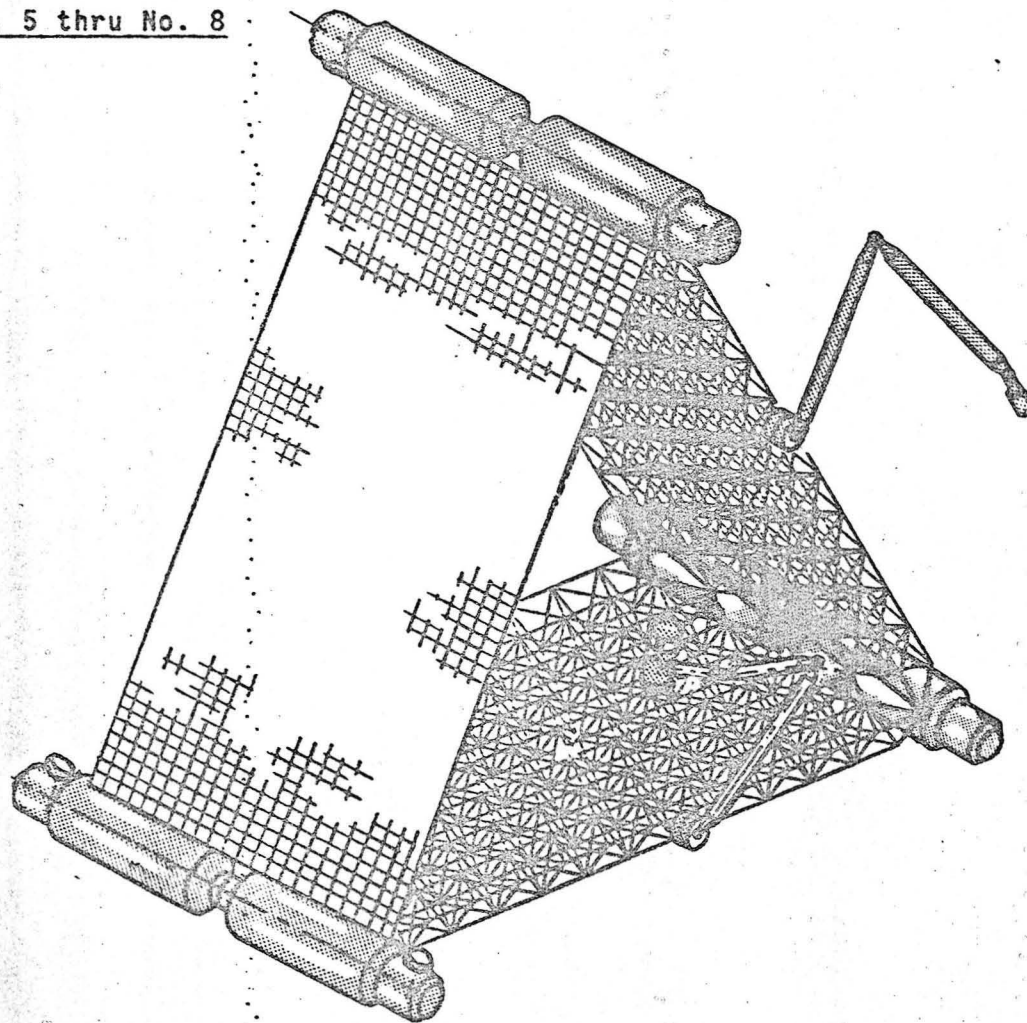
The next four flights are to be used to complete the six module Space Station as shown in figure 4.6. After these modules are positioned and fastened into place, the three connecting tunnels are installed into place as shown in Figure 4.7. Buildup can be on an as-needed schedule (i.e., all 6 modules are not required for the Space Station to be completely functional). Figure 4.8 shows the Space Station fully completed and operational.

Hydrazine tanks, antennas, RCS thrusters, and other equipment, will be taken into orbit as needed on module flights and assembled by EVA crewmen. Many of these items can be brought to orbit inside the modules, removed and relocated later.

The logistics module is used for the storage of consumables, spare parts and equipment, and the stowage of waste products for return from orbit. Because not all of the consumables or spares will be used between each supply or crew rotation period, it would seem more practical to leave the logistics module in place and have smaller containers of consumables to take to orbit and smaller containers of garbage and other wastes to be returned to earth.

Delivery Flights No. 5 thru No. 8

• Modules 3 thru 6.



ORIGINAL PAGE IS
OF POOR QUALITY

Fig. 4.6. Delivery Flights No. 5 thru No. 8.

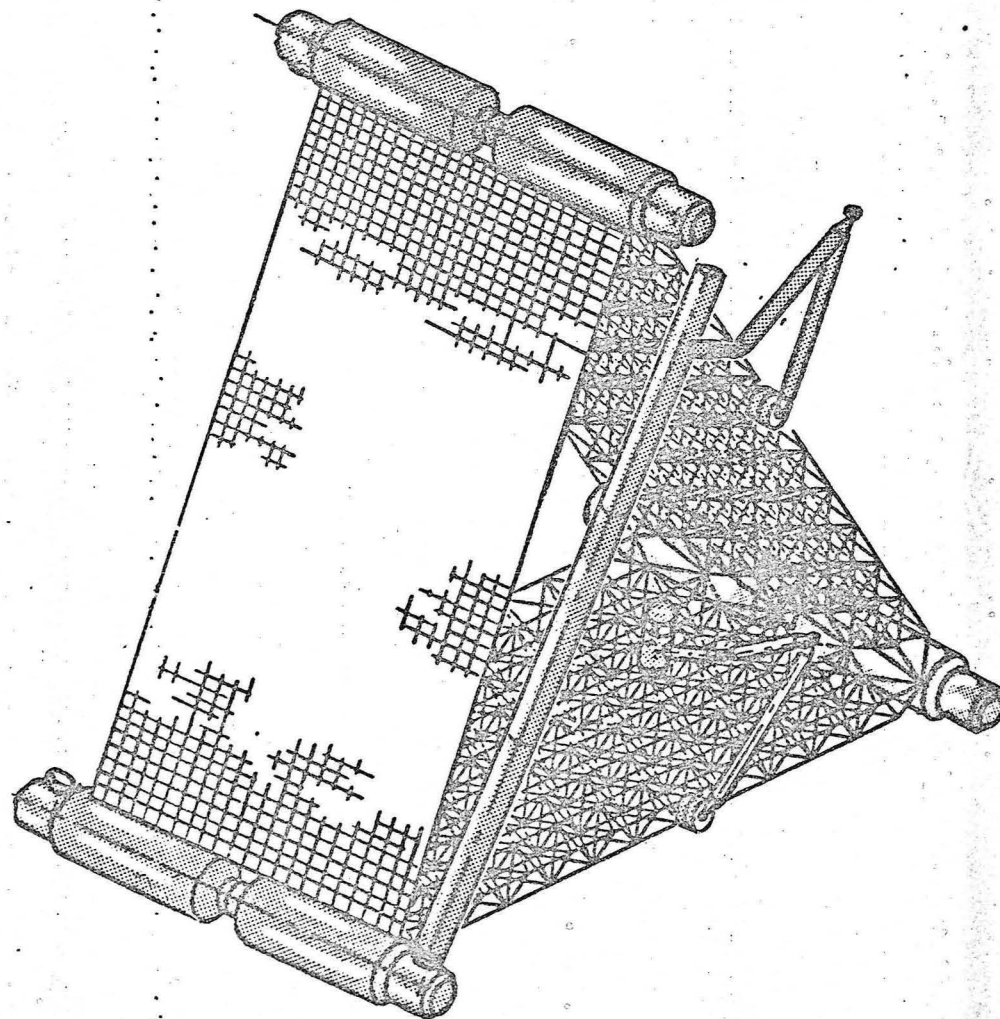
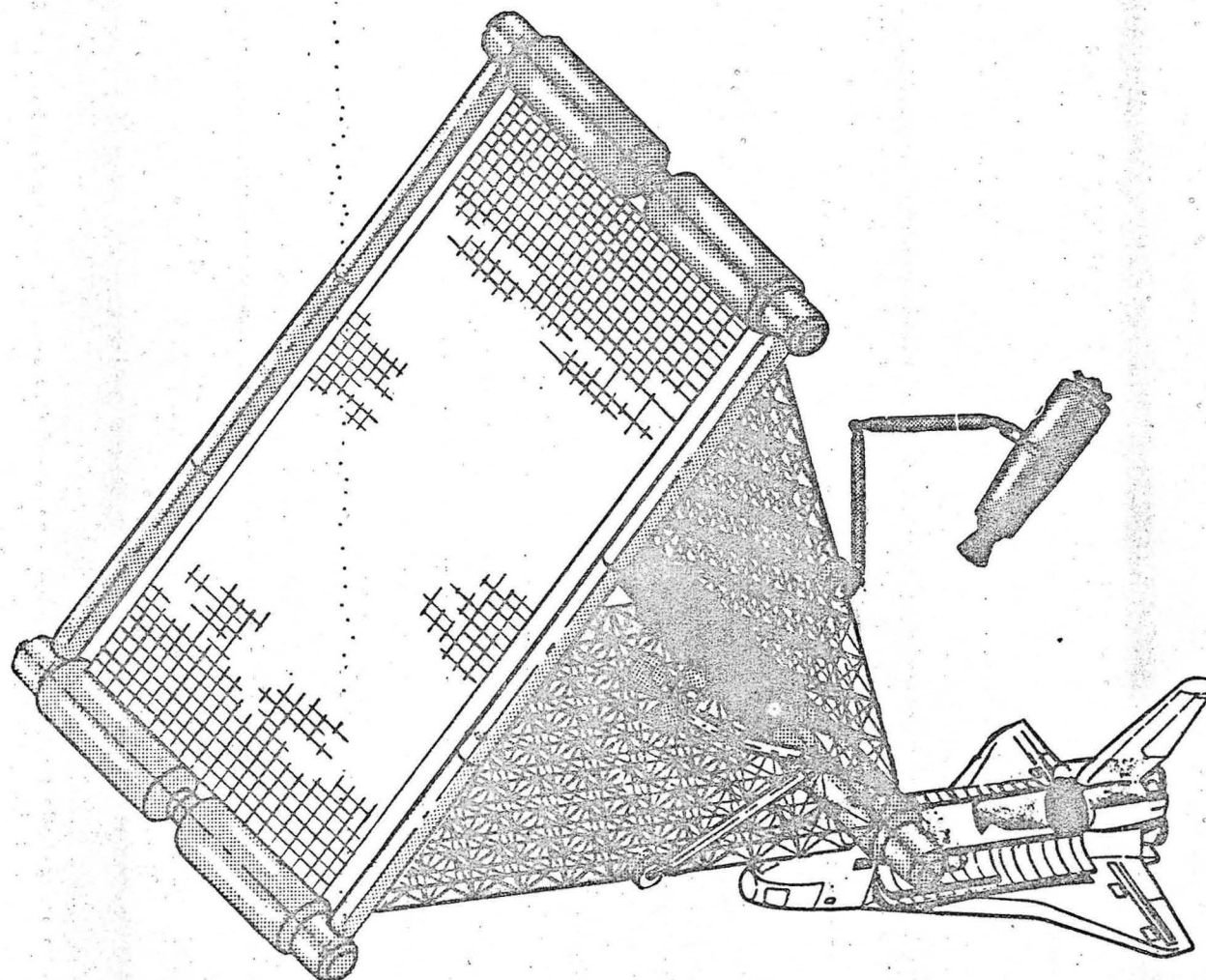


Fig. 4.7. Positioning the Tunnels into Position.



ORIGINAL PAGE IS
OF POOR QUALITY

Fig. 4.8 . The Complete and Operational Space Station.

5.0 CONCLUDING REMARKS

The results of a 3-month preliminary design and analysis effort has been presented in this report. The configuration that emerged consists of a very stiff deployable truss structure with an overall triangular cross section having universal modules attached at the apexes. Sufficient analysis has been performed to show feasibility of the configuration.

This study emphasized an evaluation of the structure required to accomplish the Space Station objectives. Desirable attributes of this configuration are

a) The solar cells, radiators, and antennas will be mounted to stiff structure to minimize control problems during orbit maintenance and correction, docking, and attitude control.

b) Large flat areas are available for mounting and servicing of equipment (OTV's, storage containers, large antennas, etc.).

c) Large mass items can be mounted near the center of gravity of the system to minimize gravity gradient torques (and resulting control required) or can be relocated to help stabilize the system by mass redistribution.

d) The trusses are lightweight structures and can be transported into orbit in one Shuttle flight.

e) The trusses are expandable and will require a minimum of EVA for initial Space Station buildup.

f) The modules are anticipated to be structurally identical except for internal equipment to minimize cost.

It is hoped that the work accomplished during this study will have a impact on future Space Station configurations.

**END
DATE
FILMED**

JAN 23 1986

